R/V Mirai Cruise Report
MR14-02

February 15, 2014 – March 23, 2014
Tropical Ocean Climate Study (TOCS)

Japan Agency for Marine-Earth Science and Technology (JAMSTEC)
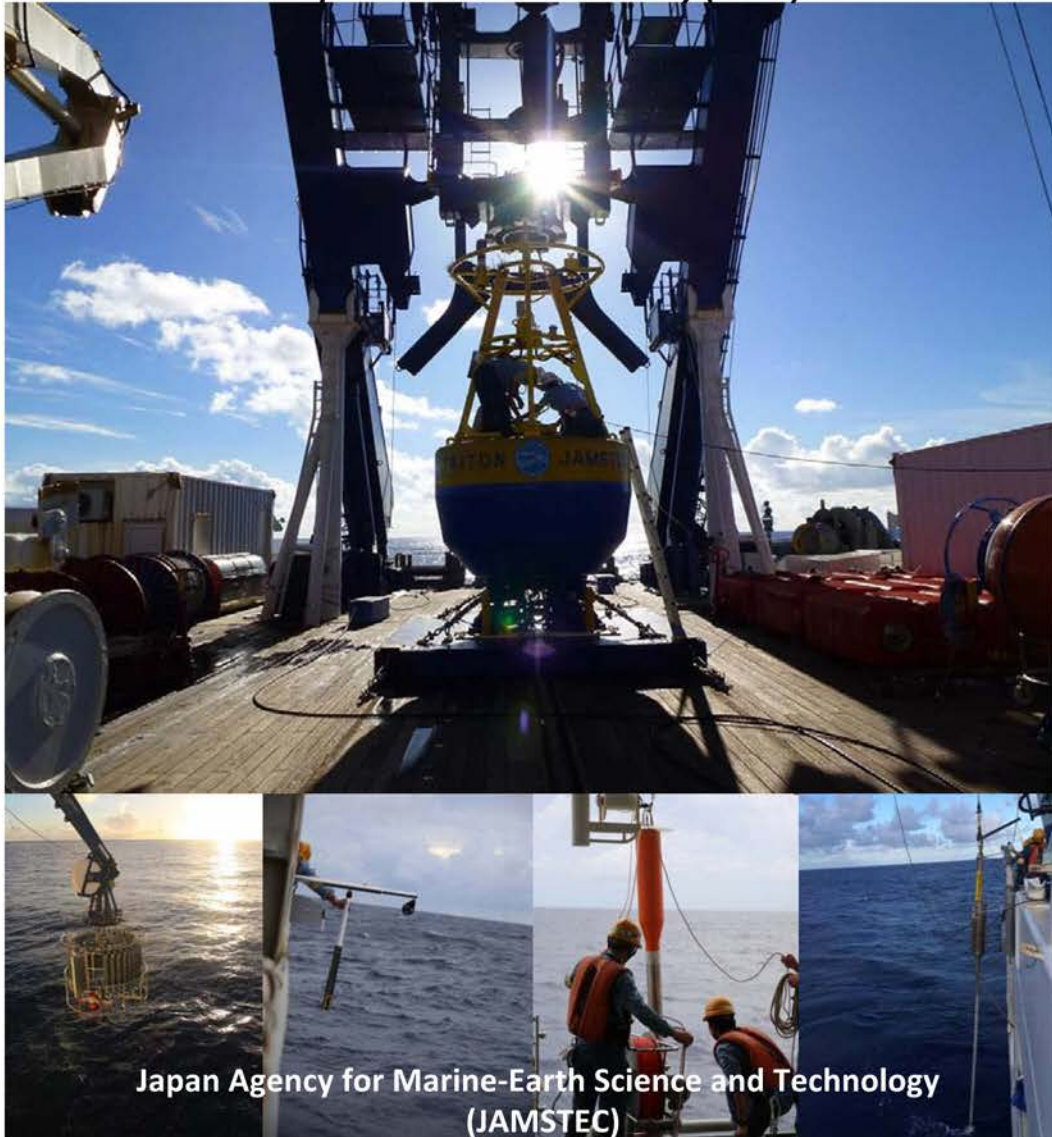
Cruise Report ERRATA of the Nutrients part

page	Error	Correction
155	potassium nitrate CAS No. 7757-91-1	potassium nitrate CAS No. 7757-79-1

Contents

Note:

This cruise report is a preliminary documentation as of the end of the cruise. It may not be revised even if new findings and others are derived from observation results after publication. It may also be changed without notice. Data on the cruise report may be raw or not processed. Please ask the chief scientist for the latest information before using this report. Users of data or results of this cruise are requested to submit their results to Data Integration and Analysis Group (DIAG), JAMSTEC (e-mail: diag-dmd@jamstec.go.jp).

1. Cruise name and code

Cruise name: Tropical Ocean Climate Study

Cruise code: MR14-02

Ship name: R/V MIRAI

Captain: Yoshiharu Tsutsumi

2. Introduction and observation summary

2.1. Introduction

It is well recognized that the evolution of an El Niño/Southern Oscillation (ENSO) event is closely related to the tropical oceanic and atmospheric variations in the Pacific Ocean. Because an El Niño event has a great impact on not only the equatorial Pacific region but also the basin and global climate systems, it strongly affects the natural environment and human society in the world. It is therefore necessary to better understand the physical mechanism of the onset of an El Niño event and improve our skill to predict it.

To improve our understandings of ENSO nature and to monitor the onset of ENSO event, one of the main missions of this cruise is to deploy and recover the TRITON (TRIangle Trans Ocean buoy Network) buoys along 147E and 156E. Also various observations using subsurface ADCP (Acoustic Doppler Current Profiler) moorings, CTD (Conductivity, Temperature and Depth)/XCTD (expendable CTD) measurements and meteorological observation were conducted for understanding oceanic and atmospheric variability in the warm water pool region. In addition, in order to understand mixing effect in the upper ocean changes, CTD with Lowered ADCP (LADCP) observations and ocean turbulence observations were also conducted along 147E and 156E lines, collaborating with International Pacific Research Center (IPRC)/University of Hawaii.

Recently numerical model study implies that oceanic volume transports of low-latitude western boundary currents (LLWBCs) in the tropical South Pacific around Papua New Guinea have interannual variation in association with ENSO events. To understand the role LLWBCs in the tropical South Pacific in oceanic changes of the center of the warm pool, UnderwayCTD (UCTD) and XCTD observations were conducted across the Solomon Strait. In addition, two subsurface

ADCP moorings that were deployed in the coastal region off New Ireland Island during MR12-03 were successfully recovered in this cruise. The ADCPs have measured the current speed of New Ireland Island Coastal Undercurrent (NICU) that is one of the LLWBCs around Papua New Guinea. These observations within the EEZ and territorial water of Papua New Guinea contribute to the SPICE (Southwest Pacific Ocean Circulation and Climate Experiment) project, which was endorsed by CLIVAR.

In addition to the observations related to physical oceanography as mentioned above, we also conducted piston coring at four sites in this cruise. The purpose of the piston coring is to obtained sediment records for paleomagnetic and biogeochemical studies in the western tropical Pacific. Furthermore, in the north of the equator along 156E line, CTD deep casts were conducted at six stations to explore oxygen isotope and related biochemical characteristics from the surface to bottom water in the North Pacific to focus on North Pacific Intermdiate Water (NPIW) changing process in the subtropical/tropical region.

Other observations including continuous oceanic and atmospheric observations have been also successfully conducted along the cruise track.

2.2. Overview

(1) Ship

Ship name: R/V MIRAI

Captain: Yoshiharu Tsutsumi

(2) Cruise code

MR14-02

(3) Project name

Tropical Ocean Climate Study (TOCS)

(Name and representative proposer of each public application project are shown in the Appendix)

(4) Undertaking institution

Japan Agency for Marine-Earth Science and Technology (JAMSTEC)

2-15, Natsushima-cho, Yokosuka 237-0061, Japan

(5) Chief Scientist

Takuya Hasegawa (JAMSTEC)

(6) Period

February 15th, 2014 (Koror) – March 23th, 2014 (Sekinehama)

(7) Research Participants

Total 28 scientists and technical staffs participated from 7 different institutions and companies.

(8) **Research Area**

Western Tropical Pacific

2.3. Observation summary

(1) Number of observation site/launch

TRITON buoy deployment: 7 sites

TRITON buoy recovery: 9 sites

Subsurface ADCP buoy deployment: 1 site

Subsurface ADCP buoy recovery: 3 sites

CTD including water sampling: 37 cites (including 6 CTD deep casts)

XCTD: 31 sites (38 casts)

UCTD: 10 sites (including 2 test sites)

Ocean turbulence observation: 23 stations (31 casts including 5 test casts)

Argo float: 4 launches

Piston Coring: 4 sites

Surface meteorology: continuous

Shipboard ADCP measurement: continuous

Geophysics measurement: continuous

Surface temperature and salinity measurements by intake method pCO2 measurements: continuous

*** Other specially designed observations have been carried out successfully.

(2) Observed oceanic and atmospheric conditions

Very strong westerly wind (westerly wind burst: WWB) up to 25 m/s occurred over the western equatorial Pacific during the present cruise, due to Madden-Julian Oscillation (MJO) (-like) atmospheric pattern coming from the Indian Ocean. Corresponding to the WWB, there were anomalously strong westward surface currents exceeding 1.0 m/s centered the equator, which could bring the warm water in the warm pool region toward the central Pacific. Based on past

studies on onset of ENSO event, such oceanic and atmospheric condition could cause El Niño event in this year.

Also we confirmed that NICU show large northwestward current speed off New Ireland Island, contributing warm water volume transportation to the center of the Pacific warm pool. The NICU-related transportation also may affect the oceanic changes in the warm pool before onset of El Niño event. If El Niño event occur in this year, the data observed by MR14-02 cruise would be very useful to understand the oceanic and atmospheric changes over the western tropical Pacific that will lead the El Niño event.

(3) Overview

Along 147E and 156E lines we deployed seven TRITON buoys and recovered nine TRITON buoys. We only recovered the buoys at two sites of 5N-156E and 8N-156E, and did not deploy at the two sites since the two sited are closed at this year. We also deployed one subsurface ADCP buoys at EQ-156E, and recovered three subsurface ADCP buoys including CLIVAR-SPICE-related two moorings off New Ireland Island.

Various CTD observations including UCTD were conducted during this cruise. Along 147E and 156E lines we measured vertical micro structure profile (MSP) and turbulent in upper ocean using CTD/LADCP and turbmap every 60 miles from 5S and 5N (and 30 miles between 2S and 2N). Unfortunately water leak and trouble of conductivity sensor of turbomap, we miss conductivity data at almost all stations of the MSP observation. The UCTD is one of the new oceanic observational tools. It can measure temperature, conductivity and pressure during the ship runs. JAMSTE conducted the first UCTD observation during MR13-03. In this cruise, first we did test observation of the UCTD at two sites in the 147E line, and then conducted UCTD with XCTD observations near New Ireland Island and across Solomon Strait with high spatial resolution from

10 miles to 30 miles. We also did UCTD and CTD comparison on the CTD stations south of EQ along 156E to confirm the performance of CTD sensor of UCTD.

In addition to the observations related to TOCS and CLIVAR-SPICE projects as mentioned above, piston coring and CTD deep casts were also conducted during this cruise. Other continuous measurements of surface oceanic and low-level atmospheric conditions were also conducted along the cruise track.

3. Period, ports of call, cruise log and cruise track

3.1 Period
15th February 2014 – 23th March 2014

3.2 Ports of call
Koror, Republic of Palau (Departure: 15th February 2014)
Hachinohe, Japan (Arrival: 21th March 2014)
Hachinohe, Japan (Departure: 21th March 2014)
Sekinehama, Japan (Arrival: 23th March 2014)

3.3 Cruise Log

SMT	UTC	Event
Feb. 15th (Sat.) 2014		
09:00	00:00	Departure from Palau
		[Ship Mean Time (SMT) = UTC+9h]
11:00	02:00	Safety guidance
13:15	04:15	Emergency drill
15:00	06:00	Observation Meeting
16:45	07:45	Konpira ceremony
17:00	08:00	Palau EEZ out
		Continuous observations start
		Surface sea water sampling start
Feb. 16th (Sun.) 2014		
13:21	04:21	XCTD observation (for MBES) (#01)
14:00	05:00	MBES/SBP Survey Line PC01 in
Feb. 17th (Mon.) 2014		
05:05	20:05 (-1day)	MBES/SBP Survey Line PC01 out
05:12	20:12 (-1day)	Arrival at PC01
06:41 - 10:31	21:41 (-1day) - 01:31	Piston Corer penetrate (#01)
		(6-30.04N, 138-56.53E)
10:36	01:36	Departure from PC01
Feb. 18th (Tue.) 2014		
00:23	15:23 (-1day)	XCTD observation (for MBES) (#02)
00:55	15:55 (-1day)	MBES/SBP Survey Line PC02 in

SMT	UTC	Event
Feb. 18th (Tue.) 2014		
05:12	20:12 (-1day)	MBES/SBP Survey Line PC02 out
06:00	21:00 (-1day)	Arrival at PC02
08:01 - 09:23	23:01 (-1day) - 00:23	Piston Corer penetrate (#02)
		(3-52.66N, 141-24.05E)
09:30	00:30	Departure from PC02
Feb. 19th (Wed.) 2014		
09:06	00:06	Arrival at TRITON buoy TR07 station
09:10 - 09:50	00:10 - 00:50	CTD dC01M01 (800m) (#01)
09:57 - 10:26	00:57 - 01:26	MSP observation (500m) (#01)
10:27 - 10:56	01:27 - 01:56	MSP observation (500m) (#02)
13:04 - 16:57	04:04 - 07:57	Recovery of TRITON buoy 07 (#01)
17:00	08:00	Departure from TRITON buoy TR07 station
Feb. 20th (Thu.) 2014		
05:12	20:12 (-1day)	Arrival at TRITON buoy TR08 station
05:27 - 06:07	20:27 (-1day) - 21:07 (-1day)	CTD dC02M01 (800m) (#02)
06:12 - 06:46	21:12 (-1day) - 21:46 (-1day)	MSP observation (500m) (#03)
08:04 – 11:33	23:04 (-1day) - 02:33	Recovery of TRITON buoy 08 (#02)
11:36	02:36	Departure from TRITON buoy TR08 station
13:36	04:36	Arrival at CTD point (2-30N, 147-00E)
13:40 – 14:11	04:40 – 05:11	CTD dC03M01 (500m) (#03)

14:12	05:12	Departure from CTD point (2-30N, 147-00E)
16:24	07:24	Arrival at CTD point (3-00N, 147-00E)
16:25 - 16:58	07:25 – 07:58	CTD dC04M01 (500m) (#04)
17:00	08:00	Departure from CTD point (3-00N, 147-00E)

Feb. 21st (Fri.) 2014

00:00	15:00 (-1day)	Arrival at TRITON buoy TR08 station
08:17 - 11:40	23:17 (-1day) - 02:40	Deployment of TRITON buoy 08 (#01) (Fixed position: 01-59.4969N, 147-01.1695E)
12:37	03:37	XCTD observation (#03)
12:42	03:42	Departure from TRITON buoy TR08 station
14:42	05:42	Arrival at CTD point (1-30N, 147-00E)

SMT	UTC	Event

Feb. 21st (Fri.) 2014

14:48 - 15:20	05:48 - 06:20	CTD dC05M01 (500m) (#05)
15:28 - 16:02	06:28 - 07:02	MSP observation (500m) (#04)
16:09 - 16:20	07:09 - 07:20	Underway CTD (250m) (#01)
16:24	07:24	Departure from CTD point (1-30N, 147-00E)
18:18	09:18	Arrival at CTD point (1-00N, 147-00E)
18:36 - 19:06	09:36 - 10:06	CTD dC06M01 (500m) (#06)
19:06	10:06	Departure from CTD point (1-00N, 147-00E)

Feb. 22nd (Sat.) 2014

02:30	17:30 (-1day)	Arrival at CTD point (EQ, 147-00E)
05:30 - 06:12	20:30 (-1day) - 21:12 (-1day)	CTD dC07M01 (800m) (#07)
08:22 - 12:38	23:22 (-1day) - 03:38	Recovery of TRITON Buoy 09 (#03)
13:30 - 14:00	04:30 - 05:00	CTD dC08M01 (500m) (#08)
14:00	05:00	Departure from CTD point (EQ, 147-00E)
16:00	07:00	Arrival at CTD point (0-30N, 147-00E)
16:01 - 16:32	07:01 - 07:32	CTD dC09M01 (500m) (#09)
16:36 - 16:54	07:36 - 07:54	Underway CTD (1000m) (#02)
17:00	08:00	Departure from CTD point (0-30N, 147-00E)
19:42	10:42	Arrival at TRITON buoy TR09 station
19:46 - 20:07	10:46 - 11:07	Calibration for magnetometer (#01)

Feb. 23rd (Sun.) 2014

08:28 - 11:34	23:28 (-1day) - 02:34	Deployment of TRITON buoy 09 (#02) (Fixed position: 00-01.4896N, 147-00.0927E)
12:36	03:36	XCTD observation (#04)
13:36	04:36	Departure from TRITON buoy TR09 station
14:45	05:45	Cesium magnetometer towing start

Feb. 24th (Mon.) 2014

22:00	12:00	Time adjustment +1 hour (SMT=UTC+10h)

Feb. 25th (Tue.) 2014

00:32	14:32 (-1day)	Cesium magnetometer towing finish
03:52	17:52 (-1day)	XCTD observation (#05)
05:41	19:41 (-1day)	XCTD observation (#06)

SMT	UTC	Event

Feb. 25th (Tue.) 2014

07:30	21:30 (-1day)	Arrival at ADCP mooring station (2-38.1S, 153-21.0E)
08:00 - 08:43	22:00 (-1day) - 22:43 (-1day)	CTD dC10M01 (1000m) (#10)
09:28 - 12:06	23:28 (-1day) - 02:06	Recovery ADCP mooring (#01)
12:06	02:06	Departure from ADCP mooring station (2-38.1S, 153-21.0E)
13:18	03:18	Arrival at ADCP mooring station (2-48.0S, 153-21.0E)
13:19 - 14:05	03:19 - 04:05	CTD dC11M01 (1000m) (#11)
14:44 - 17:03	04:44 - 07:03	Recovery of ADCP mooring (#02)
17:11	07:11	XCTD observation (#07)
17:12	07:12	Departure from ADCP mooring station

SMT	UTC	Event
19:20	09:20	XCTD observation (#08)
21:30	11:30	XCTD observation (#09)
23:23	13:23	XCTD observation (#10)
Feb. 26th (Wed.) 2014		
02:18	16:18 (-1day)	XCTD observation (#11)
05:59 - 06:21	19:59 (-1day) - 20:21 (-1day)	MSP observation (300m) (#05)
06:57	20:57 (-1day)	XCTD observation (#12)
07:03 - 07:32	21:03 (-1day) - 21:32 (-1day)	Underway CTD (1000m) (#03)
08:36 - 09:07	22:36 (-1day) - 23:07 (-1day)	Underway CTD (1000m) (#04)
10:07	00:07	XCTD observation (#13)
10:14 - 10:44	00:14 - 00:44	Underway CTD (1000m) (#05)
11:41 - 12:15	01:41 - 02:15	Underway CTD (1000m) (#06)
13:09	03:09	XCTD observation (#14)
13:21 - 13:53	03:21 - 03:53	Underway CTD (1000m) (#07)
14:42 - 15:16	04:42 - 05:16	Underway CTD (1000m) (#08)
16:04	06:04	XCTD observation (#15)
16:10 - 16:46	06:10 - 06:46	Underway CTD (1000m) (#09)
17:39 - 18:14	07:39 - 08:14	Underway CTD (1000m) (#10)
19:03	09:03	XCTD observation (#16)
SMT	UTC	Event
Feb. 26th (Wed.) 2014		
20:31	10:31	XCTD observation (#17)
22:03	12:03	XCTD observation (#18)
23:38	13:38	XCTD observation (#19)
Feb. 27th (Thu.) 2014		
01:14	15:14 (-1day)	XCTD observation (#20)
03:00	17:00 (-1day)	Arrival at TRITON buoy TR06 station
08:12 - 10:20	22:12 (-1day) - 00:20	Deployment of TRITON buoy 06 (#03) (Fixed position: 04-57.9932N, 156-00.9964E)
11:44	01:44	XCTD observation (#21)
13:00 - 13:23	03:00 - 03:23	MSP observation (300m) (#06)
13:24	03:24	Departure from TRITON buoy TR06 station
15:30	05:30	Arrival at CTD point (4-30S, 156-00E)
15:30 - 16:02	05:30 - 06:02	CTD dC12M01 (500m) (#12)
16:06	06:06	Departure from CTD point (4-30S, 156-00E)
18:12	08:12	Arrival at CTD point (4-00S, 156-00E)
18:15 - 18:46	08:15 - 08:46	CTD dC13M01 (500m) (#13)
18:50 - 19:12	08:50 - 09:12	MSP observation (300m) (#07)
19:12	09:12	Departure from CTD point (4-00S, 156-00E)
Feb. 28th (Fri.) 2014		
03:00	17:00 (-1day)	Arrival at TRITON buoy TR06 station
04:23 - 04:50	18:23 (-1day) - 18:50 (-1day)	Calibration for magnetometer (#02)
05:29 - 06:09	19:29 (-1day) - 20:09 (-1day)	CTD dC14M01 (800m) (#14)
08:04 - 10:43	22:04 (-1day) - 00:43	Recovery of TRITON buoy 06 (#04)
10:48	00:48	Departure from TRITON buoy TR06 station
18:00	08:00	Arrival at CTD point (3-30S, 156-00E)
18:15 - 18:47	08:15 - 08:47	CTD dC15M01 (500m) (#15)
18:51 - 19:14	08:51 - 09:14	MSP observation (300m) (#08)
19:18	09:18	Departure from CTD point (3-30S, 156-00E)
Mar. 1st (Sat.) 2014		
03:00	17:00 (-1day)	Arrival at TRITON buoy TR05 station
SMT	UTC	Event
Mar. 1st (Sat.) 2014		
08:15 - 10:18	22:15 (-1day) - 00:18	Deployment of TRITON buoy 05 (#04) (Fixed position: 01-58.9967S, 156-01.9862E)
10:44	00:44	XCTD observation (#22)
11:36	01:36	Departure from TRITON buoy TR05 station

13:54	03:54	Arrival at CTD point (2-30S, 156-00E)
13:59 - 14:29	03:59 - 04:29	CTD dC16M01 (500m) (#16)
14:30 - 15:08	04:30 - 05:08	MSP observation (300m) (#09)
15:21 - 15:42	05:21 - 05:42	MSP observation (300m) (#10)
15:42	05:42	Departure from CTD point (2-30S, 156-00E)
18:00	08:00	Arrival at CTD point (3-00S, 156-00E)
18:00 - 18:31	08:00 - 08:31	CTD dC17M01 (500m) (#17)
18:36 - 18:59	08:36 - 08:59	MSP observation (300m) (#11)
19:00	09:00	Departure from CTD point (3-00S, 156-00E)

Mar. 2nd (Sun.) 2014

02:30	16:30 (-1day)	Arrival at TRITON buoy TR05 station
05:29 - 06:10	19:29 (-1day) - 20:10 (-1day)	CTD dC18M01 (800m) (#18)
06:15 - 06:33	20:15 (-1day) - 20:33 (-1day)	MSP observation (300m) (#12)
06:34 - 06:54	20:34 (-1day) - 20:54 (-1day)	MSP observation (300m) (#13)
08:07 - 10:51	22:07 (-1day) - 00:51	Recovery of TRITON buoy 05 (#05)
10:54	00:54	Departure from TRITON buoy TR05 station
13:12	03:12	Arrival at CTD point (1-30S, 156-00E)
13:13 - 13:48	03:13 - 03:48	CTD dC19M01 (500m) (#19)
13:54 - 14:12	03:54 - 04:12	MSP observation (300m) (#14)
14:13 - 14:35	04:13 - 04:35	MSP observation (300m) (#15)
14:36	04:36	Departure from CTD point (1-30S, 156-00E)
16:48	06:48	Arrival at CTD point (1-00S, 156-00E)
16:48 - 17:17	06:48 - 07:17	CTD dC20M01 (500m) (#20)
17:22 - 17:40	07:22 - 07:40	MSP observation (300m) (#16)
17:41 - 18:03	07:41 – 08:03	MSP observation (300m) (#17)
18:06	08:06	Departure from CTD point (1-00S, 156-00E)
SMT	UTC	Event

Mar. 3rd (Mon.) 2014

01:30	15:30 (-1day)	Arrival at TRITON buoy TR04 station
08:11 - 10:29	22:11 (-1day) - 00:29	Deployment of TRITON Buoy 04 (#05)
		(Fixed position: 00-00.9973S, 155-57.7969E)
11:31	01:31	XCTD observation (#23)
13:02 - 13:48	03:02 - 03:48	CTD dC21M01 (800m) (#21)
13:54 - 14:27	03:54 - 04:27	MSP observation (500m) (#18)
14:29 - 15:05	04:29 - 05:05	MSP observation (500m) (#19)
15:06	05:06	Departure from TRITON buoy 04 station
17:18	07:18	Arrival at CTD point (0-30S, 156-00E)
17:19 - 17:51	07:19 - 07:51	CTD dC22M01 (500m) (#22)
18:18	08:18	Departure from CTD point (0-30S, 156-00E)
22:12	12:12	Arrival at TRITON buoy TR04 station

Mar. 4th (Tue.) 2014

08:03 - 11:08	22:03 (-1day) - 01:08	Recovery of TRITON buoy 04 (#06)
12:59 - 14:46	02:59 - 04:46	CTD dC22M02 (1945m) (#23)

Mar. 5th (Wed.) 2014

08:12 - 09:42	22:12 (-1day) - 23:42 (-1day)	Recovery of ADCP mooring (#03)
13:03 - 14:01	03:03 - 04:01	Deployment of ADCP mooring (#01)
		(Fixed position: 00-02.1869S, 156-08.0406E)
14:42 - 15:20	04:42 - 05:20	MSP observation (300m) (#20)
15:28	05:28	XCTD observation (#24)
17:00	07:00	Departure from TRITON buoy TR04 station
17:00	07:00	MBES/SBP Survey Line PC03 in

Mar. 6th (Thu.) 2014

04:00	18:00 (-1day)	MBES/SBP Survey Line PC03 out
06:36 - 09:20	20:36 (-1day) - 23:20 (-1day)	Arrival at PC03
08:01	22:01 (-1day)	Piston Corer penetrate (#03)
		(0-12.00S, 155-57.95E)
09:24	23:24 (-1day)	Departure from PC03

SMT	UTC	Event
Mar. 6th (Thu.) 2014		
12:48	02:48	Arrival at CTD point (0-30N, 156-00E)
12:59 - 13:32	02:59 - 03:32	CTD dC23M01 (500m) (#24)
13:36 - 13:58	03:36 - 03:58	MSP observation (300m) (#21)
14:00 - 14:23	04:00 - 04:23	MSP observation (300m) (#22)
14:24	04:24	Departure from CTD point (0-30N, 156-00E)
20:24	10:24	MBES/SBP Survey Line PC04 in
Mar. 7th (Fri.) 2014		
04:15	18:15 (-1day)	MBES/SBP Survey Line PC04 out
06:34 - 09:36	20:34 (-1day) - 23:36 (-1day)	Arrival at PC04
08:06	22:06 (-1day)	Piston Corer penetrate (#04)
		(2-02.98N, 156-06.54E)
09:36	23:36 (-1day)	Departure from PC04
12:48	02:48	Arrival at CTD point (1-00N, 156-00E)
12:57	02:57	XCTD observation (#25)
13:06 - 13:28	03:06 - 03:28	MSP observation (300m) (#23)
13:35 - 14:05	03:35 - 04:05	CTD dC24M01 (500m) (#25)
14:06	04:06	Departure from CTD point (1-30N, 156-00E)
16:12	06:12	Arrival at CTD point (1-00N, 156-00E)
16:14	06:14	XCTD observation (#26)
16:19 - 16:42	06:19 - 06:42	MSP observation (300m) (#24)
16:52 - 17:27	06:52 - 07:27	CTD dC25M01 (500m) (#26)
17:30	07:30	Departure from CTD point (1-00N, 156-00E)
Mar. 8th (Sat.) 2014		
00:30	14:30 (-1day)	Arrival at TRITON buoy TR03 station
08:07 - 10:23	22:07 (-1day) - 00:23	Deployment of TRITON buoy 03 (#06)
		(Fixed position: 01-57.1916N, 155-59.9678E)
11:01	01:01	XCTD observation (#27)
12:58	02:58	XCTD observation (#28)
13:03 - 13:23	03:03 - 03:23	MSP observation (300m) (#25)
13:24 - 13:44	03:24 - 03:44	MSP observation (300m) (#26)

SMT	UTC	Event
Mar. 8th (Sat.) 2014		
13:54 - 14:36	03:54 - 04:36	CTD dC26M01 (800m) (#27)
Mar. 9th (Sun.) 2014		
08:03	22:03 (-1day)	Recovery of TRITON buoy 03 (#07)
11:24	01:24	Departure from TRITON buoy TR03 station
15:00	05:00	Arrival at CTD point (3-00N, 156-00E)
15:03	05:03	XCTD observation (#29)
15:08 - 15:30	05:08 - 05:30	MSP observation (300m) (#27)
15:39 - 16:01	05:39 - 06:01	MSP observation (300m) (#28)
16:07 - 16:37	06:07 - 06:37	CTD dC27M01 (500m) (#28)
16:42	06:42	Departure from CTD point (3-00N, 156-00E)
Mar. 10th (Mon.) 2014		
02:00	16:00	Arrival at TRITON buoy TR02 station
08:10	22:10	Deployment of TRITON Buoy 02 (#07)
		(Fixed position: 04-58.4511N, 156-02.0429E)
11:34	01:34	XCTD observation (#30)
11:42	01:42	Departure from TRITON buoy TR02 station
15:36	05:36	Arrival at CTD point (4-00N, 156-00E)
15:41	05:41	XCTD observation (#31)
15:48 - 16:10	05:48 - 06:10	MSP observation (300m) (#29)
16:19 - 16:49	06:19 - 06:49	CTD dC28M01 (500m) (#29)
16:53 - 17:14	06:53 - 07:14	MSP observation (300m) (#30)
17:18	07:18	Departure from CTD point (4-00N, 156-00E)
Mar. 11th (Tue.) 2014		

00:30	14:30 (-1day)	Arrival at TRITON buoy TR02 station
05:27	19:27 (-1day)	XCTD observation (#32)
05:32 - 05:55	19:32 (-1day) - 19:55 (-1day)	MSP observation (300m) (#31)
06:01 - 06:41	20:01 (-1day) - 20:41 (-1day)	CTD dC29M01 (800m) (#30)
08:06 - 11:28	22:06 (-1day) - 01:28	Recovery of TRITON buoy 02 (#08)
13:03 - 15:56	03:03 - 05:56	CTD dC30M01 (3595m) (#31)
16:00	06:00	Departure from TRITON buoy TR02 station
18:00	08:00	XCTD observation (#33)

SMT	UTC	Event
Mar. 11th (Tue.) 2014		
20:02	10:02	XCTD observation (#34)
22:03	12:03	XCTD observation (#35)
00:03	14:03 (-1day)	XCTD observation (#36)
Mar. 12th (Wed.) 2014		
02:11	16:11 (-1day)	XCTD observation (#37)
05:42	19:42 (-1day)	Arrival at TRITON buoy TR01 station
05:59 - 06:44	19:59 (-1day) - 20:44(-1day)	CTD dC31M01 (1000m) (#32)
06:05	20:05 (-1day)	XCTD observation (Auto+Hand) (#38, #39)
06:14	20:14 (-1day)	XCTD observation (Auto+Hand) (#40, #41)
06:21	20:21 (-1day)	XCTD observation (Auto+Hand) (#42, #43)
06:29	20:29 (-1day)	XCTD observation (Auto+Hand) (#44, #45)
08:04 - 11:40	22:04 (-1day) - 01:40	Recovery of TRITON Buoy 01 (#09)
11:48	01:48	Departure from TRITON buoy TR01 station
21:48	11:48	Arrival at CTD point (10-00N, 155-12E)
21:57 - 01:51 (+1day)	11:57 - 15:51	CTD dC32M01 (5451m) (#33)
Mar. 13th (Thu.) 2014		
01:54	15:54	Departure from CTD point (10-00N, 155-12E)
Mar. 14th (Fri.) 2014		
07:42	21:42 (-1day)	Arrival at CTD point (15-00N, 153-12E)
07:54 - 12:00	21:54 (-1day) - 02:00	CTD dC33M01 (5975m) (#34)
12:06	02:06	Departure from CTD point (15-00N, 153-12E)
Mar. 15th (Sat.) 2014		
05:42	19:42	Arrival at CTD point (18-18N, 151-54E)
05:55 - 07:06	19:55 - 21:06	CTD dC34M01 (2000m) (#35)
07:13	21:13	Deployment of Argo float (#01)
07:18	21:18	Departure from CTD point (18-18N, 151-54E)
19:12	09:12	Arrival at CTD point (20-40N, 150-57E)
19:30 - 23:40	09:30 - 13:40	CTD dC35M01 (6022m) (#36)
23:46	13:46	Deployment of Argo float (#02)
23:48	13:48	Departure from CTD point (20-40N, 150-57E)

| SMT	UTC	Event
Mar. 16th (Sun.) 2014		
07:48	21:48	Arrival at CTD point (22-00N, 150-24E)
07:59 - 09:10	21:59 - 23:10	CTD dC36M01 (2000m) (#37)
09:16	23:16	Deployment of Argo float (#03)
09:18	23:18	Departure from CTD point (22-00N, 150-24E)
05:48	19:48	Arrival at CTD point (25-00N, 149-12E)
Mar. 17th (Mon.) 2014		
05:58 - 09:56	19:58 - 23:56	CTD dC37M01 (5715m) (#38)
10:01	00:01	Deployment of Argo float (#04)
10:06	00:06	Departure from CTD point (25-00N, 149-12E)
15:26 - 15:50	05:26 - 05:50	Calibration for magnetometer (#03)
Mar. 18th (Tue.) 2014		
22:00	13:00	Time adjustment -1 hour (SMT=UTC+9h)
Mar. 19th (Wed.) 2014		
19:38	10:38	Surface sea water sampling finish
Mar. 21st (Fri.) 2014		
13:00	04:00	Arrival at Hachinohe
18:00	09:00	Departure from Hachinohe

Mar. 23rd (Sun.) 2014
   09:10   00:10   Arrival at Sekinehama *

---

  * Due to bad weather condition between Hachinohe and Sekinehama, arrival at Sekinehama was one day late behind the original plan.

3.4 Cruise Track

MR14-02 Cruise Track
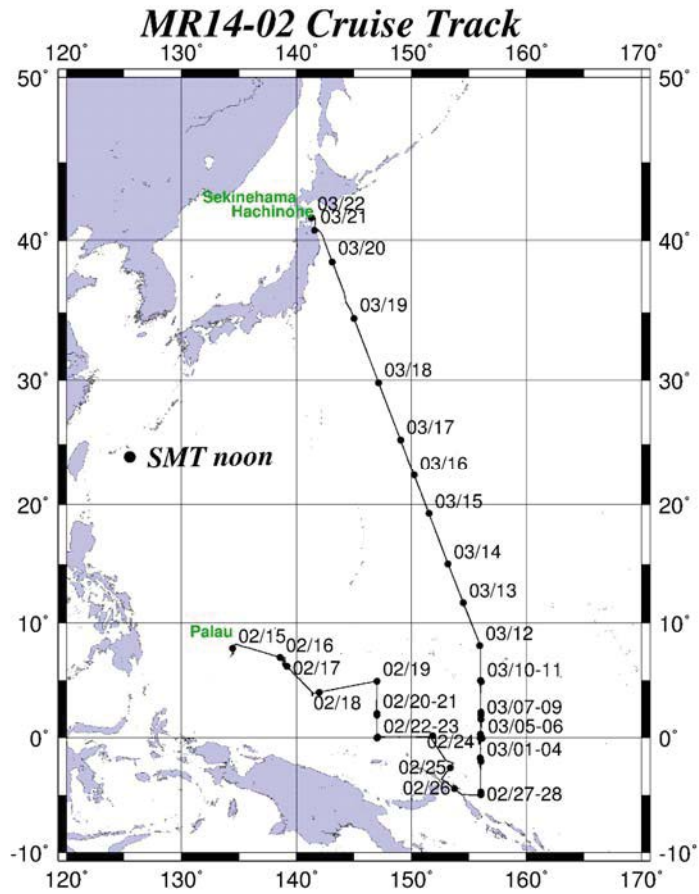
4. Chief scientist

Chief Scientist: Takuya Hasegawa

Senior Research Scientist

Research Institute for Global Change (RIGC)

Japan Agency for Marine-Earth Science and Technology (JAMSTEC)

2-15, Natsushima-cho, Yokosuka, 237-0061, Japan

Tel: +81-46-867-9457,   FAX: +81-46-867-9255

e-mail: takuyah@jamstec.go.jp

5. Participants list

5.1 R/V MIRAI scientists and technical staffs

Name	Affiliation	Occupation	Onboard section
Takuya Hasegawa	JAMSTEC	Chief Scientist	Koror - Sekinehama
Junichiro Kuroda	JAMSTEC	Scientist	Koror - Sekinehama
Toshitsugu Yamazaki	AORI, University of Tokyo	Scientist	Koror - Sekinehama
Haruka Takagi	Waseda University/JAMSTEC	Scientist	Koror - Sekinehama
Toshihiro Yoshimura	JAMSTEC	Scientist	Koror - Sekinehama
Kensuke Watari	JAMSTEC	Scientist	Koror - Sekinehama
Osamu Abe	Nagoya University	Scientist	Koror - Sekinehama
Habeeb Rahman Keedakkadan	Nagoya University	Scientist	Koror - Sekinehama
Kelvin Richards	University of Hawaii	Scientist	Koror - Hachinohe
Kazuho Yoshida	Global Ocean Development Inc.	Technical Staff	Koror - Sekinehama
Masanori Murakami	Global Ocean Development Inc.	Technical Staff	Koror - Sekinehama
Miki Morioka	Global Ocean Development Inc.	Technical Staff	Koror - Sekinehama
Keisuke Matsumoto	Marine Works Japan Ltd.	Technical Staff	Koror - Sekinehama
Tomohide Noguchi	Marine Works Japan Ltd.	Technical Staff	Koror - Sekinehama
Hiroki Ushiromura	Marine Works Japan Ltd.	Technical Staff	Koror - Sekinehama
Akira Watanabe	Marine Works Japan Ltd.	Technical Staff	Sekinehama - Sekinehama
Shungo Oshitani	Marine Works Japan Ltd.	Technical Staff	Koror - Sekinehama
Sonoka Wakatsuki	Marine Works Japan Ltd.	Technical Staff	Koror - Sekinehama
Makito Yokota	Marine Works Japan Ltd.	Technical Staff	Koror - Sekinehama
Kai Fukuda	Marine Works Japan Ltd.	Technical Staff	Koror - Sekinehama
Yoshiko Ishikawa	Marine Works Japan Ltd.	Technical Staff	Koror - Sekinehama
Yasuhiro Arii	Marine Works Japan Ltd.	Technical Staff	Koror - Sekinehama
Kanako Yoshida	Marine Works Japan Ltd.	Technical Staff	Koror - Sekinehama
Masahiro Orui	Marine Works Japan Ltd.	Technical Staff	Koror - Sekinehama
Mika Yamaguchi	Marine Works Japan Ltd.	Technical Staff	Koror - Sekinehama
Hiroyuki Hayashi	Marine Works Japan Ltd.	Technical Staff	Koror - Sekinehama
Yuki Miyajima	Marine Works Japan Ltd.	Technical Staff	Koror - Sekinehama
Yasumi Yamada	Marine Works Japan Ltd.	Technical Staff	Koror - Sekinehama

5.2 R/V MIRAI crew members

Name	Rank
Yoshiharu Tsutsumi	Master
Haruhiko Inoue	Chief Officer
Takeshi Isohi	1st Officer
Toshihisa Akutagawa	Jr. 1st Officer
Nobuo Fukaura	2nd Officer
Takahiro Noguchi	3rd Officer
Minoru Maruta	Chief Engineer
Ryo Sakata	1st Engineer
Naoto Miyazaki	2nd Engineer
Wataru Okuma	3rd Engineer
Toshitaka Oki	Jr. 3rd Engineer
Ryo Kimura	Technical Officer
Yosuke Kuwahara	Boatswain
Kazuyoshi Kudo	Able Seaman
Tsuyoshi Sato	Able Seaman
Tsuyoshi Monzawa	Able Seaman
Hiromu Hirokawa	Able Seaman
Masaya Tanikawa	Able Seaman
Hideaki Tamotsu	Ordinary Seaman
Hideyuk Okubo	Ordinary Seaman
Shohei Uehara	Ordinary Seaman
Tetsuya Sakamoto	Ordinary Seaman
Tenki Yamashiro	Ordinary Seaman
Kazumi Yamashita	No.1 Oiler
Toshiyuki Furuki	Oiler
Keisuke Yoshida	Oiler
Shintaro Abe	Wiper
Hiromi Ikuta	Wiper
Hitoshi Ota	Chief Steward
Sakae Hoshikuma	Cook
Tsuneaki Yoshinaga	Cook
Yukio Chiba	Cook
Shigenori Yamaguchi	Cook
Shohei Maruyama	Steward

6. General observation

6.1 Meteorological measurement

6.1.1 Surface meteorological observations

(1) Personnel

Takuya Hasegawa	(JAMSTEC) *Principal Investigator
Kazuho Yoshida	(Global Ocean Development Inc., GODI)
Masanori Murakami	(GODI)
Miki Morioka	(GODI)
Ryo Kimura	(MIRAI Crew)

(2) Objective

Surface meteorological parameters are observed as a basic dataset of the meteorology. These parameters bring us the information about the temporal variation of the meteorological condition surrounding the ship.

(3) Instruments and Methods

Surface meteorological parameters were observed throughout the MR14-02 cruise. We used two systems for the observation, during this cruise.

i)   MIRAI Surface Meteorological observation (SMet) system

Instruments of SMet system are listed in Table.6.1.1-1 and measured parameters are listed in Table.6.1.1-2. Data were collected and processed by KOAC-7800 weather data processor made by Koshin-Denki, Japan. The data set consists of 6-second averaged data.

ii)   Shipboard Oceanographic and Atmospheric Radiation (SOAR) system

SOAR system designed by BNL (Brookhaven National Laboratory, USA) consists of major three parts.
a)   Portable Radiation Package (PRP) designed by BNL - short and long wave downward radiation.
b)   Zeno Meteorological (Zeno/Met) system designed by BNL - wind, air temperature, relative humidity, pressure, and rainfall measurement.
c)   Photosynthetically Available Radiation (PAR) sensor manufactured by Biospherical Instruments Inc. (USA) - PAR measurement.
d)   Scientific Computer System (SCS) developed by NOAA (National Oceanic and Atmospheric Administration, USA) - centralized data acquisition and logging of all data sets.

SCS recorded PRP data every 6 seconds, while Zeno/Met data every 10 seconds. Instruments and their locations are listed in Table.6.1.1-3 and measured parameters are listed in Table.6.1.1-4.

For the quality control as post processing, we checked the following sensors, before and after the cruise.

  i) Young Rain gauge (SMet and SOAR)
       Inspect of the linearity of output value from the rain gauge sensor to change Input value by adding fixed quantity of test water.
  ii. Barometer (SMet and SOAR)
       Comparison with the portable barometer value, PTB220CASE, VAISALA.
  iii. Thermometer (air temperature and relative humidity) (SMet and SOAR)
       Comparison with the portable thermometer value, HMP41/45, VAISALA.

(4) Preliminary results

Figure 6.1.1-1 show the time series of the following parameters;
    Wind (SOAR)
    Air temperature (SMet)
    Relative humidity (SMet)
    Precipitation (SOAR, capacitive rain gauge)
    Short/long wave radiation (SOAR)
    Pressure (SMet)
    Sea surface temperature (SMet)
    Significant wave height (SMet)

(5) Data archives

These meteorological data will be submitted to the Data Management Group (DMG) of JAMSTEC just after the cruise.

(6) Remarks

1. Data acquisition was suspended in the territorial waters of Palau.

2. During the following period, SST (Sea Surface Temperature) data were available.
     04:51UTC 15 Feb. 2014 - 01:29UTC 19 Mar. 2014

3. At the following time, increasing of SMet capacitive rain gauge data were invalid due to transmitting for MF/HF radio.
     05:41UTC 18 Mar. 2014
     05:43UTC 18 Mar. 2014

4. During the following periods, optical rain gauge, atmospheric pressure, relative wind direction and relative wind speed data of SOAR was invalid due to system trouble.
     04:16:58UTC 15 Feb. 2014 - 04:17:46UTC 15 Feb. 2014
     05:57:52UTC 15 Feb. 2014 - 05:58:28UTC 15 Feb. 2014
     08:47:39UTC 15 Feb. 2014 - 08:48:39UTC 15 Feb. 2014
     09:29:53UTC 15 Feb. 2014 - 09:31:05UTC 15 Feb. 2014
     09:31:11UTC 15 Feb. 2014 - 09:31:23UTC 15 Feb. 2014

5. During the following period, FRSR data acquisition was suspended to prevent damage to the shadow-band from freezing.

08:42UTC 20 Mar. 2014 to the end of this cruise

6. During the following period, Latitude, Longitude, heading and LOG data were invalid due to communication trouble of the network server side.
09:37UTC 20 Mar. 2014 - 11:45UTC 20 Mar. 2014

7. During the following period, Latitude, Longitude were invalid due to GPS trouble.
18:05UTC 20 Mar. 2014 - 18:12UTC 20 Mar. 2014

Table.6.1.1-1 Instruments and installations of MIRAI
Surface Meteorological observation system

Sensors	Type	Manufacturer	Location (altitude from surface)
Anemometer	KE-500	Koshin Denki, Japan	foremast (24 m)
Tair/RH	HMP155	Vaisala, Finland	compass deck (21 m)
			starboard and port side
	with 43408 Gill aspirated radiation shield	R.M. Young, USA	
Thermometer (SST)	RFN1-0	Koshin Denki, Japan	4th deck (-1m, inlet -5m)
Barometer	Model-370	Setra System, USA	captain deck (13 m)
			weather observation room
Rain gauge	50202	R. M. Young, USA	compass deck (19 m)
Optical rain gauge	ORG-815DS	Osi, USA	compass deck (19 m)
Radiometer (short wave)	MS-802	Eiko Seiki, Japan	radar mast (28 m)
Radiometer (long wave)	MS-202	Eiko Seiki, Japan	radar mast (28 m)
Wave height meter	WM-2	Tsurumi-seiki, Japan	bow (10 m)
			port side stern (8 m)

Table.6.1.1-2 Parameters of MIRAI Surface Meteorological observation system

	Parameter	Units	Remarks
1	Latitude	degree	
2	Longitude	degree	
3	Ship's speed	knot	MIRAI log, DS-30 Furuno
4	Ship's heading	degree	MIRAI gyro, TG6000, Tokimec
5	Relative wind speed	m/s	6sec./10min. averaged
6	Relative wind direction	degree	6sec./10min. averaged
7	True wind speed	m/s	6sec./10min. averaged
8	True wind direction	degree	6sec./10min. averaged
9	Barometric pressure	hPa	adjusted to sea surface level
			6sec. averaged
10	Air temperature (starboard)	degC	6sec. averaged
11	Air temperature (port side)	degC	6sec. averaged
12	Dewpoint temperature (starboard)	degC	6sec. averaged
13	Dewpoint temperature (side)	degC	6sec. averaged
14	Relative humidity (starboard)	%	6sec. averaged
15	Relative humidity (port side)	%	6sec. averaged
16	Sea surface temperature	degC	6sec. averaged

17	Rain rate (optical rain gauge)	mm/hr	hourly accumulation
18	Rain rate (capacitive rain gauge)	mm/hr	hourly accumulation
19	Down welling shortwave radiation	W/m^2	6sec. averaged
20	Down welling infra-red radiation	W/m^2	6sec. averaged
21	Significant wave height (bow)	m	hourly
22	Significant wave height (aft)	m	hourly
23	Significant wave period (bow)	second	hourly
24	Significant wave period (aft)	second	hourly

Table.6.1.1-3 Instruments and installation locations of SOAR system

Sensors (Zeno/Met)	Type	Manufacturer	Location (altitude from surface)
Anemometer	05106	R.M. Young, USA	foremast (25 m)
Tair/RH	HMP155	Vaisala, Finland	foremast (23 m)
		with 43408 Gill aspirated radiation shield	R.M. Young, USA
Barometer	61302V	R.M. Young, USA	foremast (23 m)
		with 61002 Gill pressure port	R.M. Young, USA
Rain gauge	50202	R.M. Young, USA	foremast (24 m)
Optical rain gauge	ORG-815DA	Osi, USA	foremast (24 m)

Sensors (PRP)	Type	Manufacturer	Location (altitude from surface)
Radiometer (short wave)	PSP	Epply Labs, USA	foremast (25 m)
Radiometer (long wave)	PIR	Epply Labs, USA	foremast (25 m)
Fast rotating shadowband radiometer		Yankee, USA	foremast (25 m)

Sensor (PAR)	Type	Manufacturer	Location (altitude from surface)
PAR sensor	PUV-510	Biospherical Instruments Inc., USA	Navigation deck (18m)

Table.6.1.1-4 Parameters of SOAR system

|	Parameter	Units	Remarks
1	Latitude	degree	
2	Longitude	degree	
3	SOG	knot	
4	COG	degree	
5	Relative wind speed	m/s	
6	Relative wind direction	degree	
7	Barometric pressure	hPa	
8	Air temperature	degC	
9	Relative humidity	%	
10	Rain rate (optical rain gauge)	mm/hr	
11	Precipitation (capacitive rain gauge)	mm	reset at 50 mm
12	Down welling shortwave radiation	W/m^2	
13	Down welling infra-red radiation	W/m^2	
14	Defuse irradiance	W/m^2	
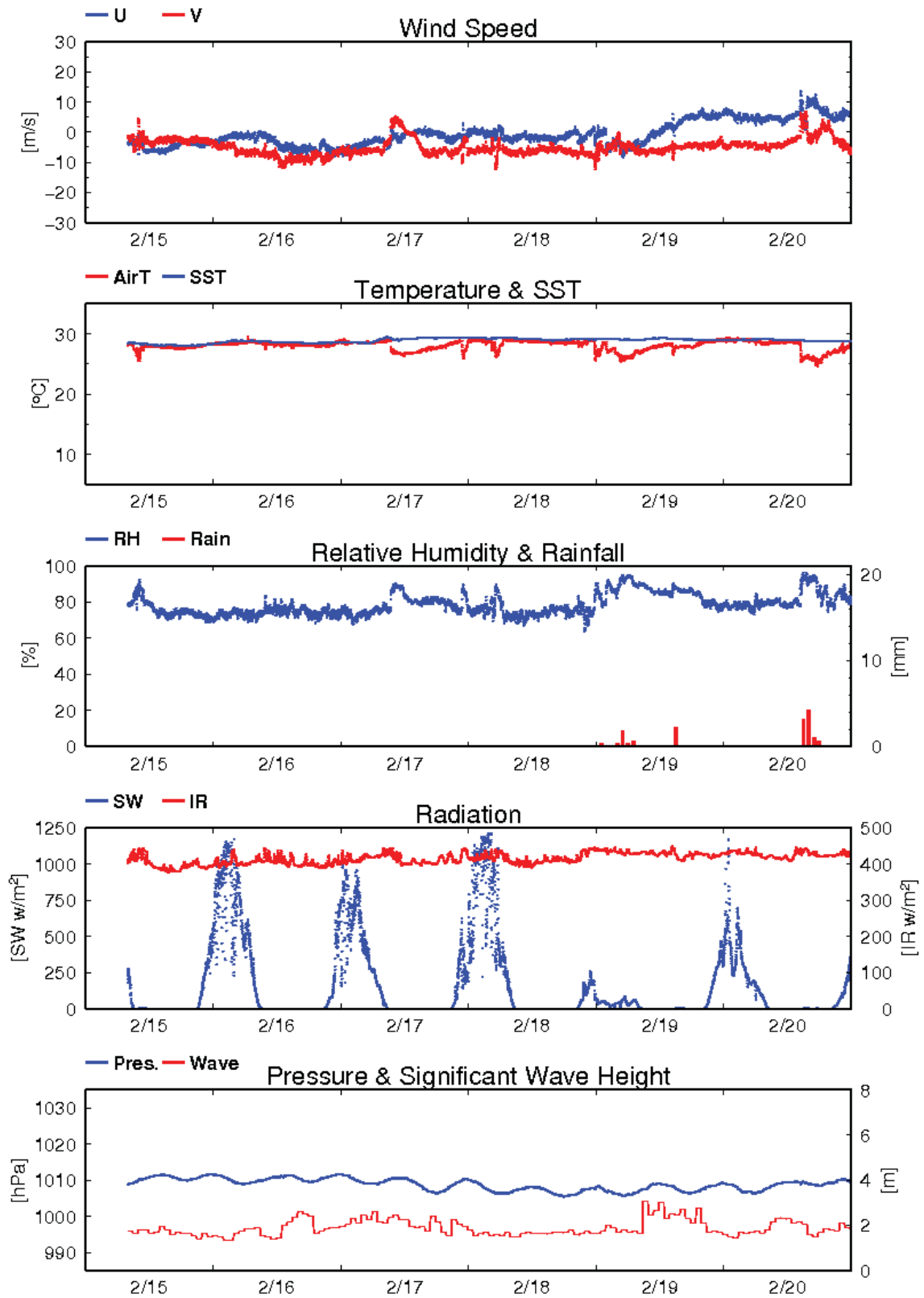
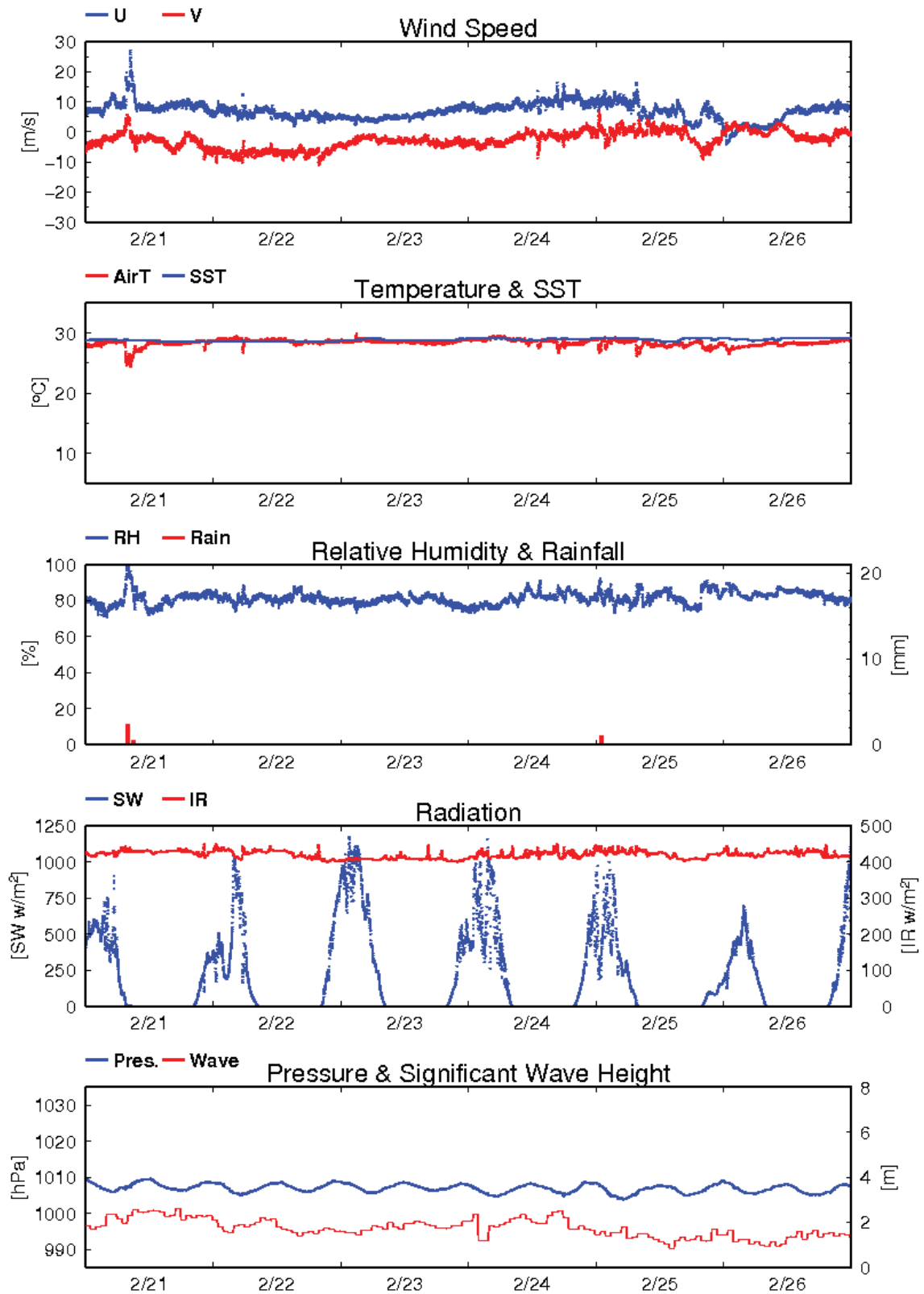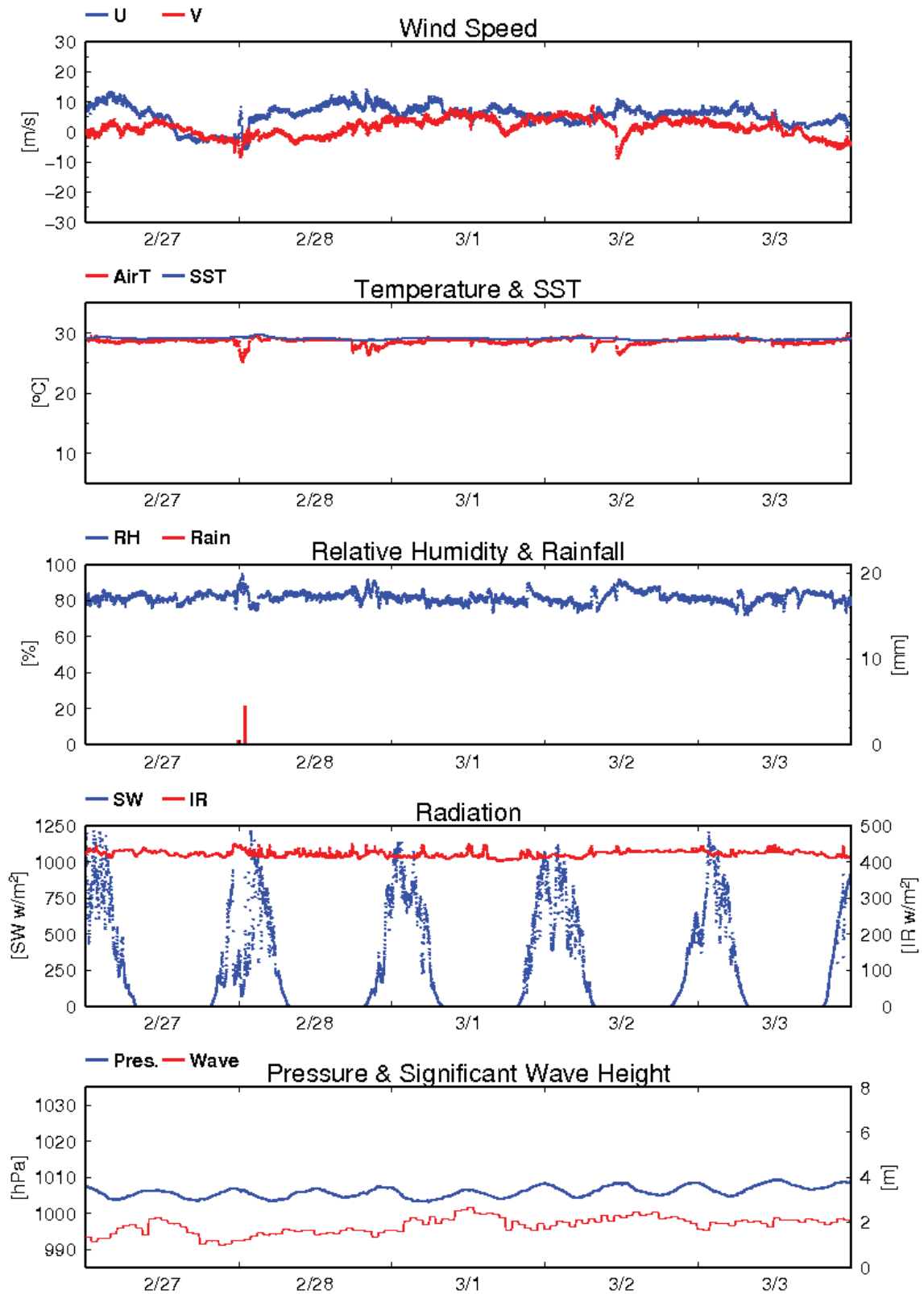Fig.6.1.1-1 Time series of surface meteorological parameters during the MR14-02

23

Fig.6.1.1-1 (Continued)

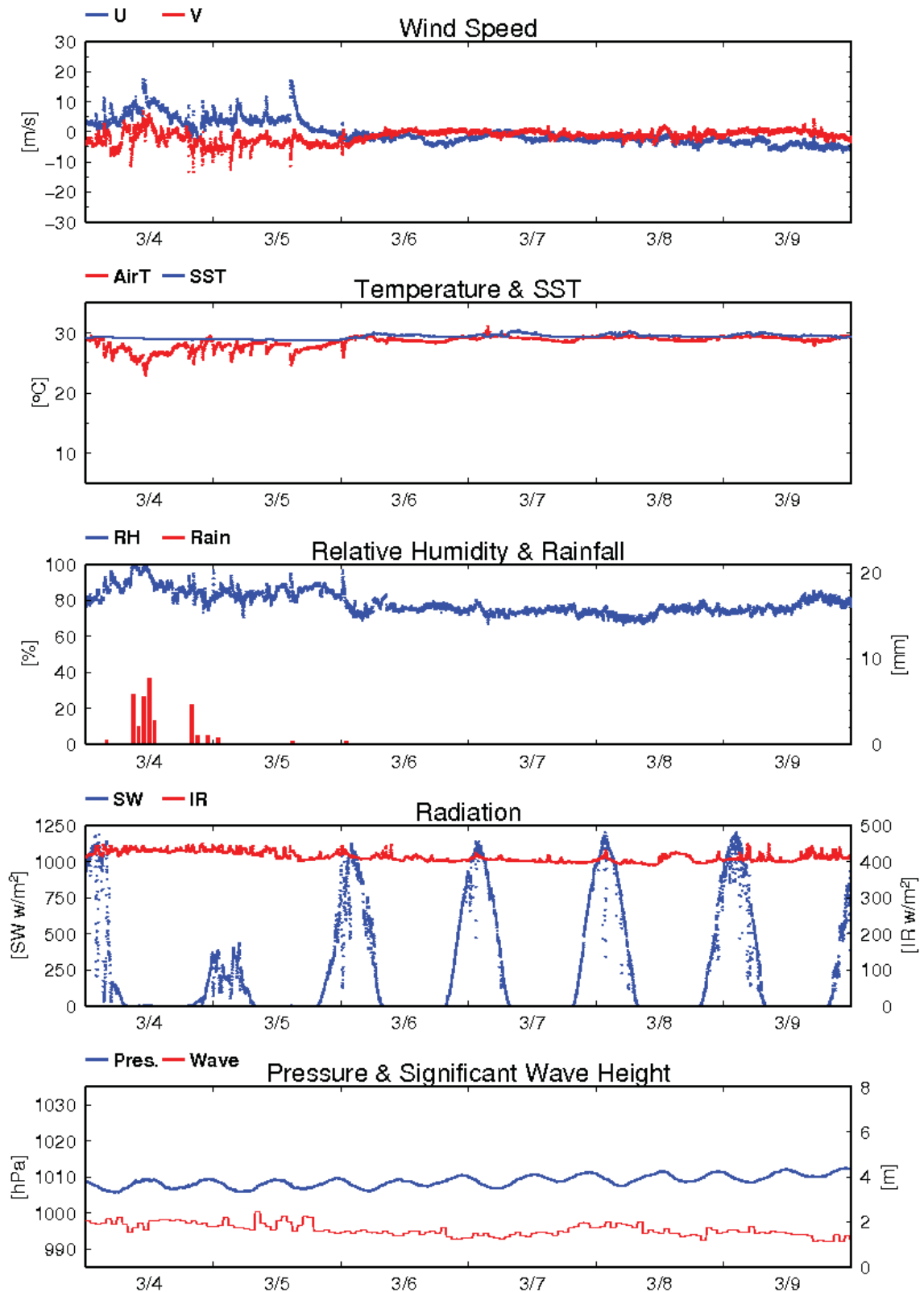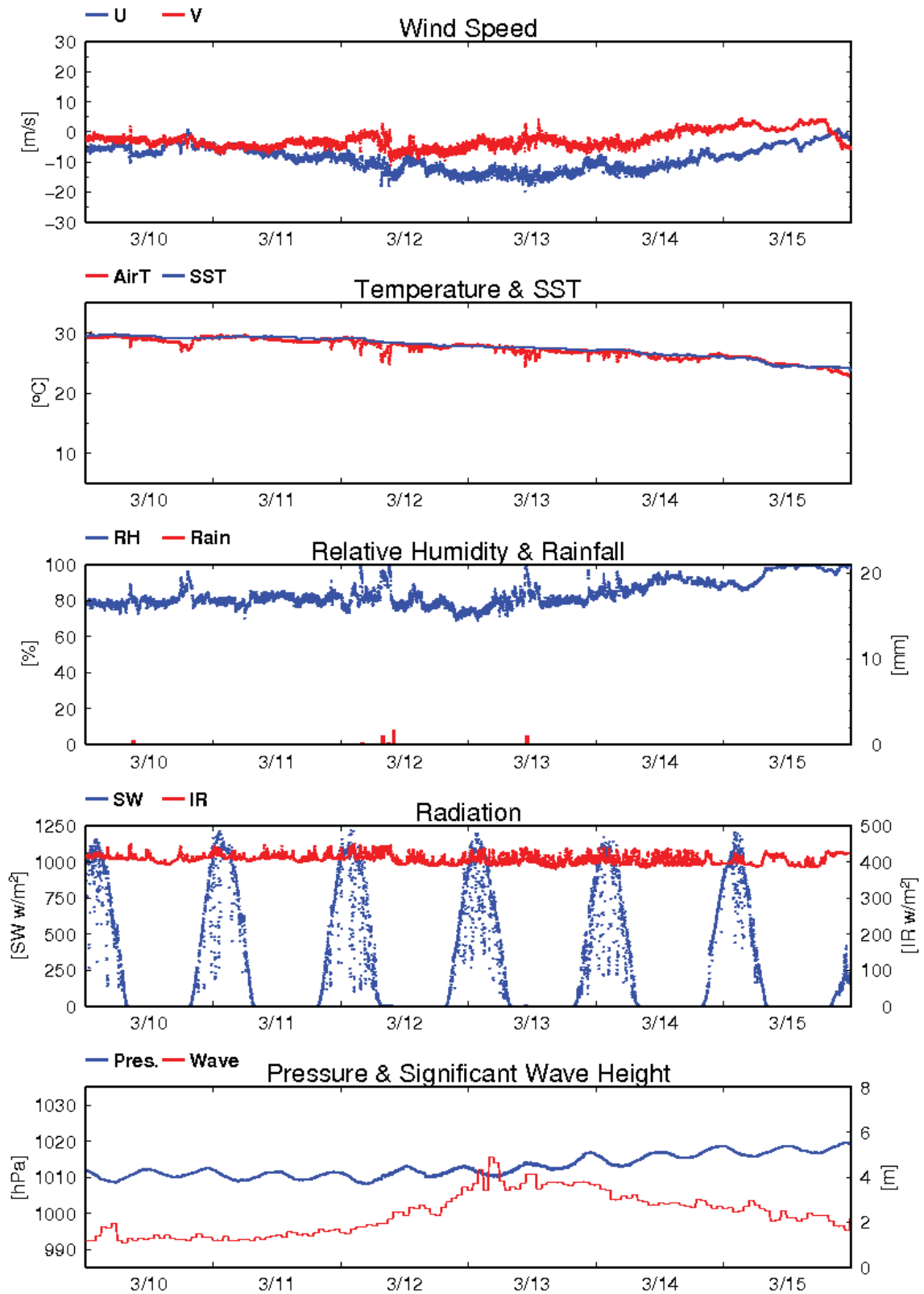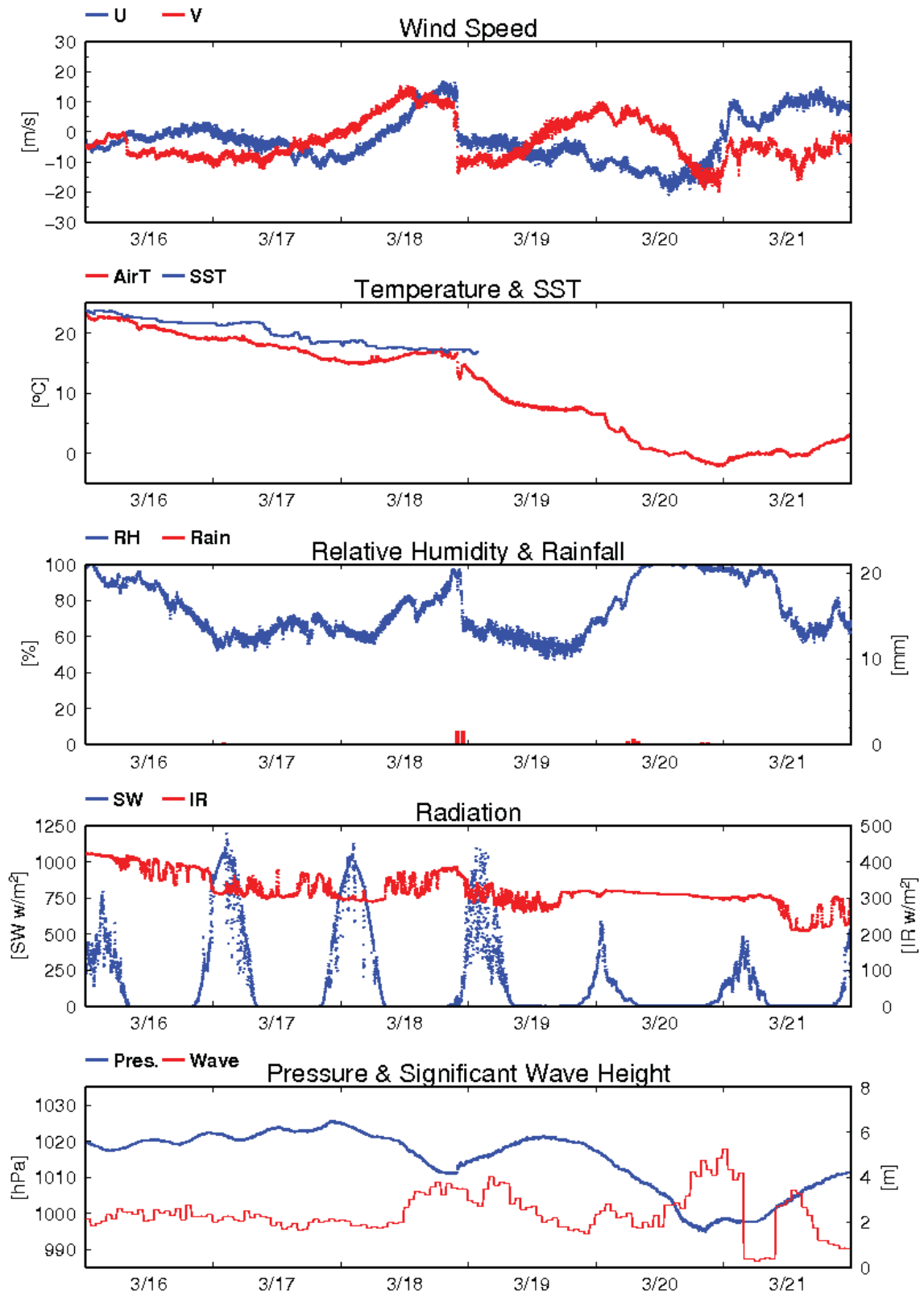Fig.6.1.1-1 (Continued)

Fig.6.1.1-1 (Continued)

Fig.6.1.1-1 (Continued)

Fig.6.1.1-1 (Continued)

6.1.2 Ceilometer

(1) Personnel
Takuya Hasegawa   (JAMSTEC) *Principal Investigator
Kazuho Yoshida   (Global Ocean Development Inc., GODI)
Masanori Murakami   (GODI)
Miki Morioka   (GODI)
Ryo Kimura   (Mirai Crew)

(2) Objectives
  The information of cloud base height and the liquid water amount around cloud base is important to understand the process on formation of the cloud. As one of the methods to measure them, the ceilometer observation was carried out.

(3) Paramters
  1. Cloud base height [m].
  2. Backscatter profile, sensitivity and range normalized at 10 m resolution.
  3. Estimated cloud amount [oktas] and height [m]; Sky Condition Algorithm.

(4) Methods
  We measured cloud base height and backscatter profile using ceilometer (CL51, VAISALA, Finland) throughout the MR14-02 cruise.

Major parameters for the measurement configuration are as follows;

Laser source:	Indium Gallium Arsenide (InGaAs) Diode Laser
Transmitting center wavelength:	910±10 nm at 25 degC
Transmitting average power:	19.5 mW
Repetition rate:	6.5 kHz
Detector:	Silicon avalanche photodiode (APD)
Cloud detection range:	0 ~ 13 km
Measurement range:	0 ~ 15 km
Resolution:	10 meter in full range
Sampling rate:	36 sec
Sky Condition:	Cloudiness in octas (0 ~ 9)
	(0: Sky Clear, 1:Few, 3:Scattered, 5-7: Broken,
	8: Overcast, 9: Vertical Visibility)

  On the archive dataset, cloud base height and backscatter profile are recorded with the resolution of 10 m (33 ft).

(5) Preliminary results
  Fig.6.1.2-1 shows the time series plot of the lowest, second and third cloud base height during the cruise.

(6) Data archives
  The raw data obtained during this cruise will be submitted to the Data Management Group (DMG) in JAMSTEC.

(7) Remarks
1. Data acquisition was suspended in the territorial waters of Palau.

2. Window Cleaning;
        22:58UTC 21 Feb. 2014

01:08UTC 27 Feb. 2014
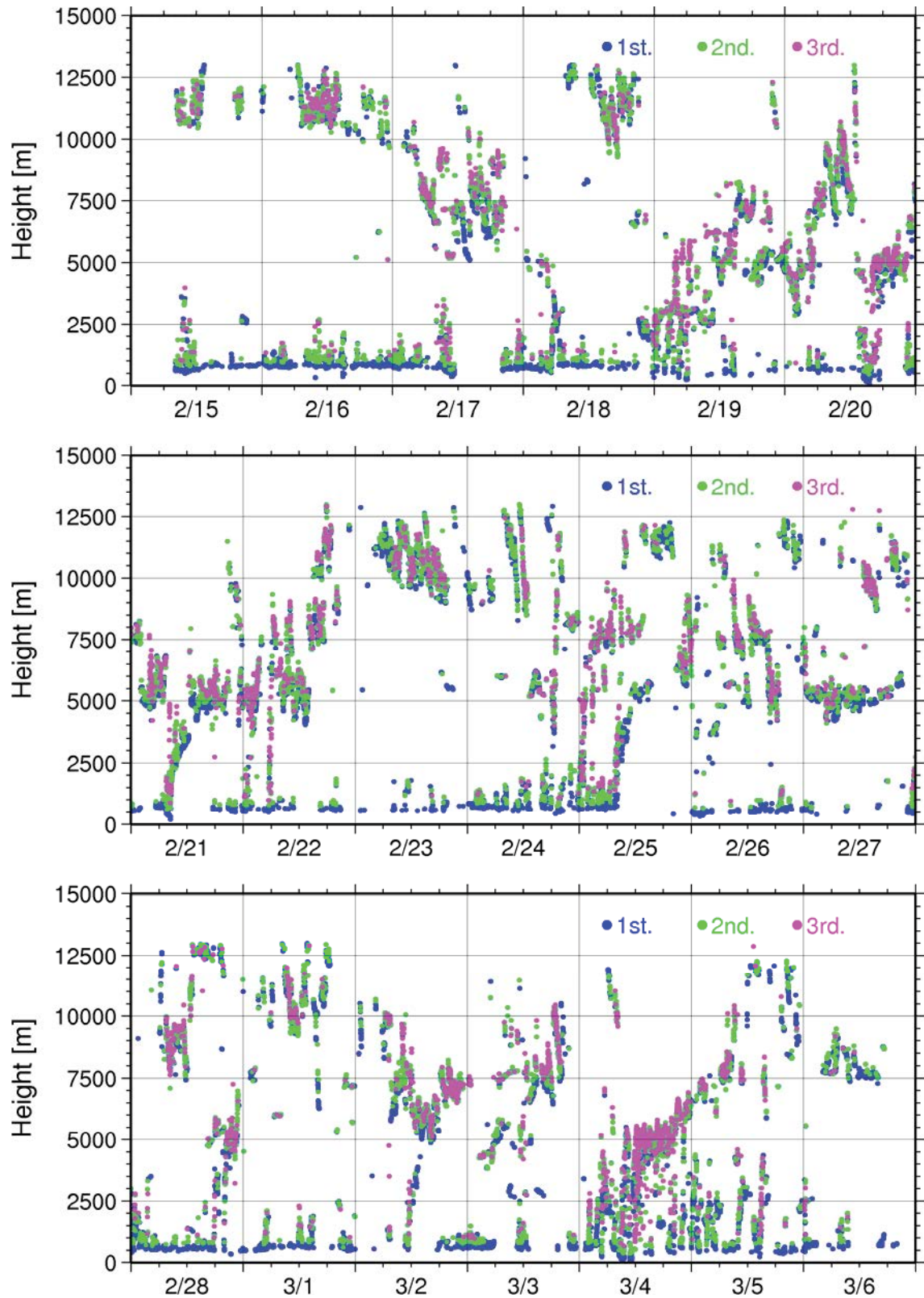23:16UTC 06 Mar. 2014
05:13UTC 14 Mar. 2014

Fig. 6.1.2-1 First (Blue), 2nd (Green) and 3rd (Red) lowest cloud base height during the cruise.
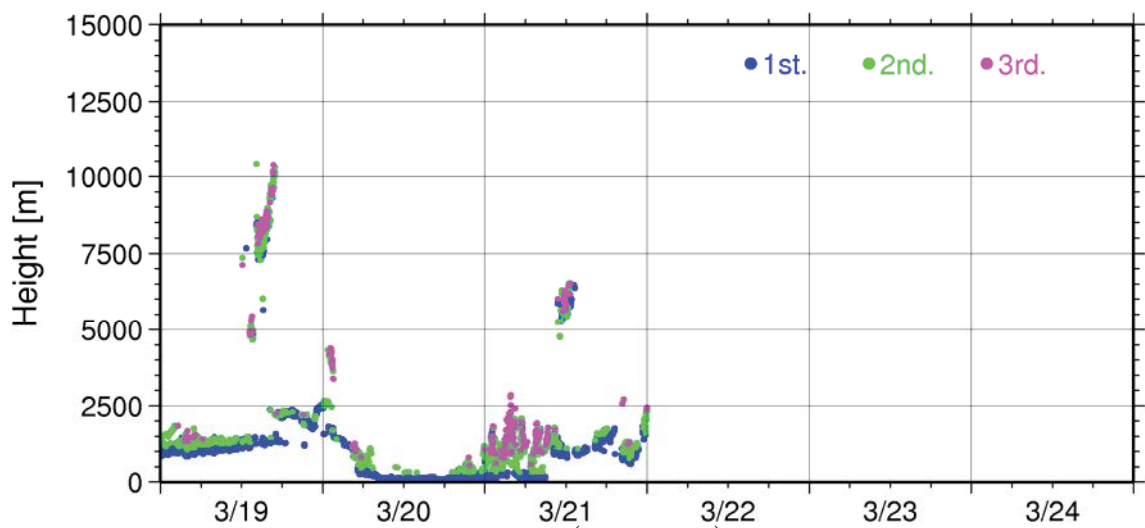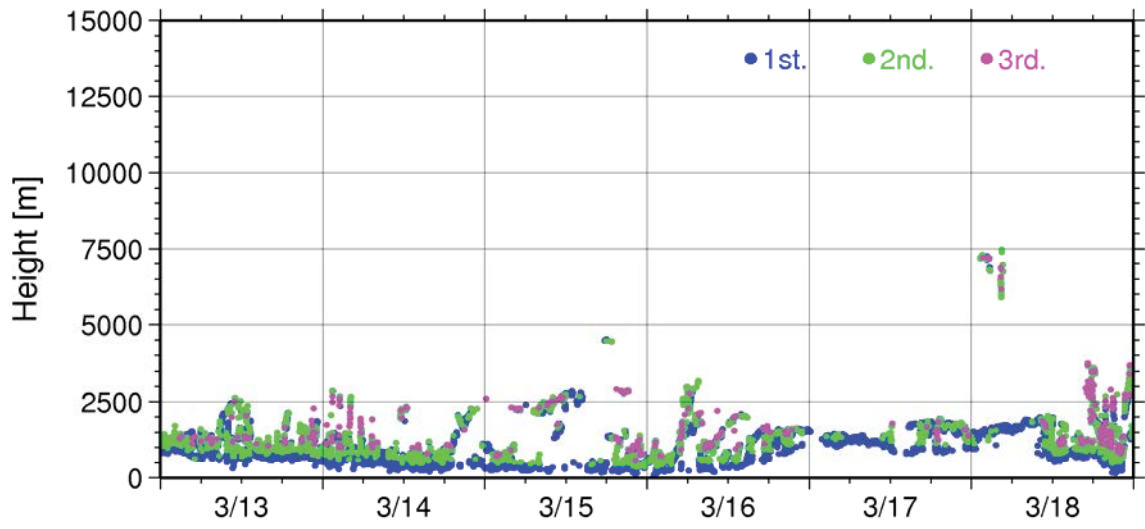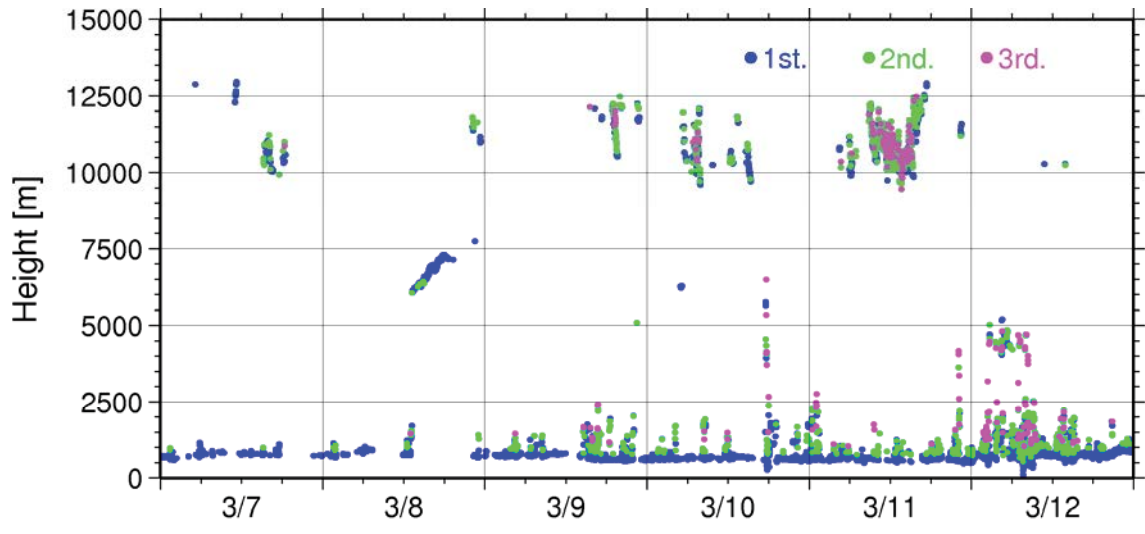
Fig. 6.1.2-1 (Continued)

6.1.3 Disdrometers

(1) Personnel
Masaki KATSUMATA　　　(JAMSTEC)　　　　　- Principal Investigator (not on board)

(2) Objectives
The disdrometer can continuously obtain size distribution of raindrops. The objective of this observation is (a) to reveal microphysical characteristics of the rainfall, depends on the type, temporal stage, etc. of the precipitating clouds, (b) to retrieve the coefficient to convert radar reflectivity to the rainfall amount, and (c) to validate the algorithms and the product of the satellite-borne precipitation radars; TRMM/PR and GPM/DPR.

(3) Methods
Four different types of disdrometers are utilized to obtain better reasonable and accurate value on the moving vessel. Three of the disdrometers and one optical rain gauge are installed in one place, the starboard side on the roof of the anti-rolling system of R/V Mirai, as in Fig. 6.1.3-1. One of the disdrometers named "micro rain radar" is installed at the starboard side of the anti-rolling systems (see Fig. 6.1.3-2).

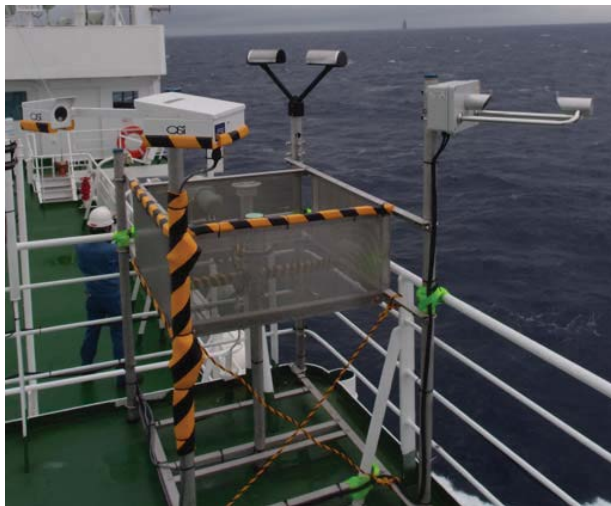The details of the sensors are described below. All the sensors archive data every one minute.

Fig. 6.1.3-1: The three disdrometers (Parsivel, LPM and Joss-Waldvogel disdrometer) and an optical rain gauge, installed on the roof of the anti-rolling tank.

Fig. 6.1.3-2: The micro rain radar, installed on the starboard side of the anti-rolling tank.

(3-1) Joss-Waldvogel type disdrometer

The "Joss-Waldvogel-type" disdrometer system (RD-80, Disdromet Inc.) (hereafter JW) equipped a microphone on the top of the sensor unit. When a raindrop hit the microphone, the magnitude of induced sound is converted to the size of raindrops. The logging program "DISDRODATA" determines the size as one of the 20 categories as in Table 6.1.3-1, and accumulates the number of raindrops at each category. The rainfall amount could be also retrieved from the obtained drop size distribution. The number of raindrops in each category, and converted rainfall amount, are recorded every one minute.

(3-2) Laser Precipitation Monitor (LPM) optical disdrometer

The "Laser Precipitation Monitor (LPM)" (Adolf Thies GmbH & Co) is an optical disdrometer. The instrument consists of the transmitter unit which emit the infrared laser, and the receiver unit which detects the intensity of the laser come thru the certain path length in the air. When a precipitating particle fall thru the laser, the received intensity of the laser is reduced. The receiver unit detect the magnitude and the duration of the reduction and then convert them onto particle size and fall speed. The sampling volume, i.e. the size of the laser beam "sheet", is 20 mm (W) x 228 mm (D) x 0.75 mm (H).

The number of particles are categorized by the detected size and fall speed and counted every minutes. The categories are shown in Table 6.1.3-2.

(3-3) "Parsivel" optical disdrometer

The "Parsivel" (Adolf Thies GmbH & Co) is another optical disdrometer. The principle is same as the LPM. The sampling volume, i.e. the size of the laser beam "sheet", is 30 mm (W) x 180 mm (D). The categories are shown in Table 6.1.3-3.

(3-4) Optical rain gauge

The optical rain gauge, which detect scintillation of the laser by falling raindrops, is installed beside the above three disdrometers to measure the exact rainfall. The ORG-815DR (Optical Scientific Inc.) is utilized with the controlling and recording software (manufactured by Sankosha Co.).

(3-5) Micro rain radar

The MRR-2 (METEK GmbH) was utilized. The specifications are in Table 6.1.3-4. The antenna unit was installed at the starboard side of the anti-rolling systems (see Fig. 6.1.3-2), and wired to the junction box and laptop PC inside the vessel.

The data was averaged and stored every one minute. The vertical profile of each parameter was obtained every 200 meters in range distance (i.e. height) up to 6200 meters, i.e. well beyond the melting layer. The drop size distribution is recorded, as well as radar reflectivity, path-integrated attenuation, rain rate, liquid water content and fall velocity.

(4) Preliminary Results

The data were obtained continuously thru the cruise except in the territorial water and in the EEZ without permissions. The further analyses will be done after the cruise.

(5) Data Archive

All data obtained during this cruise will be submitted to the JAMSTEC Data Integration and Analysis Group (DIAG).

(6) Acknowledgment

Table 6.1.3-1: Category number and corresponding size of the raindrop for JW disdrometer.

Category	Corresponding size range [mm]		
1	0.313	-	0.405
2	0.405	-	0.505
3	0.505	-	0.696
4	0.696	-	0.715
5	0.715	-	0.827
6	0.827	-	0.999
7	0.999	-	1.232
8	1.232	-	1.429
9	1.429	-	1.582
10	1.582	-	1.748
11	1.748	-	2.077
12	2.077	-	2.441
13	2.441	-	2.727
14	2.727	-	3.011
15	3.011	-	3.385
16	3.385	-	3.704
17	3.704	-	4.127
18	4.127	-	4.573
19	4.573	-	5.145
20	5.145	or larger	

Table 6.1.3-2: Categories of the size and the fall speed for LPM.

Particle Size				Fall Speed		
Class	Diameter [mm]	Class width [mm]		Class	Speed [m/s]	Class width [m/s]
1	≥ 0.125	0.125		1	≥ 0.000	0.200
2	≥ 0.250	0.125		2	≥ 0.200	0.200
3	≥ 0.375	0.125		3	≥ 0.400	0.200
4	≥ 0.500	0.250		4	≥ 0.600	0.200
5	≥ 0.750	0.250		5	≥ 0.800	0.200
6	≥ 1.000	0.250		6	≥ 1.000	0.400
7	≥ 1.250	0.250		7	≥ 1.400	0.400
8	≥ 1.500	0.250		8	≥ 1.800	0.400
9	≥ 1.750	0.250		9	≥ 2.200	0.400
10	≥ 2.000	0.500		10	≥ 2.600	0.400
11	≥ 2.500	0.500		11	≥ 3.000	0.800
12	≥ 3.000	0.500		12	≥ 3.400	0.800
13	≥ 3.500	0.500		13	≥ 4.200	0.800
14	≥ 4.000	0.500		14	≥ 5.000	0.800
15	≥ 4.500	0.500		15	≥ 5.800	0.800
16	≥ 5.000	0.500		16	≥ 6.600	0.800
17	≥ 5.500	0.500		17	≥ 7.400	0.800
18	≥ 6.000	0.500		18	≥ 8.200	0.800
19	≥ 6.500	0.500		19	≥ 9.000	1.000
20	≥ 7.000	0.500		20	≥ 10.000	10.000
21	≥ 7.500	0.500				
22	≥ 8.000	unlimited				

Table 6.1.3-3: Categories of the size and the fall speed for Parsivel.

Particle Size				Fall Speed		
Class	Average Diameter [mm]	Class spread [mm]		Class	Average Speed [m/s]	Class Spread [m/s]
1	0.062	0.125		1	0.050	0.100
2	0.187	0.125		2	0.150	0.100
3	0.312	0.125		3	0.250	0.100
4	0.437	0.125		4	0.350	0.100
5	0.562	0.125		5	0.450	0.100
6	0.687	0.125		6	0.550	0.100
7	0.812	0.125		7	0.650	0.100
8	0.937	0.125		8	0.750	0.100
9	1.062	0.125		9	0.850	0.100
10	1.187	0.125		10	0.950	0.100
11	1.375	0.250		11	1.100	0.200
12	1.625	0.250		12	1.300	0.200
13	1.875	0.250		13	1.500	0.200
14	2.125	0.250		14	1.700	0.200
15	2.375	0.250		15	1.900	0.200
16	2.750	0.500		16	2.200	0.400
17	3.250	0.500		17	2.600	0.400
18	3.750	0.500		18	3.000	0.400
19	4.250	0.500		19	3.400	0.400
20	4.750	0.500		20	3.800	0.400
21	5.500	1.000		21	4.400	0.800
22	6.500	1.000		22	5.200	0.800
23	7.500	1.000		23	6.000	0.800
24	8.500	1.000		24	6.800	0.800
25	9.500	1.000		25	7.600	0.800
26	11.000	2.000		26	8.800	1.600
27	13.000	2.000		27	10.400	1.600
28	15.000	2.000		28	12.000	1.600
29	17.000	2.000		29	13.600	1.600
30	19.000	2.000		30	15.200	1.600
31	21.500	3.000		31	17.600	3.200
32	24.500	3.000		32	20.800	3.200

Table 6.1.3-4: Specifications of the MRR-2.

Transmitter power	50 mW
Operating mode	FM-CW
Frequency	24.230 GHz (modulation 1.5 to 15 MHz)
3dB beam width	1.5 degrees
Spurious emission	< -80 dBm / MHz
Antenna Diameter	600 mm
Gain	40.1 dBi

6.2. CTD/UCTD/XCTD

6.2.1 CTD

(1) Personnel
Takuya Hasegawa   (JAMSTEC): Principal investigator
Shungo Oshitani   (MWJ): Operation leader
Tomohide Noguchi (MWJ)

(2) Objective
Investigation of oceanic structure and water sampling.

(3) Parameters
Temperature (Primary and Secondary)
Conductivity (Primary and Secondary)
Pressure
Dissolved Oxygen (Primary and Secondary)
Fluorescence
Altimeter

(4) Instruments and Methods
　CTD/Carousel Water Sampling System, which is a 36-position Carousel water sampler (CWS) with Sea-Bird Electronics, Inc. CTD (SBE9plus), was used during this cruise. 12-litter Niskin Bottles were used for sampling seawater. The sensors attached on the CTD were temperature (Primary and Secondary), conductivity (Primary and Secondary), pressure and dissolved oxygen （Primary and Secondary）. Salinity was calculated by measured values of pressure, conductivity and temperature. The CTD/CWS was deployed from starboard on working deck.
　The CTD raw data were acquired on real time using the Seasave-Win32 (ver.7.22.5) provided by Sea-Bird Electronics, Inc. and stored on the hard disk of the personal computer. Seawater was sampled during the up cast by sending fire commands from the personal computer. We stop at each layer for 1 minute or 30 seconds to stabilize then fire.
　38 casts of CTD measurements were conducted (Table 6.2.1-1).
　Data processing procedures and used utilities of SBE Data Processing-Win32 (ver.7.22.5a) and SEASOFT were as follows:

(The process in order)
　DATCNV: Convert the binary raw data to engineering unit data. DATCNV also extracts bottle
　　　　　　information where scans were marked with the bottle confirm bit during
　　　　　　acquisition. The duration was set to 3.0 seconds, and the offset was set to 0.0
　　　　　　seconds.

　BOTTLESUM: Create a summary of the bottle data. The data were averaged over 3.0 seconds.

　ALIGNCTD: Convert the time-sequence of sensor outputs into the pressure sequence to ensure
　　　　　　that all calculations were made using measurements from the same parcel of
　　　　　　water. Dissolved oxygen data are systematically delayed with respect to depth
　　　　　　mainly because of the long time constant of the dissolved oxygen sensor and of
　　　　　　an additional delay from the transit time of water in the pumped pluming line.
　　　　　　This delay was compensated by 5 seconds advancing dissolved oxygen sensor
　　　　　　output (dissolved oxygen voltage) relative to the temperature data.

　WILDEDIT: Mark extreme outliers in the data files. The first pass of WILDEDIT obtained an

accurate estimate of the true standard deviation of the data. The data were read in blocks of 1000 scans. Data greater than 10 standard deviations were flagged. The second pass computed a standard deviation over the same 1000 scans excluding the flagged values. Values greater than 20 standard deviations were marked bad. This process was applied to pressure, depth, temperature, conductivity and dissolved oxygen voltage.

CELLTM: Remove conductivity cell thermal mass effects from the measured conductivity. Typical values used were thermal anomaly amplitude alpha = 0.03 and the time constant 1/beta = 7.0.

FILTER: Perform a low pass filter on pressure with a time constant of 0.15 second. In order to produce zero phase lag (no time shift) the filter runs forward first then backward

SECTIONU (original module of SECTION): Select a time span of data based on scan number in order to reduce a file size. The minimum number was set to be the starting time when the CTD package was beneath the sea-surface after activation of the pump. The maximum number of was set to be the end time when the package came up from the surface.

LOOPEDIT: Mark scans where the CTD was moving less than the minimum velocity of 0.0 m/s (traveling   backwards due to ship roll).

DERIVE: Compute dissolved oxygen (SBE43).

BINAVG: Average the data into 1-dbar pressure bins.

BOTTOMCUT (original module): Bottom cut deletes discontinuous scan bottom data if it's created by BINAVG.

DERIVE: Compute salinity, potential temperature, and sigma-theta.

SPLIT: Separate the data from an input .cnv file into down cast and up cast files.

Configuration file
   MR1402A.xmlcon:

Specifications of the sensors are listed below.
      CTD: SBE911plus CTD system
      Under water unit:
            SBE9plus
            S/N 09P38273-0786 (Sea-Bird Electronics, Inc.)
                  Pressure sensor: Digiquartz pressure sensor (S/N 94766)
                        Calibrated Date: 03 Apr. 2013
            Temperature sensors:
                  Primary: SBE03 (S/N 031464, Sea-Bird Electronics, Inc.)
                        Calibrated Date: 04 Oct. 2013
                  Secondary: SBE03-04/F (S/N 031524, Sea-Bird Electronics, Inc.)
                        Calibrated Date: 12 Nov. 2013
            Conductivity sensors:
                  Primary: SBE04-04/0 (S/N 041203, Sea-Bird Electronics, Inc.)

Calibrated Date: 13 Nov. 2013
Secondary: SBE04-04/0 (S/N 041206, Sea-Bird Electronics, Inc.)
Calibrated Date: 13 Nov. 2013
Dissolved Oxygen sensors:
Primary: SBE43 (S/N 432036, Sea-Bird Electronics, Inc.)
Calibrated Date: 21 Aug. 2013
Secondary: SBE43 (S/N 430205, Sea-Bird Electronics, Inc.)
Calibrated Date: 08 Nov. 2013
Fluorescence:
Chlorophyll Fluorometer (S/N 3054, Seapoint Sensors, Inc.)

Altimeter
Benthos PSA-916T (S/N 1100, Teledyne Benthos, Inc.)

Carousel water sampler:
SBE32 (S/N 3227443-0391, Sea-Bird Electronics, Inc.)

Deck unit: SBE11plus (S/N 11P9833-0344, Sea-Bird Electronics, Inc.)

(5) Preliminary Results
During this cruise, 38 casts of CTD observation were carried out. Date, time and locations of the CTD casts are listed in Table 6.2.1.
Vertical profile (down cast) of primary temperature, salinity and dissolved oxygen with pressure are shown in Figure 6.2.1-1 - 6.2.1-10.

(6) Data archive
All raw and processed data files were copied onto HD provided by Data Management Office (DMO); JAMSTEC will be opened to public via **"Data Research for Whole Cruise Information in JAMSTEC"** in the JAMSTEC home page.

Table 6.2.1. MR14-02 CTD casttable

Stnnbr	Castno	Date(UTC) (mmddyy)	Time(UTC) Start	End	BottomPosition Latitude	Longitude	Depth	Wire Out	HT Above Bottom	Max Depth	Max Pressure	CTD Filename	Remark
C01	1	021914	00:15	00:46	04-56.54N	147-00.75E	4386.0	796.0	-	796.0	802.0	C01M01	Recovery point of T07
C02	1	021914	20:33	21:04	02-03.51N	146-58.87E	4488.0	796.0	-	797.0	803.0	C02M01	Recovery point of T08
C03	1	022014	04:45	05:08	02-29.99N	146-59.97E	4423.0	494.3	-	496.7	500.0	C03M01	
C04	1	022014	07:30	07:56	03-00.01N	147-00.06E	4428.0	496.3	-	498.6	502.0	C04M01	
C05	1	022114	05:54	06:17	01-29.92N	147-00.10E	4511.0	497.6	-	500.6	504.0	C05M01	Deployment point of T08
C06	1	022114	09:41	10:03	01-00.02N	147-00.24E	4523.0	495.0	-	498.6	502.0	C06M01	
C07	1	022114	20:36	21:08	00-03.94N	147-02.17E	4487.0	791.8	-	795.1	801.0	C07M01	Recovery point of T09
C07	2	022214	04:35	04:56	00-03.97N	147-02.17E	4490.0	498.3	-	500.6	504.0	C07M02	
C08	1	022214	07:07	07:29	00-30.01N	147-00.18E	4469.0	495.7	-	498.6	502.0	C08M01	
C09	1	022414	22:05	22:42	02-38.52S	153-22.54E	3259.0	996.1	-	996.1	1004.0	C09M01	Recovery point of ADCP
C10	1	022514	03:24	04:01	02-48.27S	153-14.29E	3475.0	996.3	-	995.1	1003.0	C10M01	Recovery point of ADCP
C11	1	022714	05:38	05:59	04-30.06S	155-59.79E	1721.0	495.2	-	498.6	502.0	C11M01	
C12	1	022714	08:20	08:43	03-59.99S	155-59.76E	1782.0	501.6	-	503.6	507.0	C12M01	
C13	1	022714	19:35	20:05	05-02.07S	155-59.86E	1544.0	792.9	-	797.0	803.0	C13M01	Recovery point of T06
C14	1	022814	08:20	08:42	03-29.96S	155-59.64E	1895.0	494.8	-	497.6	501.0	C14M01	
C15	1	030114	04:04	04:25	02-29.98S	156-00.19E	1740.0	495.4	-	498.6	502.0	C15M01	
C16	1	030114	08:06	08:28	02-59.82S	156-00.01E	1813.0	494.4	-	497.6	501.0	C16M01	
C17	1	030114	19:34	20:06	01-59.99S	155-58.14E	1746.0	792.1	-	795.1	801.0	C17M01	Recovery point of T05
C18	1	030214	03:21	03:44	01-30.02S	156-00.41E	1811.0	504.4	-	498.6	502.0	C18M01	

|													
C19	1	030214	06:54	07:14	00-59.98S	156-00.42E	2081.0	502.7	-	501.6	505.0	C19M01	
C20	1	030314	03:10	03:41	00-01.06S	156-00.71E	1948.0	806.1	-	799.0	805.0	C20M01	Recovery point of T04
C21	1	030314	07:25	07:47	00-29.91S	156-00.37E	1954.0	504.0	-	501.6	505.0	C21M01	
C22	1	030414	03:05	04:43	00-00.14S	156-01.57E	1957.0	1946.3	9.7	1946.1	1966.0	C22M01	Nagoya Univ
C23	1	030614	03:05	03:27	00-29.97N	156-00.51E	2142.0	507.9	-	503.6	507.0	C23M01	
C24	1	030714	03:40	04:01	01-29.82N	156-00.30E	2381.0	497.9	-	498.6	502.0	C24M01	
C25	1	030714	07:00	07:22	00-59.58N	156-00.66E	2244.0	500.5	-	500.6	504.0	C25M01	
C26	1	030814	04:00	04:32	02-03.12N	156-02.50E	2543.0	791.4	-	795.1	801.0	C26M01	Recovery point of T03
C27	1	030914	06:12	06:34	03-00.80N	156-00.21E	2886.0	501.6	-	500.6	504.0	C27M01	
C28	1	031014	06:25	06:46	04-00.45N	156-00.63E	3479.0	494.4	-	498.6	502.0	C28M01	
C29	1	031014	20:06	20:37	05-02.24N	155-57.33E	3600.0	794.5	-	796.0	802.0	C29M01	Recovery point of T02
C30	1	031114	03:09	05:52	05-00.34N	155-59.98E	3608.0	3599.6	9.9	3595.8	3647.0	C30M01	Nagoya Univ
C31	1	031114	20:04	20:41	07-57.66N	156-00.67E	4865.0	991.0	-	993.0	1001.0	C31M01	
C32	1	031214	12:05	15:48	10-00.44N	155-11.69E	5469.0	5476.6	9.6	5452.1	5554.0	C32M01	Nagoya Univ
C33	1	031314	22:00	02:00	15-00.76N	153-11.35E	5999.0	6061.5	9.0	5976.8	6097.0	C33M01	Nagoya Univ
C34	1	031414	20:01	21:05	18-18.26N	151-54.08E	5251.0	1982.1	-	1980.5	2002.0	C34M01	Argo
C35	1	031514	09:35	13:37	20-39.97N	150-56.96E	6042.0	6020.7	10.0	6024.3	6148.0	C35M01	Nagoya Univ, Argo
C36	1	031514	22:04	23:07	21-59.99N	150-23.87E	5689.0	1985.6	-	1981.0	2003.0	C36M01	Argo
C37	1	031614	20:03	23:54	24-59.90N	149-11.20E	5717.0	5758.7	9.8	5716.0	5831.0	C37M01	Nagoya Univ, Argo
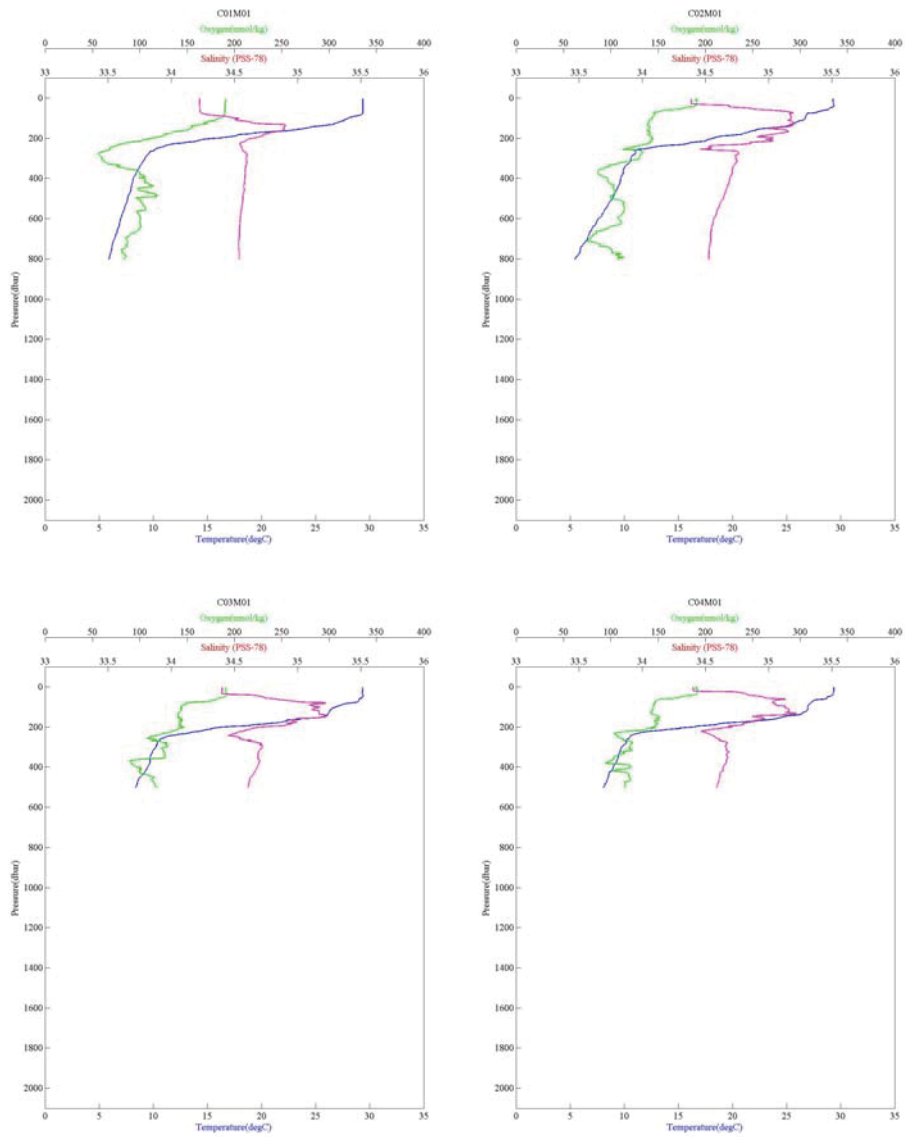
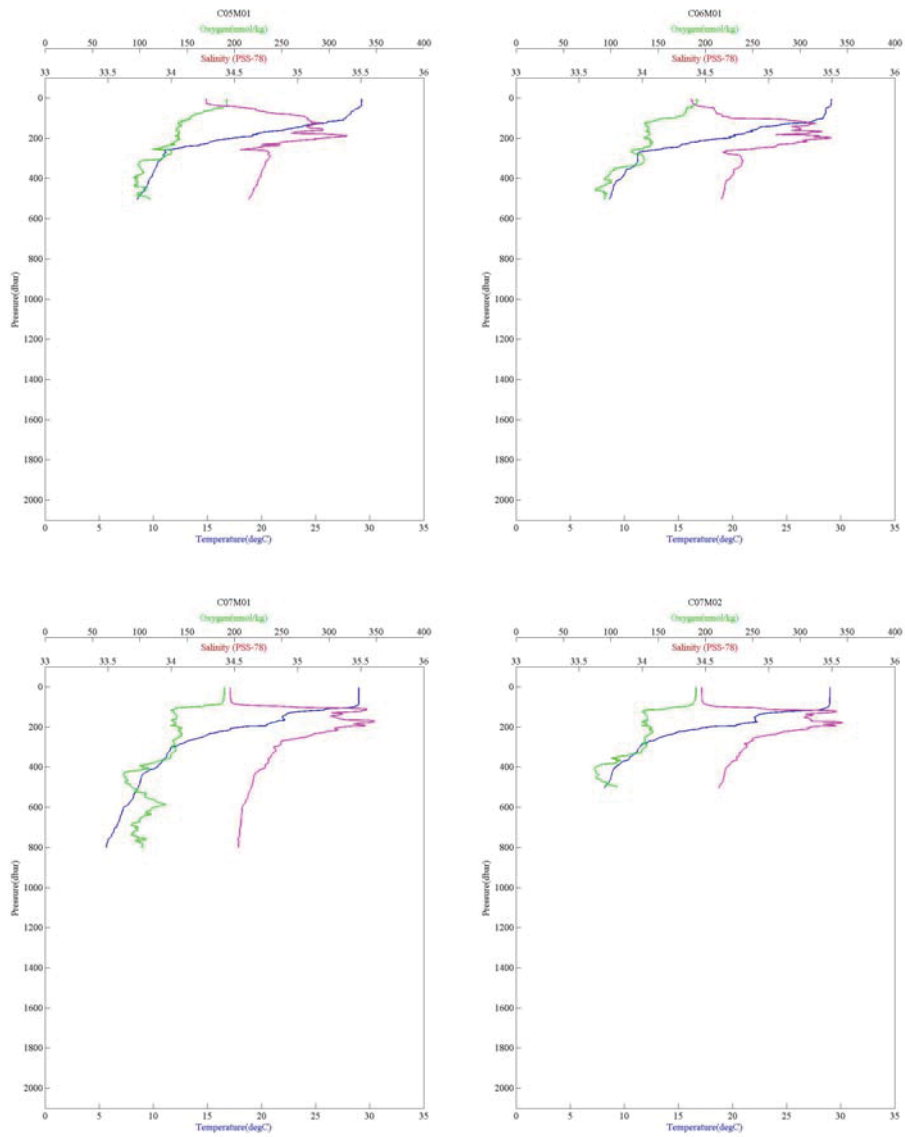Figure 6.2.1-1 CTD profile (C01M01, C02M01, C03M01 and C04M01)

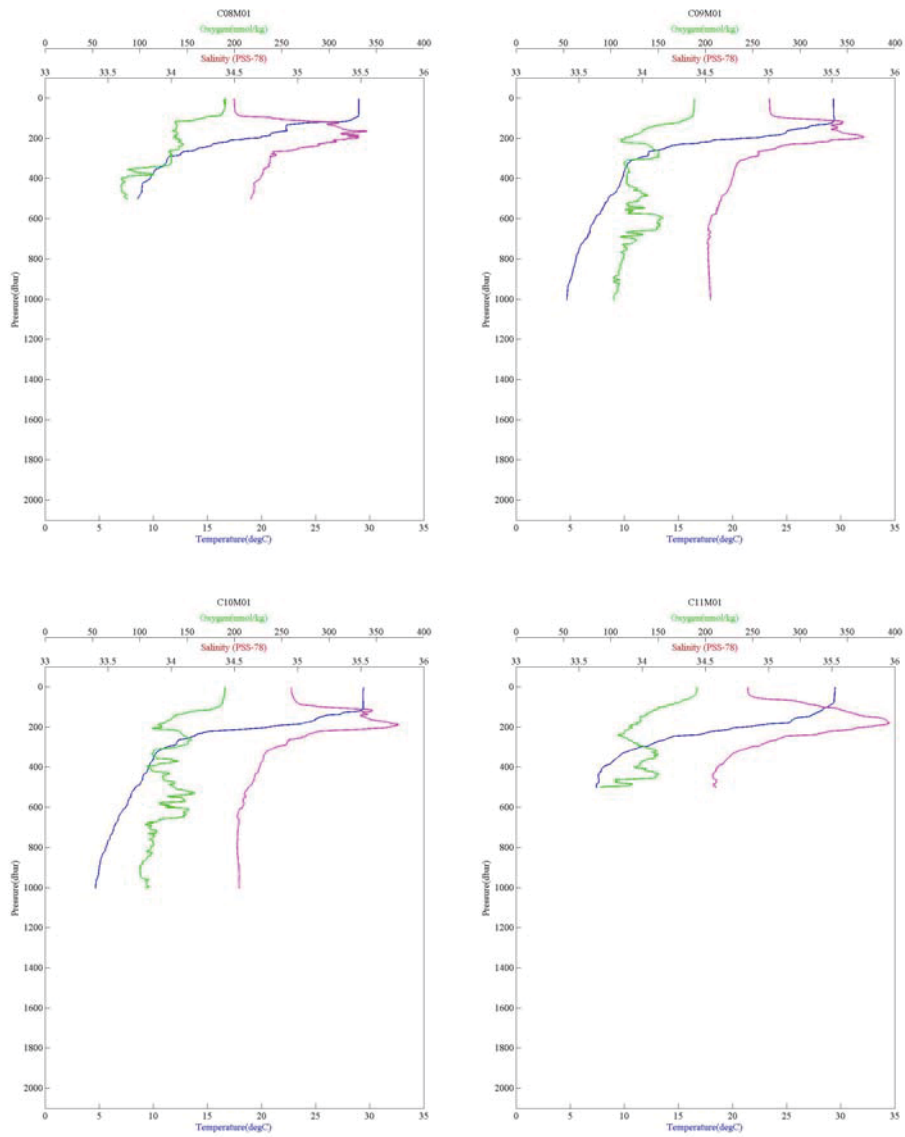Figure 6.2.1-2 CTD profile (C05M01, C06M01, C07M01 and C07M02)

Figure 6.2.1-3 CTD profile (C08M01, C09M01, C10M01 and C11M01)
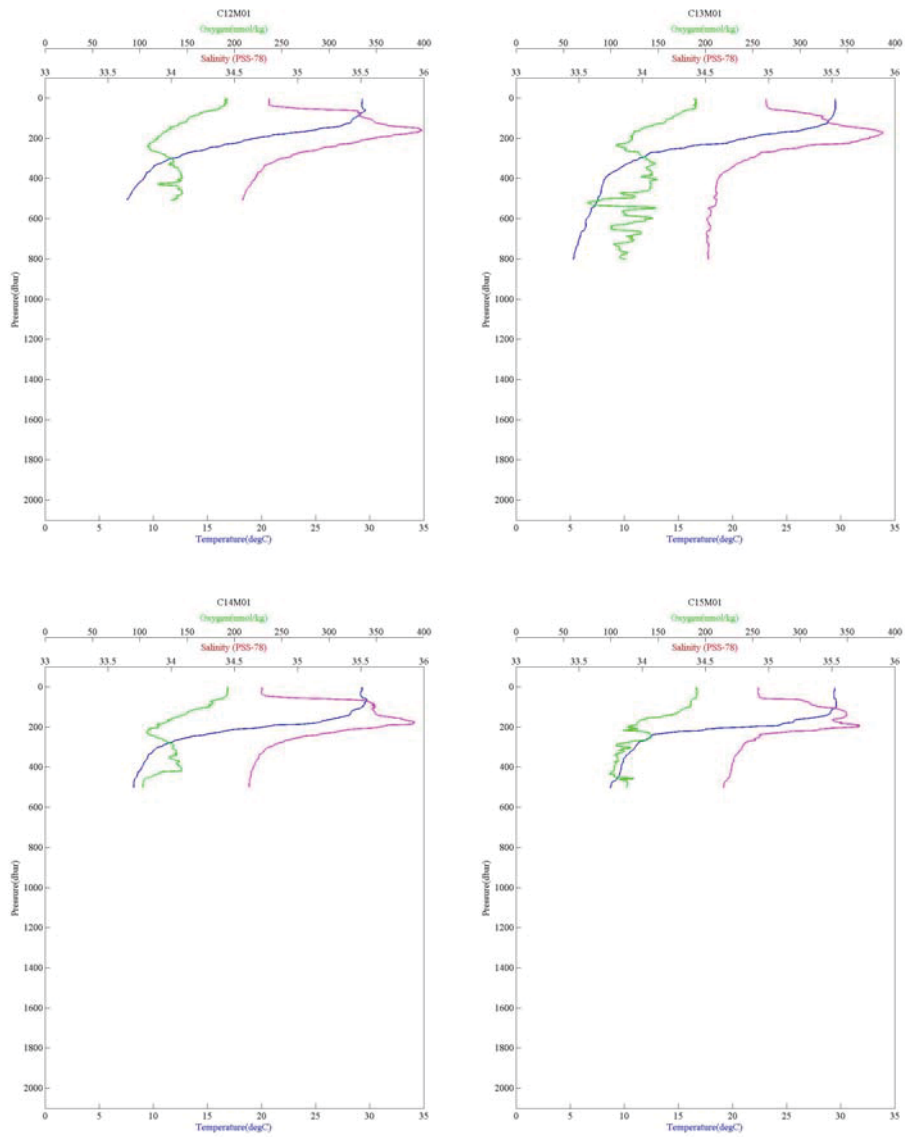
Figure 6.2.1-4 CTD profile (C12M01, C13M01, C14M01 and C15M01)
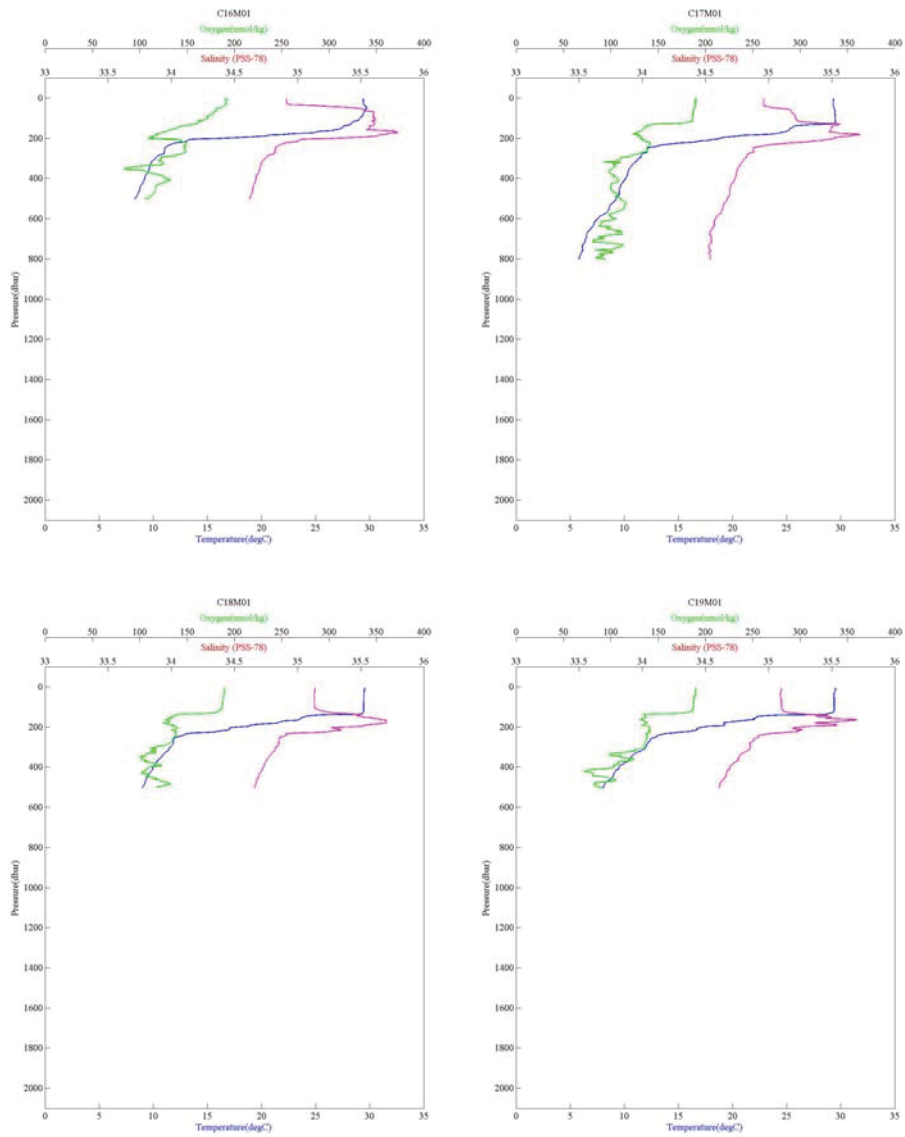
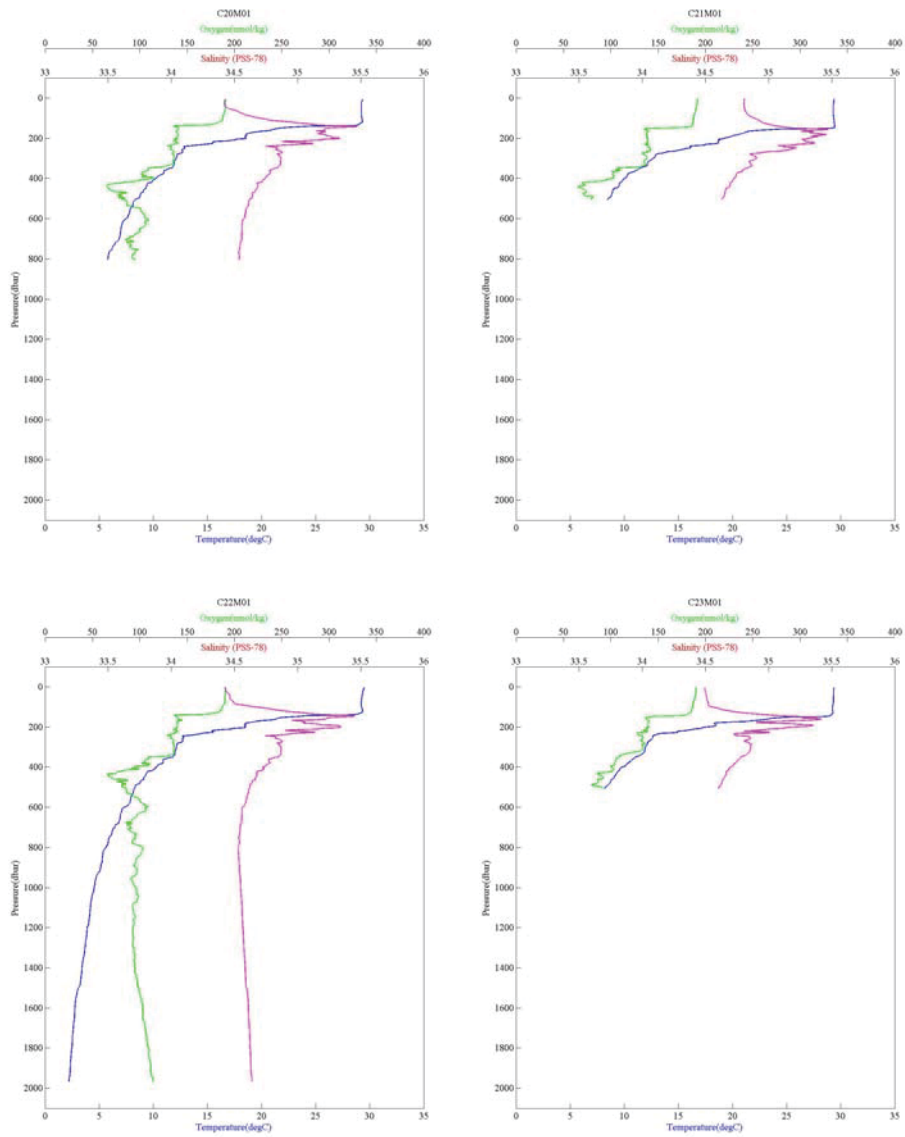Figure 6.2.1-5 CTD profile (C16M01, C17M01, C18M01 and C19M01)

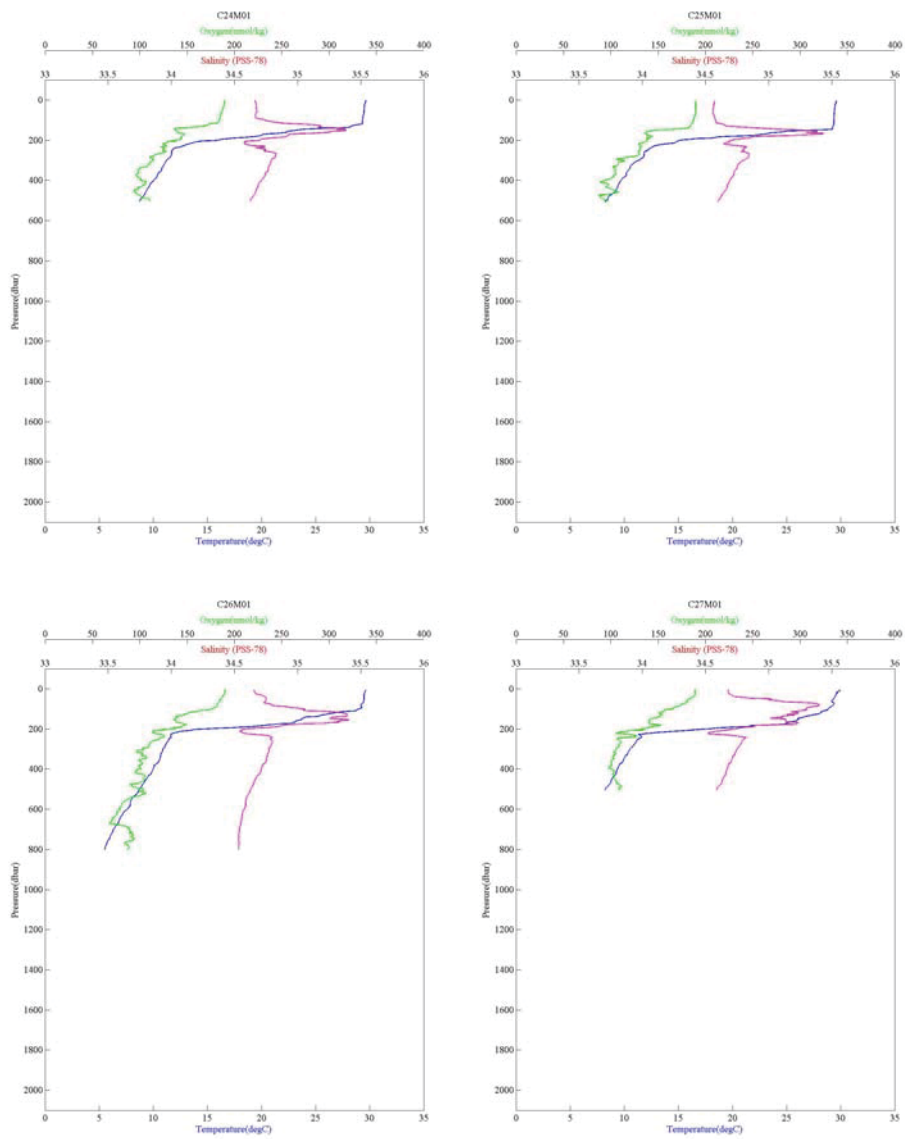Figure 6.2.1-6 CTD profile (C20M01, C21M01, C22M01 and C23M01)

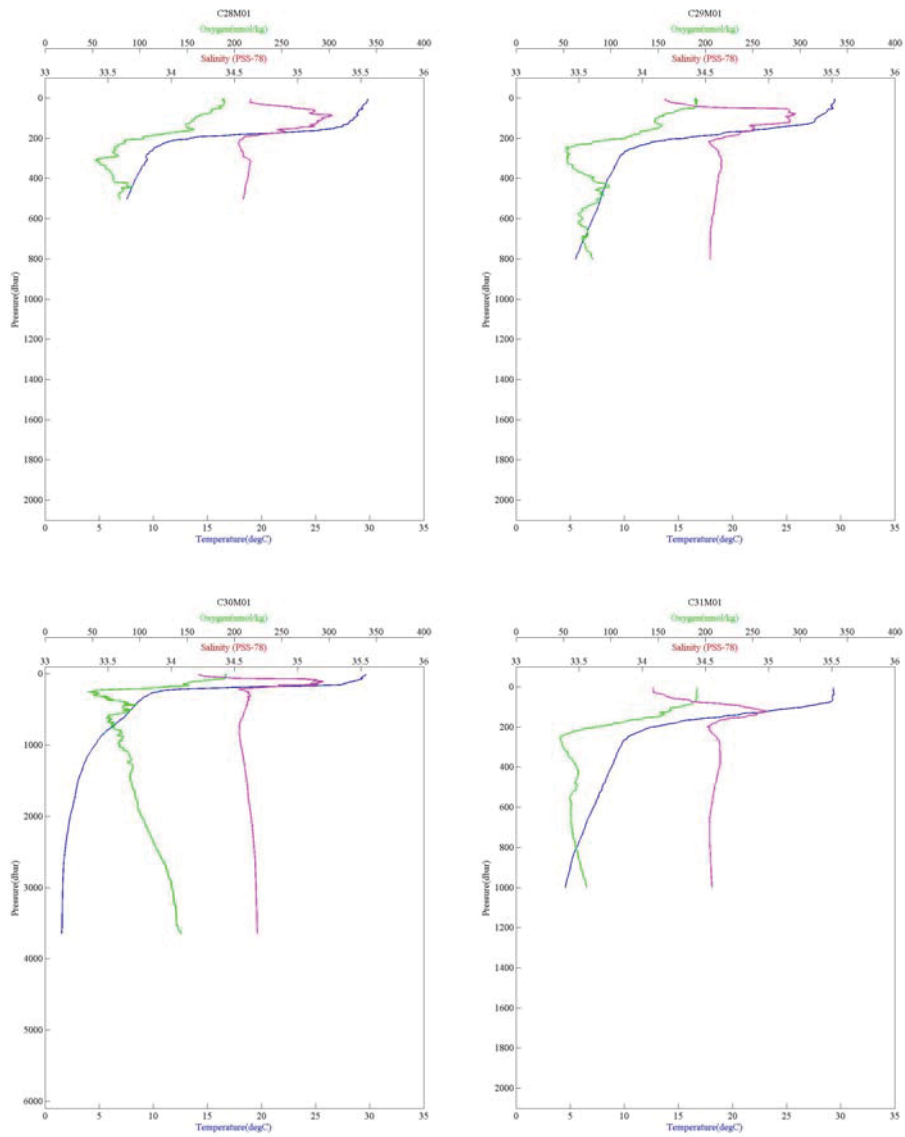Figure 6.2.1-7 CTD profile (C24M01, C25M01, C26M01 and C27M01)

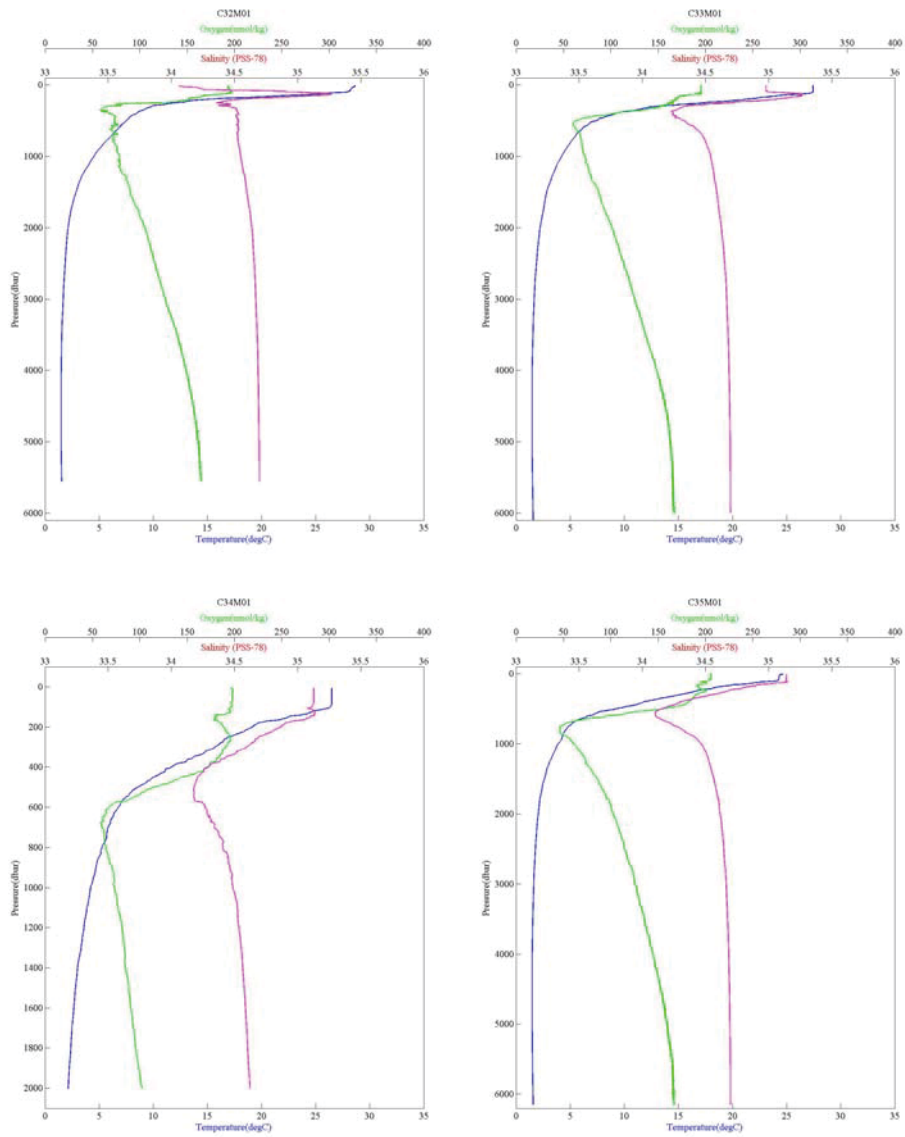Figure 6.2.1-8 CTD profile (C28M01, C29M01, C30M01 and C31M01)

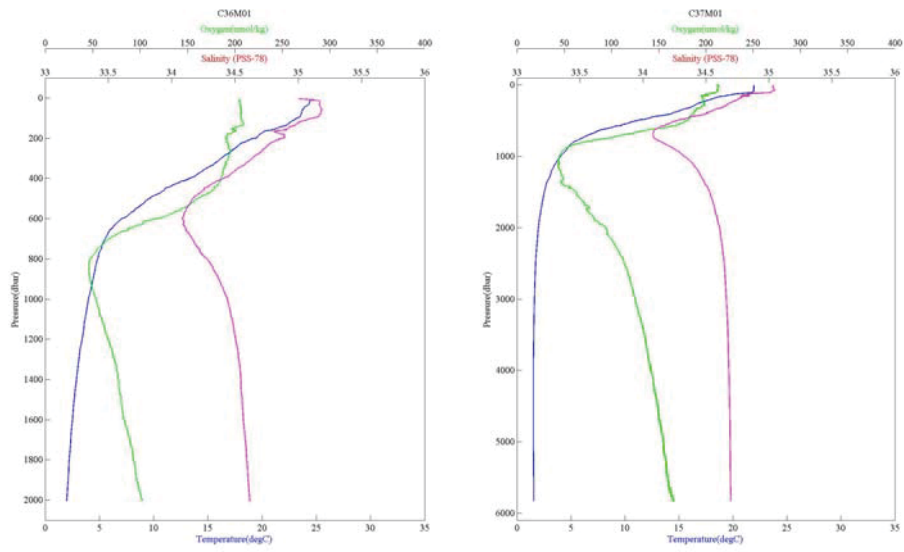Figure 6.2.1-9 CTD profile (C32M01, C33M01, C34M01 and C35M01)

Figure 6.2.1-10 CTD profile (C36M01 and C37M01)

6.2.2 Underway CTD

(1) Personal

Takuya HASEGAWA (JAMSTEC) - Principal Investigator
Kensuke Watari (JAMSTEC) – Monitoring of an ammeter of the winch
Hiroki Ushiromura (MWJ) - Operation Leader/Operator for test casts
Shungo Oshitani (MWJ) - Operator for observations across Solomon Strait
Tomohide Noguchi (MWJ) - Operator for CTD/UCTD comparison observation
Keisuke Matsumoto (MWJ) – Withdrawal of the UCTD items from the deck

(2) Objective

The "Underway CTD" (UCTD) system measures vertical profiles of temperature, conductivity and pressure like traditional CTD system. The strongest point of the UCTD system is to obtain good-quality CTD profiles from moving vessels with repeatable operation. In addition, the UCTD data are more accurate than those from XCTD because the sensor of the UCTD is basically same as that used in the traditional CTD system.

The purpose of UCTD observation in this cruise is to explore oceanic vertical structure of temperature and salinity across Solomon Strait as a part of SPICE. We also check the moving speed during the UCTD sensor recovery. Also we did UCTD and CTD comparison experiments south of EQ along 156E to check the performance of UCTD like MR13-03.

(3) Methods

The UCTD system, manufactured by Oceanscience Group, is utilized in this cruise.

The system consists of the probe unit and on-deck unit with the winch and the rewinder, as in Fig. 6.2.2-1. After spooling the line for certain length onto the probe unit (in "tail spool" part), the probe unit is released from the vessels into the ocean, and then measure temperature, conductivity and pressure during its free-fall with speed of roughly 4 m/s in the ocean. The probe unit is physically connected to the winch on the vessel by line. Releasing the line from the tail spool ensure the probe unit to be fall without physical forcing by the movement of the vessel. After the probe unit reaches the deepest layer for observation, it is recovered by using the winch on the vessel. The observed data are stored in the memory within the probe unit. The dataset can be downloaded into PCs via Bluetooth communication on the deck.

The specifications of the sensors are in Table 6.2.2-1. The UCTD system used in this cruise can observe temperature, conductivity and pressure from surface to 1000 m depth with 16 Hz sampling rate.

During the profiling, the vessel can be cruised (straight line recommended). The manufacturer recommends the maximum speed of the vessel during the profiling as in Table 6.2.2-2. In this cruise, we examine various cruising speed up to 12 knot and confirm there are no apparent problem for the examined speeds.

Table 6.2.2-1: Specification of the sensors of the UCTD system in this cruise.

Parameter	Accuracy	Resolution	Range
Temperature (deg.C)	0.004	0.002	-5 to 43
Conductivity (S/m)	0.0003	0.0005	0 to 9
Pressure (dbar)	1.0	0.5	0 to 2000

Table 6.2.2-2: Maximum depth and speed of the vessel during profile

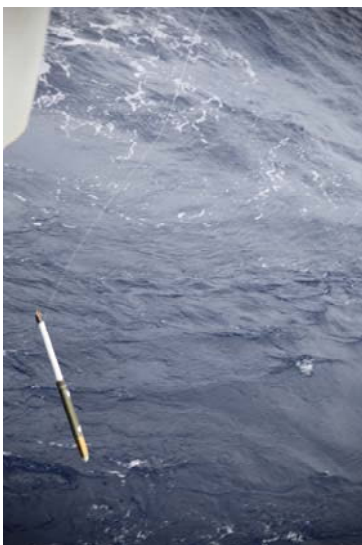| Maximum depth to profile	Maximum ship speed (knot)
0 to 350 m	13
350 m to 400 m	12
400 to 450 m	11
450 to 500 m	10
500 to 550 m	8
550 to 600 m	6
600 to 650 m	4
650 to 1000 m	2

Fig. 6.2.2-1: UCTD system installed and operated on R/V Mirai. (Top) On-deck unit, consists of the winch and the rewinder. (Middle) Probe unit, consists of sensor probe (bottom half) and tail spool (top half): it is just before towing from the deck. (bottom): Probe unit towing from the deck; just above the sea surface.

(4) Preliminary Results

(a) Test casts

Before the observation around New Ireland Island, we conducted two test casts of UCTD along 147E line. For example, we show profiles of temperature, conductivity, salinity and decent rate at test002C01 (Fig. 6.2.2-2). It shown that the descent rates range from 3.5 to 4.5 m/s above 650m depth, implying free fall in upper ocean above 650 m depth. Below 650 m depth, the descent rate reduces, but there are no large noises in salinity profile in all depths. Based on this result, it is confirmed that the UCTD system works well. The all stations of UCTD conducted in this cruise are listed in Table 6.2.2-3.
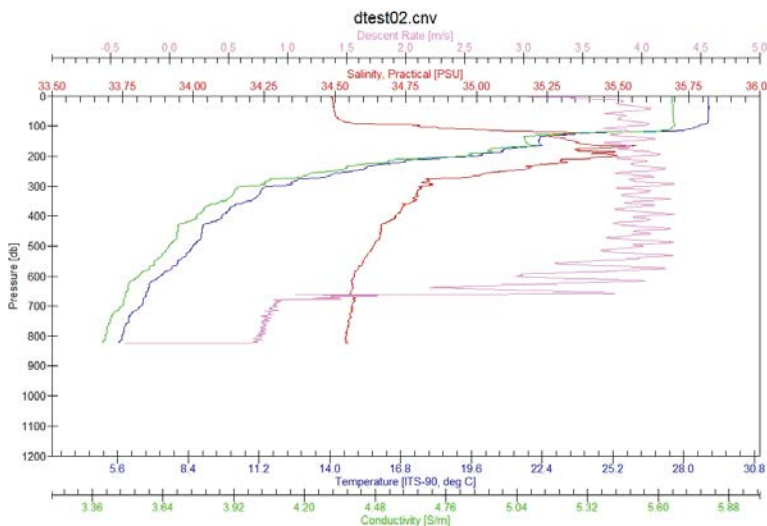

Figure 6.2.2-2: Profiles of temperature (blue line), salinity (red line), density (green line), and descent rate (purple line) at test001C01. All of variables are 1-db vertical averaged.

(b) Result of Solomon Strait observations

As a mission related to CLIVAR-SPICE international project, we conducted UCTD observation across Solomon Strait together with XCTD observations. The purpose is to explore sea water characteristics along the Solomon Strait, because the water in this region can be transported to NICU area, especially western side of the Solomon Strait.

In Fig. 6.2.2-3, we show the profile at u001C01 station (western part of the Solomon Strait) and at u008C01 station (eastern part of the Solomon Strait). Large differences between the western and eastern sides appear in the salinity profile. That is, both sites show salinity maxima around at 200 m depth, but the values of salinity in the eastern side (roughly 35.6) is less than

that of western side (roughly 35.9). It may be due to the effect of local rainfall, oceanic advection, and river input.
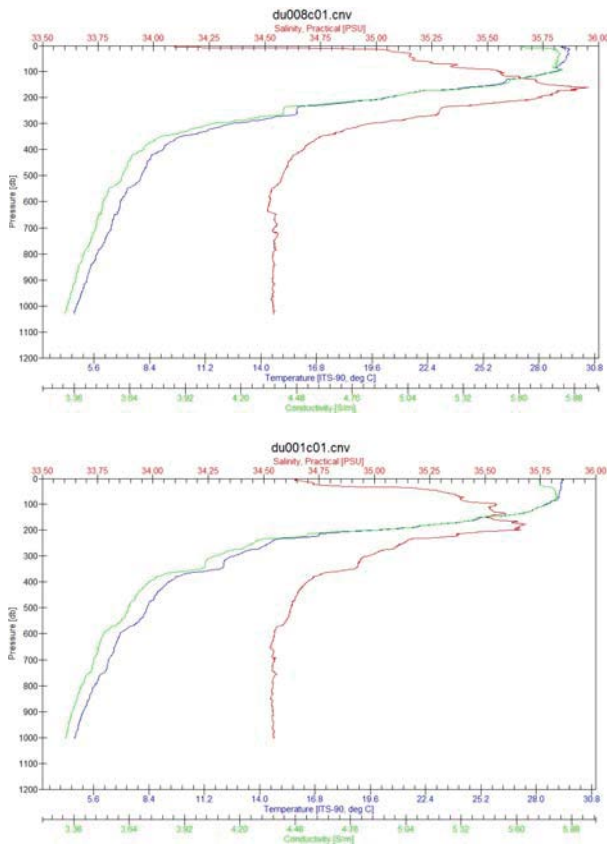
Fig. 6.2.2-3: Profiles of temperature (blue line), salinity (red line), and density (green line) at u001C01 (top) and u008C01 (bottom) stations. All of variables are 1-db vertical averaged.

(C) Comparison between UCTD and CTD

The accuracy of UCTD-derived parameters is ensured by comparing the results to these from CTD measurements at CTD stations from C11 to C21, like MR13-03 cruise. First, the two UCTD probes (S/N of sensor probe: 145 and 146) were attached to the metal frame for CTD system when CTD was deployed onto the sea. For example, the result at station C11 is shown in Fig. 6.2.2-4. Figure 6.2.2-4 indicates the values from two systems match excellently (lines of UCTD and CTD for temperature and conductivity are almost identical and hard to distinguish). Difference between two UCTD sensor probes is also very small (not shown here).

Fig. 6.2.2-4: Vertical profiles of temperature and conductivity from UCTD (S/N of sensor probe is 145; temperature is shown by black line; conductivity is shown by light blue line) and CTD (CTD profile is shown by gray line for temperature and conductivity) at C21 CTD station (station/cast number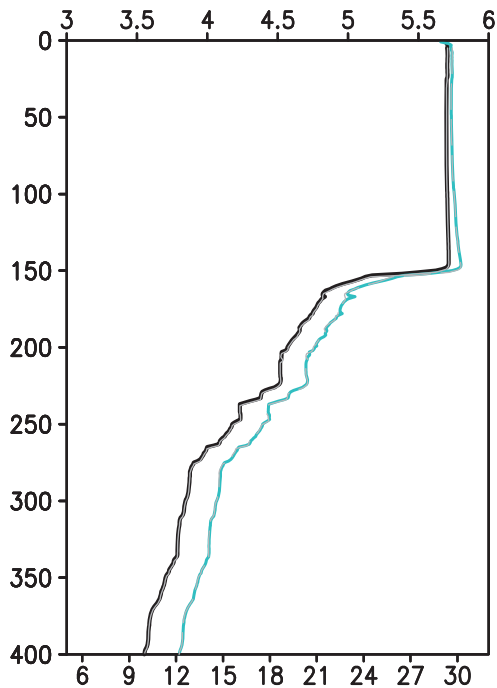 is C21M01). The x-axis in the bottom is for temperature (deg_C), and one in the top is for conductivity (S/m). The CTD system was deployed with UCTD probe attached at the frame of CTD system.

(d) Ship speeds during sensor probe recovery

As mentioned above, UCTD observation can be conducted without stopping the vessel. In future observation, spatially high-resolution UCTD observation for wide area can be done during a short period as compared to CTD observation, which can explore detailed spatial and/or temporal change of upper ocean structure related to barrier layer and other oceanic and atmospheric phenomena.

During the present cruise, we did recovery of the sensor probe with higher speeds shown in the official manual in order to obtain information for saving ship time in future cruises.

Such operation could be done since we newly attached an ammeter that measures a power current of the winch. If the power current reaches the maximum values that warrant safety use of the winch (i.e., 35 A), we stop the increase in the ship speed. We conducted the 1000 m depth casts with various ship speed from 2 knot to seven knots. Two knots of the ship speed is the recommended ship speed at the 1000 m depth cast by the official manual.

We confirmed that the power current is less than 20 A at the two knot of the ship speed at the first cast. The values of power current is much less than the maximum value of 35 A. Finally it was confirmed that the power current is around 25 A at the ship speed of seven knots. Because of limitation of the ship time, we could not test higher ship speed than seven knot during this cruise. However, the present result can contribute to saving the ship time by moving

of the ship at higher speed than that shown in the official manual during the recovery of UCTD sensor probe.

(5) Data Archive

All data obtained during this cruise will be submitted to the JAMSTEC Data Management Group (DMG).

Table 6.2.2-3: List of UCTD stations during MR14-02 cruise

Station Number	Cast Number	Time Towed (UTC)	Position Towed Lat. (deg–min)	Position Towed Lon. (deg–min)	Depth to go (m)	Ship speed (knot) Tow	Ship speed (knot) Recovery	S/N of sensor	Notes
test001	c01	Feb. 21 07:03	01–29.61N	147–00.50E	250	2.0	10.3	145	Test cast
test002	c01	Feb. 22 07:32	00–29.99N	147–00.20E	1000	2.0	2.1	145	Test cast
u001	c01	Feb. 25 21:04	04–05.29S	153–15.11E	1000	2.0	2.1 – 3.0	145	
u002	c01	Feb. 25 22:37	04–12.50S	153–24.30E	1000	2.0	2.2	145	
u003	c01	Feb. 26 00:14	04–20.04S	153–34.05E	1000	2.0	3.0	145	
u004	c01	Feb. 26 01:41	04–26.86S	153–43.19E	1000	2.0	4.0	145	
u005	c01	Feb. 26 03:22	04–34.31S	153–53.01E	1000	2.0	5.0	146	
u006	c01	Feb. 26 04:42	04–40.73S	154–00.92E	1000	2.0	6.0	146	
u007	c01	Feb. 26 06:11	04–47.32S	154–08.89E	1000	2.0	4.0	146	
u008	c01	Feb. 26 07:39	04–53.56S	154–16.92E	1000	2.0	7.0	146	
u011	c01	Feb. 27 05:30	04–30.00S	156–00.04E	500	–	–	145/146	Attached on CTD frame at CTD C11M01
u012	c01	Feb. 27 08:14	04–00.25S	156–00.00E	500	–	–	145/146	Attached on CTD frame at CTD C12M01
u013	c01	Feb. 27 19:29	05–02.20S	155–59.97E	800	–	–	145/146	Attached on CTD frame at CTD C13M01
u014	c01	Feb. 28 18:15	03–29.94S	155–59.88E	500	–	–	145/146	Attached on CTD frame at CTD C14M01
u015	c01	Mar. 01 03:59	02–29.91S	156–00.19E	500	–	–	145/146	Attached on CTD frame at CTD C15M01
u016	c01	Mar. 01 08:00	02–59.64S	156–00.16E	500	–	–	145/146	Attached on CTD frame at CTD C16M01
u017	c01	Mar. 01 19:28	01–59.99S	155–58.17E	800	–	–	145/146	Attached on CTD frame at CTD C17M01
u018	c01	Mar. 02 03:13	01–30.17S	156–00.17E	500	–	–	145/146	Attached on CTD frame at CTD C18M01
u019	c01	Mar. 02 06:48	01–00.09S	156–00.19E	500	–	–	145/146	Attached on CTD frame at CTD C19M01
u020	c01	Mar. 03 03:20	00–00.78S	155–59.68E	800	–	–	145/146	Attached on CTD frame at CTD C20M01
u021	c01	Mar. 03 07:18	00–30.00S	156–00.03E	500	–	–	145/146	Attached on CTD frame at CTD C21M01

6.2.3 XCTD

(1) Personnel

Takuya Hasegawa   (JAMSTEC): Principal Investigator

Kazuho Yoshida   (Global Ocean Development Inc.: GODI)

Masanori Murakami (GODI)

Miki Morioka   (GODI)

Ryo Kimura   (MIRAI Crew)

(2) Objectives

Investigation of oceanic structure.

(3) Parameters

Parameters of XCTD-1 (eXpendable Conductivity, Temperature & Depth profiler; Tsurumi-Seiki Co..) are as follows;

Parameter	Range	Accuracy
Conductivity	0 ~ 60 [mS/cm]	+/- 0.03 [mS/cm]
Temperature	-2 ~ 35 [deg-C]	+/- 0.02 [deg-C]
Depth	0 ~ 1000 [m]	5 [m] or 2 [%] (whichever is greater)

(4) Methods

We observed the vertical profiles of the sea water temperature and salinity measured by XCTD system. We launched 41 XCTD-1 probes (No.1-.38, 40, 42, 44) by using the automatic launcher, MK-150N digital converter (Tsurumi-Seiki Co.) and AL-12B software (Ver.1.1.4; Tsurumi-Seiki Co.), and 4 probes (No.39, 41, 43, 45) by the hand launcher, MK-130 digital converter (Tsurumi-Seiki Co.) and MK-130 software (Ver. 3.11; Tsurumi-Seiki Co.) . The summary of XCTD observations were shown in Table 6.2.2.

(5) Preliminary results

Position map of XCTD observations was shown in Fig. 6.2.3-1. Vertical section of temperature and salinity were shown from Fig.6.2.3-2 to Fig.6.2.3-4.

(6) Data archive

These data obtained in this cruise will be submitted to the Data Management Group (DMG) of JAMSTEC, and will be opened to the public via **"Data Research for Whole Cruise Information in JAMSTEC"** in JAMSTEC home page.

Table 6.2.3 Summary of XCTD observation and launching log

No	Station	Date (UTC)	Time (UTC)	Latitude [deg-min]	Longitude [deg-min]	Depth [m]	SST [deg-C]	SSS [PSU]	Probe S/N
01	PC01	2014/02/16	04:21	6-57.15N	138-49.91E	3457	29.261	33.976	11011557
02	PC02	2014/02/17	15:23	4-02.60N	141-17.15E	2731	29.607	34.671	11125648
03	TR08DEP	2014/02/21	03:37	1-59.15N	147-01.81E	4517	29.265	34.417	13093857
04	TR09DEP	2014/02/23	03:36	0-00.99N	147-00.95E	4526	29.281	34.411	13093858
05	XCTD-p17	2014/02/24	17:52	2-14.00S	153-37.84E	3853	29.406	34.955	13093861
06	XCTD-p16	2014/02/24	19:41	2-30.07S	153-25.98E	5057	29.330	35.007	13093860
07	XCTD-p15	2014/02/25	07:11	2-48.48S	153-15.73E	3445	29.392	34.951	13093866
08	XCTD-p14	2014/02/25	09:20	3-03.02S	153-01.02E	2336	29.297	34.888	13093863
09	XCTD-p13	2014/02/25	11:30	3-20.00S	152-49.03E	2269	29.163	34.815	13093862
10	XCTD-p12	2014/02/25	13:23	3-35.97S	152-37.03E	1074	28.885	34.729	13093865
11	XCTD-p11	2014/02/25	16:18	3-50.26S	152-55.96E	2414	29.340	34.669	13093864
12	XCTD-p10	2014/02/25	20:57	4-05.28S	153-15.06E	2646	29.378	34.643	13093859
13	XCTD-p9	2014/02/26	00:07	4-19.94S	153-33.93E	3547	29.510	34.549	13093873
14	XCTD-p8	2014/02/26	03:09	4-34.21S	153-52.78E	3840	29.331	34.477	13093871
15	XCTD-p7	2014/02/26	06:04	4-47.32S	154-08.89E	2942	29.106	34.103	13093874
16	XCTD-p6	2014/02/26	09:03	4-59.88S	154-25.19E	994	29.337	34.195	13093872
17	XCTD-p5	2014/02/26	10:31	4-57.99S	154-44.01E	2349	29.260	34.904	13093870
18	XCTD-p4	2014/02/26	12:03	5-00.01S	155-03.00E	3305	29.524	34.908	13093868
19	XCTD-p3	2014/02/26	13:38	5-00.00S	155-22.00E	3023	29.473	34.899	13093869
20	XCTD-p2	2014/02/26	15:14	5-00.05S	155-41.00E	2061	29.486	34.964	13093867
21	TR06DEP	2014/02/27	01:44	4-57.78S	156-01.60E	1498	29.569	34.952	13093875
22	TR05DEP	2014/03/01	00:44	1-59.33S	156-02.49E	1764	29.305	34.921	13093876
23	TR04DEP	2014/03/03	01:31	0-00.55S	155-58.52E	1938	29.271	34.422	13093877
24	MSP_20	2014/03/05	05:28	0-03.23S	156-11.29E	1959	29.304	34.412	13093878
25	MSP_23	2014/03/07	02:57	1-29.98N	156-00.06E	2382	30.150	34.659	13093879
26	MSP_24	2014/03/07	06:14	0-59.88N	156-00.20E	2255	30.523	34.576	13093880
27	TR03DEP	2014/03/08	01:01	1-57.44N	156-00.50E	2562	30.032	34.654	13093881
28	MSP_25,26	2014/03/08	02:58	2-03.00N	156-02.72E	2538	30.136	34.651	13093882
29	MSP_27,28	2014/03/09	05:03	3-00.10N	155-59.98E	2876	30.383	34.678	13093883
30	TR02DEP	2014/03/10	01:34	4-57.71N	156-02.04E	3606	29.970	34.322	13093885
31	MSP_29,30	2014/03/10	05:41	4-00.05N	156-00.03E	3475	30.178	34.610	13093884
32	MSP_31	2014/03/10	19:27	5-02.10N	155-57.52E	3601	29.442	34.174	13093886
33	XCTD_08	2014/03/11	08:00	5-30.05N	155-59.98E	3737	29.600	33.990	13093890
34	XCTD_09	2014/03/11	10:02	5-59.99N	155-59.99E	4146	29.716	34.168	13093891
35	XCTD_10	2014/03/11	12:03	6-30.01N	155-59.99E	4411	29.713	34.195	13093892
36	XCTD_11	2014/03/11	14:03	7-00.00N	156-00.01E	4448	29.642	34.210	13093889

Table 6.2.3 Summary of XCTD observation and launching log (continued)

37	XCTD_12	2014/03/11	16:11	7-30.00N	156-00.01E	4398	29.311	33.982	13093887
38	TR01REC	2014/03/11	20:05	7-57.67N	156-00.71E	4849	29.325	34.077	13093895
39*	TR01REC	2014/03/11	20:05	7-57.67N	156-00.71E	4849	29.325	34.077	13093893
40	TR01REC	2014/03/11	20:21	7-57.67N	156-00.67E	4858	29.318	34.078	13093888
41*	TR01REC	2014/03/11	20:21	7-57.67N	156-00.67E	4858	29.318	34.078	13093894
42	TR01REC	2014/03/11	20:21	7-57.67N	156-00.67E	4858	29.318	34.078	13093888
43*	TR01REC	2014/03/11	20:21	7-57.67N	156-00.67E	4858	29.318	34.078	13093896
44	TR01REC	2014/03/11	20:29	7-57.66N	156-00.66E	4853	29.315	34.078	13093899
45*	TR01REC	2014/03/11	20:29	7-57.66N	156-00.66E	4853	29.315	34.078	13093898

Attached symbol and acronyms in Table XCTD observation log are as follows;

* :   Observed by using the hand launcher, MK-130 digital converter and MK-130 software (ver.3.11)

Depth: The depth of water [m]

SST: Sea Surface Temperature [deg-C] measured by TSG (ThermoSalinoGraph).

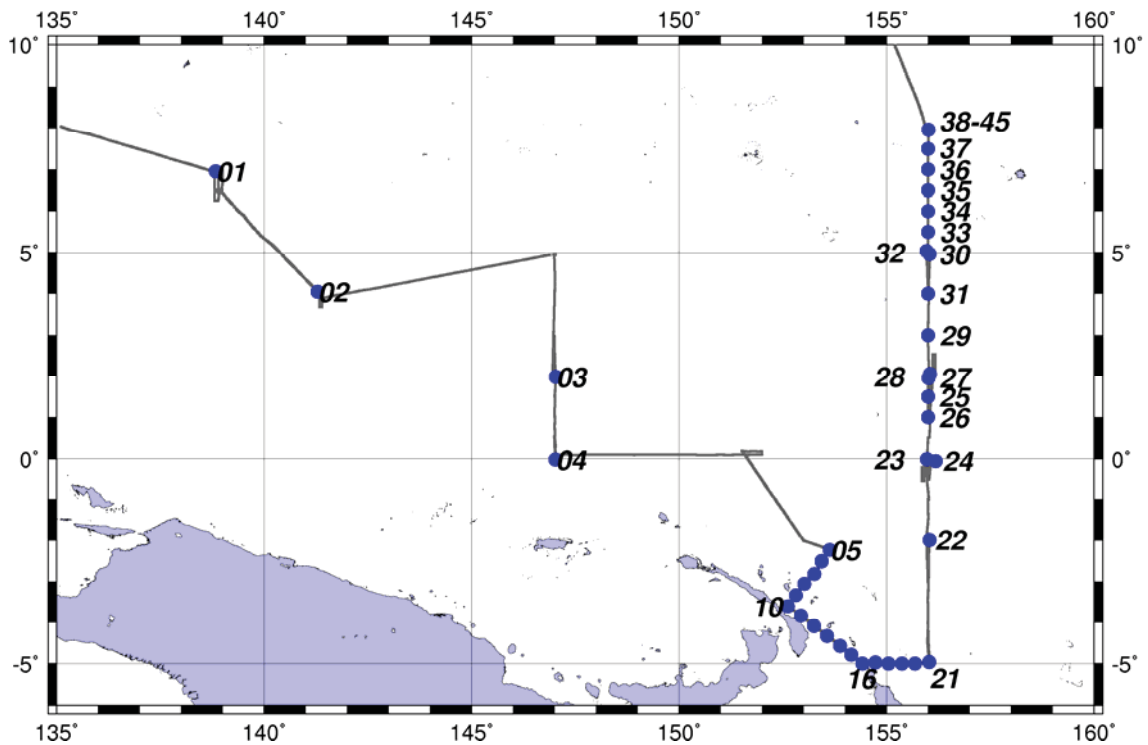SSS: Sea Surface Salinity [PSU] measured by TSG.

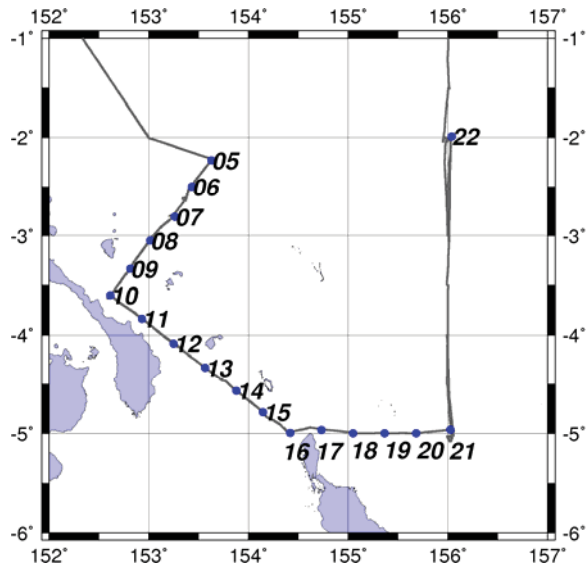Fig. 6.2.3-1 Position map of XCTD observations.

Fig. 6.2.3-1 Position map of XCTD observations around Solomon Straight..

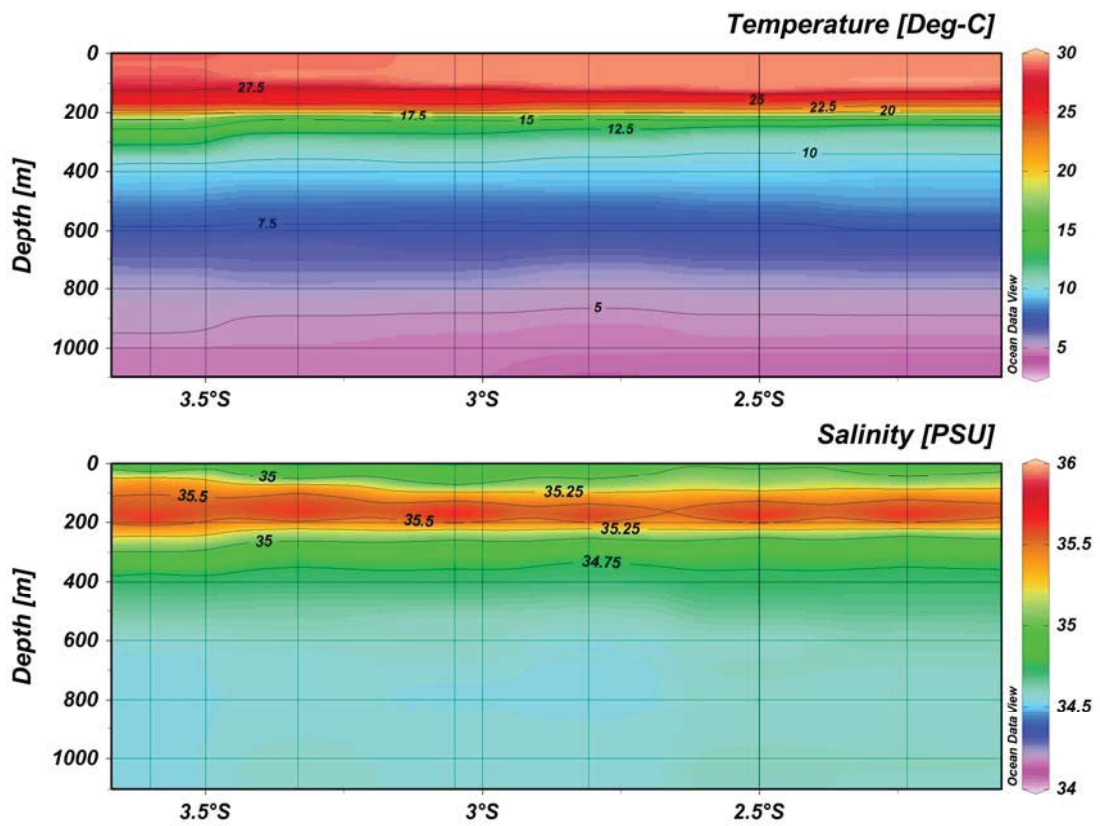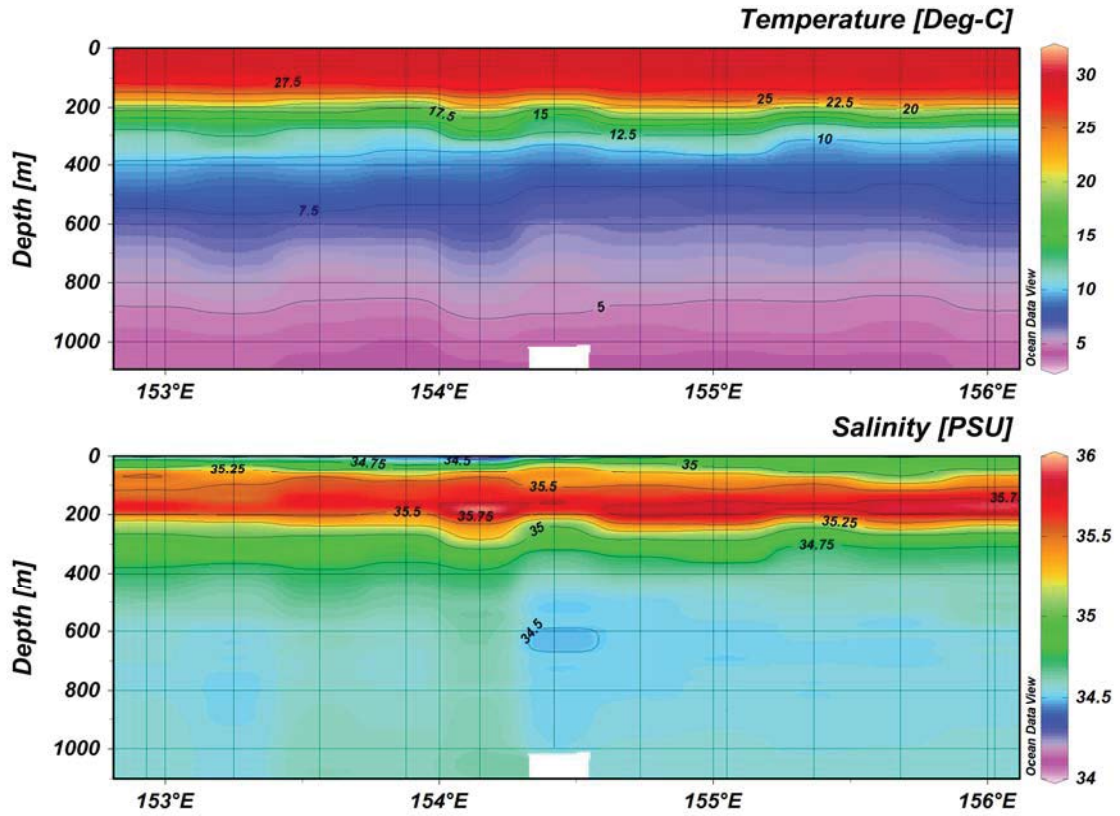Fig. 6.2.3-2 Vertical section of temperature (upper) and salinity (lower)

Fig. 6.2.3-3 Vertical section of temperature (upper) and salinity (lower)
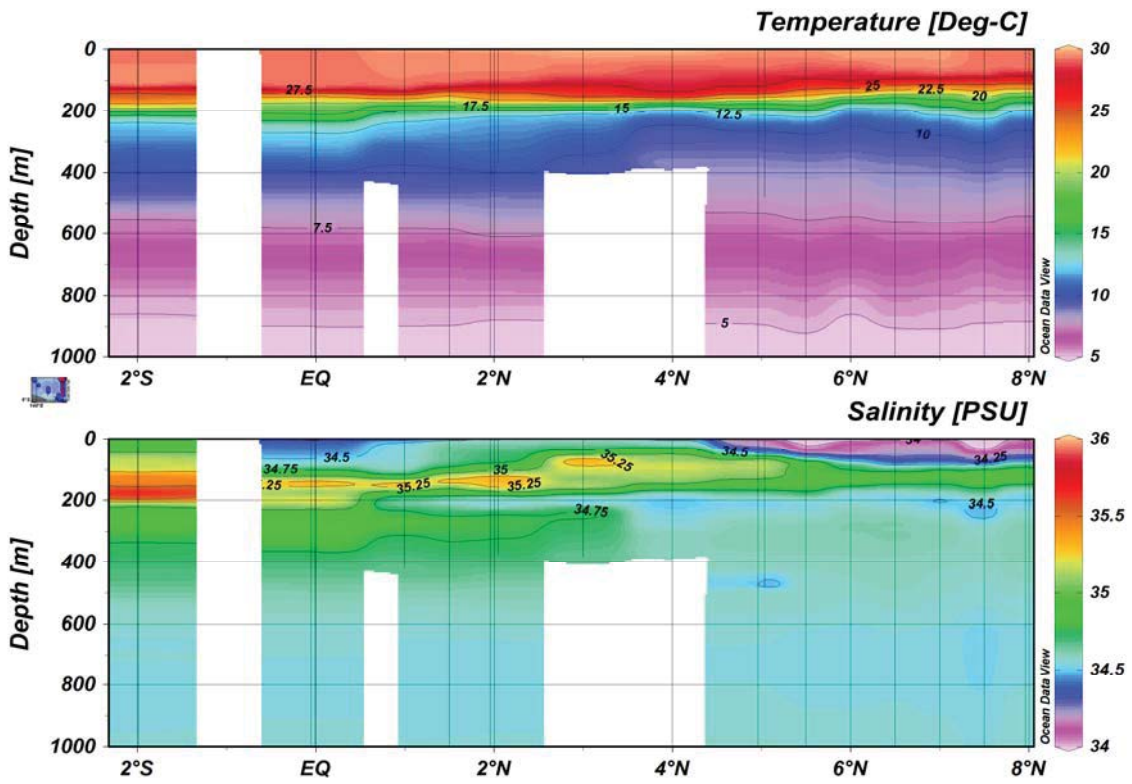
from Station XCTD p-12 to TR06DEP. (No. 10 to No. 21)

Fig. 6.2.3-4 Vertical section of temperature (upper) and salinity (lower) along 156E(No. 22 to No.38)

6.3 Water sampling (salinity) for TOCS

(1) Personnel

Takuya Hasegawa　　　　　　　　　(JAMSTEC): Principal Investigator

Hiroki Ushiromura　　　　　　　　 (MWJ): Technical Staff (Operation Leader)

Sonoka Wakatsuki　　　　　　　　　(MWJ): Technical Staff

(2) Objective

To measure bottle salinity obtained by CTD casts and the continuous sea surface water   monitoring system (TSG).

(3) Method

a. Salinity Sample Collection

Seawater samples were collected with 12 liter Niskin-X bottles and TSG. The salinity sample bottle of the 250ml brown glass with GL32 screw cap was used for collecting the sample seawater. Each bottle was rinsed 3 times with the sample seawater, and was filled with sample seawater to the bottle shoulder. All of sample bottles were sealed with a plastic cone and a screw cap because we took into consideration the possibility of storage for about a month. The cone was rinsed 3 times with the sample seawater before its use. Each bottle was stored for more than 12 hours in the laboratory before the salinity measurement.

Types and numbers (n) of samples are shown in Table 6.3-1.

Table 6.3-1 Types and numbers (n) of samples

Types	numbers of samples
Samples for CTD	64
Samples for TSG	32
Total	96

b. Instruments and Method

The salinity measurement was carried out on R/V MIRAI during the cruise of MR14-02 using the salinometer (Model 8400B "AUTOSAL" ;　Guildline Instruments Ltd.: S/N 62556) with an additional peristaltic-type intake pump (Ocean Scientific International, Ltd.).

One pair of precision digital thermometers (Model 9540 ;　Guildline Instruments Ltd.) were used. One thermometer monitored the ambient temperature and the

other monitored the bath temperature of the salinometer.

The specifications of the AUTOSAL salinometer and thermometer are shown as follows；

Salinometer (Model 8400B "AUTOSAL"； Guildline Instruments Ltd.)
   Measurement Range： 0.005 to 42 (PSU)
   Accuracy： Better than ±0.002 (PSU) over 24 hours
              without re-standardization
   Maximum Resolution： Better than ±0.0002 (PSU) at 35 (PSU)

Thermometer (Model 9540； Guildline Instruments Ltd.)
   Measurement Range   ： -40 to +180 deg C
   Resolution   ： 0.001
   Limits of error ±deg C   ： 0.01 (24 hours @ 23 deg C ±1 deg C)
   Repeatability   ： ±2 least significant digits

The measurement system was almost the same as Aoyama *et al.* (2002). The salinometer was operated in the air-conditioned ship's laboratory at a bath temperature of 24 deg C. The ambient temperature varied from approximately 21.6 deg C to 23.6 deg C, while the bath temperature was very stable and varied within +/- 0.003 deg C on rare occasion.

The measurement for each sample was done with a double conductivity ratio and defined as the median of 31 readings of the salinometer. Data collection was started 10 seconds after filling the cell with the sample and it took about 10 seconds to collect 31 readings by the personal computer. Data were taken for the sixth and seventh filling of the cell. In the case of the difference between the double conductivity ratio of these two fillings being smaller than 0.00002, the average value of the double conductivity ratio was used to calculate the bottle salinity with the algorithm for the practical salinity scale, 1978 (UNESCO, 1981). If the difference was greater than or equal to 0.00003, an eighth filling of the cell was done. In the case of the difference between the double conductivity ratio of these two fillings being smaller than 0.00002, the average value of the double conductivity ratio was used to calculate the bottle salinity. In the case of the double conductivity ratio of eighth filling did not satisfy the criteria above, we measured a ninth or tenth filling of the cell and calculated the bottle salinity. The conductivity cell was cleaned with detergent after the measurement of the day.

(4) Results

　　a. Standard Seawater (SSW)

The specifications of SSW used in this cruise are shown as follows；

　　　　Batch： P156

　　　　Conductivity Ratio： 0.99984

　　　　Salinity： 34.994

　　　　Use By： 23rd July 2016

Standardization control of the salinometer S/N 62556 was set to 690 and all measurements were carried out at this setting. The value of STANDBY was 24+5198~5199 and that of ZERO was 0.0+0001~0.0-0000. 21 bottles of SSW were measured.

Fig.6.3.1-1 shows the time series of the double conductivity ratio of SSW batch P156 before correction. The average of the double conductivity ratio was 1.99967 and the standard deviation was 0.00001, which is equivalent to 0.0003 in salinity.
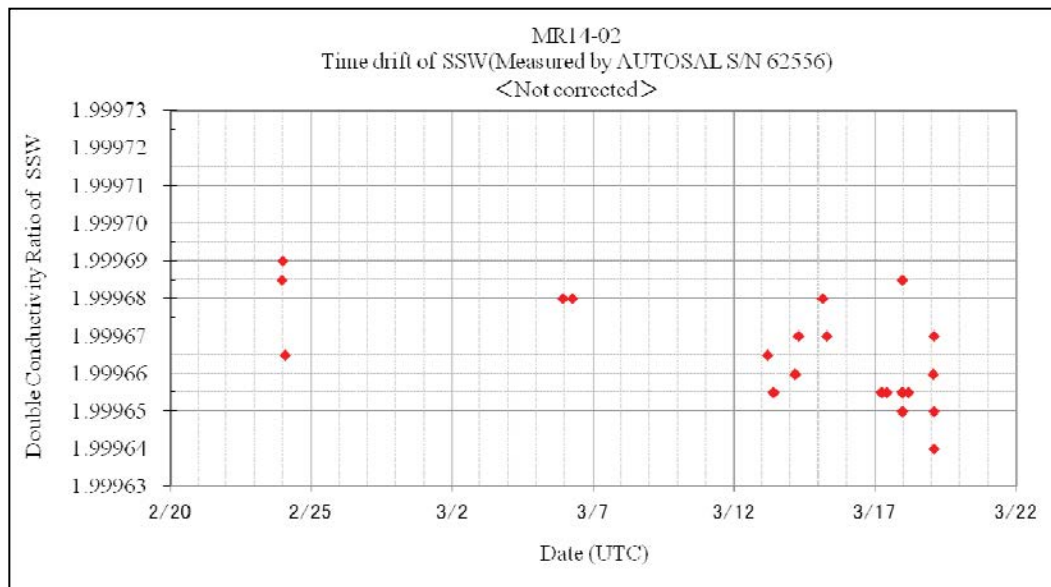

Fig. 6.3.1-1 Time series of double conductivity ratio for the Standard Seawater batch P156
(before correction)

Fig.6.3.1-2 shows the time series of the double conductivity ratio of SSW batch P156 after correction. The average of the double conductivity ratio was 1.99968 and the standard deviation was 0.00001, which is equivalent to 0.0002 in salinity.
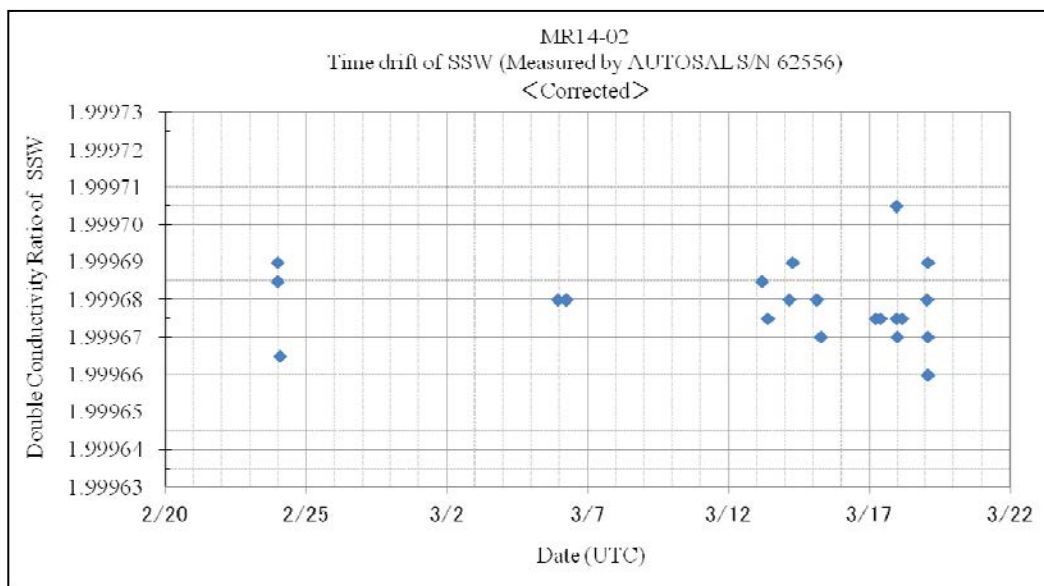
Fig.6.3.1-2 Time series of double conductivity ratio for the Standard Seawater batch P156
(after correction)

b. Sub-Standard Seawater

Sub-standard seawater was made from surface sea water filtered by a pore size of 0.22 micrometer and stored in a 20 liter container made of polyethylene and stirred for at least 24 hours before measuring. It was measured about every 6 samples in order to check for the possible sudden drifts of the salinometer.

c. Replicate Samples

We estimated the precision of this method using 32 pairs of replicate samples taken from the same Niskin bottle. Fig.6.3.2 shows the histogram of the absolute difference between each pair of the replicate samples. The average and the standard deviation of absolute difference among 32 pairs of replicate samples were 0.0003 and 0.0003 in salinity, respectively.

70
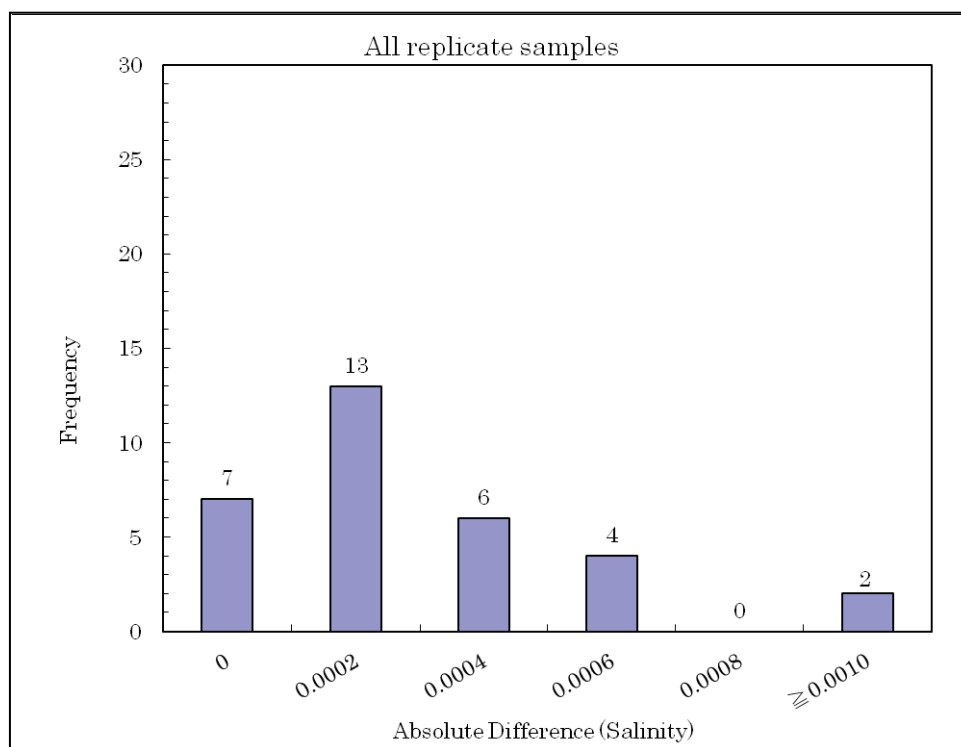
Fig.6.3.2 Histogram of the absolute difference between replicate samples

(5) Data archive

These raw datasets will be submitted to JAMSTEC Data Management Office (DMO).

(6) Reference

・Aoyama, M. T. Joyce, T. Kawano and Y. Takatsuki : Standard seawater comparison up to P129. Deep-Sea Research, I, Vol. 49, 1103～1114, 2002

・UNESCO : Tenth report of the Joint Panel on Oceanographic Tables and Standards. UNESCO Tech. Papers in Mar. Sci., 36, 25 pp., 1981

6.4 Continuous monitoring of surface seawater : Temperature, salinity, dissolved oxygen

1. Personnel

Takuya HASEGAWA (JAMSTEC): Principal Investigator

Kanako YOSHIDA (Marine Works Japan Co. Ltd): Operation Leader

Masahiro ORUI (Marine Works Japan Co. Ltd)

2. Objective

Our purpose is to obtain temperature, salinity and dissolved oxygen data continuously in near-sea surface water.

3. Instruments and Methods

The Continuous Sea Surface Water Monitoring System (Marine Works Japan Co. Ltd.) has four sensors and automatically measures temperature, salinity and dissolved oxygen in near-sea surface water every one minute. This system is located in the "*sea surface monitoring laboratory*" and connected to shipboard LAN-system. Measured data, time, and location of the ship were stored in a data management PC. The near-surface water was continuously pumped up to the laboratory from about 4.5 m water depth and flowed into the system through a vinyl-chloride pipe. The flow rate of the surface seawater was adjusted to be 5 dm^3 min^{-1}.

a. Instruments

Software

Seamoni-kun Ver.1.50

Sensors

Specifications of the each sensor in this system are listed below.

Temperature and Conductivity sensor

Model:	SBE-45, SEA-BIRD ELECTRONICS, INC.
Serial number:	4563325-0362
Measurement range:	Temperature -5 to +35 ºC
	Conductivity 0 to 7 S m^{-1}
Initial accuracy:	Temperature 0.002 ºC
	Conductivity 0.0003 S m^{-1}

Typical stability (per month):	Temperature 0.0002 °C
	Conductivity 0.0003 S m^{-1}
Resolution:	Temperatures 0.0001 °C
	Conductivity 0.00001 S m^{-1}

Bottom of ship thermometer

Model:	SBE 38, SEA-BIRD ELECTRONICS, INC.
Serial number:	3857820-0540
Measurement range:	-5 to +35 °C
Initial accuracy:	±0.001 °C
Typical stability (per 6 month):	0.001 °C
Resolution:	0.00025 °C

Dissolved oxygen sensor

Model:	OPTODE 3835, AANDERAA Instruments.
Serial number:	1519
Measuring range:	0 - 500 mmol dm^{-3}
Resolution:	< 1 mmol dm^{-3}
Accuracy:	< 8 mmol dm^{-3} or 5 % whichever is greater
Settling time:	< 25 s

Dissolved oxygen sensor

Model:	RINKO II, ARO-CAR/CAD
Serial number:	13
Measuring range:	0 - 540 mmol dm^{-3}
Resolution:	< 0.1 mmol dm^{-3}
	or 0.1 % of reading whichever is greater
Accuracy:	< 1 mmol dm^{-3}
	or 5 % of reading whichever is greater

b. Measurements

　　Periods of measurement, maintenance, and problems during MR14-02 are listed in Table 6.4-1.

Table 6.4-1 Events list of the Sea surface water monitoring during MR14-02

System Date [UTC]	System Time [UTC]	Events	Remarks
2014/02/15	08:00	All the measurements started and data was available.	Cruise start
2014/03/19	01:37	All the measurements stopped.	Cruise end

4.　Preliminary Result

　　We took the surface water samples to compare sensor data with bottle data of salinity. The results are shown in Fig.6.4-1. All the salinity samples were analyzed by the Guideline 8400B "AUTOSAL". Preliminary data of temperature, salinity, and dissolved oxygen at sea surface are shown in Fig.6.4-2.

5.　Data archive

　　These data obtained in this cruise will be submitted to the Data Management Office (DMO) of JAMSTEC, and will be opened to the public via **"Data Research for Whole Cruise Information in JAMSTEC"** in JAMSTEC home page.
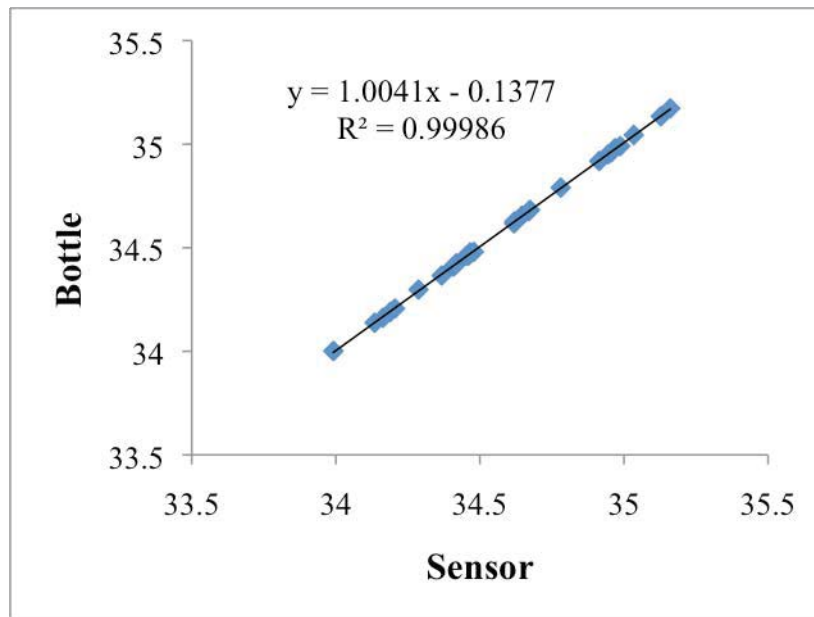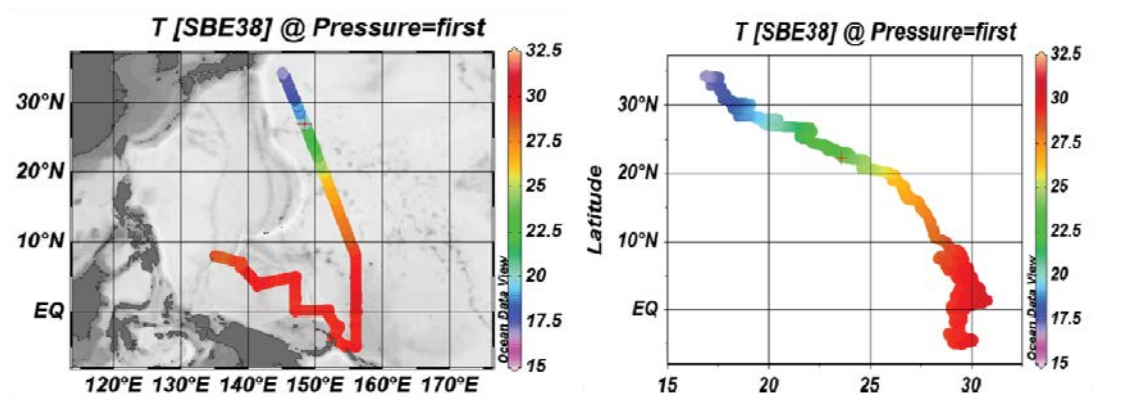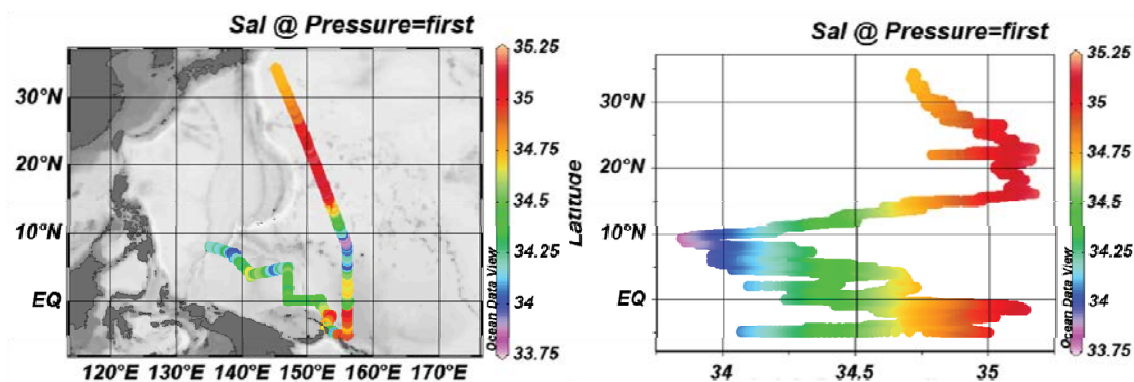
Fig 6.4-1 Correlation of salinity between sensor data and bottle data.

(a) Temperature

(b) Salinity

(c) Dissolved oxygen

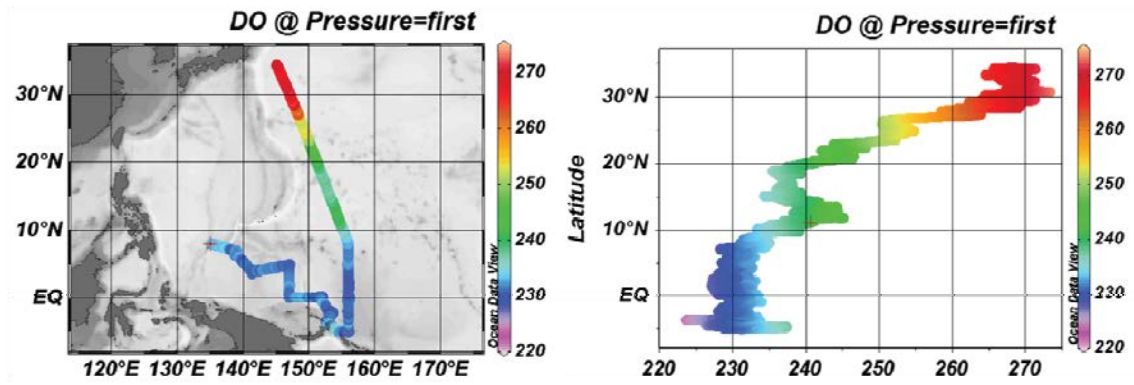

Fig.6.4 -2 Spatial and temporal distribution of (a) temperature by SBE38 (b) salinity (c) dissolved oxygen in MR14-02 cruise.

6.5 Shipboard ADCP

(1) Personnel

Takuya Hasegawa	(JAMSTEC): Principal Investigator
Kazuho Yoshida	(Global Ocean Development Inc., GODI)
Masanori Murakami	(GODI)
Miki Morioka	(GODI)
Ryo Kimura	(MIRAI Crew)

(2) Objective

To obtain continuous measurement of the current profile along the ship's track.

(3) Methods

Upper ocean current measurements were made in MR14-02 cruise, using the hull-mounted Acoustic Doppler Current Profiler (ADCP) system. For most of its operation the instrument was configured for water-tracking mode. Bottom-tracking mode, interleaved bottom-ping with water-ping, was made to get the calibration data for evaluating transducer misalignment angle. The system consists of following components;

1) R/V MIRAI has installed the Ocean Surveyor for vessel-mount (acoustic frequency 76.8 kHz; Teledyne RD Instruments). It has a phased-array transducer with single ceramic assembly and creates 4 acoustic beams electronically. We mounted the transducer head rotated to a ship-relative angle of 45 degrees azimuth from the keel

2) For heading source, we use ship's gyro compass (Tokimec, Japan), continuously providing heading to the ADCP system directory. Additionally, we have Inertial Navigation System (INS) which provide high-precision heading, attitude information, pitch and roll, are stored in ".N2R" data files with a time stamp.

3) DGPS system (Trimble SPS751 & StarFixXP) providing position fixes.

4) We used VmDas version 1.46.5 (TRD Instruments) for data acquisition.

5) To synchronize time stamp of ping with GPS time, the clock of the logging computer is adjusted to GPS time every 1 minute

6) Fresh water is charged in the sea chest to prevent biofouling at transducer face.

7) The sound speed at the transducer does affect the vertical bin mapping and vertical velocity measurement, is calculated from temperature, salinity (constant value; 35.0 psu) and depth (6.5 m; transducer depth) by equation in Medwin (1975).

Data was configured for 16 m intervals starting 23 m below sea surface. Every ping was recorded as raw ensemble data (.ENR). Also, 60 seconds and 300 seconds averaged data were recorded as short term average (.STA) and long term average (.LTA) data, respectively. Major parameters for the measurement (Direct Command) are shown in Table 6.5-1.

(4) Preliminary results

Fig.6.5-1 shows the surface current vector along the ship's track.

(5) Data archive

These data obtained in this cruise will be submitted to the Data Management Group (DMG) of JAMSTEC, and will be opened to the public via JAMSTEC home page.

(6) Remarks

1. Data acquisition was suspended in the territorial waters of Palau.

2. The following periods, navigation data was invalid due to GPS position fix error or GPS system trouble.

    11:06UTC 15 Mar. 2014
    11:08UTC 15 Mar. 2014 - 11:10UTC 15 Mar. 2014
    11:12UTC 15 Mar. 2014 - 11:13UTC 15 Mar. 2014
    11:20UTC 15 Mar. 2014
    10:03UTC 16 Mar. 2014
    18:04UTC 20 Mar. 2014 - 18:24UTC 20 Mar. 2014

Table 6.5-1 Major parameters

Bottom-Track Commands

   BP = 001   Pings per Ensemble (almost less than 1300m depth)
          13:25UTC 25 Feb. to 18:57UTC 25 Feb., 2014
          08:47UTC 26 Feb. to 10:17UTC 26 Feb., 2014
          08:34UTC 20 Mar. to 00:00UTC 23 Mar., 2014

Environmental Sensor Commands

   EA = +04500 Heading Alignment (1/100 deg)

EB	=	+00000	Heading Bias (1/100 deg)
ED	=	00065	Transducer Depth (0 - 65535 dm)
EF	=	+001	Pitch/Roll Divisor/Multiplier (pos/neg) [1/99 - 99]
EH	=	00000	Heading (1/100 deg)
ES	=	35	Salinity (0-40 pp thousand)
EX	=	00000	Coord Transform (Xform:Type; Tilts; 3Bm; Map)
EZ	=	10200010	Sensor Source (C; D; H; P; R; S; T; U)

C (1): Sound velocity calculates using ED, ES, ET (temp.)

D (0): Manual ED

H (2): External synchro

P (0), R (0): Manual EP, ER (0 degree)

S (0): Manual ES

T (1): Internal transducer sensor

U (0): Manual EU

Timing Commands

| TE | = | 00:00:02.00 | Time per Ensemble (hrs:min:sec.sec/100) |
| TP | = | 00:02.00 | Time per Ping (min:sec.sec/100) |

Water-Track Commands

WA	=	255	False Target Threshold (Max) (0-255 count)
WB	=	1	Mode 1 Bandwidth Control (0=Wid, 1=Med, 2=Nar)
WC	=	120	Low Correlation Threshold (0-255)
WD	=	111 100 000	Data Out (V; C; A; PG; St; Vsum; Vsum^2;#G;P0)
WE	=	1000	Error Velocity Threshold (0-5000 mm/s)
WF	=	0800	Blank After Transmit (cm)
WG	=	001	Percent Good Minimum (0-100%)
WI	=	0	Clip Data Past Bottom (0 = OFF, 1 = ON)
WJ	=	1	Rcvr Gain Select (0 = Low, 1 = High)
WM	=	1	Profiling Mode (1-8)
WN	=	40	Number of depth cells (1-128)
WP	=	00001	Pings per Ensemble (0-16384)
WS	=	1600	Depth Cell Size (cm)
WT	=	000	Transmit Length (cm) [0 = Bin Length]
WV	=	0390	Mode 1 Ambiguity Velocity (cm/s radial)
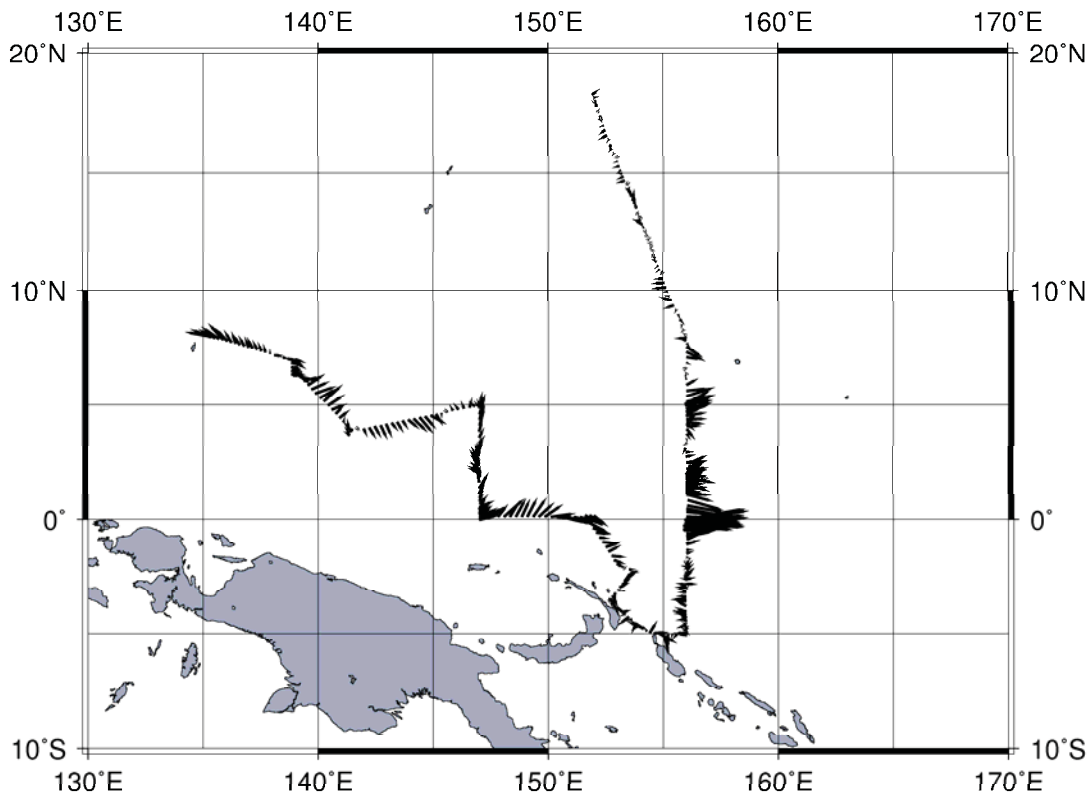
Fig 6.5-1. Surface current vector along the ship's track. (TRITON area)

6.6 Underway geophysics

6.6.1. Sea surface gravity

(1) Personnel

Masao Nakanishi	(Chiba University): Principal Investigator (Not on-board)
Takeshi Matsumoto	(University of the Ryukyus): Principal Investigator (Not on-board)
Takuya Hasegawa	(JAMSTEC)
Kazuho Yoshida	(Global Ocean Development Inc., GODI)
Masanori Murakami	(GODI)
Miki Morioka	(GODI)
Ryo Kimura	(MIRAI Crew)

(2) Introduction

The local gravity is an important parameter in geophysics and geodesy. We collected gravity data at the sea surface.

(3) Parameters

Relative Gravity [CU: Counter Unit]

[mGal] = (coef1: 0.9946) * [CU]

(4) Data Acquisition

We measured relative gravity using LaCoste and Romberg air-sea gravity meter S-116 (Micro-g LaCoste, LLC) in the MR14-02 cruise.

We measured gravity to convert the relative gravity to absolute one, using portable gravity meter (Scintrex gravity meter CG-5) at Sekinehama as the reference point.

(5) Preliminary Results

Absolute gravity shown in Table 6.6.1-1

(6) Data Archives

Surface gravity data obtained during this cruise will be submitted to the Data Management Group (DMG) in JAMSTEC, and will be archived there.

(7) Remarks

1. Data acquisition was suspended in the territorial waters of Palau.

2. The following period, heading data was invalid due to communication trouble between the network server and Gyro compass.

   09:37:08UTC 20 Mar. 2014 - 11:46:28UTC 20 Mar. 2014

3. The following period, EOTVOS correction, Longitude, Latitude, SOG and COG data were invalid due to GPS trouble.

   18:05:13UTC 20 Mar. 2014 - 19:04:02UTC 20 Mar. 2014

Table 6.6.1-1

No	Date	UTC	Port	Absolute Gravity [mGal]	Sea Level [cm]	Draft [cm]	Gravity at Sensor [1] [mGal]	L&R[2] Gravity [mGal]
#1	06 Jan.	06:45	Sekinehama	980,371.94	259	630	980,372.97	12,662.89
#2	24 Mar.	07:32	Sekinehama	980,371.92	310	600	980,373.03	12,666.28

[1]: Gravity at Sensor = Absolute Gravity + Sea Level*0.3086/100 + (Draft-530)/100*0.222

[2]: LaCoste and Romberg air-sea gravity meter S-116

6.6.2 Sea surface magnetic field

1) Three-component magnetometer

(1) Personnel

Masao Nakanishi	(Chiba University) : Principal Investigator (Not on-board)
Takeshi Matsumoto	(University of the Ryukyus): Principal Investigator (Not on-board)
Takuya Hasegawa	(JAMSTEC)
Kazuho Yoshida	(Global Ocean Development Inc., GODI)
Masanori Murakami	(GODI)
Miki Morioka	(GODI)
Ryo Kimura	(MIRAI Crew)

(2) Introduction

Measurement of magnetic force on the sea is required for the geophysical investigations of marine magnetic anomaly caused by magnetization in upper crustal structure. We measured geomagnetic field using a three-component magnetometer during the MR14-02 cruise.

(3) Principle of shipboard geomagnetic vector measurement

The relation between a magnetic-field vector observed on-board, $\mathbf{H}$ob, (in the ship's fixed coordinate system) and the geomagnetic field vector, $\mathbf{F}$, (in the Earth's fixed coordinate system) is expressed as:

$$\mathbf{H}ob = \widetilde{\mathbf{A}} \ \widetilde{\mathbf{R}} \ \widetilde{\mathbf{P}} \ \widetilde{\mathbf{Y}} \ \mathbf{F} + \mathbf{H}p \qquad (a)$$

Where $\widetilde{\mathbf{R}}$, $\widetilde{\mathbf{P}}$ and $\widetilde{\mathbf{Y}}$ are the matrices of rotation due to roll, pitch and heading of a ship, respectively. $\widetilde{\mathbf{A}}$ is a 3 x 3 matrix that represents magnetic susceptibility of the ship, and $\mathbf{H}p$ is a magnetic field vector produced by a permanent magnetic moment of the ship's body. Rearrangement of Eq. (a) makes

$$\widetilde{\mathbf{B}} \ \mathbf{H}ob + \mathbf{H}bp = \widetilde{\mathbf{R}} \ \widetilde{\mathbf{P}} \ \widetilde{\mathbf{Y}} \ \mathbf{F} \qquad (b)$$

Where $\widetilde{\mathbf{B}} = \widetilde{\mathbf{A}}^{-1}$, and $\mathbf{H}bp = -\widetilde{\mathbf{B}} \ \mathbf{H}p$. The magnetic field, $\mathbf{F}$, can be obtained by measuring $\widetilde{\mathbf{R}}$, $\widetilde{\mathbf{P}}$, $\widetilde{\mathbf{Y}}$ and $\mathbf{H}ob$, if $\widetilde{\mathbf{B}}$ and $\mathbf{H}bp$ are known. Twelve constants in $\widetilde{\mathbf{B}}$ and $\mathbf{H}bp$ can be determined by measuring variation of $\mathbf{H}ob$ with $\widetilde{\mathbf{R}}$, $\widetilde{\mathbf{P}}$ and $\widetilde{\mathbf{Y}}$ at a place where the geomagnetic field, $\mathbf{F}$, is known.

(4) Instruments on R/V MIRAI

A shipboard three-component magnetometer system (Tierra Tecnica SFG1214) is equipped on-board R/V MIRAI. Three-axes flux-gate sensors with ring-cored coils are fixed on the fore

mast. Outputs from the sensors are digitized by a 20-bit A/D converter (1 nT/LSB), and sampled at 8 times per second. Ship's heading, pitch, and roll are measured by the Inertial Navigation System (INS) for controlling attitude of a Doppler radar. Ship's position (GPS) and speed data are taken from LAN every second.

(5) Data Archives

These data obtained in this cruise will be submitted to the Data Management Group (DMG) of JAMSTEC.

(6) Remarks

1. Data acquisition was suspended in the territorial waters of Palau.

2. For calibration of the ship's magnetic effect, we made a "figure-eight" turn (a pair of clockwise and anti-clockwise rotation) three times as follows;
   10:46UTC - 11:07UTC 22 Feb. 2014 around 00-02N, 147-00E
   18:23UTC - 18:50UTC 27 Feb. 2014 around 05-04S, 156-02E
   05:26UTC - 05:49UTC 17 Mar. 2014 around 25-59N, 148-47E

3. The following period, Latitude, Longitude, Heading and SOG data were invalid due to communication trouble between the network server, gyro compass and GPS .
   09:37:05UTC 20 Mar. 2014 - 11:45:17UTC 20 Mar. 2014

4. The following period, Latitude, Longitude and SOG data were invalid due to GPS trouble.
   18:05:03UTC 20 Mar. 2014 - 18:12:46UTC 20 Mar. 2014

2) Cesium magnetometer

(1) Personnel

Masao Nakanishi   (Chiba University) : Principal Investigator (Not on-board)

Takeshi Matsumoto   (University of the Ryukyus): Principal Investigator (Not on-board)

Takuya Hasegawa   (JAMSTEC)

Kazuho Yoshida   (Global Ocean Development Inc., GODI)

Masanori Murakami   (GODI)

Miki Morioka   (GODI)

Ryo Kimura   (MIRAI Crew)

(2) Introduction

Measurement of total magnetic force on the sea is required for the geophysical investigations of marine magnetic anomaly caused by magnetization in upper crustal structure.

(3) Data Period

05:10UTC 23 Feb. 2014 - 20:12UTC 24 Feb. 2014

(4) Specification

We measured total geomagnetic field using a cesium marine magnetometer (Geometrics Inc., G-882) and recorded by G-882 data logger (Clovertech Co., Ver.1.0.0). The G-882 magnetometer uses an optically pumped Cesium-vapor atomic resonance system. The sensor fish towed 500 m behind the vessel to minimize the effects of the ship's magnetic field.

Table 6.6.2-1 shows system configuration of MIRAI cesium magnetometer system.

Table 6.6.2-1 System configuration of MIRAI cesium magnetometer system.

Dynamic operating range:		20,000 to 100,000 nT
Absolute accuracy:		<±2 nT throughout range
Setting:	Cycle rate;	0.1 sec
	Sensitivity;	0.001265 nT at a 0.1 second cycle rate
	Sampling rate;	1 sec

(5) Data Archives

Total magnetic force data obtained during this cruise was submitted to the Data Management Group (DMG) of JAMSTEC, and archived there.

6.6.3. Swath Bathymetry

(1) Personnel

Masao Nakanishi   (Chiba University) : Principal Investigator (Not on-board)

Takeshi Matsumoto   (University of the Ryukyus): Principal Investigator (Not on-board)

Takuya Hasegawa   (JAMSTEC)

Junichiro Kuroda   (IFREE, JAMSTEC)

Toshitsugu Yamazaki   (AORI, The University of Tokyo)

Kazuho Yoshida   (Global Ocean Development Inc., GODI)

Masanori Murakami   (GODI)

Miki Morioka   (GODI)

Ryo Kimura   (MIRAI Crew)

(2) Introduction

R/V MIRAI is equipped with a Multi narrow Beam Echo Sounding system (MBES), SEABEAM 3012 Upgrade Model (L3 Communications ELAC Nautik) and Sub-bottom Profiler (SBP), Bathy2010 (SyQwest). The objective of MBES is collecting continuous bathymetric data along ship's track to make a contribution to geological and geophysical investigations and global datasets.

(3) Data Acquisition

The "SEABEAM 3012 Upgrade Model" on R/V MIRAI was used for bathymetry mapping during the MR14-02 cruise.

To get accurate sound velocity of water column for ray-path correction of acoustic multibeam, we used Surface Sound Velocimeter (SSV) data to get the sea surface (6.62m) sound velocity, and the deeper depth sound velocity profiles were calculated by temperature and salinity profiles from CTD, XCTD and Argo float data by the equation in Del Grosso (1974) during the cruise.

Table 6.6.3-1 shows system configuration and performance of SEABEAM 3012 Upgrade Model. Table 6.6.3-2 shows system configuration and performance of Sub-Bottom Profiler, Bathy2010.

Table 6.6.3-1 System configuration and performance of SEABEAM 3012 Upgrade Model

----

Frequency: 12 kHz
Transmit beam width: 1.6 degree
Transmit power: 20 kW
Transmit pulse length: 2 to 20 msec.

Receive beam width:	1.8 degree
Depth range:	100 to 11,000 m
Beam spacing:	0.5 degree athwart ship
Swath width:	150 degree (max)
	120 degree to 4,500 m
	100 degree to 6,000 m
	90 degree to 11,000 m
Depth accuracy:	Within < 0.5% of depth or ±1m, whichever is greater, over the entire swath. (Nadir beam has greater accuracy; typically within < 0.2% of depth or ±1m, whichever is greater)

Table 6.6.3-2 System configuration and performance of Sub-Bottom Profiler, Bathy2010

Frequency:	3.5 kHz
Transmit beam width:	23 degree
Transmit pulse length:	0.5 to 50 msec
Strata resolution:	Up to 8 cm with 300+ Meters of bottom penetration; bottom type dependant
Depth resolution:	0.1 Feet, 0.1 Meters
Depth accuracy:	±10 cm to 100 m, ±0.3% to 6,000 m

(4) Preliminary Results

The results will be published after primary processing.

(5) Data Archives

Bathymetric data obtained during this cruise will be submitted to the Data Management Group (DMG) in JAMSTEC, and will be archived there.

(6) Remarks

1. Data acquisition was suspended in the territorial waters of Palau.

2. Site survey around the stations of Piston corer sampling

PC01(around 6-40N 138-55E)	;	05:00UTC -20:05UTC 17 Feb. 2014
PC02(around 3-52N 141-20E)	;	15:55UTC -20:12UTC 18 Feb. 2014
PC03(around 0-00S 156-00E)	;	07:00UTC -18:00UTC 5 Mar. 2014
PC04(around 2-00N 156-00E)	;	10:24UTC -18:15UTC 6 Mar. 2014

3. The following period, SSV(Surface Sound Velocity) of MBES was updated by manual setting.

01:06UTC 09 Mar. 2014 -　14:01UTC 20 Mar. 2014

7. Special observations

7.1 Operation of TRITON buoys

(1) Personnel

Takuya Hasegawa	(JAMSTEC): Principal Investigator
Keisuke Matsumoto	(MWJ): Operation Leader
Akira Watanabe	(MWJ): Technical Leader
Makito Yokota	(MWJ): Technical Staff
Kai Hukuda	(MWJ): Technical Staff
Tomohide Noguchi	(MWJ): Technical Staff
Hiroki Ushiromura	(MWJ): Technical Staff
Shungo Oshitani	(MWJ): Technical Staff
Sonoka Wakatsuki	(MWJ): Technical Staff
Yoshiko Ishikawa	(MWJ): Technical Staff
Yasuhiro Arii	(MWJ): Technical Staff
Masahiro Ohrui	(MWJ): Technical Staff
Kanako Yoshida	(MWJ): Technical Staff
Hiroyuki Hayashi	(MWJ): Technical Staff
Yuki Miyajima	(MWJ): Technical Staff
Yasumi Yamada	(MWJ): Technical Staff
Mika Yamaguchi	(MWJ): Technical Staff

(2) Objectives

The large-scale air-sea interaction over the warmest sea surface temperature region in the western tropical Pacific Ocean called warm pool that affects the global atmosphere and causes El Nino phenomena. The formation mechanism of the warm pool and the air-sea interaction over the warm pool have not been well understood. Therefore, long term data sets of temperature, salinity, currents and meteorological elements have been required at fixed locations. The TRITON program aims to obtain the basic data to improve the predictions of El Nino and variations of Asia-Australian Monsoon system.

TRITON buoy array is integrated with the existing TAO(Tropical Atmosphere Ocean) array, which is presently operated by the Pacific Marine Environmental Laboratory/National Oceanic and Atmospheric Administration of the United States. TRITON is a component of international research program of CLIVAR (Climate Variability and Predictability), which is a

major component of World Climate Research Program sponsored by the World Meteorological Organization, the International Council of Scientific Unions, and the Intergovernmental Oceanographic Commission of UNESCO. TRITON will also contribute to the development of GOOS (Global Ocean Observing System) and GCOS (Global Climate Observing System).

Nine TRITON buoys have been recovered and seven TRITON buoys have been deployed during this R/V MIRAI cruise (MR14-02).

(3) Measured parameters

Meteorological parameters: wind speed, direction, atmospheric pressure, air temperature, relative humidity, radiation, precipitation.

Oceanic parameters: water temperature and conductivity at 1.5m, 25m, 50m, 75m, 100m, 125m, 150m, 200m, 300m, 500m 750m, depth at 300m and 750m, currents at 10m.

(4) Instrument

1) CTD and CT

SBE-37 IM MicroCAT

A/D cycles to average : 4

Sampling interval : 600sec

Measurement range, Temperature : -5～+35 deg-C

Measurement range, Conductivity : 0～7　S/m

Measurement range, Pressure : 0～full scale range

2) CRN(Current meter)

SonTek Argonaut ADCM

Sensor frequency : 1500kHz

Sampling interval : 1200sec

Average interval : 120sec

3) Meteorological sensors

Precipitation

R.M.YOUNG COMPANY MODEL50202/50203

Atmospheric pressure

PAROPSCIENTIFIC.Inc. DIGIQUARTZ FLOATING BAROMETER 6000SERIES

Relative humidity/air temperature,Shortwave radiation, Wind speed/direction

Woods Hole Institution ASIMET

Sampling interval : 60sec

Data analysis : 600sec averaged

(5) Locations of TRITON buoys deployment

Nominal location	5N, 156E
ID number at JAMSTEC	02015
Number on surface float	T01
ARGOS PTT number	27388
ARGOS backup PTT number	24234, 134002
Deployed date	10 Mar. 2014
Exact location	04° 58.5N, 156° 02.0E
Depth	3,600 m

Nominal location	2N, 156E
ID number at JAMSTEC	03016
Number on surface float	T04
ARGOS PTT number	27399
ARGOS backup PTT number	24244
Deployed date	08 Mar. 2014
Exact location	01° 57.2N, 156° 00.0E
Depth	2,563 m

Nominal location	EQ, 156E
ID number at JAMSTEC	04016
Number on surface float	T21
ARGOS PTT number	27400
ARGOS backup PTT number	24246, 24238
Deployed date	03 Mar. 2014
Exact location	00° 01.0S, 155° 57.8E
Depth	1,939 m

Nominal location	2S, 156E
ID number at JAMSTEC	05014
Number on surface float	T15
ARGOS PTT number	29765
ARGOS backup PTT number	24239
Deployed date	01 Mar. 2014

Exact location	01° 59.0S, 156° 02.0E
Depth	1,757 m

Nominal location	5S, 156E
ID number at JAMSTEC	06014
Number on surface float	T20
ARGOS PTT number	30787
ARGOS backup PTT number	24241
Deployed date	27 Feb. 2014
Exact location	04° 58.0S, 156° 01.0E
Depth	1,509m

Nominal location	2N, 147E
ID number at JAMSTEC	08013
Number on surface float	T23
ARGOS PTT number	29639
ARGOS backup PTT number	24242
Deployed date	21 Feb. 2014
Exact location	01° 59.5N, 147° 01.2E
Depth	4,517m

Nominal location	EQ, 147E
ID number at JAMSTEC	09014
Number on surface float	T26
ARGOS PTT number	27394
ARGOS backup PTT number	24243
Deployed date	22 Feb. 2014
Exact location	00° 01.5S, 147° 00.1E
Depth	4,553 m

(6) TRITON recovered

Nominal location	8N, 156E
ID number at JAMSTEC	01014
Number on surface float	T02
ARGOS PTT number	28154
ARGOS backup PTT number	11592

Deployed date	21 Aug. 2012
Recovered date	11 Mar. 2014
Exact location	07° 58.0N, 156° 01.9E
Depth	4,846 m
Nominal location	5N, 156E
ID number at JAMSTEC	02014
Number on surface float	T03
ARGOS PTT number	27275
ARGOS backup PTT number	24235
Deployed date	18 Aug. 2012
Recovered date	10 Mar. 2014
Exact location	05° 01.2N, 155° 58.0E
Depth	3,605 m
Nominal location	2N, 156E
ID number at JAMSTEC	03015
Number on surface float	T09
ARGOS PTT number	30841
ARGOS backup PTT number	29698
Deployed date	15 Aug. 2012
Recovered date	08 Mar. 2014
Exact location	02° 02.3N, 156° 01.3E
Depth	2,573 m
Nominal location	EQ, 156E
ID number at JAMSTEC	04015
Number on surface float	T10
ARGOS PTT number	29759
ARGOS backup PTT number	24715
Deployed date	10 Aug. 2012
Recovered date	03 Mar. 2014
Exact location	00° 01.0N, 156° 02.5E
Depth	1,953 m
Nominal location	2S, 156E

ID number at JAMSTEC	05013
Number on surface float	T11
ARGOS PTT number	32293
ARGOS backup PTT number	29708
Deployed date	09 Aug. 2012
Recovered date	01 Mar. 2014
Exact location	02° 01.0S, 155° 57.5E
Depth	1,749 m

Nominal location	5S, 156E
ID number at JAMSTEC	06013
Number on surface float	T17
ARGOS PTT number	29767
ARGOS backup PTT number	29738
Deployed date	03 Aug. 2012
Recovered date	27 Feb. 2014
Exact location	05° 02.0S, 156° 01.5E
Depth	1,523m

Nominal location	5N, 147E
ID number at JAMSTEC	07013
Number on surface float	T18
ARGOS PTT number	29719
ARGOS backup PTT number	24230
Deployed date	25 Jul. 2012
Recovered date	19 Feb. 2014
Exact location	04° 57.8N, 147° 01.6E
Depth	4,293 m

Nominal location	2N, 147E
ID number at JAMSTEC	08012
Number on surface float	T19
ARGOS PTT number	28157
ARGOS backup PTT number	24240
Deployed date	28 Jul. 2012
Recovered date	19 Feb. 2014

Exact location	02° 04.5N, 146° 57.1E	
Depth	4,491 m	

Nominal location	EQ, 147E
ID number at JAMSTEC	09013
Number on surface float	T22
ARGOS PTT number	28320
ARGOS backup PTT number	24229
Deployed date	29 Jul. 2012
Recovered date	21 Feb. 2014
Exact location	00° 03.5N, 147° 00.7E
Depth	4,473 m

*: Dates are UTC and represent anchor drop times for deployments and release time for recoveries, respectively.

(7) Details of deployed

We had deployed seven TRITON buoys, described them details in the list.

Deployment TRITON buoys

Observation No.	Location	Details
02015	5N156E	Deploy with full spec.
03016	2N156E	Deploy with full spec and 1 optional unit. SBE37 (CT) : 175m
04016	EQ156E	Deploy with full spec and 2 optional sensors. Security camera : with TRITON top buoy SBE37 (CT) : 175m
05014	2S156E	Deploy with full spec.
06014	5S156E	Deploy with full spec.
08013	2N147E	Deploy with full spec and 1 optional unit. SBE37 (CT) : 175m
09014	EQ147E	Deploy with full spec and 1 optional unit. SBE37 (CT) : 175m

(8) Data archive

Hourly averaged data are transmitted through ARGOS satellite data transmission system

in almost real time. The real time data are provided to meteorological organizations via Global Telecommunication System and utilized for daily weather forecast. The data will be also distributed world wide through Internet from JAMSTEC and PMEL home pages. All data will be archived at JAMSTEC Mutsu Institute.

TRITON Homepage :　http://www.jamstec.go.jp/jamstec/triton

7.2 Subsurface ADCP moorings

(1) Personnel

Takuya Hasegawa	(JAMSTEC): Principal Investigator
Tomohide Noguchi	(MWJ): Operation leader
Keisuke Matsumoto	(MWJ): Technical staff
Hiroki Ushiromura	(MWJ): Technical staff
Masahiro Orui	(MWJ): Technical staff
Kanako Yosida	(MWJ): Technical staff

(2) Objectives

The purpose of this ADCP observation is to get knowledge of physical process underlying the dynamics of oceanic circulation in the western equatorial Pacific Ocean. We have been observing subsurface currents using ADCP moorings along the equator. In this cruise (MR14-02), we recovered three subsurface ADCP moorings at Eq-156E, 2.6S-153E and 2.8S-153E. And we deployed one subsurface ADCP moorings at Eq-156E.

Recovery of the ADCP mooring at 2.6S-153E and 2.8S-153E (off PNG) is new one. Components of this mooring are depicted in Figure 7.2-1, Figure 7.2-2 and Figure 7.2-3.

(3) Parameters

・Current profiles

・Echo intensity

・Pressure, Temperature and Conductivity

(4) Methods

Two instruments are mounted at the top float of the mooring. One is ADCP (Acoustic Doppler Current Profiler) to observe upper-ocean currents from subsurface down to around 300m depths. The second instrument mounted below the float is CTD, which observes pressure, temperature and salinity for correction of sound speed and depth variability. Additionally, there are ADCP and CTD at intermediate part mooring rope. Details of the instruments and their parameters are as follows:

1) ADCP

Broadband ADCP 150 kHz (Teledyne RD Instruments, Inc.)

Distance to first bin : 8 m

Pings per ensemble : 16 (Only Eq-156E is 10 pings.)

Time per ping : 2.00 seconds

Number of depth cells : 40

Bin length : 8.00 m

Sampling Interval : 3600 seconds

Recovered ADCP

- ・ Serial Number : 1224 (Mooring No.120812-00156E)
- ・ Serial Number : 1152 (Mooring No.120801-2.6S153E)

Work horse ADCP 75 kHz (Teledyne RD Instruments, Inc.)

Distance to first bin : 7.04 m

Pings per ensemble : 27

Time per ping : 6.66 seconds

Number of depth cells : 60

Bin length : 8.00 m

Sampling Interval : 3600 seconds

Recovered ADCP

- ・ Serial Number : 3200 (Mooring No.120801-2.6S153E)
- ・ Serial Number : 7176 (Mooring No.120801-2.8S153E)
- ・ Serial Number : 2541 (Mooring No.120801-2.8S153E)

Deployed ADCP

- ・ Serial Number : 1645 (Mooring No.140305-00156E)

2) CTD

SBE-16 (Sea Bird Electronics Inc.)

Sampling Interval : 1800 seconds

Recovered CTD

- ・ Serial Number : 1282 (Mooring No. 120812-00156E)
- ・ Serial Number : 2611 (Mooring No.120801-2.6S153E)
- ・ Serial Number : 1276 (Mooring No.120801-2.6S153E)
- ・ Serial Number : 1283 (Mooring No.120801-2.8S153E)
- ・ Serial Number : 1280 (Mooring No.120801-2.8S153E)

Deployed CTD

- ・ Serial Number : 1288 (Mooring No. 140305-00156E)

3) Other instrument

(a) Acoustic Releaser (BENTHOS,Inc.)

Recovered Acoustic Releaser

- Serial Number : 719 (Mooring No.101212-00156E)
- Serial Number : 634 (Mooring No.101212-00156E)
- Serial Number : 956 (Mooring No.120801-2.6S153E)
- Serial Number : 716 (Mooring No.120801-2.6S153E)
- Serial Number : 694 (Mooring No.120801-2.8S153E)
- Serial Number : 632 (Mooring No.120801-2.8S153E)

Deployed Acoustic Releaser
- Serial Number : 960 (Mooring No. 140305-00156E)
- Serial Number : 677 (Mooring No. 140305-00156E)

(b) Transponder (BENTHOS,Inc.)

Recovered Transponder
- Serial Number : 46472 (Mooring No.120801-2.6S153E)
- Serial Number : 56413 (Mooring No.120801-2.8S153E)

Deployed Transponder
- Serial Number : 61939 (Mooring No. 140305-00156E)

(5) Deployment

Deployment of the ADCP mooring at Eq-156E was planned to mount the ADCP at about 400m depths. During the deployment, we monitored the depth of the acoustic releaser after dropped the anchor.

The position of the mooring No. 140305-00156E

Date: 05 Mar. 2014   Lat: 00-02.19S   Long: 156-08.04E   Depth: 1,950m

(6) Recovery

We recovered three ADCP moorings. One was deployed on 01 Aug. 2012 and the other was deployed on 12 Aug. 2012 (MR12-03cruise). After the recovery, we uploaded CTD data into a computer, and then raw data were converted into ASCII code. However, ADCP recovered at Eq-156E was not able to collect data. The results of mooring show from Figure 7.2-4 to Figure 7.2-12.

(7) Data archive

All data will be opened at the following web page:.

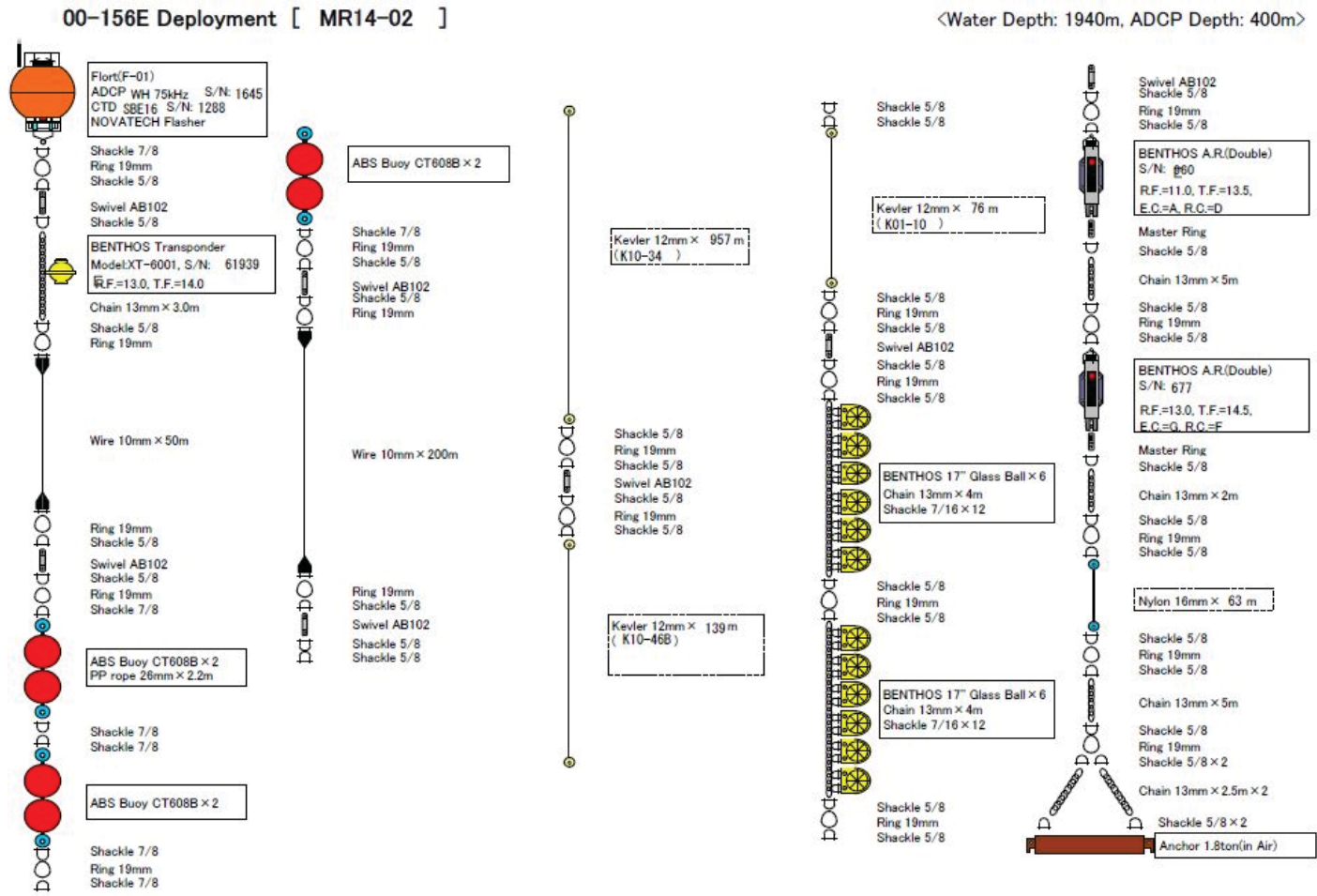http://www.jamstec.go.jp/rigc/j/tcvrp/ipocvrt/adcp_data.html

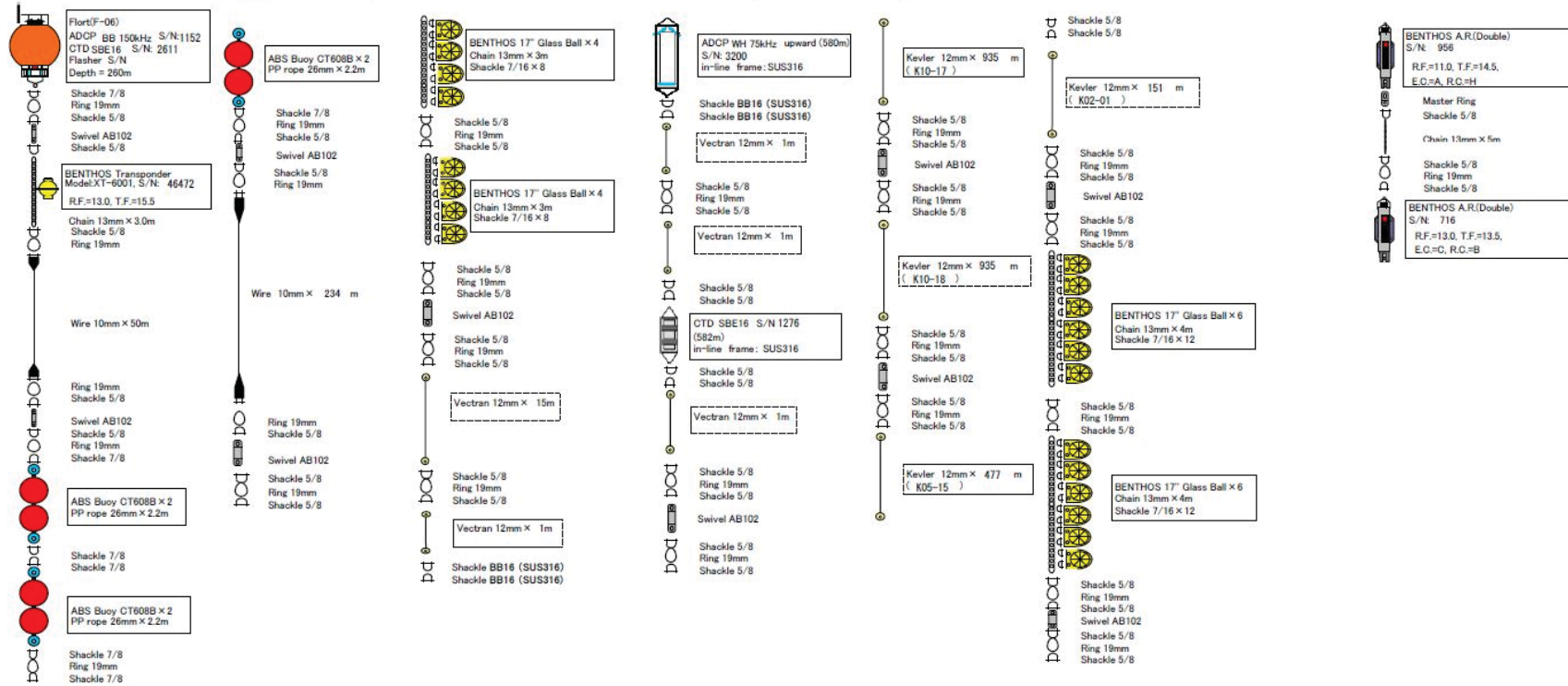Fig.7.2-1 Mooring diagram of Deploy mooring (Eq-156E)

Fig.7.2-2 Mooring diagram of Deploy mooring (2.6S-153E)

101

2.805S-153.220E Recovery [MR14-02]

<Water Depth: 3470m, ADCP Depth:340 m>

Flort(F-06)
ADCP WH 75kHz S/N: 7176
CTD SBE16 S/N: 1283
Flasher S/N
Depth = 340m

Shackle 7/8
Ring 19mm
Shackle 5/8
Swivel AB102
Shackle 5/8

BENTHOS Transponder
Model: XT-6001 S/N: 56413
R.F.=13.0. T.F.=14.5.

Chain 13mm × 3.0m
Shackle 5/8
Ring 19mm

Wire 10mm × 50m

Ring 19mm
Shackle 5/8
Swivel AB102
Shackle 5/8
Ring 19mm
Shackle 7/8

ABS Buoy CT608B × 2
PP rope 26mm × 2.2m

Shackle 7/8
Shackle 7/8

ABS Buoy CT608B × 2
PP rope 26mm × 2.2m

Shackle 7/8
Ring 19mm
Shackle 7/8

ABS Buoy CT608B × 2
PP rope 26mm × 2.2m

Shackle 7/8
Ring 19mm
Shackle 5/8
Swivel AB102
Shackle 5/8
Ring 19mm

Shackle 5/8
Shackle 5/8
Ring 19mm

Wire 10mm × 234 m

Ring 19mm
Shackle 5/8

Swivel AB102

Shackle 5/8
Ring 19mm
Shackle 5/8

BENTHOS 17'' Glass Ball × 4
Chain 13mm × 3m
Shackle 7/16 × 8

Shackle 5/8
Ring 19mm
Shackle 5/8

BENTHOS 17'' Glass Ball × 4
Chain 13mm × 3m
Shackle 7/16 × 8

Shackle 5/8
Ring 19mm
Shackle 5/8

Swivel AB102

Shackle 5/8
Shackle 5/8
Ring 19mm
Shackle 5/8

Vectran 12mm × 15m

Shackle 5/8
Ring 19mm
Shackle 5/8

Vectran 12mm × 1m

Shackle BB16 (SUS316)
Shackle BB16 (SUS316)

ADCP WH 75kHz upward (660m)
S/N: 2541
in-line frame: SUS316

Shackle BB16 (SUS316)
Shackle BB16 (SUS316)

Vectran 12mm × 1m

Shackle 5/8
Ring 19mm
Shackle 5/8

Vectran 12mm × 1m

Shackle 5/8
Shackle 5/8

CTD SBE16 S/N 1280
(662m)
in-line frame: SUS316

Shackle 5/8
Shackle 5/8

Vectran 12mm × 1m

Shackle 5/8
Ring 19mm
Shackle 5/8

Swivel AB102

Shackle 5/8
Ring 19mm
Shackle 5/8

Vectran 12mm × 1000
m V10-01
( )

Shackle 5/8
Ring 19mm
Shackle 5/8

Swivel AB102

Shackle 5/8
Ring 19mm
Shackle 5/8

Kevler 12mm × 967 m
(K10-40)

Shackle 5/8
Ring 19mm
Shackle 5/8

Swivel AB102

Shackle 5/8
Ring 19mm
Shackle 5/8

Kevler 12mm × 476 m
(K05-12)

Shackle 5/8
Shackle 5/8

Kevler 12mm × 213 m
(K10-10B)

Shackle 5/8
Ring 19mm
Shackle 5/8

Swivel AB102

BENTHOS 17'' Glass Ball × 6
Chain 13mm × 4m
Shackle 7/16 × 12

Shackle 5/8
Ring 19mm
Shackle 5/8

BENTHOS 17'' Glass Ball × 6
Chain 13mm × 4m
Shackle 7/16 × 12

Shackle 5/8
Ring 19mm
Shackle 5/8
Swivel AB102
Shackle 5/8
Ring 19mm
Shackle 5/8

BENTHOS A.R.(Double)
S/N: 694
R.F.=13.0, T.F.=14.5,
E.C.=G, R.C.=F

Master Ring
Shackle 5/8

Chain 13mm × 5m

Shackle 5/8
Ring 19mm
Shackle 5/8

BENTHOS A.R.(Double)
S/N: 632
R.F.=13.0, T.F.=14.0,
E.C.=D, R.C.=C
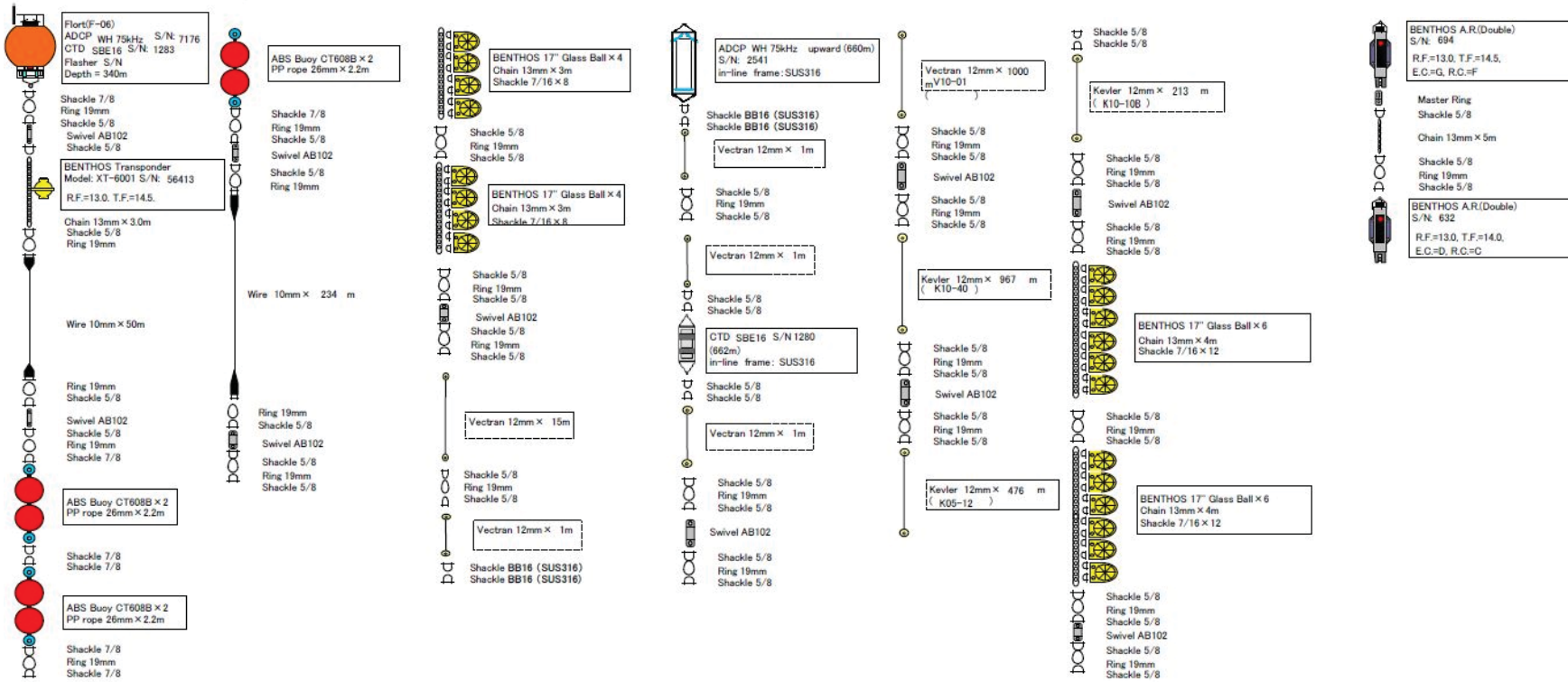
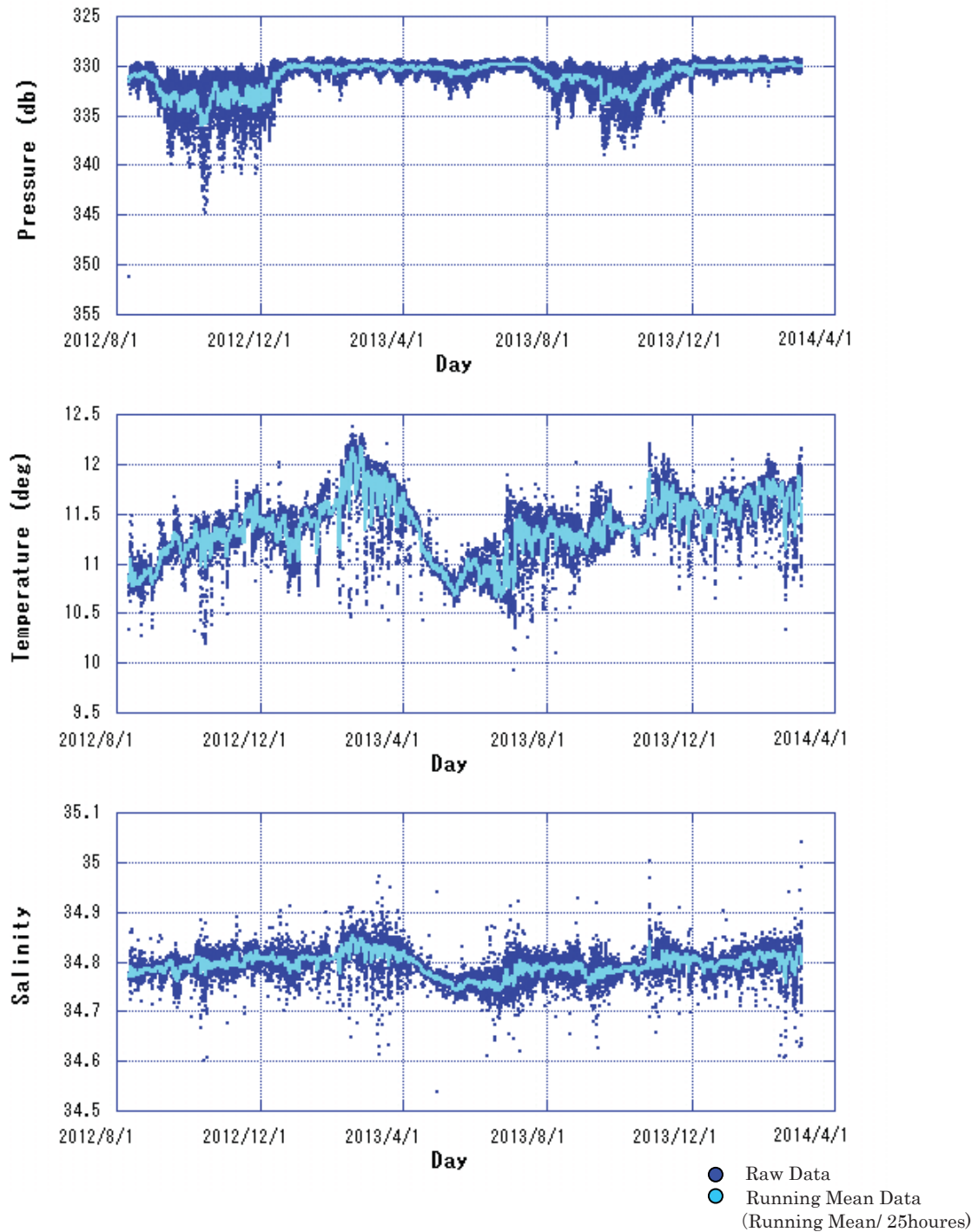Fig.7.2-3 Mooring diagram of Deploy mooring (2.8S-153E)

Fig.7.2-4 Time-series of the observed pressure (*top panel*), temperature (*middle panel*) and salinity (*bottom panel*) obtained from CTD at Eq-156E. The *dark-blue* curve indicates the raw data, while the *light-blue* curve shows the filtered data from 25 hours running-mean.
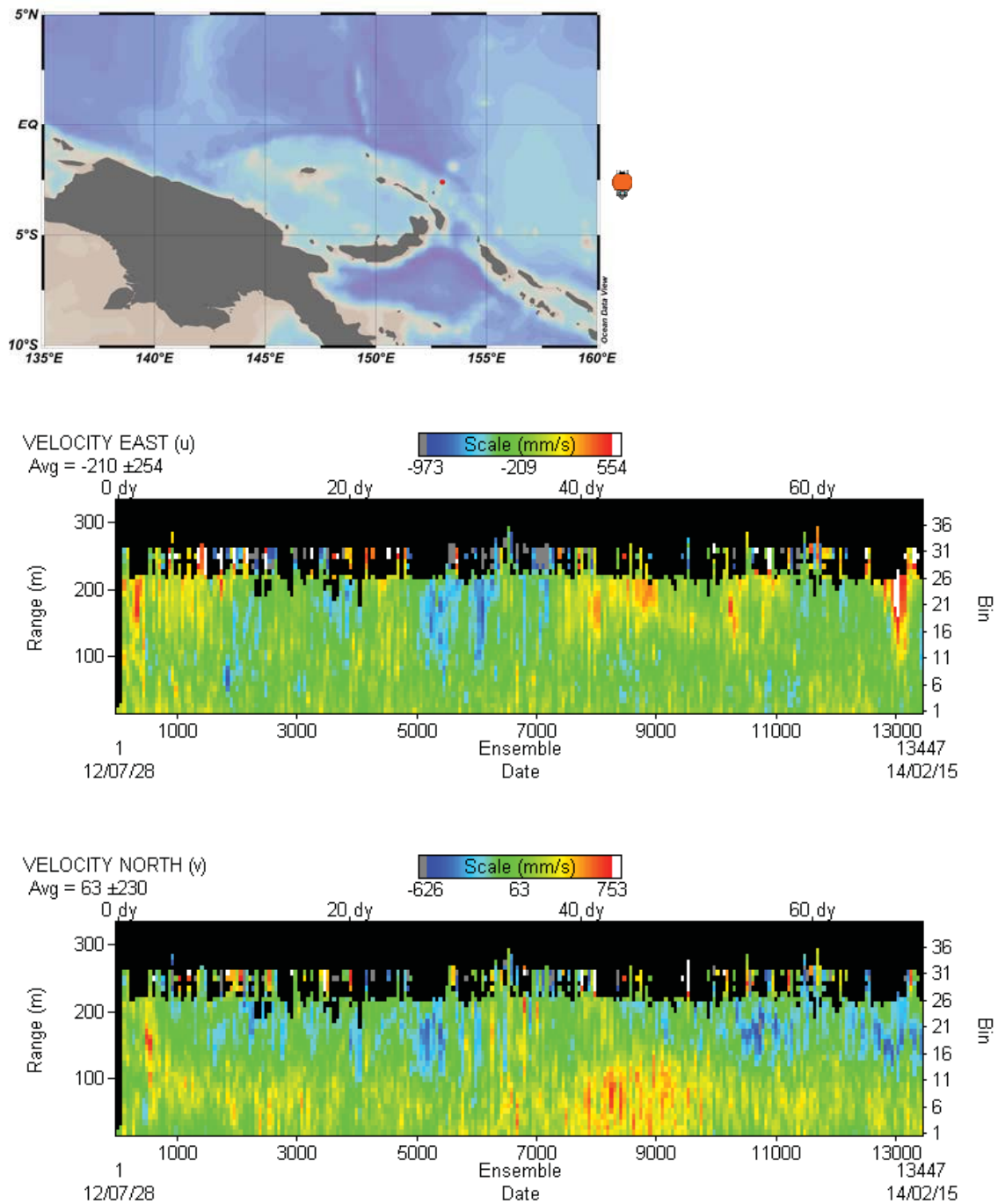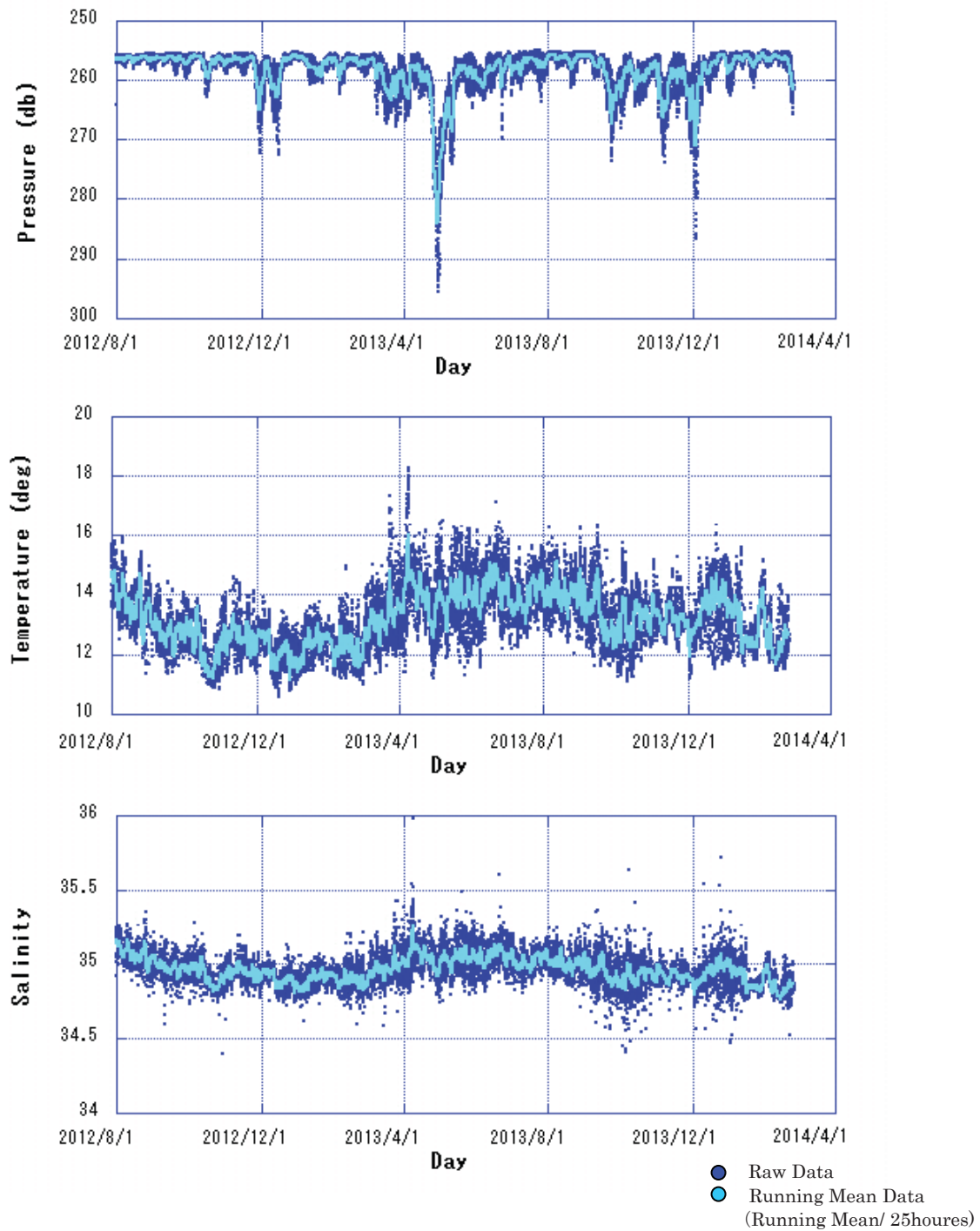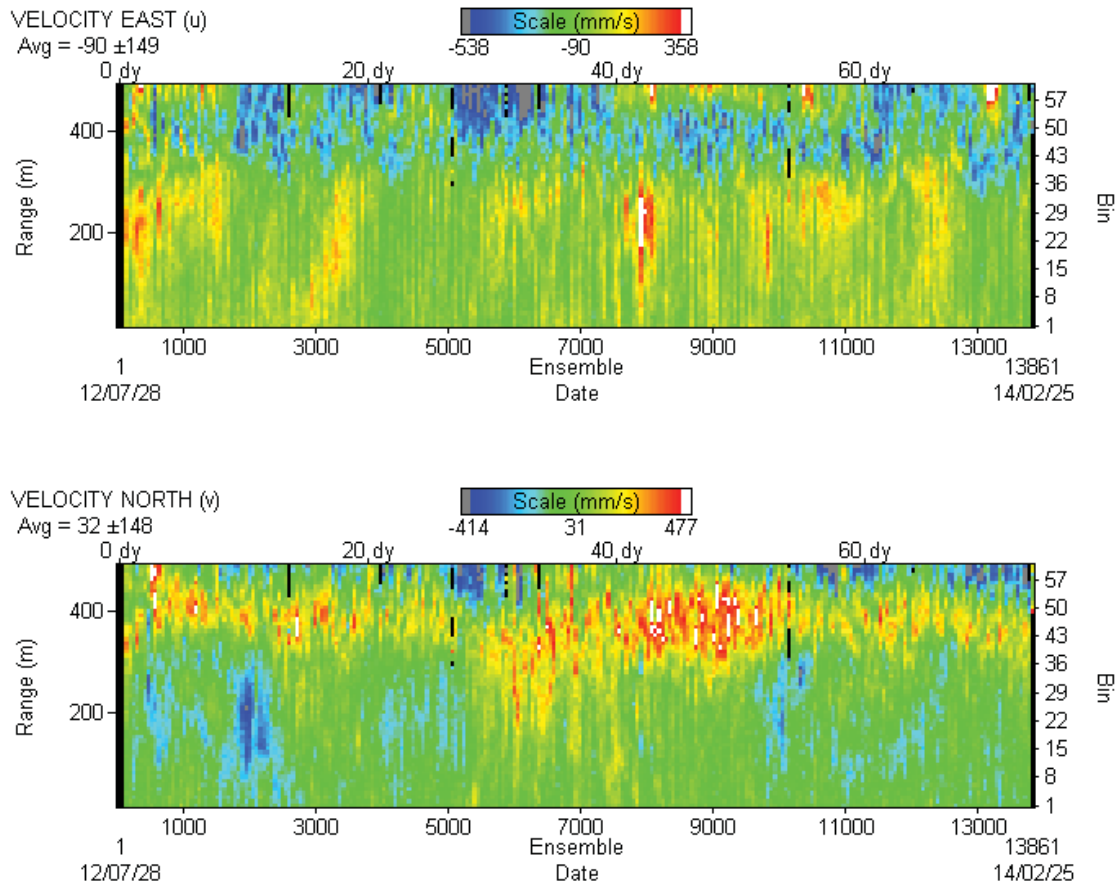
(2012/08/12-2014/03/04)

103

2.6S153E ADCP (Upper)

Fig.7.4-5 Time-depth sections of observed zonal (*top panel*) and meridional (*bottom panel*) currents
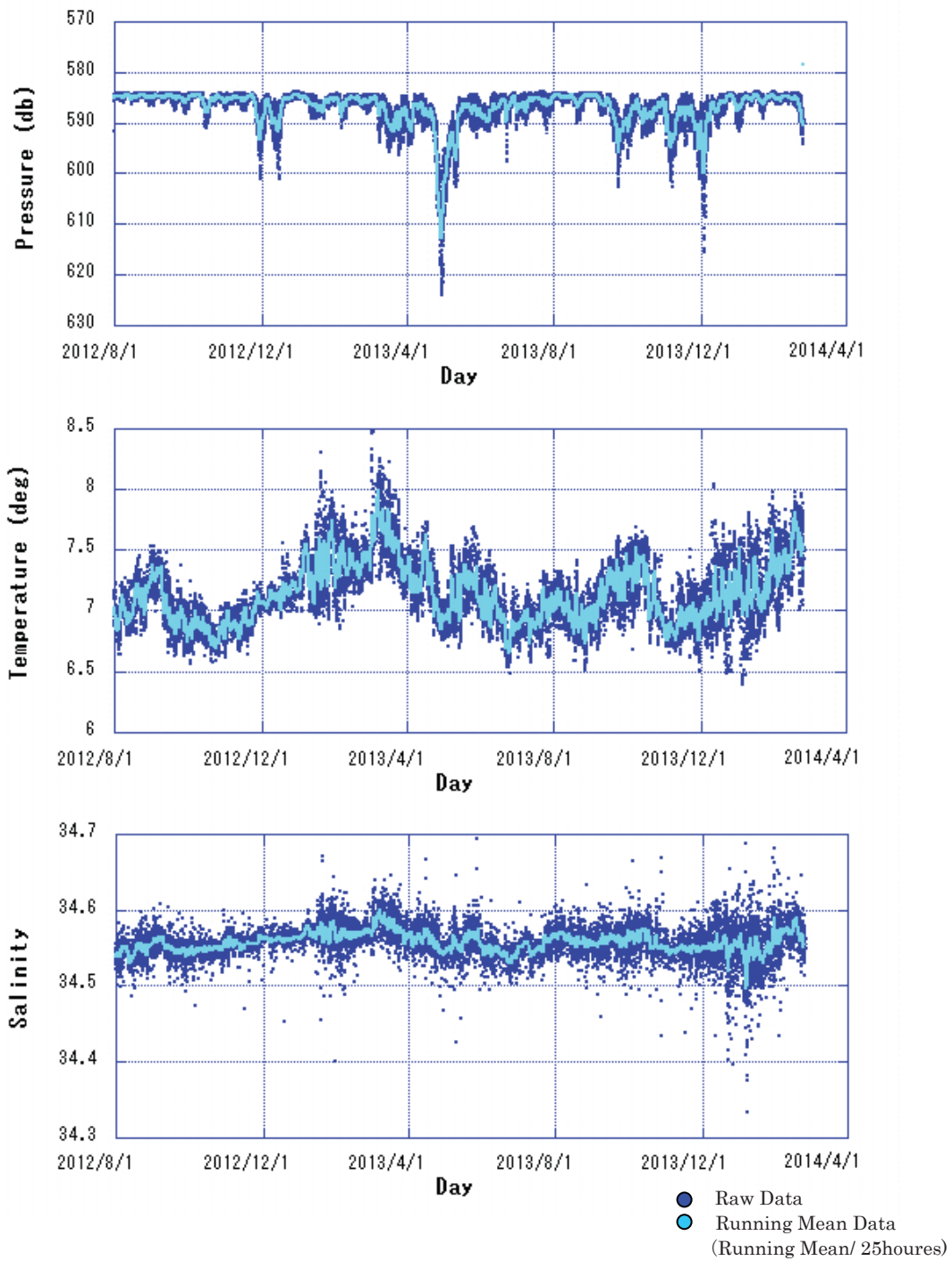obtained from ADCP mooring at 2.6S-153E.
(2012/08/01-2014/02/16)

Fig.7.2-6 Time-series of the observed pressure (*top panel*), temperature (*middle panel*) and salinity (*bottom panel*) obtained from CTD at2.6S-153E . The *dark-blue* curve indicates the raw data, while the *light-blue* curve shows the filtered data from 25 hours running-mean.

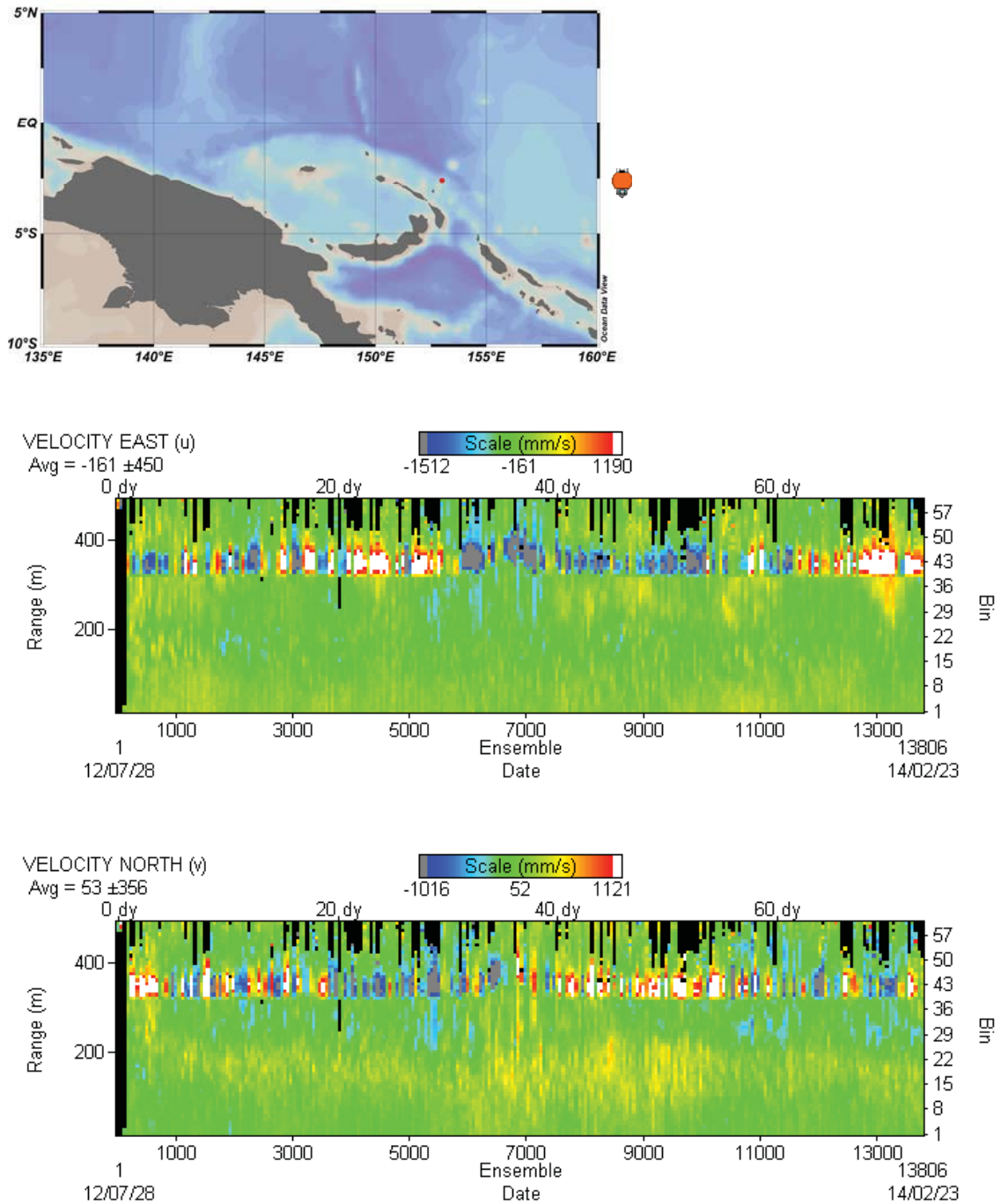(2012/08/01-2014/02/25)

2.6S153E ADCP (Lower)

Fig.7.4-7 Time-depth sections of observed zonal (*top panel*) and meridional (*bottom panel*) currents
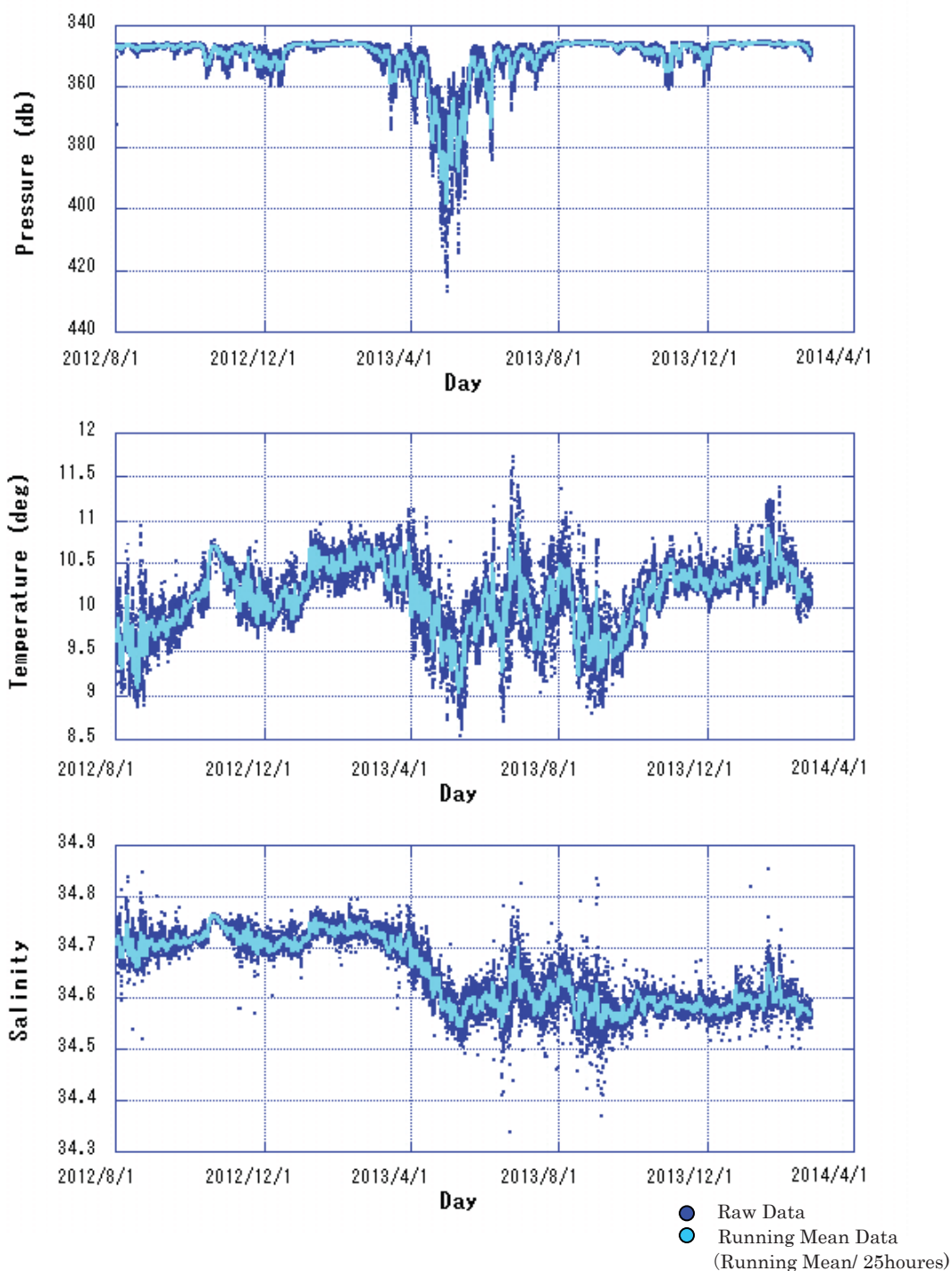   obtained from ADCP mooring at 2.6S-153E.
   (2012/08/01-2014/02/25)

Fig.7.2-8 Time-series of the observed pressure (*top panel*), temperature (*middle panel*) and salinity (*bottom panel*) obtained from CTD at 2.6S-153E . The *dark-blue* curve indicates the raw data, while the *light-blue* curve shows the filtered data from 25 hours running-mean.

(2012/08/01-2014/02/25)

107

2.8S153E ADCP (Upper)

VELOCITY EAST (u)
Avg = -161 ±450

VELOCITY NORTH (v)
Avg = 53 ±356

Fig.7.4-9 Time-depth sections of observed zonal (*top panel*) and meridional (*bottom panel*) currents obtained from ADCP mooring at 2.8S-153E. (2012/08/01-2014/02/25)

2.8S153E CTD(Upper)

Fig.7.2-10 Time-series of the observed pressure (*top panel*), temperature (*middle panel*) and salinity (*bottom panel*) obtained from CTD at 2.8S-153E . The *dark-blue* curve indicates the raw data, while the *light-blue* curve shows the filtered data from 25 hours running-mean.

(2012/08/01-2014/02/25)
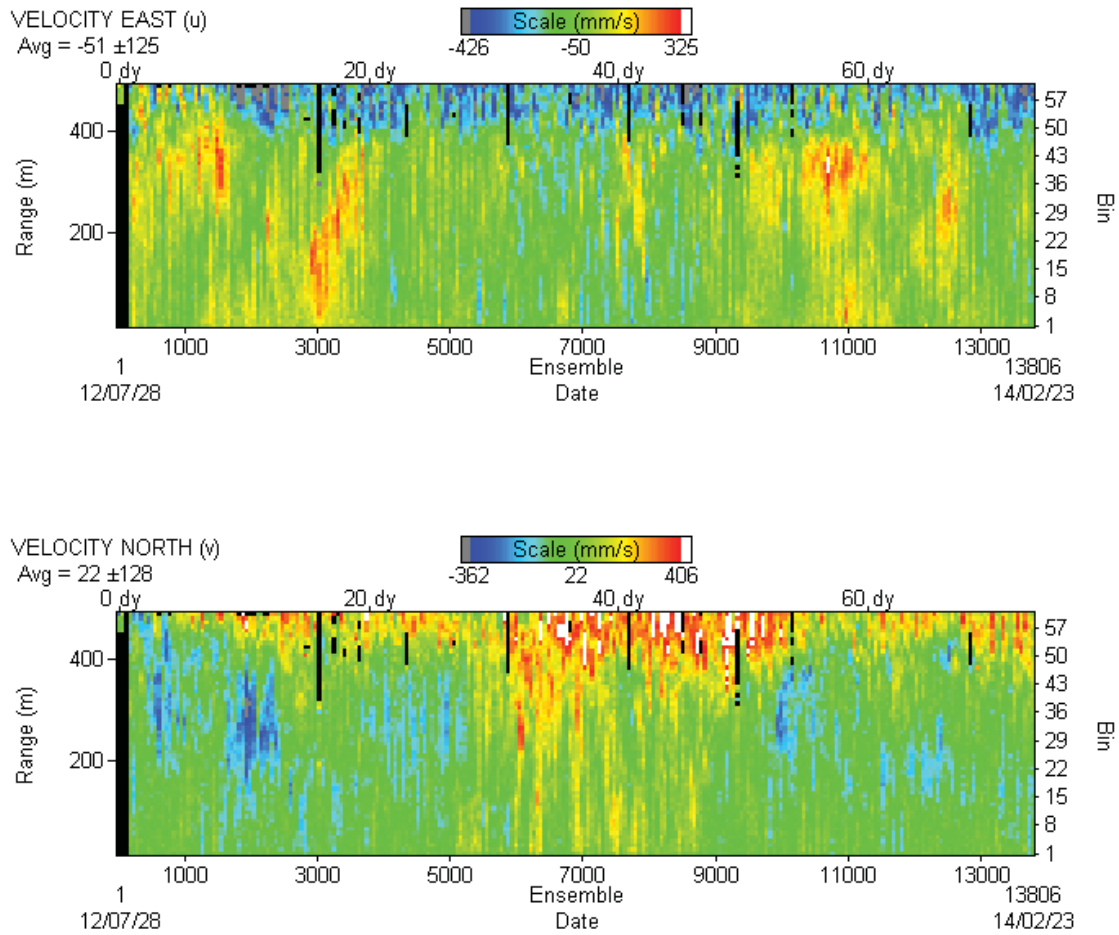
2.8S153E ADCP (Lower)

Fig.7.4-11 Time-depth sections of observed zonal (*top panel*) and meridional (*bottom panel*) currents obtained from ADCP mooring at 2.8S-153E. (2012/08/01-2014/02/25)
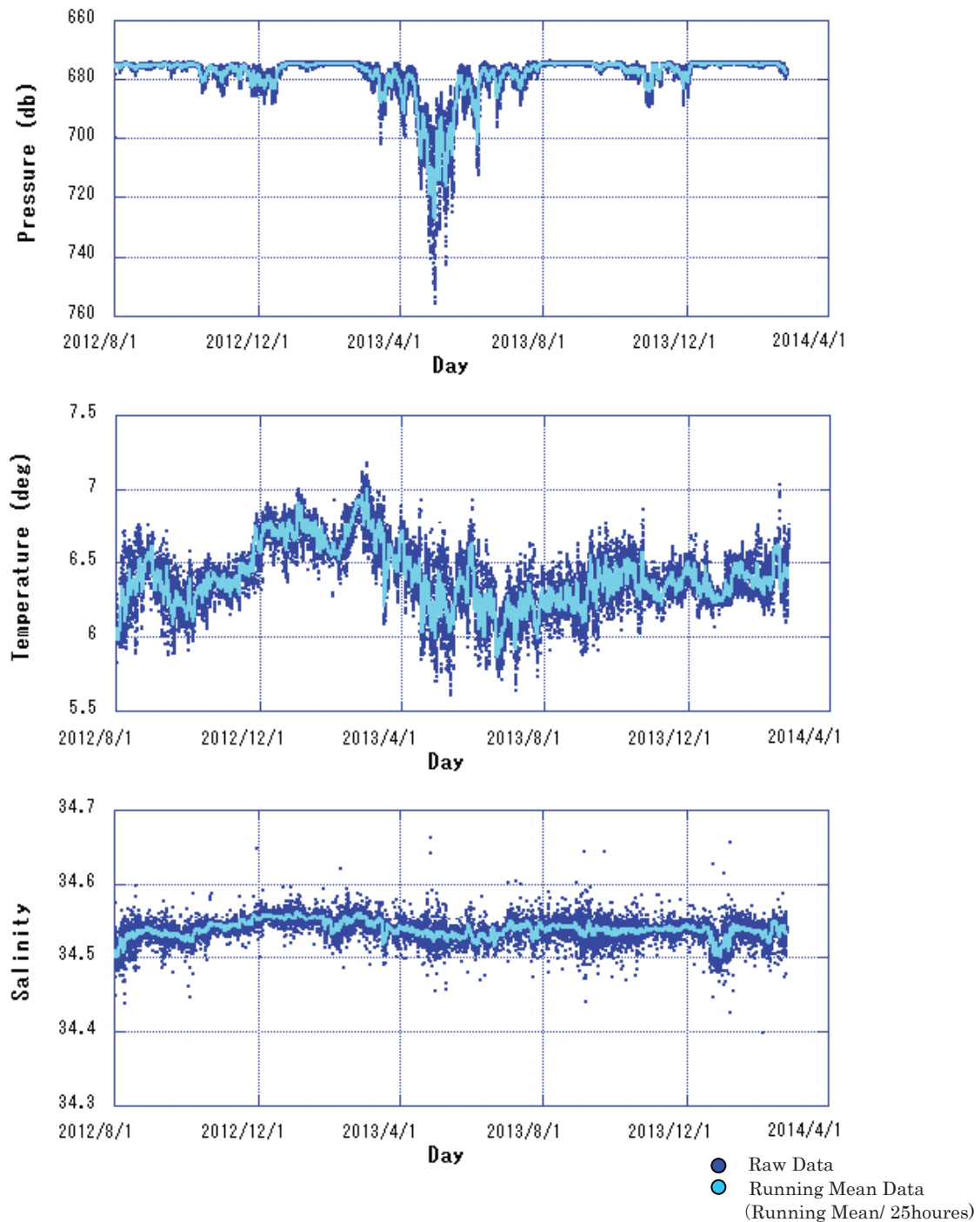
Fig.7.2-12 Time-series of the observed pressure (*top panel*), temperature (*middle panel*) and salinity (*bottom panel*) obtained from CTD at 2.8S-153E . The *dark-blue* curve indicates the raw data, while the *light-blue* curve shows the filtered data from 25 hours running-mean.

(2012/08/01-2014/02/25)

111

7.3 current profile observations using LADCP

(1) Personnel

Kelvin Richards (IPRC, University of Hawaii)

Takuya Hasegawa (JAMSTEC)

(2) Objective

To measure small vertical scale (SVS) velocity structures in the upper ocean.

(3) Overview of instrument and operation

In order to measure the velocity structure at fine vertical scales a high frequency ADCP was used in lowered mode (LADCP). The instrument was a Teledyne RDI Workhorse Sentinel 600kHz ADCP rated for 1000m depth. The instrument was attached to the frame of the CTD system using a mounting bracket (see Figure 7.3.1). The instrument was deployed on all 500m and 800m casts at CTD stations C1-C29 (excluding the full depth cast at station C22). The instrument performed well throughout its use.

Fig 7.3.1 Mounting of LADCP on the CTD Frame

The instrument is self-contained with an internal battery pack. The health of the battery is monitored by the recorded voltage count.

(4) Setup and Parameter settings

The LADCP was controlled at deploy and recover stages by a Linux PC using the python script **ladcp600.py** (written by Eric Firing, University of Hawai`i) The commands sent to the instrument at setup were contained in **ladcp600.cmd**.   The instrument was setup to have a relatively small bin depth (2m) and a fast ping rate (every 0.25 sec). The full list of commands sent to the instrument were:

CR1	# Retrieve parameter (default)
TC2	# Ensemble per burst
WP1	# Pings per ensemble
TE 00:00:00.00	# Time per ensemble (time between data collection cycles)
TP 00:00.25	# Time between pings in mm:ss
WN25	# Number of Depth cells
WS0200	# Depth cell size (in cms)
WF0088	# Blank after transit (recommended setting for 600kHz)
WB0	# Mode 1 bandwidth control (default - wide)
WV250	# Ambiguity velocity (in cm/s)
EZ0111101	# Sensor source (speed of sound excluded)
EX00000	# Beam coordinates
CF11101	# Data flow control parameters

(see the RDI Workhorse "Commands and Data Output Format" document for details.)

(5) Data processing

An initial sampling of the data was made using the following scripts to check that the instrument was performing correctly

plot_PTCV.py plot pressure, temperature, voltage and current counts
plot_vel.py   plot velocity from all 4 beams

Onboard data processing was performed using the Lamont Doherty Earth Observatory (LDEO, Columbia University) LADCP software package (available at ftp://ftp/ldeo.columbia.edu/pub/ant/LADCP) and software developed by Eric Firing (university of Hawai`i). The LDEO package is based on a number of matlab scripts. The package performs an inverse of the LADCP data, incorporating CTD (for depth) and GPS data, to provide a vertical profile of the horizontal components of velocity, U and V (eastward and northward, respectively), that is a best fit to specified constraints. The down- and up-casts are solved separately, as well as the full cast inverse. The package also calculates U and V from the vertical shear of velocity. The software is run using the matlab script **process_cast.m** with the configuration file **set_cast_params.m.** Frequent CTD data are required. Files of 1 second averaged CTD data were prepared for each station. Accurate time keeping is also required, particularly between the CTD and GPS data. To ensure this the CTD data records also included the GPS position. The LDEO software allows the ship's ADCP data (SADCP) to be included in the inverse calculation. The SADCP data were not included in this case so as to provide an independent check on the functioning of the LADCP.

LADCP data were also processed using the python script shearcalc.py developed by Eric Firing. This script is based on a shear method: the baroclinic velocity is got by vertically integrating the shear between bins, the barotropic velocity is got by integrating with time, and depth and the ship's velocity are got from the CTD pressure and GPS, respectively.

Because of the short range of the 600 kHz instrument (20-40m in this case) the analysis is very sensitive to the presence of the wake of the CTD system on up-casts. Individual beams can be affected; indicated by a reduced velocity over the top few bins shown in the velocity plot produced by plot_vel.py. In most cases only one out of the four beams was severely affected. In these cases calculating a 3-beam solution of the LDEO software, by ignoring the affected beam, produced much better results than the full 4 beam solution.

On-station SADCP velocity profiles were produced by averaging the five minute averaged profiles (mr140200x_000000.LTA produced using VmDAS) over the period of the CTD/LADCP cast. Care was taken to ensure the average did not contain any spurious data from periods when the ship was maneuvering.

(6) Preliminary results

An example of the on-board processed data is presented in Figure 7.3.2. Figure 7.3.2

compares the inverse (LDEO) and shear method (EF) solutions for the zonal (U) and meridional (V) components of the velocity vector with the corresponding SADCP profile for Station C20M01. The LADCP velocity has been fitted to the SADCP velocity using a second order polynomial. There is a very good correspondence between the general structure of all velocity profiles. While the large vertical scale flow is in a good agreement with the SADCP data (gray line), the LADCP solutions show a lot of smaller scale structure, not resolved by the SADCP. Especially noticeable in Figure 7.3.2 are the strong surface current (in excess of 1.2 m/s), which was in response to strong westerlies, and small vertical scale features, particularly in V that are poorly resolved by the SADCP.
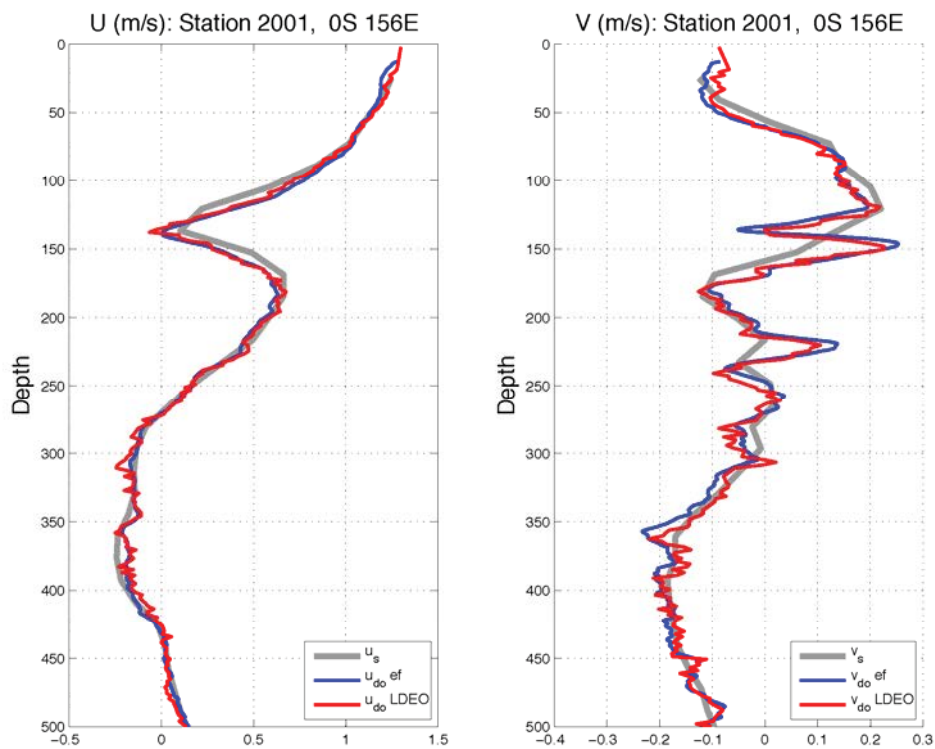

Figure 7.3.2 CTD Station C20M01: Vertical profiles of U and V calculated by the inverse (LDEO) and shear (EF) methods using LADCP data. Also shown are the profiles using SADCP data (gray lines).

7.4 Observation of ocean turbulence

(1) Personnel

> Takuya Hasagawa (RIGC, JAMSTEC)
> Kelvin Richards (IPRC)
> Kazuho Yoshida (Global Ocean Development Inc.)
> Masanori Murakami (Global Ocean Development Inc.)
> Miki Morioka (Global Ocean Development Inc.)
> Ryo Ohyama (Mirai crew, Global Ocean Development Inc.)

(2) Introduction

The western equatorial Pacific is called "Water Mass Crossroad" (Fine et al., 1994) because of complicated ocean structure due to various water masses from the northern and southern Pacific oceans. Small structure associated with ocean mixing such as interleaving was sometimes observed. Because this mixing effect is not fully implemented in the ocean general circulation model presently, it should be evaluated by in-situ observation. Considering this background, JAMSTEC started collaboration research with International Pacific Research Center (IPRC) of Univ. of Hawaii since 2007, and observations using lowered acoustic Doppler current profiler (LADCP) with high frequency were carried out since MR07-07 Leg 1. These observations revealed interesting fine structures with vertical scale of order 10m and horizontal scale of order 100km. For better understanding of ocean fine structures involving this phenomenon, we observe ocean turbulence using a Turbulence Ocean Microstructure Acquisition Profiles, Turbo Map-L, developed by JFE Advantech Co Ltd. during this cruise.

(3) Casts

Details of each cast are given in Table 7.4.1. Casts were made to a nominal 300m or 500m depth. Casts labeled 'test cast' were pressure tests with dummy probes only (with the exception of cast 20 which had 1 shear probe).

All but one cast (cast 20) was associated with a CTD/LADCP cast. The order of operations varied during the cruise.:

CTD-TMAP: casts 1-19, 21-22 and 30
XCTD-TMAP-CTD: casts 23-28 and 31
XCTD-TMAP: cast 29

XCTD deployments were made because of the lack of a conductivity measurement on the Turbo Map-L.

Using the Turbo Map-L, various parameters such as horizontal current shear are measured (see Appendix in the last part of this section).

(4) Operation and data processing

We operated the Turbo Map-L by a crane which is usually used for foods supply and installed in the middle of ship. We lowered it at the starboard of R/V Mirai (Photo 7 4-1).
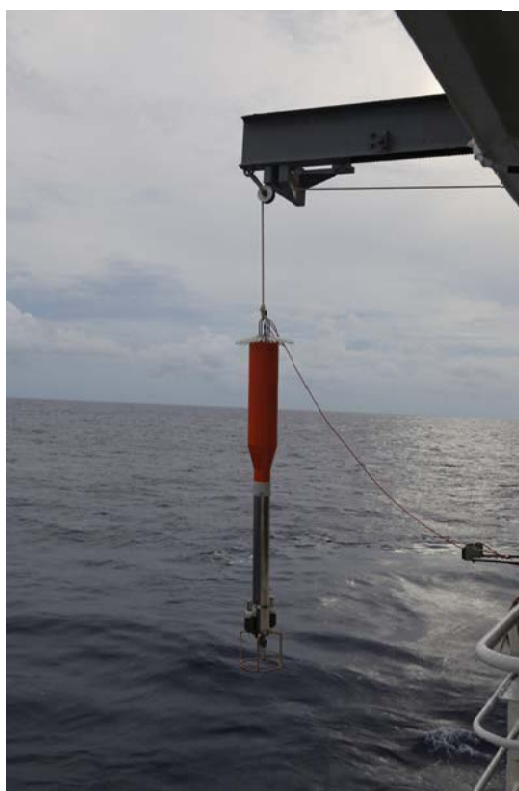

Photo 7-4-1. Observation using Turbo Map-L.

Descent rate of the Turbo Map-L was 0.5 – 0.7 m s-1. Data acquisition and processing were carried out using a PC in the Atmospheric Gas Observation Room of R/V Mirai (Photo 7-4-2). Data processing software was TM-Tool ver 3.04D provided by JFE Advantech Co Ltd.

Photo 7-4-2. Data acquisition and processing in the Atmospheric Gas Observation Room

(5) Performance

The quality of the data collected was variable. Casts 1 and 2 were fine. Cast 9 should be disregarded, as the configuration file was bad. From Cast 3 onwards various probes produced unusable data:

Shear probe 1: Bad on casts 3 and 4, but otherwise good

Shear probe 2: Bad on all casts from cast 3 onwards (no probe fitted cast 20 onwards)

CTD temperature: Good on all casts

CTD conductivity: Bad on all casts from cast 3 onwards

FP07 temperature: Good on all casts except cast 20 (no probe fitted)

(5) Preliminary results

The turbulent kinetic energy dissipation rate, ε, was calculated from data from the shear probes using software developed at the University of Hawai`i. The data were binned at 2m intervals. When available, the difference between the result from shear probes 1 and 2 is used to indicate possible bad data. If the difference is too large the lower value is taken. This was only possible on casts 1 and 2. Fig 7-4-1 shows the calculated ε from shear probe 1 for the two casts of TurboMAP at station C20. Surface induced turbulence penetrates down to ~20m. Below this layer ε increases with depth down to ~160m, presumed to be induced by a combination of the strong shear of the eastward jet and the shear associated with the small vertical scale structures in velocity between 120-160m (see Fig X.2). There is an additional region of elevated ε between

220-260m that again appears to be associated with the presence of small vertical scale flow features.
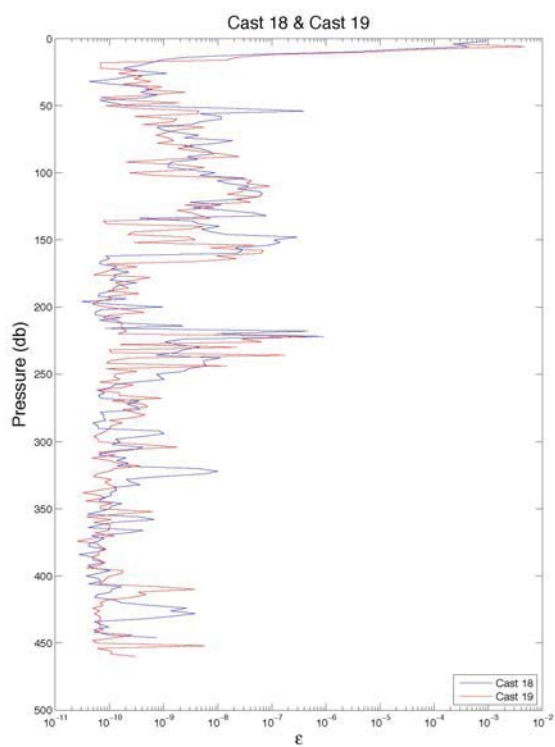

Figure 7-4-1. The turbulence kinetic energy dissipation rate, ε (W/kg), as a function of depth for casts 18 and 19 of the Turbo Map-L at station C20.

No.	Date [YYYY/MM/DD]	Longitude [deg-min]	Latitude [deg-min]	CTD Station	Logging Time Start	Stop	Depth [m]	Observation Depth[m]	Wire Length [m]	File name	FPO7	Shear 1	Shear 2	Winch	Monitor	Remarks
01	2014/02/19	147-00.58E	04-56.61N	C01	0:57	1:15	4385	605	840	MR1402-1.BIN	220	718	876	Yoshida, Murakami	Kimura, Morioka	
02	2014/02/19	147-00.36E	04-56.62N	C01	1:26	1:42	4389	596	780	MR1402-2.BIN	220	718	876	Yoshida, Murakami	Kimura, Morioka	
03	2014/02/19	146-58.77E	02-03.33N	C02	21:12	21:29	4486	511	930	MR1402-3.BIN	220	718	876	Yoshida, Morioka	Kimura, Murakami	
04	2014/02/21	147-00.22E	01-29.80N	C05	6:28	6:46	4509	556	980	MR1402-4.BIN	229	922	771	Yoshida, Murakami	Kimura, Morioka	
05										MR1402-5.BIN						Test cast
06										MR1402-6.BIN						Test cast
07										MR1402-7.BIN						Test cast
08										MR1402-8.BIN						Test cast
09	2014/03/01	156-00.24E	02-29.99S	C16	4:47	4:58	1740	362	450	MR1402-9.BIN	229	922	771	Murakami, Yoshida	Kimura, Morioka	※1 Shere 1 probe is replaced by spare (S/N: 877→S/N: 922) ※2 Config file is broken after this cast ※3 Shear2 data has large noise
10	2014/03/01	156-00.33E	02-29.99S	C16	5:21	5:31	1740	345	480	MR1402-10.BIN	229	922	771	Murakami	Kimura	Before the cast, config file is re-set.
11	2014/03/01	155-59.98E	02-29.91S	C15	8:35	8:46	1815	351	490	MR1402-11.BIN	229	922	771	Yoshida	Murakami, Kimura	
12	2014/03/01	155-58.16E	01-59.98S	C17	20:14	20:25	1748	340	490	MR1402-12.BIN	229	922	771	Yoshida	Morioka, Kimura	
13	2014/03/01	155-58.19E	02-00.04S	C17	20:33	20:44	-	345	520	MR1402-13.BIN	229	922	771	Yoshida	Morioka, Kimura	2nd cast
14	2014/03/02	156-00.63E	01-30.12S	C18	3:54	4:04	1811	326	500	MR1402-14.BIN	229	922	771	Yoshida	Kimura, Murakami	
15	2014/03/02	156-00.63E	01-30.12S	C18	4:12	4:21	-	321	510	MR1402-15.BIN	229	922	771	Yoshida	Kimura, Murakami	2nd cast ※ Descent speed rapidly decreases at 280 m depth: so, not free fall at this depth.
16	2014/03/02	156-00.62E	00-59.96S	C19	7:22	7:32	2081	341	500	MR1402-16.BIN	229	922	771	Murakami	Kimura, Yoshida	
17	2014/03/02	156-00.93E	00-59.89S	C19	7:40	7:50	2081	333	470	MR1402-17.BIN	229	922	771	Murakami, Yoshida	Kimura	2nd cast
18	2014/03/03	156-01.45E	00-01.23S	C20	3:55	4:08	1947	448	1050	MR1402-18.BIN	229	922	771	Yoshida, Murakami	Morioka, Kimura	Software finished just after the bottom: re-start the software during upward
19	2014/03/03	156-02.68E	00-01.49S	C20	4:29	4:41	1947	464	1050	MR1402-19.BIN	229	922	771	Yoshida, Murakami	Morioka, Kimura	2nd cast
20	2014/03/05	156-09.78E	00-02.53S	no CTD	4:42	4:53	1948	306	780	MR1402-20.BIN	-	922	-	Murakami	Morioka, Yoshida	Test cast
21	2014/03/06	156-00.87E	00-29.80N	C23	3:36	3:46	2139	310	550	MR1402-21.BIN	229	922	-	Murakami, Yoshida	Morioka, Yoshida	※ Shear2: dummy probe, and connector for Shear2 is not connected to the electronic circuit.
22	2014/03/06	156-01.38E	00-29.57N	C23	3:59	4:08	-	313	580	MR1402-22.BIN	229	922	-	Murakami, Yoshida	Morioka, Yoshida	2nd cast
23	2014/03/07	155-59.96E	01-29.96N	C24	3:06	3:16	2385	338	500	MR1402-23.BIN	229	922	-	Murakami	Morioka, Yoshida	※1 Shear2: dummy probe, and connector for Shear2 is not connected to the electronic circuit. ※2 Conductivity sensor: sensor is covered by rubber tape; connector for conductivity sensor is not connected to the electronic circuit.
24	2014/03/07	156-00.17E	00-59.83N	C25	6:19	6:29	2258	321	510	MR1402-24.BIN	229	922	-	Murakami	Morioka, Yoshida	※1 Shear2: dummy probe, and conneter for Shear2 is not connected to the electronic circuit. ※2 Conductivity sensor: sensor is covered by rubber tape; connector for conductivity sensor is not connected to the electronic circuit.
25	2014/03/08	156-02.69E	02-03.04N	C26	3:03	3:14	2538	365	530	MR1402-25.BIN	229	922	-	Murakami	Morioka, Yoshida	※1 Shear2: dummy probe, and connector for Shear2 is not connected to the electronic circuit. ※2 Conductivity sensor: sensor is covered by rubber tape; connector for conductivity sensor is not connected to the electronic circuit.
26	2014/03/08	156-02.63E	02-03.10N	C26	3:24	3:33	-	355	530	MR1402-26.BIN	229	922	-	Murakami	Morioka, Yoshida	2nd cast
27	2014/03/09	156-00.03E	03-00.22N	C27	5:07	5:17	2876	345	540	MR1402-27.BIN	229	922	-	Murakami	Morioka, Yoshida	※1 Shear2: dummy probe, and connector for Shear2 is not connected to the electronic circuit. ※2 Conductivity sensor: sensor is covered by rubber tape; connector for conductivity sensor is not connected to the electronic circuit.
28	2014/03/09	156-00.03E	03-00.48N	C27	5:39	5:49	2873	366	520	MR1402-28.BIN	229	877	-	Murakami	Morioka, Yoshida	2nd cast ※ Just before this cast, Shear1 probe is replaced by spare one: S/N 922→S/N 877
29	2014/03/10	156-00.18E	04-00.07N	C28	5:48	5:58	3477	354	500	MR1402-29.BIN	229	922	-	Murakami	Morioka, Yoshida	※1 Shear2: dummy probe, and conneter for Shear2 is not connected on the electronic circuit. ※2 Conductivity sensor: sensor is covered by rubber tape; connecter for conductivity sensor is not connected to the electronic circuit. ※3 Shear1: large noizes appear below 80m depth ※4 The Shear 1 is changed to S/N 877 to S/N 922
30	2014/03/10	156-00.75E	04-00.60N	C28	6:53	7:03	3477	338	500	MR1402-30.BIN	229	877	-	Murakami	Morioka, Yoshida	2nd cast ※ Just before this cast, Shear1 probe was replaced by spare one: S/N 922→S/N 877
31	2014/03/10	155-57.50E	05-02.12N	C29	19:32	19:41	3599	311	540	MR1402-31.BIN	229	877	-	Murakami	Kimura, Morioka	※1 Shear2: dummy probe, and connetor for Shear2 is not connected to the electronic circuit. ※2 Conductivity sensor: sensor is covered by rubber tape; connector for conductivity sensor is not connected to the electronic circuit.

Table 7-4-1. Details of Turbo Map-L casts

Appendix: Parameters

Using the Turbo Map-L, following parameters are measured.

Parameter	Type	Range	Accuracy	Sample Rate
$\partial u/\partial z$	Shear probe	0~10 /s	5%	512Hz
T+∂T/∂z	EPO-7 thermistor	−5~45℃	±0.01℃	512Hz
T	Platinum wire thermometer	−5~45℃	±0.01℃	64Hz
Conductivity	Inductive Cell	0~70mS	±0.01mS	64Hz
Depth	Semiconductor strain gauge	0~1000m	±0.2%	64Hz
x- acceleration	Solid-state fixed mass	±2G	±1%	256Hz
y- acceleration	Solid-state fixed mass	±2G	±1%	256Hz
z- acceleration	Solid-state fixed mass	±2G	±1%	64Hz
Chlorophyll	Fluorescence	0~100 μ g/Lm	0.5 μ g/L or ±1%	256Hz
Turbidity	Backscatter	0~100ppm	1ppm or ±2%	256Hz
$\partial u/\partial z$	Shear probe	0~10 /s	5%	512Hz

7.5 Piston core sampling

Personnel: Junichiro Kuroda (IFREE, JAMSTEC)

Toshitsugu Yamazaki (AORI, Univ. Tokyo)

Toshihiro Yoshimura (Biogeos, JAMSTEC)

Haruka Takagi (RIGC, JAMSTEC / Waseda Univ.)

Hiroyuki Hayashi (Marine Works Japan Ltd.)

Yuki Miyajima (Marine Works Japan Ltd.)

Yasumi Yamada (Marine Works Japan Ltd.)

Mika Yamaguchi (Marine Works Japan Ltd.)

Kazuho Yoshida (Global Ocean Development Inc.)

Masanori Murakami (Global Ocean Development Inc.)

Miki Morioka (Global Ocean Development Inc.)

Ryo Kimura (Mirai Crew)

7.5.1 Scientific objectives

In this cruise we aim to sample Quaternary sediment records from the western equatorial Pacific by a piston core sampler. We chose four sites (Fig. 7.5-1), i.e., West Caroline Basin (PC01), Eauripik Rise (PC02), and Ontong Java Plateau (PC03 and PC04) to achieve 1) a depth transect from shallow (PC03, 1923 m) to deep sea (PC01, 3855 m), as well as a longitudinal transect from east (PC02, 141°24′E) to west (PC04, 156°06′E) at the similar water depths (2243 to 2447 m) and latitude (2°03′N to 3°53′N). Sediments recovered from the four sites were expected to provide continuous geological records from Pleistocene to Holocene, containing well-preserved calcareous microfossils (e.g., foraminifers) which are essential to achieve a reliable stratigraphy based on stable isotopic compositions ($\delta^{18}O$ of calcium carbonate). We address the following primary scientific objectives:

Paleomagnetism. We aim to obtain reliable paleomagnetic records during the last ca 2 Ma, in particular for paleointensity variations. For this purpose, it is necessary to evaluate influence of sediment lithological and magnetic-property changes as a recording media of geomagnetic field variations. We will attempt to extract lithological contamination to paleomagnetic records using the phase shift of carbon cycle that have occurred at approximately 1.1 Ma in the Pacific: a shift from higher to lower carbonate contents in interglacials. We will also examine influence of changes in the relative abundance of detrital and biogenic magnetic mineral components.

Radiogenic isotopes. We aim to obtain continuous isotopic records of osmium ($^{187}Os/^{188}Os$) of seawater in the Pleistocene to Holocene periods to understand processes that cause changes in seawater osmium isotopic ratios in the glacial-interglacial timescale. We also aim to identify

massive eruptive and bolide impact events in this time period to investigate either these events worked as a trigger of rapid climate change during the Pleistocene. Sediments enriched in calcareous microfossils (foraminifers) are thought to be one of the best suitable materials to reconstruct isotopic composition of osmium of seawater in the geological past.

Interstitial water chemistry. Although trace elements serve important roles as regulators of biogeochemical processes, existing knowledge is insufficient to assess a role of organic compounds (e.g., adsorption, complexation) on trace element cycles in the sediments. Insight into the effect of organic compounds on the trace element dynamics between sediments and interstitial water will involve understanding of sedimentary biogeochemical cycles.

Change in water column properties. Geochmical thermometry such as Mg/Ca ratios of calcium carbonate of planktonic foraminifers, which have different depth habitats will provide crucial information to reconstruct the time-series changes in water column properties (e.g., change in thermocline depth) of the Western Pacific Warm Pool during the Pleistocene to Holocene.
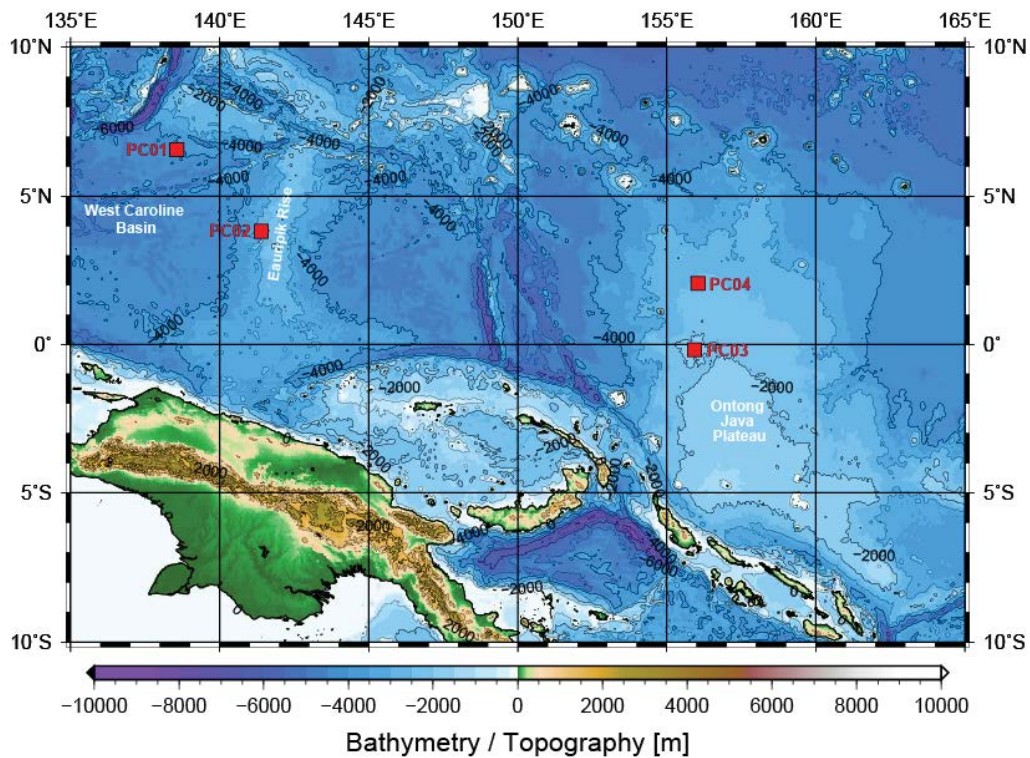

Fig. 7.5-1. Bathymetric/topographic map of the western equatorial Pacific. Stations PC 01 to PC04 are shown as red squares.

7.5.2 Explanatory notes

Site survey

We chose sites for piston coring based on detail bathymetric mapping by a multi narrow beam echo sounding system, and shallow sub-bottom structures obtained by a sub-bottom

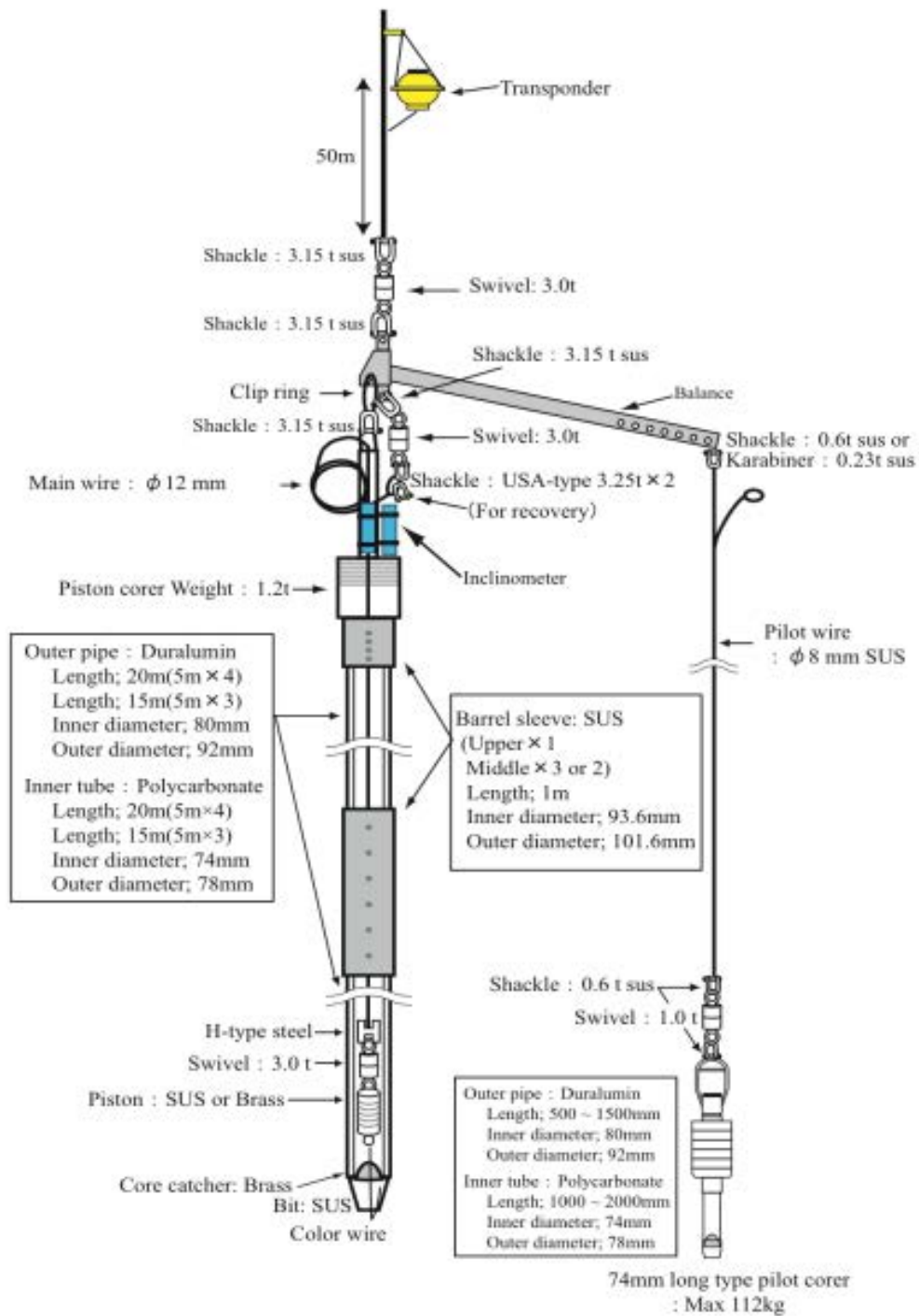profiler. For detail operations of these systems, see chapter 6.6.3.

Piston core sampling system

Piston core sampler system (PC) consists of a main weight, duralumin pipes (5 m-long each), trigger which works as a balance and a pilot core sampler (PL). Liner tubes made of polycarbonate (5 m-long per tube) are set inside of the duralumin pipes. The inner diameter (I.D.) of liner tubes is 74 mm. The outer diameter of the main winch wire is 17 mm.

In this cruise, we used a main weight of 1.2 t. The total length of duralumin pipes and liner tubes were 20 m. The pipe length was decided based on the results of site survey data. We used a 74 mm (I.D.) Long Type Pilot Corer ("74 Corer") for surface sediment sampling. The total weight of the PC system was approximately 1.4 t in water. The constructions of the PC system in this cruise are showed in Fig. 7.5-2 and Table 7.5-1. Polycarbonate tubes used as liner tubes were annealed before this cruise in order to minimize internal transformation (deformation) when split. We used a piston made of SUS body with single or double O-rings (size: P63), which was connected to the main wire via a swivel and an H-shape steel. An inclinometer was equipped on the main weight to monitor inclination and acceleration when the trigger was released. A transponder was equipped ~50 m above the trigger to monitor position and water depth of the corer.

Coring operations

A swell compensator was activated at wire out of 200 m. After that, wire was gradually let out at the speed of 1.0 m/s. The winch was stopped at a depth about 100 m above the seafloor for 3 minutes to reduce pendulum motion of the PC system. After that, the wire was stored out at the speed of 0.3 m/s. When the wire tension decreased suddenly by the release of the weight from the trigger, we confirmed the PC hit the bottom. After that, the winch was rolled up at the speed of 0.3 m/s until the tension gauge indicated the PC was completely lifted off the bottom. After leaving the bottom, the winch speed was increased to the maximum speed of 1.0 m/s.

Transponder

50m

Shackle : 3.15 t sus

Swivel: 3.0t

Shackle : 3.15 t sus

Shackle : 3.15 t sus

Clip ring

Balance

Shackle : 3.15 t sus

Swivel: 3.0t

Shackle : 0.6t sus or
Karabiner : 0.23t sus

Main wire : φ 12 mm

Shackle : USA-type 3.25t × 2

(For recovery)

Inclinometer

Piston corer Weight : 1.2t

Outer pipe : Duralumin
Length; 20m(5m × 4)
Length; 15m(5m × 3)
Inner diameter; 80mm
Outer diameter; 92mm

Barrel sleeve: SUS
(Upper × 1
Middle × 3 or 2)
Length; 1m
Inner diameter; 93.6mm
Outer diameter; 101.6mm

Inner tube : Polycarbonate
Length; 20m(5m×4)
Length; 15m(5m×3)
Inner diameter; 74mm
Outer diameter; 78mm

Pilot wire
: φ 8 mm SUS

Shackle : 0.6 t sus

Swivel : 1.0 t

H-type steel

Swivel : 3.0 t

Piston : SUS or Brass

Outer pipe : Duralumin
Length; 500 ~ 1500mm
Inner diameter; 80mm
Outer diameter; 92mm
Inner tube : Polycarbonate
Length; 1000 ~ 2000mm
Inner diameter; 74mm
Outer diameter; 78mm

Core catcher: Brass
Bit: SUS
Color wire

74mm long type pilot corer
: Max 112kg

Construction of 20m PistonCorer（MR14-02）

Fig. 7.5-2. MR14-02 Piston core sampler system（1.2t PC）

125

Table 7.5-1. Station details, operation results and specifications of the piston coring in MR14-02.

Site details							Operation results												
Area	Cruise	Station	Date (UTC)	Latitude	Longitude	Water depth (m)	Corer type	Weight (kg)	Pipe length (m)	Penet-ration (m)	Recov. (m)	Flow-in (m)	Rate (%)	Pilot wt. (kg)	Pilot recovery (cm)	Tot. wt. in water (kg)	Major lithology	MAX. tension (t)	Wire out (m)
West Caroline Basin	MR14-02	PC01	20140216	06-29.9885N	138-56.5092E	3855	IN	1200	20.0	17.1	**14.057**	0.0	70.3	112	**91.5**	1475	calcareous ooze	5.8	3790
Eauripik Rise	MR14-02	PC02	20140217	03-52.6255N	141-24.0303E	2243	IN	1200	20.0	20.0	**14.341**	0.0	71.7	112	**13.2**	1475	calcareous ooze	4.2	2183
Ontong Java Plateau	MR14-02	PC03	20140305	00-12.0027S	155-57.9961E	1923	IN	1200	20.0	20.0	**15.160**	0.0	75.8	112	**0.0**	1475	calcareous ooze	3.8	1861
Ontong Java Plateau	MR14-02	PC04	20140306	02-03.0006N	156-06.4828E	2447	IN	1200	20.0	18.4	**13.606**	0.0	68.0	112	**8.5**	1475	calcareous ooze	4.5	2384

Site details							Specification											Note
Area	Cruise	Station	Date (UTC)	Latitude	Longitude	Water depth (m)	Winch wire (kg/m)	Pipe OD (cm)	Main wire (m)	Pilot wire (m)	F.F. (m)	M.W. extra. (m)	Piston type	Piston O-ring	Bit type	Transponder	Inclinometer	Note
West Caroline Basin	MR14-02	PC01	20140216	06-29.9885N	138-56.5092E	3855	0.983	9.2	28.8	28.6	4.7	1.8	SUS	double	nomal	XT6001-10	APC-USB3	PL. pipe 1.0 m
Eauripik Rise	MR14-02	PC02	20140217	03-52.6255N	141-24.0303E	2243	0.983	9.2	28.8	28.6	4.7	1.8	SUS	double	nomal	XT6001-10	APC-USB3	PL. pipe 1.0 m
Ontong Java Plateau	MR14-02	PC03	20140305	00-12.0027S	155-57.9961E	1923	0.983	9.2	28.8	28.6	4.7	1.8	SUS	single (top)	nomal	XT6001-10	APC-USB3	PL. pipe 1.0 m
Ontong Java Plateau	MR14-02	PC04	20140306	02-03.0006N	156-06.4828E	2447	0.983	9.2	28.8	28.6	4.7	1.8	SUS	worked single (top)	nomal	XT6001-10	APC-USB3	PL. pipe 0.5 m

Core handling and analyses

As soon as the cores arrived on deck, core bit and core catcher were removed, and core catcher samples were obtained. Subsequently, inner tubes were pulled out of the barrel, and they were cut into sections (generally 1 m-long). The top and bottom of each section were capped with white and red lids. The core sections were left at a room temperature for overnight. The whole-round core sections were run through a multi-sensor core logger (MSCL). Interstitial water samples were taken from the whole round core sections with Rhizon samplers. The cores were then split into working and archive halves using a splitting devise with a nylon line (from bottom to top). Investigators should be aware that older material could have been transported upward on the split surface by splitting process.

White and blue plastic pins were put on the archive halves every 2 and 10 cm, respectively, as a stratigraphic marker. Archive half sections were photographed with a digital camera, measured color reflectance with a reflectance photospectrometer, and then described both macroscopically and microscopically. Small subsamples were taken from the archive-halves with toothpicks to make smear slides for microscopic analysis.

Physical property analyses

Physical properties such as gamma-ray attenuation (GRA), P-wave velocity (PWV), and magnetic susceptibility (MS) were measured on whole-round core sections with a GEOTEK multi-sensor core logger (MSCL). To equalize sediment temperature with room temperature, whole-core samples were kept in the laboratory overnight. Measurements were conducted on the cores every 1.0 and 2.0 cm for pilot cores and main piston cores, respectively.

Gamma-ray attenuation (GRA) was measured using a gamma ray source and a detector. They are mounted across the core on a sensor stand that aligns them with the center of the core. A narrow beam of gamma ray is emitted by Cesium-137 (^{137}Cs) with energies principally at 0.662 MeV. The photon of gamma ray is collimated through 5 mm diameter in a rotating shutter at the front of the housing of ^{137}Cs. The photon is partly absorbed in the core. The detector comprises a scintillator (a 2" diameter and 2" thick NaI crystal). GRA calibration assumes a two-phase system model for sediments, where the two phases are the minerals and the interstitial water. Aluminum has an attenuation coefficient similar to common minerals and is used as the mineral phase standard. Pure water is substituted as the interstitial-water phase standard. The actual standard consists of a telescoping aluminum rob (five elements of varying thickness) mounted in a piece of a core liner and filled with pure water. GRA was measured with 10 seconds counting.

P-wave velocity (PWV) was measured with a couple of oil-filled Acoustic Rolling Contact (ARC) transducers, which are mounted on the center sensor stand with the gamma-ray system. These transducers measure the velocity of P-wave through the core and the pulse frequency.

Magnetic susceptibility (MS) was measured using a Bartington loop sensor with an internal diameter of 100 mm. An oscillator circuit in the sensor produces a low intensity (approx. 80 A/m RMS) non-saturating, alternating magnetic field (0.565 kHz). MS was measured with the resolution of 1×10^{-5} SI (raw meter reading).

Core photography

Each archive-half core section was photographed with a digital camera (Camera body: Nikon D1x / Lens: Nikon AF-NIKKOR 24-50mm 1:3.3-4.5 D). Exceptionally, working halves were photographed for PC02. When using the digital camera, shutter speed was 1/8 ~ 1/100 sec, F-number was 3.5 ~ 6.3, sensitivity was ISO150. File format of raw data is JPEG. Details for settings were included on property of each file.

Color reflectance spectrophotometry

Color reference of visible light from sediment cores (hereafter CCR) was routinely measured using a Konica Minolta CM-2002 reference spectrophotometer (400 to 700 nm in wavelengths) which is capable to measure spectral reflectance of sediment surface with a scope of 8 mm diameter. Color references were expressed as L*, a*, and b* values which are referred to as the CIE (Commision International d'Eclairage) LAB system. It is visualized as a cylindrical coordinate

system in which the axis of the cylinder is the lightness variable L*, ranging from 0% to 100%. The radii are the chromaticity variables a* and b*. Variable a* is the green (negative) to red (positive) axis, and variable b* is the blue (negative) to yellow (positive) axis. Spectral data can be used to estimate the abundance of certain components of sediments.

The CM-2002 spectrophotometer has a specular component to be included (SCI) or excluded (SCE). In this study we applied the SCE mode, which is recommended for sediment analysis. The light reflects at a certain angle (angle of specular reflection), and the reflected light is trapped and absorbed on the integration sphere. Calibration was conducted before the measurement of core samples using a white calibration piece (CM-2002 standard accessories) without crystal clear polyethylene wrap. The reflectance of archive half cores (note that CCR was measured on working half cores for PC02) was measured through crystal clear polyethylene wrap. The measurements were taken at 2.0-cm spacing for both pilot and main piston cores. Measurement parameters are shown in Table 7.5-2.

Table 7.5-2. Measurement parameters for color reflectance spectrophotometry.

Instrument	Konica Minolta Photospectrometer CM-2002
Software	Sai check XP Ver.1.18
Illuminant	d/8 (SCE)
Light source	D65
Viewing angle	10 degree
Color system	$L^*a^*b^*$ system

Lithostratigraphy

The lithostratigraphy of sediments recovered in this cruise was determined by a combination of visual core description and smear slide analysis. The methods employed were based on those used during IODP Exp. 320/321 that drilled sediments in the eastern equatorial Pacific (Pälike *et al.*, 2009).

7.5.3. Results of piston core sampling

The results of this cruise are summarized in Table 7.5-1. As we expected, pelagic sediments composed mainly of calcareous microfossils (foraminifers and calcareous nannofossils) was recovered in each site. In station PC01, sediment samples are mixture of calcareous microfossils and clay minerals, forming an alternation of calcareous ooze and clayey calcareous ooze. In the other three stations, sediment samples contain abundant foraminifers, forming continuous calcareous ooze but the relative abundance of foraminifers varies frequently. In this section we describe brief results of site survey and coring. Detail results of visual descriptions, physical property measurements and microscopic analysis will be given elsewhere.

Station PC01

Location of PC01 (6°29.99′N, 138°56.51′E, Water depth of 3855 m) was selected in the West Caroline Basin based on the bathymetric and sub-bottom surveys. The coring site locates near a crest of topographic high which extends E-W direction (Fig. 7.5-3). This mound inclines gently toward the south and has a steep slope on the north side. Similar E-W trending mounds are visible around this site, most of which has ~50 m altitudes. A couple of deep valleys run around 7°N, which have WNW-ESE trends with ~800 m height steep slopes. These geographic structures may be a part of half-graven like structure.

Sub-bottom profiles around this site show many continuous layers with various thicknesses (inset of Fig. 7.5-3). In particular, top ~10 m of the seafloor sediments is characterized by clear thin layers (at least seven layers are visible).

At the station PC01, we recovered 0.915 m and 14.075 m sediment cores in pilot corer (PL01) and main piston corer (PC01), respectively (Table 7.5-3). Top 2.3 m of sediment samples in the PC01 become softer during the coring (seawater may be invaded in the inner tube). However, original structures and stratigraphy seem to be well preserved even for this interval. Inner polycarbonate tube of the upper 3.7 m of PC01 was slightly deformed to form a vertical dent during

the coring. Because the deformed part of the inner tube was stuck in the barrel and prevented us to pull out the inner tube from the duralumin barrel, we used a band saw to cut the pipes into sections from the top of Section 1 to the bottom of Section 4. These inner tubes were then pushed out from the bottom of each barrel with a squeezing devise. Thus investigators should be aware of possible contamination of duralumin and polycarbonate chips.

The major lithology of PL01 and PC01 is an alternation of light gray calcareous ooze and light brownish gray to grayish yellow brown clayey calcareous ooze, and also their mixture (i.e., light brownish gray calcareous ooze with clay). Calcareous nannofossils and clay minerals are the most abundant components in these sediments, but different relative abundances. In the clayey calcareous ooze, clay minerals comprise more than 25% in smear slides. Foraminifers are common throughout the core, but less abundant compared to calcareous nannofossils and clay minerals. Smear slide analysis shows that foraminifer abundance varies from 4 to 35% of total sediments. Minor amount of siliceous microfossils such as radiolarians and sponge spicules are also found in the top 2.5 m interval. The uppermost 6.5 m interval in PC01 is characterized by decimeter-scale alternation of light gray calcareous ooze and brownish clayey calcareous ooze. An interval between 6.5 and 8.4 m in core depth, light gray calcareous ooze is more predominant than brownish clayey calcareous ooze. Below 8.4 m to the bottom, light gray calcareous ooze is much more abundant, with thin intervals of slightly brownish and slightly enriched in clay minerals (calcareous ooze with clay minerals). Moderate to heavy bioturbation is visible throughout the core that makes the lithological boundaries unclear. Burrows are visible throughout the core. Almost every section contains one or two pieces of pumice or scoria (mainly < 1 cm diameter). Below 6.5 m, black spots are visible which are presumed as pyrite.
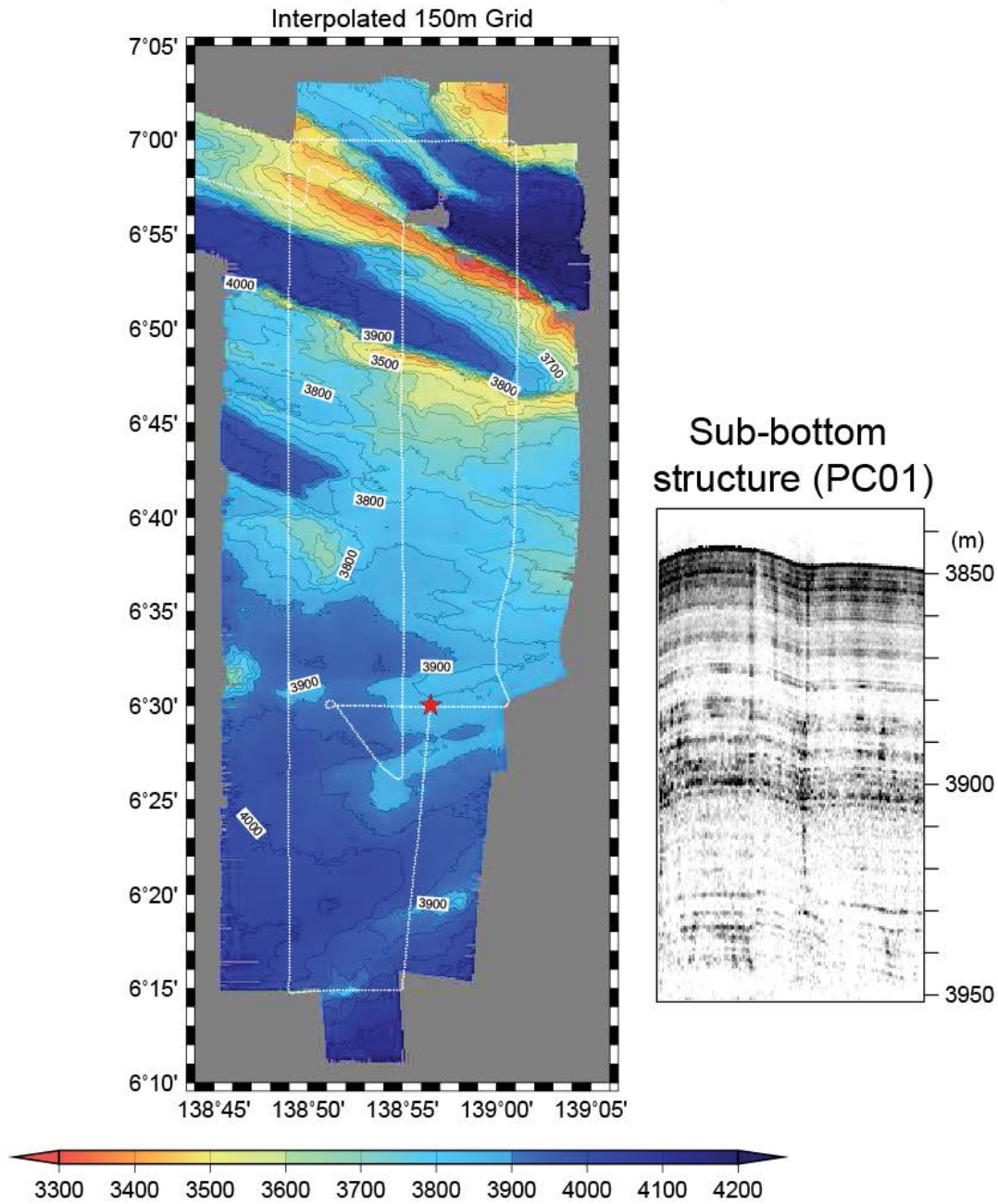
Fig. 7.5-3. Bathymetric map showing the position of PC01 (red star) and ship track (white broken line). Inset shows a sub-bottom profile on the coring site with depth from the sea surface.

130

Table 7.5-3. Lengths of sections of PL01 and PC01.

Core	Section	Length (cm)	Depth in core Top (m)	Bottom (m)
PL01		91.5	0.000	0.915
PC01	1	60.0	0.000	0.600
PC01	2	47.7	0.600	1.077
PC01	3	100.0	1.077	2.077
PC01	4	100.0	2.077	3.077
PC01	5	99.5	3.077	4.072
PC01	6	101.3	4.072	5.085
PC01	7	99.6	5.085	6.081
PC01	8	99.6	6.081	7.077
PC01	9	100.5	7.077	8.082
PC01	10	98.3	8.082	9.065
PC01	11	100.5	9.065	10.070
PC01	12	100.0	10.070	11.070
PC01	13	100.0	11.070	12.070
PC01	14	100.0	12.070	13.070
PC01	15	98.7	13.070	14.057
Total length (m)				14.057

Station PC02

Location of PC02 (3°52.63′N, 141°24.03′E, Water depth 2243 m) was selected on the Eauripik Rise based on the bathymetric and sub-bottom surveys. The coring site locates at the western end of a flat-top topographic high (Fig. 7.5-4). This topographic high dips toward west. We confirmed that there was no sea mounts or submarine channel nearby the coring site that could supply reworked materials.

Sub-bottom profiles in this site show strong reflection at the seafloor, and nearly homogenous inside the sediments but a clear reflector around 15 m beneath the seafloor (inset of Fig. 7.5-4). We speculated that the strong reflection at the sea bottom indicates calcium carbonate-rich sediments. As we expected, we recovered carbonate-rich sediments in this station with lengths of 0.132 m and 14.341 m for pilot corer (PL02) and main piston corer (PC02), respectively (Table 7.5-4). Polycarbonate inner tubes were heavily deformed in Section 6 and 0-10 cm of Section 7 (3.66-4.26 m) because the inner tube was encroached into another. In this interval inner tube was folded and formed ω-like shape. Inner tubes were also deformed in the top 65 cm (from top of Section 1 to 30 cm of Section 2) and ~276 cm interval below the Section 6 (from Section 7 to 25 cm of Section 10) to form vertical dent. Top 1.8 m of sediments becomes partly soft due to coring disturbance. In spite of those disturbances, we found that original structures and stratigraphy seem to be well preserved even for heavily deformed tubes. Because the deformed part of the inner tube was stuck in the barrel and prevented us to pull out the inner tube from the duralumin barrels, we used a band saw to cut the pipes into sections from the bottom of Section 1 to the bottom of Section 4, and the boundary between Sections 5 and 6. Top of Section 1 was cut with a hack saw. These inner tubes were then pushed out from the bottom of each barrel with a squeezing devise. Thus investigators should be aware of possible contamination of duralumin and polycarbonate chips for these section ends. In addition, a joint pipe made of SUS was also cut with duralumin barrel at the section boundary between Sections 6 and 7. Thus, SUS chips could contaminate at the section end. Because the Section 6 was encroached, a ~67 cm long sediment core was stored at the bottom of the barrel without an inner tube (Section 12). This sediment sample was pushed out from the top of the section with a rod. Because this section has a bigger diameter, we cannot conduct MSCL measurements for this section. There were 1 cm-long and 2.5 cm-long sediments at section boundaries between

131

Sections 5 and 6, and Sections 11 and 12, respectively. These extra samples were stored in plastic bags. Because working half side was heavily disturbed in Section 6, we used the working halves for description, and kept the archive halves for sampling with cubes for a paleomagnetic study.

The major lithology of PL02 and PC02 is light gray to light olive gray calcareous ooze. Foraminifers and calcareous nannofossils are the most abundant components in these sediments, with various relative abundances of these components. Microscopic analysis with smear slides shows that abundances of foraminifers and calcareous nannofossils vary from 27 to 60%, and 28 to 58% of total sediments, respectively. Clay minerals are also common, comprising 4 to 15% in smear slides. Minor amount of siliceous microfossils such as radiolarians and sponge spicules are found in the top 4.5 m interval. Sediments in PL02 and the uppermost 30 cm interval in PC02 are brownish gray, but below this level sediment color becomes light gray to light olive gray. Moderate to heavy bioturbation is visible throughout the core. Below 30 cm depth of PC02, black spots (pyrite) are visible, which occasionally fill burrows. Greenish gray to light greenish gray bands are also seen below the 30 cm level of PC02. In some places such greenish gray bands cut across burrows, indicating that they were formed diagenetically (later than burrow formations). A semi-consolidated greenish gray layer was found in the lower part of Section 9, which might correspond to the reflector seen on the sub-bottom profile of this site (Fig. 7.5-4).
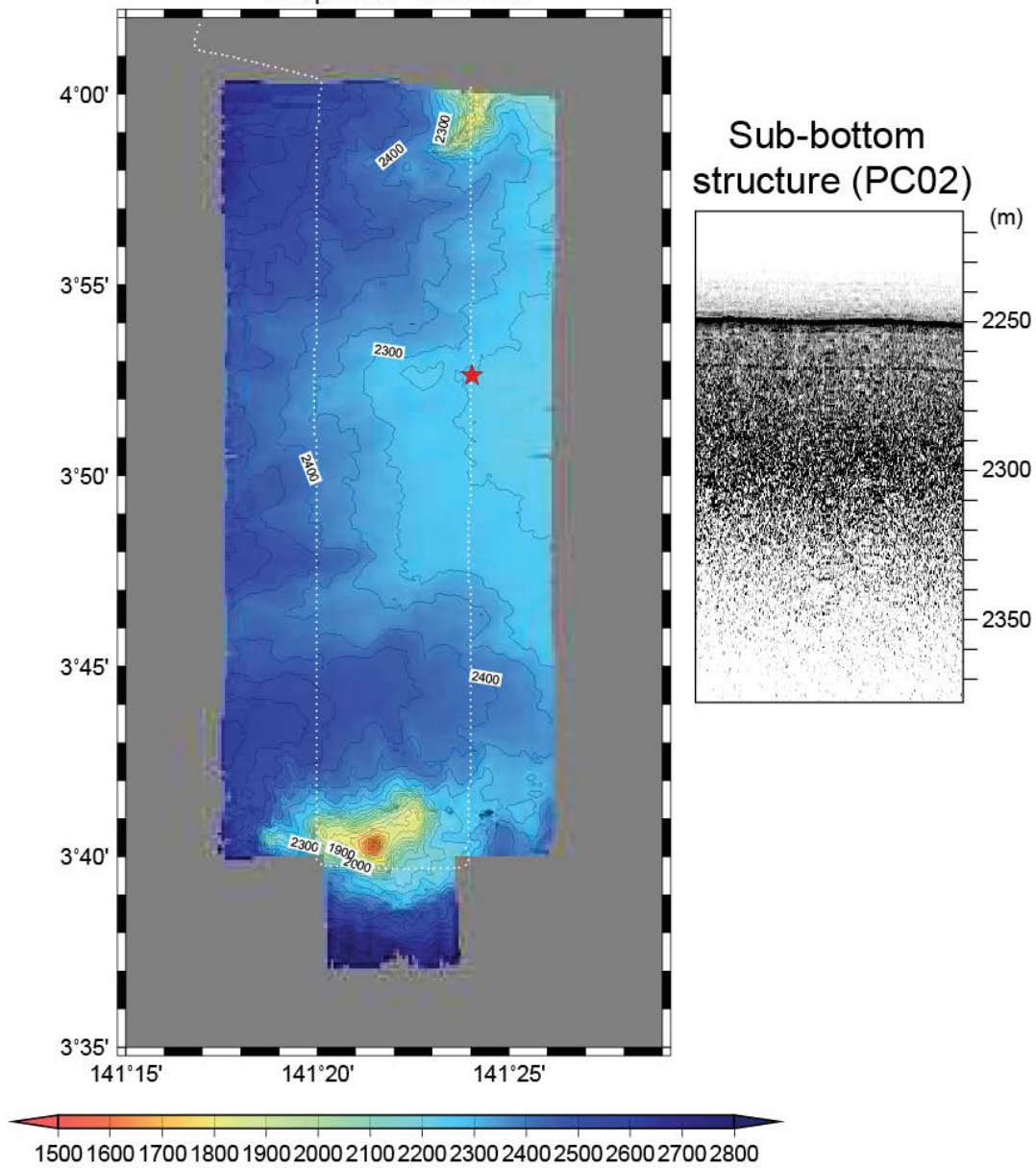
Fig. 7.5-4. Bathymetric map showing the position of PC02 (red star) and ship track (white broken line). Inset shows a sub-bottom profile on the coring site with depth from the sea surface.

133

Table 7.5-4. Lengths of sections of PL02 and PC02.

Core	Section	Length (cm)	Depth in core Top (m)	Bottom (m)
PL02		13.2	0.000	0.132
PC02	1	30.0	0.000	0.300
PC02	2	97.2	0.300	1.272
PC02	3	99.7	1.272	2.269
PC02	4	99.7	2.269	3.266
PC02	5	38.4	3.266	3.650
PC02	6	50.3	3.660	4.163
PC02	7	48.2	4.163	4.645
PC02	8	100.5	4.645	5.650
PC02	9	100.2	5.650	6.652
PC02	10	100.0	6.652	7.652
PC02	11	101.4	7.652	8.666
PC02	12	99.7	8.666	9.663
PC02	13	100.2	9.663	10.665
PC02	14	100.0	10.665	11.665
PC02	15	98.8	11.665	12.653
PC02	16	99.4	12.653	13.647
PC02	17	66.9	13.672	14.341
Total length (m)				14.341

Station PC03

Location of PC03 (0°12.00′S, 155°58.00′E, Water depth 1923 m) was selected on the Ontong Java Plateau based on the bathymetric and sub-bottom surveys. The coring site locates on a flat-top plateau (Fig. 7.5-5). We confirmed that there was no sea mounts or submarine channel nearby the coring site.

Sub-bottom profiles around this site show strong reflection at the seafloor, and nearly homogenous inside the sediments (inset of Fig. 7.5-5). We speculated that the strong reflection at the sea bottom indicates calcium carbonate-rich sediments. As we expected, we recovered carbonate-rich sediments at this station with lengths of 15.160 m (PC03), but we could not obtain surface sediments by a pilot corer (Table 7.5-5). We speculate that surface sediments were too firm to be penetrated with a 112 kg gravity pilot corer. Polycarbonate inner tubes were heavily deformed in Section 7 (4.49-5.09 m) because the inner tube was encroached into another. In this part, the inner tube was folded and formed ω-like shape. Inner tubes were also deformed above this interval, from Section 1 to Section 6 to form a vertical dent. Top 5.1 m of sediments in PC03 becomes soft due to coring disturbance. In spite of those disturbances, when the cores were split we found that original sedimentary structures and stratigraphy seem to be well preserved even for the heavily deformed tubes. Because the deformed part of the inner tube was stuck in the barrel and prevented us to pull out the inner tube from the duralumin barrels, we used a band saw to cut the pipes into sections at the top of Section 1 and from the bottom of Section 2 to the bottom of Section 7. These inner tubes were then pushed out from the bottom of each barrel with a squeezing devise. Thus investigators should be aware of possible contamination of duralumin and polycarbonate chips for these section ends. Because the Section 7 was encroached, a ~80 cm long sediment core was stored at the bottom of the barrel without an inner tube (Sections 18 and 19). This sediment sample was pushed out from the top of section with an empty polycarbonate tube. During the extraction of this core, a part of sediments was inserted in the empty tube. We set this sample as Section 18. And the other part of the sediments was set as Section 19. Because Section 19 has a bigger diameter than the other sections, we cannot

conduct MSCL measurements. ~2 cm-long sediments were left in the tube above the top of Section 1. This extra sample was stored in a plastic bag.

The major lithology of PC03 is light gray to light olive gray calcareous ooze. Foraminifers and calcareous nannofossils are the most abundant components in these sediments, with various relative abundances of these components. Microscopic analysis with smear slides shows that abundances of foraminifers and calcareous nannofossils vary from 20 to 50%, and 35 to 68% of total sediments, respectively. Clay minerals are also common, comprising 8 to 9% in smear slides. Minor amount of siliceous microfossils such as radiolarians and sponge spicules are found throughout the core. The uppermost 20 cm interval in PC03 is brownish to yellowish, but below this level sediment color becomes light gray to light olive gray. Moderate to heavy bioturbation is visible throughout the core. Below 30 cm depth of PC03, black spots (pyrite) are visible, which occasionally fill burrows. Greenish gray to light greenish gray bands are also seen frequency below the 65 cm depth of PC03.
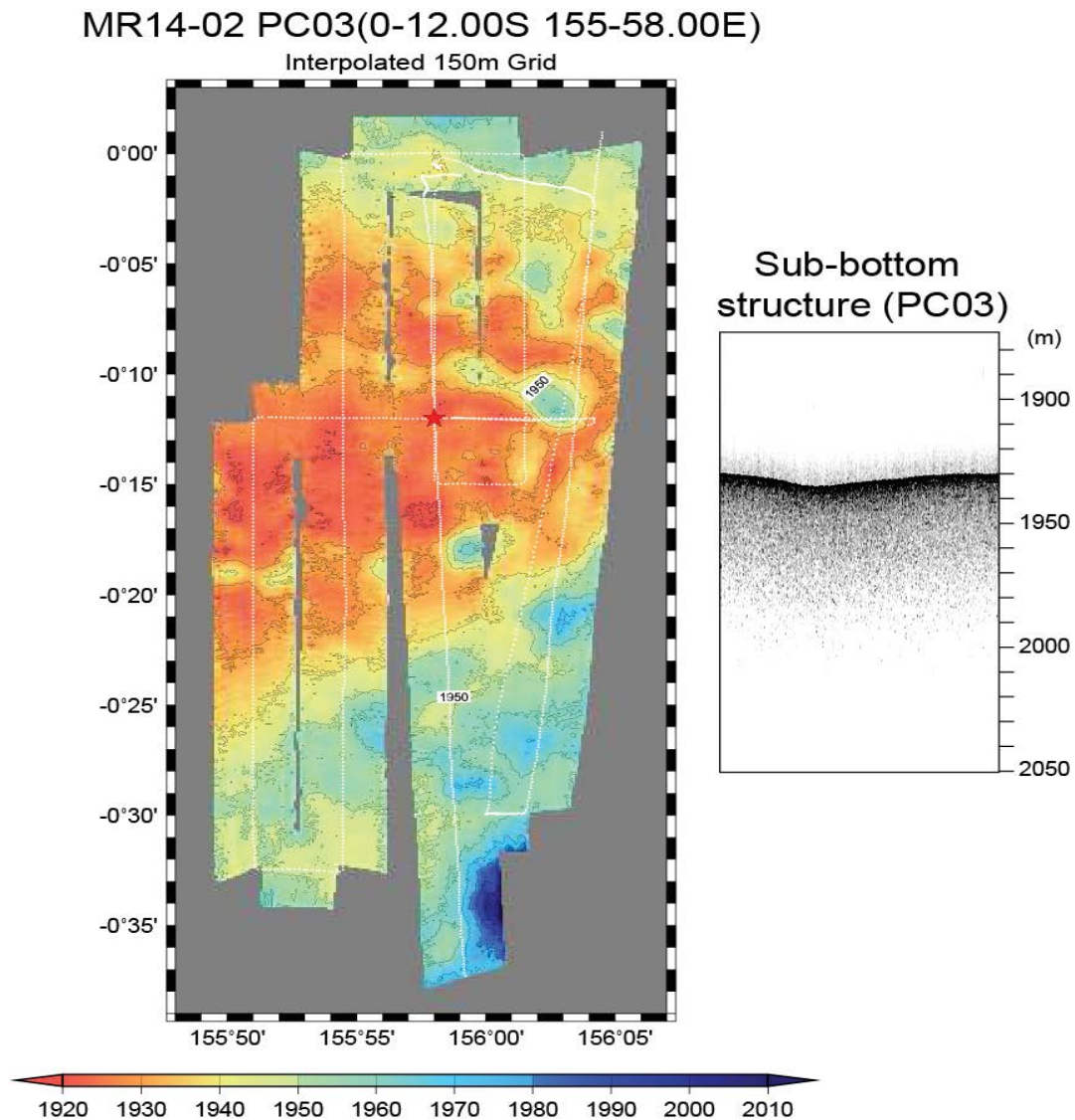

Fig. 7.5-5. Bathymetric map showing the position of PC03 (red star) and ship track (white broken line). Inset shows a sub-bottom profile on the coring site with depth from the sea surface.

Table 7.5-5. Lengths of sections of PC03.

Core	Section	Length (cm)	Depth in core Top (m)	Bottom (m)
PC03	1	24.0	0.020	0.260
PC03	2	65.2	0.260	0.912
PC03	3	61.5	0.912	1.527
PC03	4	96.2	1.527	2.489
PC03	5	100.0	2.489	3.489
PC03	6	100.0	3.489	4.489
PC03	7	60.0	4.489	5.089
PC03	8	30.0	5.089	5.389
PC03	9	98.0	5.389	6.369
PC03	10	102.4	6.369	7.393
PC03	11	100.0	7.393	8.393
PC03	12	100.0	8.393	9.393
PC03	13	98.7	9.393	10.380
PC03	14	96.5	10.380	11.345
PC03	15	102.0	11.345	12.365
PC03	16	100.0	12.365	13.365
PC03	17	99.6	13.365	14.361
PC03	18	19.4	14.361	14.555
PC03	19	60.5	14.555	15.160
Total length (m)				15.160

Station PC04

Location of PC04 (2°03.00′N, 156°06.48′E, Water depth 2447 m) was selected on the Ontong Java Plateau based on the bathymetric and sub-bottom surveys. The coring site locates on the crest of topographic high on the plateau (Fig. 7.5-6). We confirmed that there was no sea mounts or submarine channel nearby the coring site.

Sub-bottom profiles around this site show strong reflection at the seafloor, and nearly homogenous inside the sediments (inset of Fig. 7.5-6). We attributed the strong reflection at the sea bottom to calcium carbonate-rich sediments. As we expected, we recovered carbonate-rich sediments at this station with lengths of 0.085 m and 13.606 m for pilot corer (PL04) and main piston corer (PC04), respectively (Table 7.5-6). Top 0.6 m of sediments in PC04 becomes partly soft due to coring disturbance. Intervals from top to 1.3 m and from 3.6 to 7.3 m depth in PC04 were slightly deformed to form vertical dents. We used a band saw to cut the pipes into sections at the top and bottom of Section 1. The inner tube of Section 1 was then pushed out from the bottom of the barrel with a squeezing devise. Thus investigators should be aware of possible contamination of duralumin and polycarbonate chips for these section ends.

The major lithology of PL04 and PC04 is light gray to light olive gray calcareous ooze. Foraminifers and calcareous nannofossils are the most abundant components in these sediments, with various relative abundances of these components. Microscopic analysis with smear slides shows that abundances of foraminifers and calcareous nannofossils vary from 23 to 56%, and 36 to 65% of total sediments, respectively. Clay minerals are also common, comprising 7 to 13% in smear slides. Minor amount of siliceous microfossils such as radiolarians and sponge spicules are found throughout the core. Sediments in PL04 and the uppermost 30 cm interval in PC02 are brownish gray, but below this level sediment color becomes light gray to light olive gray. Moderate to heavy bioturbation is visible throughout the core. Below 85 cm depth of PC04, black spots (pyrite) are visible, which occasionally fill burrows. Greenish gray to light greenish gray bands are also seen frequently below the 85 cm level of PC04.
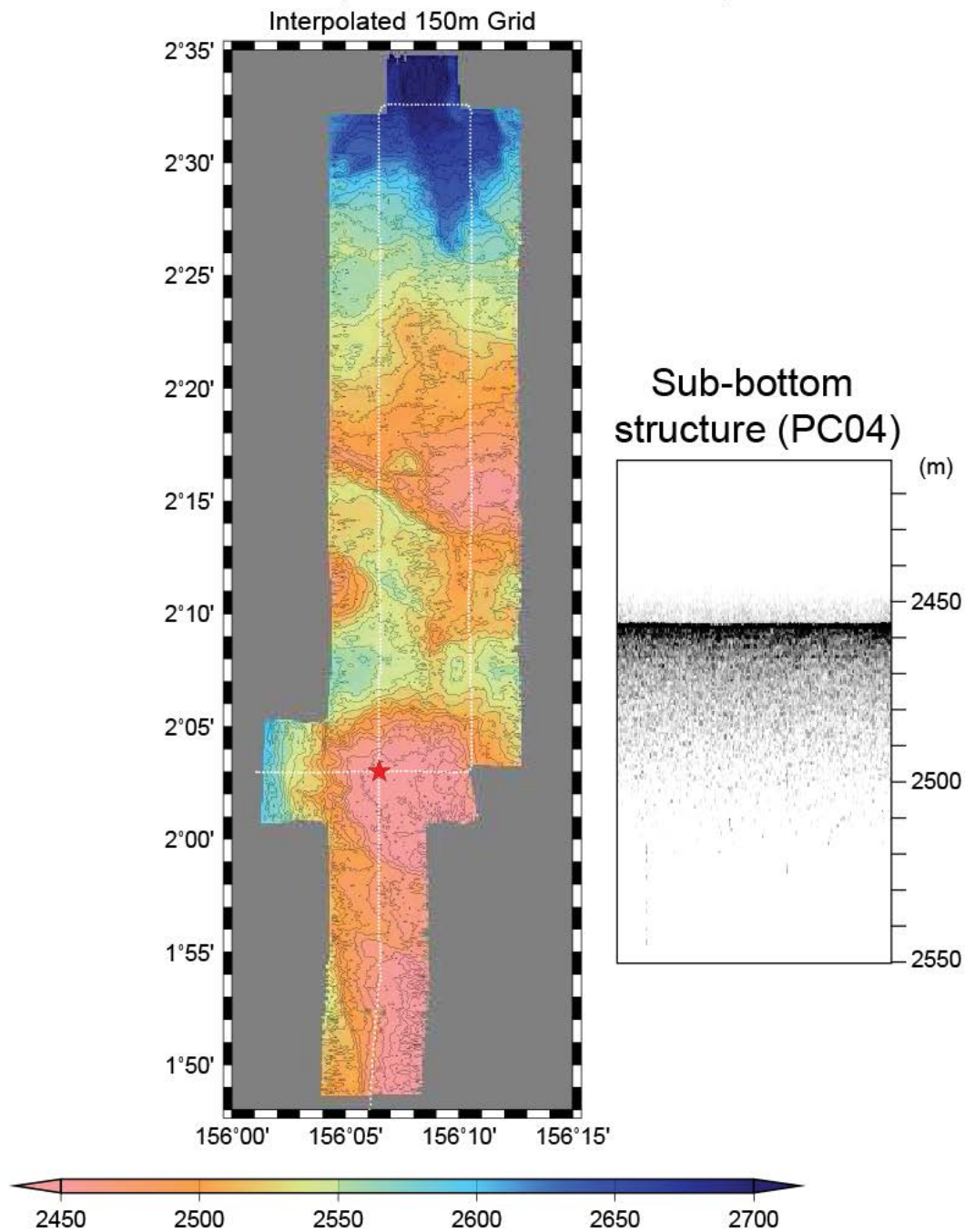
Fig. 7.5-6. Bathymetric map showing the position of PC04 (red star) and ship track (white broken line). Inset shows a sub-bottom profile on the coring site with depth from the sea surface.

137

Table 7.5-6. Lengths of sections of PL04 and PC04.

Core	Section	Length (cm)	Depth in core Top (m)	Bottom (m)
PL04		8.5	0.000	0.085
PC04	1	60.8	0.000	0.608
PC04	2	99.4	0.608	1.602
PC04	3	100.0	1.602	2.602
PC04	4	100.0	2.602	3.602
PC04	5	100.4	3.602	4.606
PC04	6	100.4	4.606	5.610
PC04	7	100.0	5.610	6.610
PC04	8	99.8	6.610	7.608
PC04	9	101.0	7.608	8.618
PC04	10	98.4	8.618	9.602
PC04	11	102.4	9.602	10.626
PC04	12	100.0	10.626	11.626
PC04	13	99.5	11.626	12.621
PC04	14	98.5	12.621	13.606
Total length (m)				13.606

References

Pälike, H., Nishi, H., Lyle, M., Raffi, I., Klaus, A., Gamage, K., and the Expedition 320/321 Scientists, 2009. Pacific Equatorial Transect. IODP Preliminary Reports, vol. 320. doi:10.2204/iodp.pr.320.2009

7.6 Water sampling and analyses for CTD bottom observation

Personal:
Osamu ABE (Nagoya Univ): Principal Investigator
Habeeb R KEEDAKKADAN (Nagoya Univ)
Hiroki USHIROMURA (MWJ)
Sonoka WAKTSUKI (MWJ)
Kanako YOSHIDA (MWJ)
Masahiro ORUI (MWJ)
Yasuhiro ARII (MWJ)
Yoshiko ISHIKAWA (MWJ)

(1) Objectives

To clarify vertical distribution of concentration and isotopic composition of dissolved oxygen, along with temperature, salinity, argon concentration, chlorophyll-a concentration and major nutrients concentrations from EQ to 25N at the northwestern Pacific.

(2) Methods

Each method is described in the following section.

(3) CTD casts and water collection

In this cruise, 6 CTD casts for collecting water samples vertically from 10m to bottom (bottom minus 10m; Table 7.6.1 and 7.6.2) were deployed. In each cast, basically 6 aliquots were collected as following orders.
1. Dissolved oxygen concentration
2. Dissolved oxygen isotope ratios
3. Dissolved argon concentration
4. Salinity
5. Nutrients concentrations (nitrate, nitrite, silicate, phosphate)
6. Chlorophyll-a concentration.

Collection depths for all stations are summarized in Table 7.6.2. As well as routine depths, depth at chlorophyll-a maximum was collected for each, which was decided by fluorescence intensity during down cast. At the chlorophyll-a maximum, samples of chlorophyll-a were collected in duplicate.

Table 7.6.0.1 CTD casts for water collection

Station	Lat-N	Long-E	Depth (m)	CTD deploy date&time Start	End	Sampling date&time Start	End
C22	-0.0023	156.0262	1957	2014/3/4 3:00	2014/3/4 4:45	2014/3/4 4:50	2014/3/4 5:59
C30	5.0057	155.9997	3608	2014/3/11 3:00	2014/3/11 5:56	2014/3/11 6:00	2014/3/11 7:08
C32	10.0073	155.1948	5469	2014/3/12 11:52	2014/3/12 15:52	2014/3/12 15:55	2014/3/12 16:56
C33	15.0127	153.1892	5999	2014/3/13 21:55	2014/3/14 2:03	2014/3/14 2:06	2014/3/14 3:03
C35	20.6662	150.9493	6042	2014/3/15 9:30	2014/3/15 13:41	2014/3/15 13:43	2014/3/15 14:43
C37	24.9983	149.1867	5717	2014/3/16 19:58	2014/3/16 23:57	2014/3/17 0:00	2014/3/17 0:51

(4) Analysis
Details of each analytical procedure are described in following sections.

Table 7.6.0.2. Detail of each CTD cast.

Station	C22	C30	C32	C33	C35	C37
Chl. Max (depth)	^{17}O, Ar (85m)	^{17}O (93m)	^{17}O, Ar (130m)	^{17}O (134m)	^{17}O, Ar (120m)	^{17}O (122m)
bott.-10 (depth)	^{17}O, Ar (1964m)	(3646m)	^{17}O, Ar (5553m)	^{17}O, Ar (6096m)	^{17}O, Ar (6146m)	^{17}O, Ar (5831m)
10dbar	^{17}O, Ar	^{17}O, Ar	^{17}O, Ar	^{17}O, Ar	^{17}O, Ar	^{17}O, Ar
30dbar	^{17}O, Ar		^{17}O, Ar		^{17}O, Ar	
50dbar	^{17}O, Ar	^{17}O, Ar	^{17}O, Ar	^{17}O, Ar	^{17}O, Ar	^{17}O, Ar
75dbar	^{17}O, Ar		^{17}O, Ar		^{17}O, Ar	
100dbar	^{17}O, Ar	^{17}O, Ar	^{17}O, Ar	^{17}O, Ar	^{17}O, Ar	^{17}O, Ar
125dbar	^{17}O, Ar		^{17}O, Ar		^{17}O, Ar	
150dbar	^{17}O, Ar	^{17}O, Ar	^{17}O, Ar	^{17}O, Ar	^{17}O, Ar	^{17}O, Ar
175dbar	^{17}O, Ar		^{17}O, Ar		^{17}O, Ar	
200dbar	^{17}O, Ar	^{17}O, Ar	^{17}O, Ar	^{17}O, Ar	^{17}O, Ar	^{17}O, Ar
300dbar	^{17}O, Ar	^{17}O*, Ar	^{17}O*, Ar	^{17}O, Ar	^{17}O, Ar	^{17}O, Ar
400dbar	^{17}O, Ar	^{17}O*, Ar	^{17}O*, Ar	^{17}O, Ar	^{17}O, Ar	^{17}O, Ar
500dbar	^{17}O, Ar	^{17}O*, Ar	^{17}O*, Ar	^{17}O*, Ar	^{17}O, Ar	^{17}O, Ar
600dbar	^{17}O, Ar	^{17}O, Ar	^{17}O, Ar	^{17}O*, Ar	^{17}O, Ar	^{17}O, Ar
700dbar	^{17}O, Ar	^{17}O, Ar	^{17}O, Ar	^{17}O*, Ar	^{17}O*, Ar	^{17}O, Ar
800dbar	^{17}O, Ar	^{17}O, Ar	^{17}O, Ar	^{17}O*, Ar	^{17}O*, Ar	^{17}O, Ar
900dbar	^{17}O, Ar	^{17}O, Ar	^{17}O, Ar	^{17}O*, Ar	^{17}O*, Ar	^{17}O*, Ar
1000dbar	^{17}O, Ar	^{17}O, Ar	^{17}O, Ar	^{17}O, Ar	^{17}O, Ar	^{17}O*, Ar
1250dbar	^{17}O, Ar	^{17}O, Ar	^{17}O, Ar	^{17}O, Ar	^{17}O, Ar	^{17}O*, Ar
1500dbar	^{17}O, Ar	^{17}O, Ar	^{17}O, Ar	^{17}O, Ar	^{17}O, Ar	^{17}O*, Ar
1750dbar	^{17}O, Ar	^{17}O, Ar	^{17}O, Ar	^{17}O, Ar	^{17}O, Ar	^{17}O, Ar
2000dbar		^{17}O, Ar	^{17}O, Ar	^{17}O, Ar	^{17}O, Ar	^{17}O, Ar
2250dbar			^{17}O		^{17}O	
2500dbar		^{17}O, Ar	^{17}O, Ar	^{17}O, Ar	^{17}O, Ar	^{17}O, Ar
2750dbar			^{17}O		^{17}O	
3000dbar			^{17}O, Ar	^{17}O, Ar	^{17}O, Ar	^{17}O, Ar
3250dbar			^{17}O		^{17}O	
3500dbar			^{17}O		^{17}O	
4000dbar			^{17}O, Ar	^{17}O, Ar	^{17}O, Ar	^{17}O, Ar
4500dbar			^{17}O		^{17}O	
5000dbar			^{17}O, Ar	^{17}O, Ar	^{17}O, Ar	^{17}O, Ar
5500dbar					^{17}O	

^{17}O: Samples for isotope ratios of dissolved oxygen collected by small vacuum flasks.
^{17}O*: Samples for isotope ratios of dissolved oxygen collected by large vacuum flasks.
Ar: Samples for dissolved argon concentration collected by 1L Duran bottles.

⬡: Depths where dissolved oxygen concentration were collected in duplicate.

▭: Depths where salinity samples were collected in duplicate.

7.6.1 Salinity

(1) Persons in charge

　Hiroki Ushiromura (MWJ): Operation Leader
　Sonoka Wakatsuki (MWJ)

(2) Objective

　　　　　　　To measure bottle salinity obtained by CTD casts.

(3) Method
a. Salinity Sample Collection

　　　　　Seawater samples were collected with 12 liter Niskin-X bottles. The salinity sample bottle of the 250ml brown glass with GL32 screw cap was used for collecting the sample seawater. Each bottle was rinsed 3 times with the sample seawater, and was filled with sample seawater to the bottle shoulder. All of sample bottles were sealed with a plastic cone and a screw cap because we took into consideration the possibility of storage for about a month. The cone was rinsed 3 times with the sample seawater before its use. Each bottle was stored for more than 12 hours in the laboratory before the salinity measurement.

　　　　Numbers (n) of samples are shown in Table 7.6.1-1.

Table 7.6.1-1 numbers (n) of samples

Types	number of samples
Samples for CTD	216

b. Instruments and Method

　　　　　The salinity measurement was carried out on R/V MIRAI during the cruise of MR14-02 using the salinometer (Model 8400B "AUTOSAL" ; Guildline Instruments Ltd.: S/N 62556) with an additional peristaltic-type intake pump (Ocean Scientific International, Ltd.).

　　　　　One pair of precision digital thermometers (Model 9540 ; Guildline Instruments Ltd.) were used. One thermometer monitored the ambient temperature and the other monitored the bath temperature of the salinometer.

　　　　　The specifications of the AUTOSAL salinometer and thermometer are shown as follows ;

　　Salinometer (Model 8400B "AUTOSAL" ; Guildline Instruments Ltd.)
　　　　Measurement Range : 0.005 to 42 (PSU)
　　　　Accuracy : Better than ±0.002 (PSU) over 24 hours
　　　　　　　　　　　　　　　　　without re-standardization
　　　　Maximum Resolution : Better than ±0.0002 (PSU) at 35 (PSU)
　　Thermometer (Model 9540 ; Guildline Instruments Ltd.)
　　　　Measurement Range : -40 to +180 deg C
　　　　Resolution : 0.001
　　　　Limits of error ±deg C : 0.01 (24 hours @ 23 deg C ±1 deg C)
　　　　Repeatability : ±2 least significant digits

　　　　　The measurement system was almost the same as Aoyama *et al.* (2002). The salinometer was operated in the air-conditioned ship's laboratory at a bath temperature of 24 deg C. The ambient temperature varied from approximately 21.6 deg C to 23.6 deg C, while the bath temperature was very stable and varied within +/- 0.003 deg C on rare occasion.

　　　　　The measurement for each sample was done with a double conductivity ratio and defined as the median of 31 readings of the salinometer. Data collection was started 10 seconds after filling the cell with the sample and it took about 10 seconds to collect 31 readings by the

personal computer. Data were taken for the sixth and seventh filling of the cell. In the case of the difference between the double conductivity ratio of these two fillings being smaller than 0.00002, the average value of the double conductivity ratio was used to calculate the bottle salinity with the algorithm for the practical salinity scale, 1978 (UNESCO, 1981). If the difference was greater than or equal to 0.00003, an eighth filling of the cell was done. In the case of the difference between the double conductivity ratio of these two fillings being smaller than 0.00002, the average value of the double conductivity ratio was used to calculate the bottle salinity. In the case of the double conductivity ratio of eighth filling did not satisfy the criteria above, we measured a ninth or tenth filling of the cell and calculated the bottle salinity. The conductivity cell was cleaned with detergent after the measurement of the day.

(4) Results
a. Standard Seawater (SSW)

The specifications of SSW used in this cruise are shown as follows ;

Batch : P156
Conductivity Ratio : 0.99984
Salinity : 34.994
Use By : 23rd July 2016

Standardization control of the salinometer S/N 62556 was set to 690 and all measurements were carried out at this setting. The value of STANDBY was 24+5198~5199 and that of ZERO was 0.0-0001~0.0-0000. 14 bottles of SSW were measured.

Fig.7.6.1-2 shows the time series of the double conductivity ratio of SSW batch P156 before correction. The average of the double conductivity ratio was 1.99967 and the standard deviation was 0.00001, which is equivalent to 0.0002 in salinity.
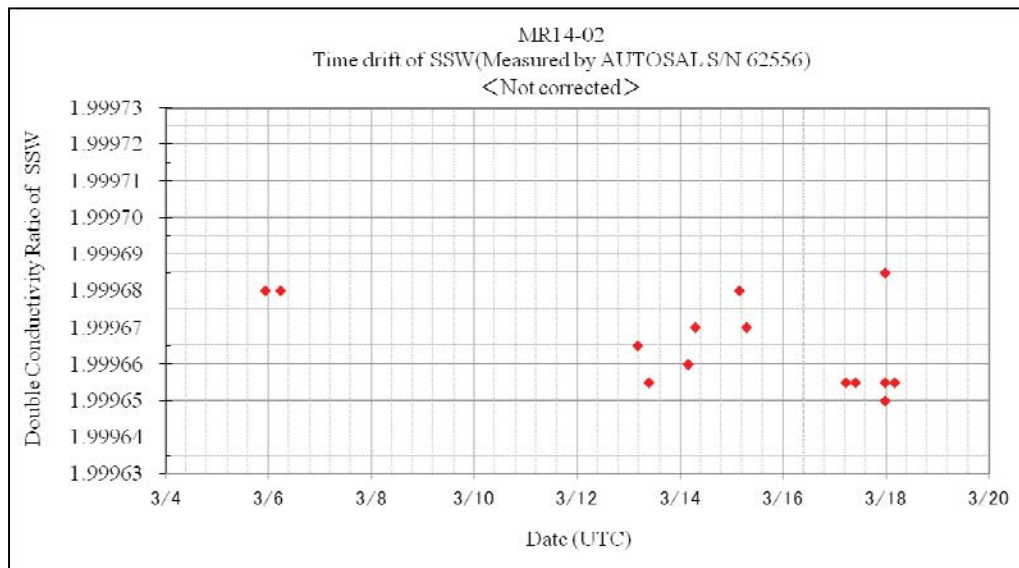
Fig. 7.6.1-2 Time series of double conductivity ratio for the Standard Seawater batch P156
(before correction)

Fig.7.6.1-3 shows the time series of the double conductivity ratio of SSW batch P156 after correction. The average of the double conductivity ratio was 1.99968 and the standard deviation was 0.00001, which is equivalent to 0.0002 in salinity.
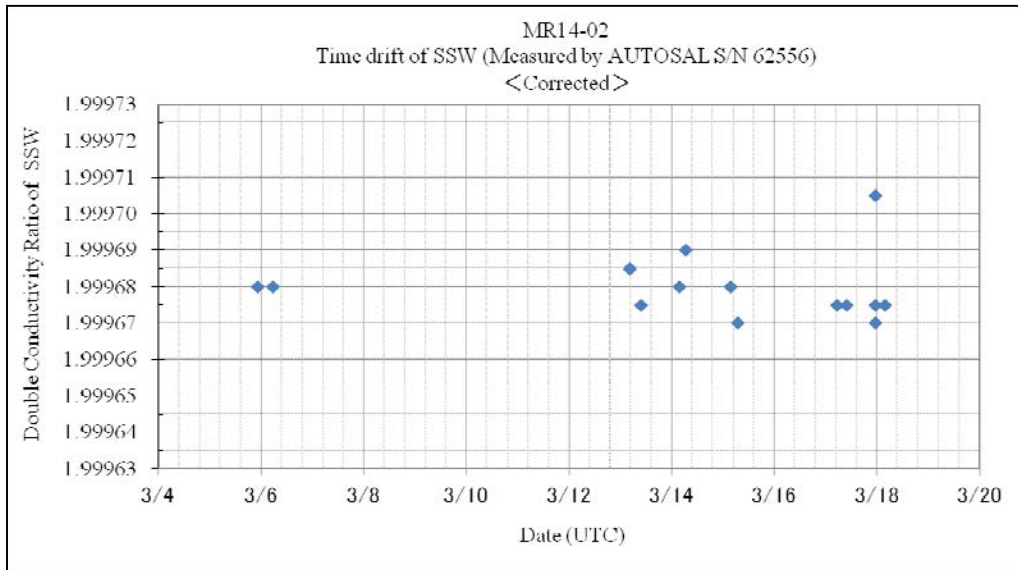
Fig.7.6.1-3 Time series of double conductivity ratio for the Standard Seawater batch P156
(after correction)

b. Sub-Standard Seawater

Sub-standard seawater was made from surface seawater filtered by a pore size of 0.22 micrometer and stored in a 20 liter container made of polyethylene and stirred for at least 24 hours before measuring. It was measured about every 6 samples in order to check for the possible sudden drifts of the salinometer.

c. Replicate Samples

We estimated the precision of this method using 36 pairs of replicate samples taken from the same Niskin bottle. Fig.7.6.1-4 shows the histogram of the absolute difference between each pair of the replicate samples. The average and the standard deviation of absolute difference among 36 pairs of replicate samples were 0.0003 and 0.0003 in salinity, respectively.
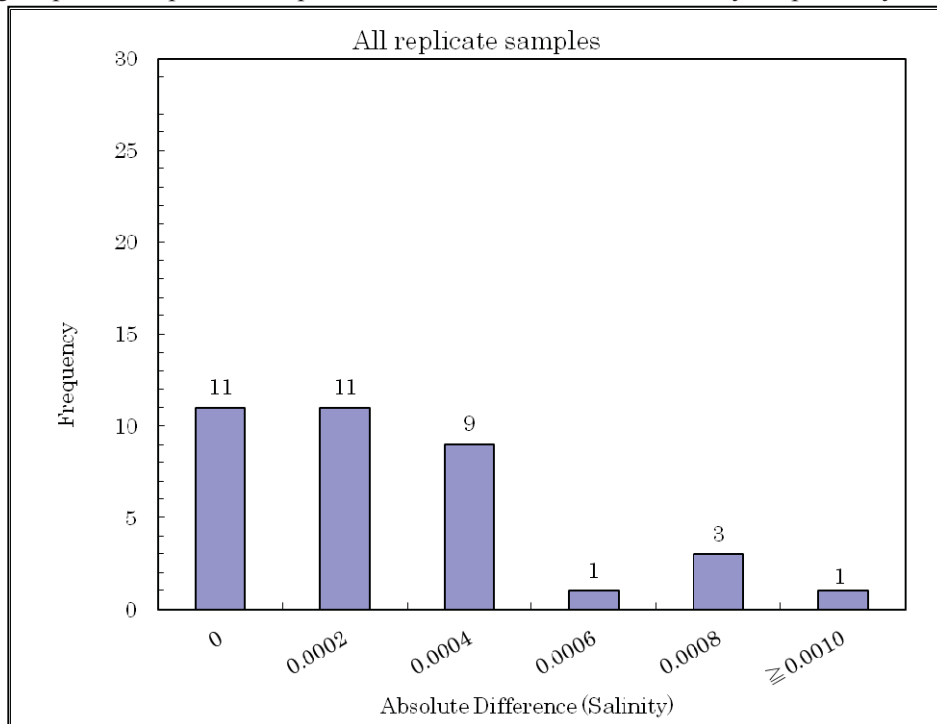
Fig.7.6.1-4 Histogram of the absolute difference between replicate samples

(5) Data archive
These raw datasets will be submitted to JAMSTEC Data Management Office (DMO).

(6) Reference

・Aoyama, M. T. Joyce, T. Kawano and Y. Takatsuki: Standard seawater comparison up to P129. Deep-Sea Research, I, Vol. 49, 1103〜1114, 2002
・UNESCO : Tenth report of the Joint Panel on Oceanographic Tables and Standards. UNESCO Tech. Papers in Mar. Sci., 36, 25 pp., 1981

7.6.2 Dissolved oxygen concentration

(1) Persons in charge
Kanako YOSHIDA (MWJ)
Masahiro ORUI (MWJ)

(2) Objectives
Determination of dissolved oxygen in seawater by Winkler titration.

(3) Parameter
Dissolved Oxygen

(4) Instruments and Methods
Following procedure is based on an analytical method, entitled by "Determination of dissolved oxygen in sea water by Winkler titration", in the WHP Operations and Methods (Dickson, 1996).

a. Instruments
Burette for sodium thiosulfate and potassium iodate;
APB-510 manufactured by Kyoto Electronic Co. Ltd. / 10 cm^3 of titration vessel
APB-620 manufactured by Kyoto Electronic Co. Ltd. / 10 cm^3 of titration vessel
Detector;
Automatic photometric titrator (DOT-01X) manufactured by Kimoto Electronic Co. Ltd.
Software;
DOT_Terminal Ver.1.2.0

b. Reagents
Pickling Reagent I: Manganese chloride solution (3 mol dm^{-3})
Pickling Reagent II: Sodium hydroxide (8 mol dm^{-3}) / sodium iodide solution (4 mol dm^{-3})
Sulfuric acid solution (5 mol dm^{-3})
Sodium thiosulfate (0.025 mol dm^{-3})
Potassium iodide (0.001667 mol dm^{-3})
CSK standard of potassium iodide:
Lot DCE2131, Wako Pure Chemical Industries Ltd., 0.0100N

c. Sampling
Seawater samples were collected with Niskin bottle attached to the CTD-system at standard depths. Seawater for oxygen measurement was transferred from sampler to a volume calibrated flask (ca. 100 cm^3). Three times volume of the flask was overflowed. Temperature was measured by digital thermometer during the overflowing. Then two reagent solutions (Reagent I and II) of 0.5 cm^3 each were added immediately into the sample flask and the stopper was inserted carefully into the flask without making any air bubble. The sample flask was then shaken vigorously to mix the contents and to disperse the precipitate finely throughout. After the precipitate has settled at least halfway down the flask, the flask was shaken again vigorously to disperse the precipitate. The sample flasks containing pickled samples were stored in a laboratory until they were titrated.

d. Sample measurement

At least two hours after the re-shaking, the pickled samples were measured on board. 1 cm^3 sulfuric acid solution and a magnetic stirrer bar were added into the sample flask and stirring began. Samples were titrated by sodium thiosulfate solution whose morality was determined by potassium iodate solution. Temperature of sodium thiosulfate during titration was recorded by a digital thermometer. During this cruise, we measured dissolved oxygen concentration using 2 sets of the titration apparatus. Dissolved oxygen concentration (μmol kg^{-1}) was calculated by knowing sample temperature during seawater sampling, salinity, flask volume, and titrated volume of sodium thiosulfate solution without the blank. When we measured low concentration samples, titration procedure was adjusted manually.

e. Standardization and determination of the blank

Concentration of sodium thiosulfate titrant was determined by potassium iodate solution. Pure potassium iodate was dried in an oven at 130 ℃. 1.7835 g potassium iodate weighed out accurately was dissolved in deionized water and diluted to final volume of 5 dm^3 in a calibrated volumetric flask (0.001667 mol dm^{-3}). 10 cm^3 of the standard potassium iodate solution was added to a flask using a volume-calibrated dispenser. Then 90 cm^3 of deionized water, 1 cm^3 of sulfuric acid solution, and 0.5 cm^3 of pickling reagent solution II and I were added into the flask in order. Amount of titrated volume of sodium thiosulfate (usually 5 times measurements average) gave the morality of sodium thiosulfate titrant.

The oxygen in the pickling reagents I (0.5 cm^3) and II (0.5 cm^3) was assumed to be 3.8 x 10^{-8} mol (Murray *et al.*, 1968). The blank due to other than oxygen was determined as follows. 1 and 2 cm^3 of the standard potassium iodate solution were added to two flasks respectively using a calibrated dispenser. Then 100 cm^3 of deionized water, 1 cm^3 of sulfuric acid solution, and 0.5 cm^3 of pickling reagent solution II and I each were added into the flask in order. The blank was determined by difference between the first (1 cm^3 of KIO$_3$) titrated volume of the sodium thiosulfate and the second (2 cm^3 of KIO$_3$) one. The results of 3 times blank determinations were averaged.

Table 7.6.2. Results of the standardization and the blank determination during this cruise.

Date	KIO$_3$ ID	Na$_2$S$_2$O$_3$	DOT-01(No.7)		DOT-01(No.8)		Stations
			E.P.	Blank	E.P.	Blank	
2014/02/12	20130510-01-04	20130514-08	3.967	0.000	-	-	-
2014/02/27	20130510-01-05	20130514-08	3.966	0.001	3.968	0.002	EQ, 5N, 10N.15N, 20N, 25N
2013/7/13	20130509-01-02	20130514-08	3.972	0.000	3.977	0.001	-

f. Repeatability of sample measurement

Replicate samples were taken at every CTD casts. Total amount of the replicate sample pairs of good measurement was 22. The standard deviation of the replicate measurement was 0.11 mmol kg^{-1} that was calculated by a procedure in Guide to best practices for ocean CO$_2$ measurements Chapter4 SOP23 Ver.3.0 (2007). .

(5) Data archive

       All data will be submitted to Chief Scientist.

(6) References

Dickson, A.G., Determination of dissolved oxygen in sea water by Winkler titration. (1996)

Dickson, A.G., Sabine, C.L. and Christian, J.R. (Eds.), Guide to best practices for ocean CO2 measurements. (2007)

Culberson, C.H., WHP Operations and Methods July-1991 "Dissolved Oxygen", (1991)

Japan Meteorological Agency, Oceanographic research guidelines（Part 1）. (1999)

KIMOTO electric CO. LTD., Automatic photometric titrator DOT-01X Instruction manual

7.6.3 Vertical distribution of isotopic composition of dissolved oxygen

(1) Persons in charge

Habeeb R Keedakkadan (Nagoya University)

Osamu ABE (Nagoya University)

(2) Objective

$\Delta^{17}O$ of dissolved O_2, which is defined approximately as $\delta^{17}O - 0.5\delta^{18}O$, is a unique tracer for primary productivity and gas transfer between atmosphere and water. This can be treated as a conservative component in subsurface (hypolimnion) waters, thus we could reconstruct past changes of productivity from subsurface $\Delta^{17}O$ values when the water was in the surface. Objective of this study is to clarify inter-annual variation of primary productivity at the subduction area of north Pacific intermediate water (NPIW) using vertical distribution $\Delta^{17}O$.

(3) Sampling

In this cruise, vertical water sampling was conducted at the stations EQ, 5N, 10N, 15N, 20N and 25N at standard CTD depths. One hundred and fifty milliliter of water was collected to vacuum flasks of 300mL except for oxygen minimum layer, which expands below 600 m. In this layer, 1L water was collected to vacuum flasks of 2L for gaining sufficient signals in IRMS. Total number of samples from each location is tabulated in 7.6.2.

After the bottling, less soluble gases such as oxygen, argon and nitrogen are released to vacuum headspaces within 24 hours at room temperature. These gases will be collected using a vacuum line in the laboratory. Then O_2 gas will be purified using specially designed molecular sieve packed column and isotope ratios were measured by isotope ratio mass spectrometer (IRMS) for $\Delta^{17}O$.

(4) Expected results

Previous investigations for $\Delta^{17}O$ has been limited to surface mixed layer and used for "present" primary productivity at the surface water. This study will first investigate whether this parameter would be really conserved the surface condition. On that basis, $\Delta^{17}O$ values for water masses from each location can be regarded as those surface values when water masses were at the surface. Compare to surface $\Delta^{17}O$, subsurface $\Delta^{17}O$ values would be controlled not only by primary productivity and gas transfer between atmosphere and water, but also by the amount of isopycnal and diapycnal mixing. With regard to gas exchanges between air-water, and stratified water masses could be quantified by measuring degrees of super-saturation for nitrogen and/or noble gases.

7.6.4 Vertical distribution of dissolved argon concentration

(1) Persons in charge
Osamu ABE (Nagoya University)

(2) Objective

As described in 7.6.3, our purpose is to clarify temporary changes of Okhotsk sea surface environments by tracing NPIW water from 25 deg.N to equator at northwestern Pacific. The unidentified influence on the isotopic composition of NPIW water is how mixed with adjacent water masses vertically (diapycnal mixing) as well as how mixed horizontally along isopycnal surface (isopycnal mixing). According to Emerson et al. (2012), the latter effect is relatively small to the former effect. Therefore, we would like to identify the effect of diapycnal mixing by using dissolved argon supersaturation, which is controlled by mixing between two temperature-different water masses.

(3) Sampling

In this cruise, vertical water sampling was conducted at the stations EQ, 5N, 10N, 15N, 20N and 25N at standard CTD depths. One liter of water was collected to Duran glass flasks, then poisoned by adding 2.5mL HgCl saturated solution. Detail of water collection points are tabulated in 7.6.2.

After the bottling, almost all of water in each bottle is transferred to 2L vacuum flask on land, then less soluble gases such as oxygen, argon and nitrogen are released to its vacuum headspace within 24 hours at room temperature. These gases will be collected using a vacuum line in the laboratory. Then O_2 and argon gases will be purified using specially designed molecular sieve packed column and O_2/Ar ratio will be measured by isotope ratio mass spectrometer (IRMS). Finally, dissolved argon concentration will be calculated from O_2/Ar ratio and O_2 concentration that was obtained by Winkler titration on board.

(4) Expected results

Emerson et al. (2012) reveals subsurface argon supersaturation at northwestern Pacific from 44 deg.N to 25 deg.N along 155 degE transect. They showed results above thermocline (approx.. shallower than 500m), and weaker supersaturation relative to northeastern Pacific. Then they showed the numerical simulation results using three-dimensional ocean model, however, as they mentioned, number of observations are very small.

This study could suffice the lack of deeper layer below 500m and expand the observation to equator. Therefore, our data must be valuable for the future understanding of diapycnal mixing process in the deep ocean.

(5) Reference
Emerson et al. (2012) Argon supersaturation indicates low decadal-scale vertical mixing in the ocean thermocline. Geophys. Res. Lett., 39, L18610.

7.6.5. Nutrients

(1) Persons in charge
    Yasuhiro ARII (MWJ): Operation leader
    Yoshiko ISHIKAWA (MWJ)

(2) Objectives
    The objective of nutrients analyses during the R/V Mirai MR14-02 cruise in the West Pacific Ocean is to describe the present status of nutrients concentration with excellent comparability.

(3) Parameters
    The determinants are nitrate, nitrite, silicate and phosphate in the West Pacific Ocean.

(4) Summary of nutrients analysis
    We made 6 QuAAtro runs for the water columns sample at 6 casts during MR14-02. The total amount of layers of the seawater sample reached up to 180. We made basically duplicate measurement. The station locations for nutrients measurement is shown in Figure 7.6.5.1
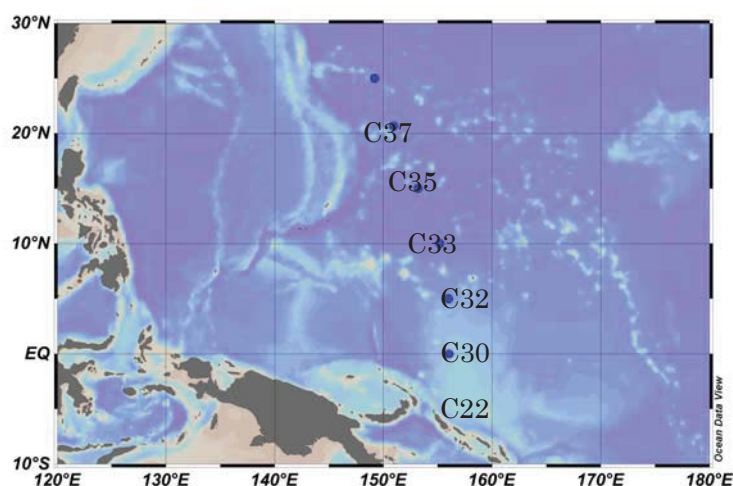
Figure 7.6.5.1 Sampling positions of nutrients sample.

(5) Instrument and Method
(5.1) Analytical detail using QuAAtro 2-HR systems (BL-Tech)
    Nitrate + nitrite and nitrite were analyzed according to the modification method of Wood et al. (1967). The sample nitrate was reduced to nitrite in a cadmium tube inside of which was coated with metallic copper. The sample streamed with its equivalent nitrite was treated with an acidic, sulfanilamide reagent and the nitrite forms nitrous acid which reacted with the sulfanilamide to produce a diazonium ion. N-1-Naphthylethylene-diamine added to the sample stream then coupled with the diazonium ion to produce a red, azo dye. With reduction of the nitrate to nitrite, both nitrate and nitrite reacted and were measured; without reduction, only nitrite reacted. Thus, for the nitrite analysis, no reduction was performed and the alkaline buffer was not necessary. Nitrate was computed by difference.
    The silicate method was analogous to that described for phosphate. The method used was essentially that of Grasshoff et al. (1983), wherein silicomolybdic acid was first formed from the silicate in the sample and added molybdic acid; then the silicomolybdic acid was reduced to silicomolybdous acid, or "molybdenum blue" using ascorbic acid as the reductant.
    The phosphate analysis was a modification of the procedure of Murphy and Riley (1962). Molybdic acid was added to the seawater sample to form phosphomolybdic acid which was in turn reduced to phosphomolybdous acid using L-ascorbic acid as the reductant.
    The details of modification of analytical methods used in this cruise are also compatible with the methods described in nutrients section in GO-SHIP repeat hydrography manual (Hydes et al., 2010).

The flow diagrams and reagents for each parameter are shown in Figures 7.6.5.2 to 7.6.5.5.

(5.2) Nitrate + Nitrite Reagents
　　Imidazole (buffer), 0.06 M (0.4 % w/v)
　　Dissolve 4 g imidazole, $C_3H_4N_2$, in ca. 1000 ml DIW; add 2 ml concentrated HCl. After mixing, 1 ml Triton®X-100 (50 % solution in ethanol) is added.

　　Sulfanilamide, 0.06 M (1 % w/v) in 1.2M HCl
　　Dissolve 10 g sulfanilamide, $4\text{-}NH_2C_6H_4SO_3H$, in 900 ml of DIW, add 100 ml concentrated HCl. After mixing, 2 ml Triton®X-100 (50 % solution in ethanol) is added.

　　N-1-Napthylethylene-diamine dihydrochloride, 0.004 M (0.1 %f w/v)
　　Dissolve 1 g NED, $C_{10}H_7NHCH_2CH_2NH_2\cdot 2HCl$, in 1000 ml of DIW and add 10 ml concentrated HCl. After mixing, 1 ml Triton®X-100 (50 % solution in ethanol) is added. This reagent is stored in a dark bottle.
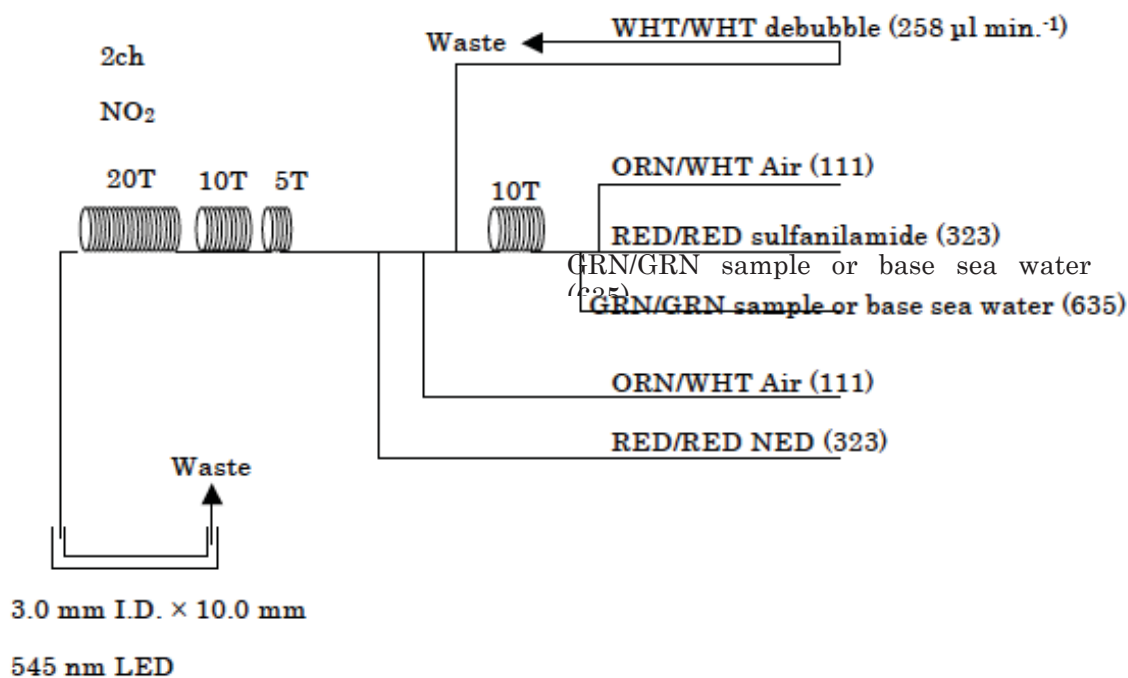

Figure7.6.5.2 NO3+NO2 (1ch.) Flow diagram.

(5.3) Nitrite Reagents
　　Sulfanilamide, 0.06 M (1 % w/v) in 1.2 M HCl
　　Dissolve 10g sulfanilamide, $4\text{-}NH_2C_6H_4SO_3H$, in 900 ml of DIW, add 100 ml concentrated HCl. After mixing, 2 ml Triton®X-100 (50 % solution in ethanol) is added.

　　N-1-Napthylethylene-diamine dihydrochloride, 0.004 M (0.1 % w/v)
　　Dissolve 1 g NED, $C_{10}H_7NHCH_2CH_2NH_2\cdot 2HCl$, in 1000 ml of DIW and add 10 ml concentrated HCl. After mixing, 1 ml Triton®X-100 (50 % solution in ethanol) is added. This reagent is stored in a dark bottle.

Figure7.6.5.3 NO₂ (2ch.) Flow diagram.

(5.4) Silicate Reagents

Molybdic acid, 0.06 M (2 % w/v)

Dissolve 15 g disodium molybdate(VI) dihydrate, $Na_2M_oO_4 \cdot 2H_2O$, in 980 ml DIW, add 8 ml concentrated H_2SO_4. After mixing, 20 ml sodium dodecyl sulphate (15 % solution in water) is added.

Oxalic acid, 0.6 M (5 % w/v)

Dissolve 50 g oxalic acid anhydrous, HOOC: COOH, in 950 ml of DIW.

Ascorbic acid, 0.01M (3 % w/v)

Dissolve 2.5g L (+)-ascorbic acid, $C_6H_8O_6$, in 100 ml of DIW. Stored in a dark bottle and freshly prepared before every measurement.
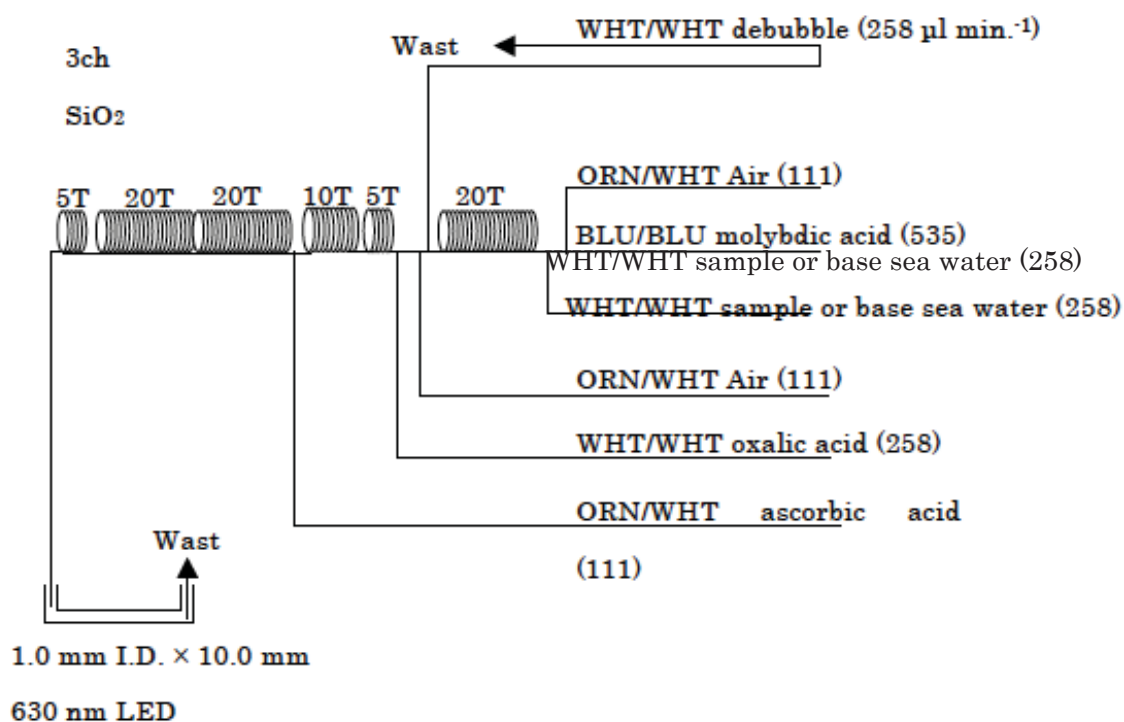
Figure7.6.5.4 SiO₂ (3ch.) Flow diagram.

(5.5) Phosphate Reagents

Stock molybdate solution, 0.03M (0.8 % w/v)

Dissolve 8 g disodium molybdate(VI) dihydrate, $Na_2M_oO_4\cdot2H_2O$, and 0.17 g antimony potassium tartrate, $C_8H_4K_2O_{12}Sb_2\cdot3H_2O$, in 950 ml of DIW and add 50 ml concentrated H_2SO_4.

Mixed Reagent

Dissolve 1.2 g L (+)-ascorbic acid, $C_6H_8O_6$, in 150 ml of stock molybdate solution. After mixing, 3 ml sodium dodecyl sulphate (15 % solution in water) is added. Stored in a dark bottle and freshly prepared before every measurement.
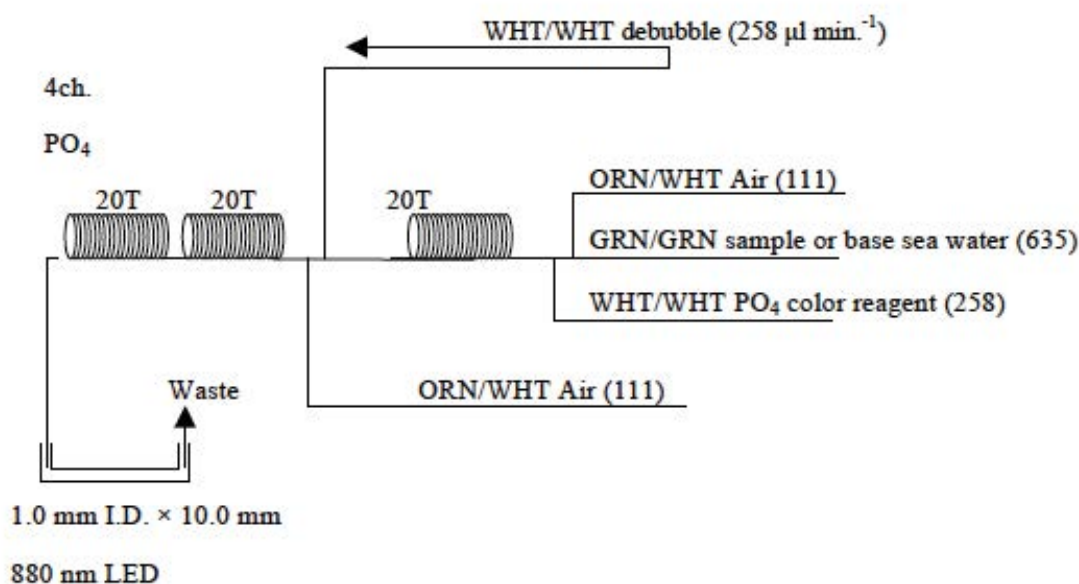
Figure 7.6.5.5 PO$_4$ (4ch.) Flow diagram.

(5.6) Sampling procedures

Sampling of nutrients followed that oxygen, salinity and trace gases. Samples were drawn into a virgin 10 ml polyacrylates vials without sample drawing tubes. These were rinsed three times before filling and vials were capped immediately after the drawing. The vials are put into water bath adjusted to ambient temperature, 21.5 ± 0.5 deg. C, in about 30 minutes before use to stabilize the temperature of samples.

No transfer was made and the vials were set an auto sampler tray directly. Samples were analyzed after collection basically within 24 hours.

(5.7) Data processing

Raw data from QuAAtro were treated as follows:
- Check baseline shift.
- Check the shape of each peak and positions of peak values taken, and then change the positions of peak values taken if necessary.
- Carry-over correction and baseline drift correction were applied to peak heights of each samples followed by sensitivity correction.
- Baseline correction and sensitivity correction were done basically using liner regression.
- Load pressure and salinity from CTD data due to calculate density of seawater.
- Calibration curves to get nutrients concentration were assumed second order equations.

(6) Nutrients standards
(6.1) Volumetric laboratory ware of in-house standards

All volumetric glass ware and polymethylpentene (PMP) ware used were gravimetrically calibrated. Plastic volumetric flasks were gravimetrically calibrated at the temperature of use within 0 to 4 K.

Volumetric flasks

Volumetric flasks of Class quality (Class A) are used because their nominal tolerances are 0.05 % or less over the size ranges likely to be used in this work. Class A flasks are made of borosilicate glass, and the standard solutions were transferred to plastic bottles as quickly as possible after they are made up to volume and well mixed in order to prevent excessive dissolution of silicate from the glass. PMP volumetric flasks were gravimetrically calibrated and used only within 0 to 4 K of the calibration temperature.

The computation of volume contained by glass flasks at various temperatures other than the

calibration temperatures were done by using the coefficient of linear expansion of borosilicate crown glass.

Because of their larger temperature coefficients of cubical expansion and lack of tables constructed for these materials, the plastic volumetric flasks were gravimetrically calibrated over the temperature range of intended use and used at the temperature of calibration within 0 to 4 K. The weights obtained in the calibration weightings were corrected for the density of water and air buoyancy.

Pipettes and pipettors
All pipettes have nominal calibration tolerances of 0.1 % or better. These were gravimetrically calibrated in order to verify and improve upon this nominal tolerance.

(6.2) Reagents, general considerations
Specifications
For nitrate standard, "potassium nitrate 99.995 suprapur®" provided by Merck, Lot. B0771365, CAS No.: 7757-91-1, was used.

For nitrite standard, "sodium nitrate" provided by Wako, CAS No.: 7632-00-0, was used. And assay of nitrite was determined according JIS K8019 and assays of nitrite salts were 98.53 %. We use that value to adjust the weights taken.

For the silicate standard, we use "Silicon standard solution SiO_2 in NaOH 0.5 mol/l CertiPUR®" provided by Merck, CAS No.: 1310-73-2, of which lot number is HC122701 are used. The silicate concentration is certified by NIST-SRM3150 with the uncertainty of 0.5 %. HC122701 is certified as 1000+-5 mg L-1, however, our direct comparison between two Merck standards and estimation based on 13 lots of RMNS gave us a factor of 975 mg L-1 for HC074650 which was exceed 5mg of certification by Merck. We use this factor throughout MR12-E03 to keep comparability for silicate concentration.

For phosphate standard, "potassium dihydrogen phosphate anhydrous 99.995 suprapur®" provided by Merck, Lot. B0691108, CAS No.: 7778-77-0, was used.

Ultra pure water
Ultra pure water (Milli-Q) freshly drawn was used for preparation of reagent, standard solutions and for measurement of reagent and system blanks.

Low-nutrients seawater (LNSW)
Surface water having low nutrient concentration was taken and filtered using 0.45 μm pore size membrane filter. This water is stored in 20 liter cubitainer with paper box. The concentrations of nutrient of this water were measured carefully in August 2012.

(6.3) Concentrations of nutrients for A, B and C standards
Concentrations of nutrients for A, B and C standards are set as shown in Table 7.6.5.1. Then the actual concentration of nutrients in each fresh standard was calculated based on the ambient, solution temperature and determined factors of volumetric laboratory wares.

The calibration curves for each run were obtained using 5 levels, C-1, C-2, C-3, C-4 and C-5.

(6.4) Renewal of in-house standard solutions
In-house standard solutions as stated in paragraph c were renewed as shown in Table 7.6.5.2.

Table 7.6.5.1 Nominal concentrations of nutrients for A, B and C.

	A	B	C-1	C-2	C-3	C-4	C-5
NO_3 (μM)	22500	900	0	9	18	36	54
NO_2 (μM)	4000	20	0	0.2	0.4	0.8	1.2
SiO_2 (μM)	35600	2850	0	29	57	114	170
PO_4 (μM)	3000	60	0	0.6	1.2	2.4	3.6

Table 7.6.5.2 Timing of renewal of in-house standards.

In-house standards	Renewal
A-1 Std. (NO_3)	maximum a month
A-2 Std. (NO_2)	maximum a month
A-3 Std. (SiO_2)	commercial prepared solution
A-4 Std. (PO_4)	maximum a month
B-1 Std. (mixture of NO_3, SiO_2, PO_4)	maximum a week
B-2 Std. (NO_2)	maximum a week
C Std. (mixture of B-1 and B-2.)	every 24 hours
D-1 Std. (3600 μM NO_3)	maximum a week
43 μM NO_3 (reduction estimation)	when C Std. renewed
47 μM NO_2 (reduction estimation)	when C Std. renewed

(7) Reference material of nutrients in seawater

To get the more accurate and high quality nutrients data to achieve the objectives stated above, huge numbers of the bottles of the reference material of nutrients in seawater (hereafter RMNS) are prepared (Aoyama et al., 2006, 2007, 2008, 2009). In the previous worldwide expeditions, such as WOCE cruises, the higher reproducibility and precision of nutrients measurements were required (Joyce and Corry, 1994). Since no standards were available for the measurement of nutrients in seawater at that time, the requirements were described in term of reproducibility. The required reproducibility was 1 %, 1 to 2 %, 1 to 3 % for nitrate, phosphate and silicate, respectively. Although nutrient data from the WOCE one-time survey was of unprecedented quality and coverage due to much care in sampling and measurements, the differences of nutrients concentration at crossover points are still found among the expeditions (Aoyama and Joyce, 1996, Mordy et al., 2000, Gouretski and Jancke, 2001). For instance, the mean offset of nitrate concentration at deep waters was 0.5 μmol kg^{-1} for 345 crossovers at world oceans, though the maximum was 1.7 μmol kg^{-1} (Gouretski and Jancke, 2001). At the 31 crossover points in the Pacific WHP one-time lines, the WOCE standard of reproducibility for nitrate of 1 % was fulfilled at about half of the crossover points and the maximum difference was 7 % at deeper layers below 1.6 deg. C in potential temperature (Aoyama and Joyce, 1996).

(7.1) RMNS for this cruise

RMNS lots BY, BW and BV, which cover full range of nutrients concentrations in the West Pacific ocean are prepared. 6 sets of BY, BW and BV are prepared.

These RMNS assignment were completely done based on random number. The RMNS bottles were stored at a room in the ship, REAGENT STORE, where the temperature was maintained around 20.0 deg. C.

(7.2) Assigned concentration for RMNSs

We assigned nutrients concentrations for RMNS lots BY, BW and BV as shown in Table 7.6.5.3.

Table 7.6.5.3 Assigned concentration of RMNSs.

unit: μmol kg^{-1}

Nitrate	Nitrite	Silicate	Phosphate	Assigned year

BY	0.07	0.03	1.54	0.070	2014
BW	24.59	0.08	58.18	1.575	2014
BV	35.32	0.06	99.55	2.541	2013

(8) Quality control
(8.1) Precision of nutrients analyses during the cruise

Precision of nutrients analyses during this cruise was evaluated based on the 6 to 8 measurements, which are measured every 9 to 11 samples, during a run at the concentration of C-5 std. Summary of precisions are shown as shown in Table 7.6.5.4. Analytical precisions previously evaluated were 0.08 % for nitrate, 0.07 % for silicate and 0.10 % for phosphate in CLIVAR P21 revisited cruise of MR09-01 cruise in 2009, respectively. During in this cruise, analytical precisions were 0.08% for nitrate, 0.08% for nitrite, 0.10% for silicate and 0.07% for phosphate in terms of median of precision, respectively. Then we can conclude that the analytical precisions for nitrate, nitrite, silicate and phosphate were maintained throughout this cruise.

Table 7.6.5.4 Summary of precision based on the replicate analyses.

	Nitrate CV %	Nitrite CV %	Silicate CV %	Phosphate CV %
Median	0.09	0.08	0.11	0.07
Mean	0.08	0.08	0.10	0.07
Maximum	0.10	0.16	0.12	0.10
Minimum	0.05	0.04	0.08	0.05
N	6	6	6	6

(8.2) Carry over

We can also summarize the magnitudes of carry over throughout the cruise. These are small enough within acceptable levels as shown in Table 7.6.5.5.

Table 7.6.5.5 Summary of carry over throughout MR14-02.

	Nitrate %	Nitrite %	Silicate %	Phosphate %
Median	0.17	0.19	0.19	0.15
Mean	0.16	0.18	0.17	0.17
Maximum	0.23	0.31	0.25	0.33
Minimum	0.11	0.04	0.10	0.08
N	6	6	6	6

(9) Problems/improvements occurred and solutions.
Nothing Special.

(10) Station list
The sampling station list for nutrients is shown in Table 7.6.5.6

Table 7.6.5.6 List of stations

Station	Cast	Latitude	Longitude
C22	1	-0.0023	156.0262
C30	1	5.0057	155.9997
C32	1	10.0073	155.1948
C33	1	15.0127	153.1892
C35	1	20.6662	150.9493
C37	1	24.9983	149.1867

(11) Data archive

    These data obtained in this cruise will be submitted to the Data Integration and Analysis Group (DIAG) of JAMSTEC, and will be opened to the public via **"Data Research for Whole Cruise Information in JAMSTEC"** in JAMSTEC home page.

(12) References

Aminot, A. and Kerouel, R. 1991. Autoclaved seawater as a reference material for the determination of nitrate and phosphate in seawater. Anal. Chim. Acta, 248: 277-283.

Aminot, A. and Kirkwood, D.S. 1995. Report on the results of the fifth ICES intercomparison exercise for nutrients in sea water, ICES coop. Res. Rep. Ser., 213.

Aminot, A. and Kerouel, R. 1995. Reference material for nutrients in seawater: stability of nitrate, nitrite, ammonia and phosphate in autoclaved samples. Mar. Chem., 49: 221-232.

Aoyama M., and Joyce T.M. 1996, WHP property comparisons from crossing lines in North Pacific. In Abstracts, 1996 WOCE Pacific Workshop, Newport Beach, California.

Aoyama, M., 2006: 2003 Intercomparison Exercise for Reference Material for Nutrients in Seawater in a Seawater Matrix, Technical Reports of the Meteorological Research Institute No.50, 91pp, Tsukuba, Japan.

Aoyama, M., Susan B., Minhan, D., Hideshi, D., Louis, I. G., Kasai, H., Roger, K., Nurit, K., Doug, M., Murata, A., Nagai, N., Ogawa, H., Ota, H., Saito, H., Saito, K., Shimizu, T., Takano, H., Tsuda, A., Yokouchi, K., and Agnes, Y. 2007. Recent Comparability of Oceanographic Nutrients Data: Results of a 2003 Intercomparison Exercise Using Reference Materials. Analytical Sciences, 23: 1151-1154.

Aoyama M., J. Barwell-Clarke, S. Becker, M. Blum, Braga E. S., S. C. Coverly,E. Czobik, I. Dahllof, M. H. Dai, G. O. Donnell, C. Engelke, G. C. Gong, Gi-Hoon Hong, D. J. Hydes, M. M. Jin, H. Kasai, R. Kerouel, Y. Kiyomono, M. Knockaert, N. Kress, K. A. Krogslund, M. Kumagai, S. Leterme, Yarong Li, S. Masuda, T. Miyao, T. Moutin, A. Murata, N. Nagai, G.Nausch, M. K. Ngirchechol, A. Nybakk, H. Ogawa, J. van Ooijen, H. Ota, J. M. Pan, C. Payne, O. Pierre-Duplessix, M. Pujo-Pay, T. Raabe, K. Saito, K. Sato, C. Schmidt, M. Schuett, T. M. Shammon, J. Sun, T. Tanhua, L. White, E.M.S. Woodward, P. Worsfold, P. Yeats, T. Yoshimura, A.Youenou, J. Z. Zhang, 2008: 2006 Intercomparison Exercise for Reference Material for Nutrients in Seawater in a Seawater Matrix, Technical Reports of the Meteorological Research Institute No. 58, 104pp.

Gouretski, V.V. and Jancke, K. 2001. Systematic errors as the cause for an apparent deep water property variability: global analysis of the WOCE and historical hydrographic data・REVIEW ARTICLE, Progress In Oceanography, 48: Issue 4, 337-402.

Wood, E.D., F.A.J. Armstrong and F.A. Richards (1967), Determination of Nitrate in Sea Water by Cadmium-Copper Reduction to Nitrite. J. Mar. Biol. Assoc. U. K. 47, 23-31

Grasshoff, K., Ehrhardt, M., Kremling K. et al. 1983. Methods of seawater anylysis. 2nd rev. Weinheim: Verlag Chemie, Germany, West.

Joyce, T. and Corry, C. 1994. Requirements for WOCE hydrographic programmed data reporting. WHPO Publication, 90-1, Revision 2, WOCE Report No. 67/91.

Kawano, T., Uchida, H. and Doi, T. WHP P01, P14 REVISIT DATA BOOK, (Ryoin Co., Ltd., Yokohama, 2009).

Kirkwood, D.S. 1992. Stability of solutions of nutrient salts during storage. Mar. Chem., 38 : 151-164.

Kirkwood, D.S. Aminot, A. and Perttila, M. 1991. Report on the results of the ICES fourth intercomparison exercise for nutrients in sea water. ICES coop. Res. Rep. Ser., 174.

Mordy, C.W., Aoyama, M., Gordon, L.I., Johnson, G.C., Key, R.M., Ross, A.A., Jennings, J.C. and Wilson. J. 2000. Deep water comparison studies of the Pacific WOCE nutrient data set. Eos Trans-American Geophysical Union. 80 (supplement), OS43.

Murphy, J., and Riley, J.P. 1962. Analytica chim. Acta 27, 31-36.

Uchida, H. & Fukasawa, M. WHP P6, A10, I3/I4 REVISIT DATA BOOK Blue Earth Global Expedition 2003 1, 2, (Aiwa Printing Co., Ltd., Tokyo, 2005).

7.6.6. Chlorophyll *a* measurements by fluorometric determination

(1) Persons in charge

Kanako YOSHIDA (MWJ): Operation Leader

Masahiro ORUI (MWJ)

(2) Objective

Phytoplankton biomass can estimate as the concentration of chlorophyll *a* (chl-*a*), because all oxygenic photosynthetic plankton contain chl-*a*. Phytoplankton exist various species in the ocean, but the species are roughly characterized by their cell size. The objective of this study is to investigate the vertical distribution of phytoplankton and their size fractionations as chl-*a* by using the fluorometric determination.

(3) Sampling

Sampling of total chl-*a* were conducted from 9 depths between the surface and 200 m at EQ station and 9 depths between surface and 300m at stations 5N, 10N, 15N, 20N and 25N. Two samples were collected at chlorophyll maximum layer.

(4) Instruments and Methods

Water samples (0.5L) for total chl-*a* were filtered (<0.02 MPa) through 25mm-diameter Whatman GF/F filter. Phytoplankton pigments retained on the filters were immediately extracted in a polypropylene tube with 7 ml of N,N-dimethylformamide (Suzuki and Ishimaru, 1990). Those tubes were stored at –20°C under the dark condition to extract chl-*a* for 24 hours or more.

Fluorescences of each sample were measured by Turner Design fluorometer (10-AU-005), which was calibrated against a pure chl-*a* (Sigma-Aldrich Co.). We applied two kind of fluorometric determination for the samples of total chl-*a*: "Non-acidification method" (Welschmeyer, 1994).

(5) Data archives

The processed data file of pigments will be submitted to the JAMSTEC Data Integration and Analysis Group (DIAG) within a restricted period. Please ask PI for the latest information.

(6) Reference

Suzuki, R., and T. Ishimaru (1990), An improved method for the determination of phytoplankton chlorophyll using N, N-dimethylformamide, *J. Oceanogr. Soc. Japan*, 46, 190-194.

Holm-Hansen, O., Lorenzen, C. J., Holmes, R.W. and J. D. H. Strickland (1965), Fluorometric determination of chlorophyll. *J. Cons. Cons. Int. Explor. Mer.* 30, 3-15.

Welschmeyer, N. A. (1994), Fluorometric analysis of chlrophyll *a* in the presence of chlorophyll *b* and pheopigments. *Limnol. Oceanogr.* 39, 1985-1992.

Table 7.6.6. Analytical conditions of "Non-acidification method" for chlorophyll *a* with Turner Designs fluorometer (10-AU-005).

	Non-acidification method
Excitation filter (nm)	436
Emission filter (nm)	680
Lamp	Blue mercury vapor

7.7. Argo floats

(1) Personnel

Toshio Suga   (JAMSTEC/RIGC): Principal Investigator (not on board)
Shigeki Hosoda   (JAMSTEC/RIGC): not on board
Kanako Sato   (JAMSTEC/RIGC): not on board
Mizue Hirano   (JAMSTEC/RIGC): not on board
Hiroki Ushiromura   (MWJ): Technical Staff (Operation Leader)
Keisuke Matsumoto   (MWJ): Technical Staff

(2) Objectives

The objective of deployment is to clarify the structure and temporal/spatial variability of water masses in the North Pacific such as North Pacific Tropical Water in the subtropical North Pacific.

The profiling floats launched in this cruise measure vertical profiles of temperature and salinity automatically every ten days.   As the vertical resolution of the profiles is very fine, the structure and variability of the water mass can be displayed well. Therefore, the profile data from the floats will enable us to understand the variability and the formation mechanism of the water mass.

(3) Parameters

・water temperature, salinity, and pressure

(4) Methods

i. Profiling float deployment

We launched three Arvor floats manufactured by nke and a Navis float manufactured by Sea-Bird Electronics Inc. These floats equip an SBE41cp CTD sensor manufactured by Sea-Bird Electronics Inc.

The floats usually drift at a depth of 1000 dbar (called the parking depth), diving to a depth of 2000 dbar and rising up to the sea surface by decreasing and increasing their volume and thus changing the buoyancy in ten-day cycles. During the ascent, they measure temperature, salinity, and pressure.   They stay at the sea surface for approximately nine hours, transmitting the CTD data to the land via the ARGOS or Iridium RUDICS system, and then return to the parking depth by decreasing volume.   The status of floats and their launches are shown in Table 4.1.1.

Table 4.1.1 Status of floats and their launches
Float(2000dbar)

Float Type	Arvor float manufactured by nke.
CTD sensor	SBE41cp manufactured by Sea-Bird Electronics Inc.
Cycle	10 days (approximately 9 hours at the sea surface)
Trans mission	ARGOS , transmit interval 30 sec
Target Parking Pressure	1000 dbar
Sampling layers	115 (2000,1950,1900,1850,1800,1750,1700,1650,1600,1550,1500, 1450, 1400, 1350, 1300, 1250, 1200, 1150, 1100, 1050, 1000, 980, 960, 940, 920, 900, 880, 860, 840, 820, 800, 780, 760, 740, 720, 700, 680, 660, 640, 620, 600, 580, 560, 540, 520, 500, 490, 480, 470, 460, 450, 440, 430, 420, 410, 400, 390, 380, 370, 360, 350, 340, 330, 320, 310, 300, 290, 280, 270, 260, 250, 240, 230, 220,210, 200, 195, 190, 185, 180, 175, 170, 165, 160, 155, 150, 145, 140, 135, 130, 125, 120, 115, 110, 105, 100, 95, 90, 85, 80, 75, 70, 65, 60, 55, 50, 45, 40, 35, 30, 25, 20, 15, 10, 4 or surface dbar)

Float Type	Navis float manufactured by Sea-Bird Electronics Inc.
CTD sensor	SBE41cp manufactured by Sea-Bird Electronics Inc.
Cycle	10 days (approximately 9 hours at the sea surface)
Trans mission	Iridium, RUDICS server
Target Parking Pressure	1000 dbar
Sampling layers	1000 (interval 2dbar . from 2000dbar to surface)

Launches

Float S/N	ARGOS ID	Date and Time of Reset (UTC)	Date and Time of Launch(UTC)	Location of Launch	CTD St. No.
OIN13JAP-ARL-35	123595	2014 /03/14 20：05	2014 /03/14 21：13	18-18.58[N] 151 -54.11[E]	C34
OIN13JAP-ARL-36	123596	2014 /03/15 12：27	2014 /03/15 13：46	20-40.53[N] 150 -56.59[E]	C35
OIN13JAP-ARL-37	123597	2014 /03/15 22：34	2014 /03/15 23：16	22-0.33[N] 150 -23.56[E]	C36
F0279			2014 /03/17 00：01	25-00.00[N] 149-09.81[E]	C37

(5) Data archive

The real-time data are provided to meteorological organizations, research institutes, and universities via Global Data Assembly Center (GDAC: http://www.usgodae.org/argo/argo.html, http://www.coriolis.eu.org/) and Global Telecommunication System (GTS), and utilized for analysis and forecasts of sea conditions.

7.8 Lidar observations of clouds and aerosols

Personal:
Nobuo SUGIMOTO (NIES)
Ichiro MATSUI (NIES)
Atsushi SHIMIZU (NIES)
Tomoaki NISHIZAWA (NIES)
(Lidar operation was supported by Global Ocean Development Inc. (GODI).)

(1) Objectives

Objectives of the observations in this cruise is to study distribution and optical characteristics of ice/water clouds and marine aerosols using a two-wavelength polarization Mie-scattering lidar.

(2) Description of instruments deployed

Vertical profiles of aerosols and clouds are measured with a two-wavelength polarization Mie-scattering lidar. The lidar employs a Nd:YAG laser as a light source which generates the fundamental output at 1064nm and the second harmonic at 532nm. Transmitted laser energy is typically 30mJ per pulse at both of 1064 and 532nm. The pulse repetition rate is 10Hz. The receiver telescope has a diameter of 20 cm. The receiver has three detection channels to receive the lidar signals at 1064 nm and the parallel and perpendicular polarization components at 532nm. An analog-mode avalanche photo diode (APD) is used as a detector for 1064nm, and photomultiplier tubes (PMTs) are used for 532 nm. The detected signals are recorded with a transient recorder and stored on a hard disk with a computer. The lidar system was installed in a container with a glass window on the roof, and the lidar was operated continuously regardless of weather. Every 10 minutes vertical profiles of four channels (532 parallel, 532 perpendicular, 1064, 532 near range) are recorded. Time-height sections of backscatter intensity and depolarization ratio on previous day are automatically generated on Mirai, and sent to NIES lidar team everyday via E-mail.

(3) Preliminary results

The two wavelength polarization Mie-scattering lidar worked well and succeeded in getting the lidar data during the whole observation period. Quicklook figures of time-height sections of measured data are depicted in Fig. 1. Left panel shows an existence of geometrically thick and optically thin cirrus clouds which spread between 10 and 16 km altitude. Right panel shows that the mixing layer near the sea surface, blow 1 km altitude, was formed. Moderate backscatter, with lower depolarization ratio, continues during whole day, which implies surface was covered by spherical particles like sulfate or organic carbons. Strong backstter from cloud bottom is confirmed at the top of mixing layer. Further analysis will be conducted after numerical data is obtained from shipborne lidar PC.
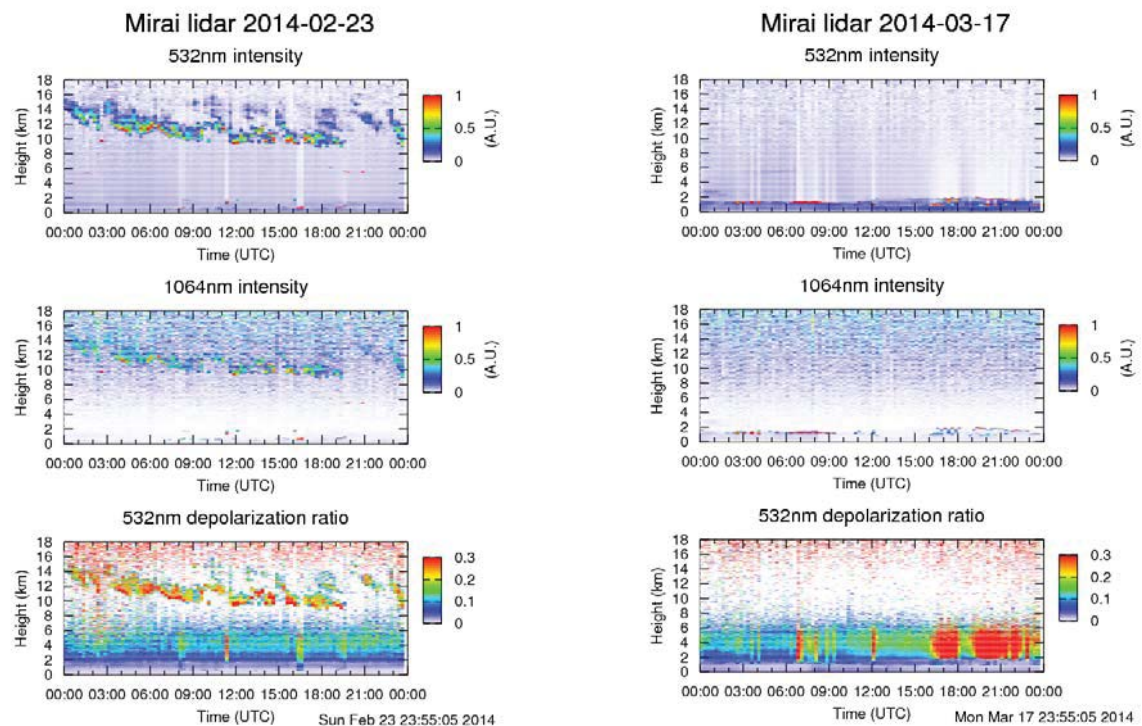
163

Figure 1: Time-height sections of backscatter intensities at 532nm /1064nm and total depolarization ratio at 532nm measured on February 23 (left) and March 17 (right), 2014.

(4) Data archive
- Raw data
temporal resolution 10min / vertical resolution 6 m (up to 18 km)
data period (UTC): February 15, 2014 ~ March 22, 2014
Backscatter intensities at 532 nm/1064 nm,   depolarization ratio at 532 nm

- Processed data (plan)
cloud base height, apparent cloud top height, phase of clouds (ice/water), cloud fraction
boundary layer height (aerosol layer upper boundary height),
backscatter coefficient of aerosols, particle depolarization ratio of aerosols

* Data policy and Citation
Contact NIES lidar team (nsugimot/i-matsui/shimizua/nisizawa@nies.go.jp) to utilize lidar data for productive use.

164

7.9. Aerosol optical characteristics measured by ship-borne sky radiometer

(1) Personnel

Kazuma Aoki (University of Toyama) Principal Investigator / not onboard
Tadahiro Hayasaka (Tohoku University) Co-worker / not onboard
Sky radiometer operation was supported by Global Ocean Development Inc.

(2) Objective

Objective of this observation is to study distribution and optical characteristics of marine aerosols by using a ship-borne sky radiometer (POM-01 MKII: PREDE Co. Ltd., Japan). Furthermore, collections of the data for calibration and validation to the remote sensing data were performed simultaneously.

(3) Parameters
- Aerosol optical thickness at five wavelengths (400, 500, 675, 870 and 1020 nm)
- Ångström exponent
- Single scattering albedo at five wavelengths
- Size distribution of volume (0.01 μm – 20 μm)
- # GPS provides the position with longitude and latitude and heading direction of the vessel, and azimuth and elevation angle of the sun. Horizon sensor provides rolling and pitching angles.

(4) Instruments and Methods

The sky radiometer measures the direct solar irradiance and the solar aureole radiance distribution with seven interference filters (0.34, 0.4, 0.5, 0.675, 0.87, 0.94, and 1.02 μm). Analysis of these data was performed by SKYRAD.pack version 4.2 developed by Nakajima *et al*. 1996.

(5) Data archives

Aerosol optical data are to be archived at University of Toyama (K.Aoki, SKYNET/SKY: http://skyrad.sci.u-toyama.ac.jp/) after the quality check and will be submitted to JAMSTEC.

7.10. Atmospheric aerosol and gas observations

(1) Personal
    Yugo KANAYA (JAMSTEC RIGC) Principal Investigator / not on board
    Fumikazu TAKETANI (JAMSTEC RIGC, not on board)
    Takuma MIYAKAWA (JAMSTEC RIGC, not on board)
    Hisahiro TAKASHIMA (JAMSTEC RIGC, not on board)
    Xiaole PAN (JAMSTEC RIGC, not on board)
    Yuichi KOMAZAKI (JAMSTEC RIGC, not on board)
    Operation was supported by Global Ocean Development Inc.

(2) Objective
    • To clarify transport processes of atmospheric pollutants from the Asian continent to the ocean
    • To investigate processes of biogeochemical cycles between the atmosphere and the ocean
    • To advance validation of satellite observations of atmospheric composition

(3) Parameters
    1. Black carbon mass concentrations and size distribution
    2. Ozone and carbon monoxide mixing ratios
    3. Aerosol composition (trace metals, water-soluble ions, carbonaceous etc)

(4) Instruments and Methods
    1. CO, O_3, and black carbon (BC)
    Carbon monoxide (CO) and ozone (O_3) measurements were also continuously conducted during the cruise. For CO and O_3 measurements, ambient air was continuously sampled on the compass deck and drawn through ~20-m-long Teflon tubes connected to a gas filter correlation CO analyzer (Model 48C, Thermo Fisher Scientific) and a UV photometric ozone analyzer (Model 49C, Thermo Fisher Scientific) in the Research Information Center.
    BC was measured by an instrument based on laser-induced incandescence (SP2, Droplet Measurement Technologies). Ambient air was sampled from the flying bridge by a 3-m-long conductive tube and then introduced to the instrument.

    2. High-volume air sampler
    Ambient aerosol particles were collected along cruise track using a high-volume air sampler (HV-525PM, SIBATA) located on the flying bridge operated at a flow rate of 500 L min^{-1}. To avoid collecting particles emitted from the funnel of the own vessel, the sampling period was controlled automatically by using a "wind-direction selection system". Coarse and fine particles separated at the diameter of 2.5 μm were collected on quartz filters. The filter samples obtained during the cruise are subject to chemical analysis of aerosol composition, including water-soluble ions and trace metals.

(5) Observation log
    The shipboard measurements and sampling were conducted in the open sea.

(6) Data archives
    These data obtained in this cruise will be submitted to the Data Management Group (DMG) of JAMSTEC, and will be opened to the public via "Data Research for Whole Cruise Information in JAMSTEC" in JAMSTEC web site.

7.11. Validation of GOSAT products over sea using a ship-borne compact system for measuring atmospheric trace gas column densities

Personal;
Kei Shiomi (JAXA EORC)
Shuji KAWAKAMI (JAXA EORC)

(1) Objective

Greenhouse gases Observing SATellite (GOSAT) was launched on 23 January 2009 in order to observe the global distributions of atmospheric greenhouse gas concentrations: column-averaged dry-air mole fractions of carbon dioxide (CO_2) and methane (CH_4). A network of ground-based high-resolution Fourier transform spectrometers provides essential validation data for GOSAT. Vertical CO_2 profiles obtained during ascents and descents of commercial airliners equipped with the in-situ CO_2 measuring instrument are also used for the GOSAT validation. Because such validation data are obtained mainly over land, there are very few data available for the validation of the over-sea GOSAT products. The objectives of our research are to acquire the validation data over the Indian Ocean and the tropical Pacific Ocean using an automated compact instrument, to compare the acquired data with the over-sea GOSAT products, and to develop a simple estimation of the carbon flux between the ocean and the atmosphere from GOSAT data.

(2) Description of instruments deployed

The column-averaged dry-air mole fractions of CO_2 and CH_4 can be estimated from absorption by atmospheric CO_2 and CH_4 that is observed in a solar spectrum. An optical spectrum analyzer (OSA, Yokogawa M&I co., AQ6370) was used for measuring the solar absorption spectra in the near-infrared spectral region. A solar tracker (PREDE co., ltd.) and a small telescope (Figure 1) collected the sunlight into the optical fiber that was connected to the OSA. The solar tracker searches the sun every one minute until the sunlight with a defined intensity. The measurements of the solar spectra were performed during solar zenith angles less than 80°.
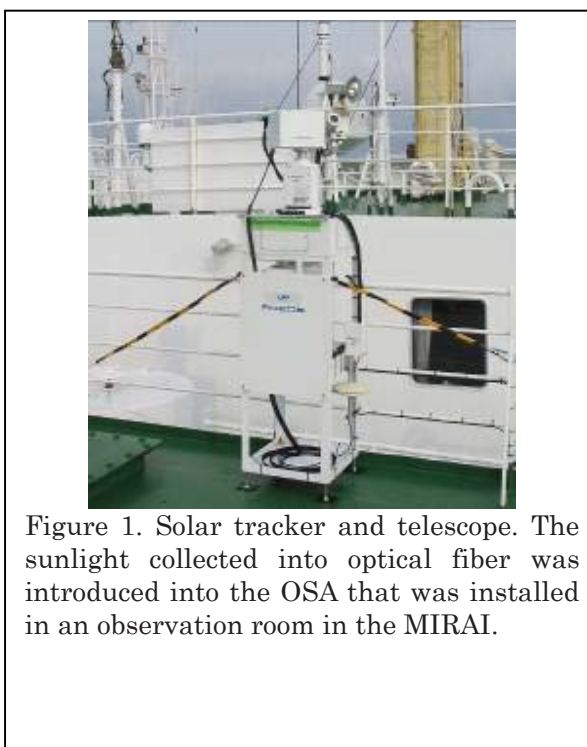

Figure 1. Solar tracker and telescope. The sunlight collected into optical fiber was introduced into the OSA that was installed in an observation room in the MIRAI.

(3) Analysis method

The CO_2 absorption spectrum at the 1.6 μm band measured with the OSA is shown in Figure 2. The absorption spectrum can be simulated based on radiative transfer theory using assumed atmospheric profiles of pressure, temperature, and trace gas concentrations. The column abundance of CO_2 (CH_4) was retrieved by adjusting the assumed CO_2 (CH_4) profile to minimize the differences between the measured and simulated spectra. Figure 3 shows an example of spectral fit performed for the spectral region with the CO_2 absorption lines. The column-averaged dry-air mole fraction of CO_2 (CH_4) was obtained by taking the ratio of the CO_2 (CH_4) column to the dry-air column.
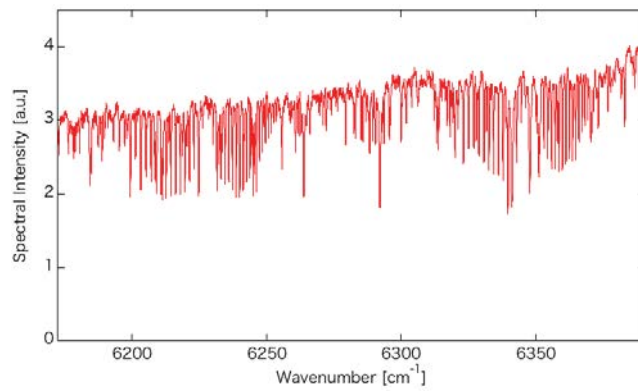
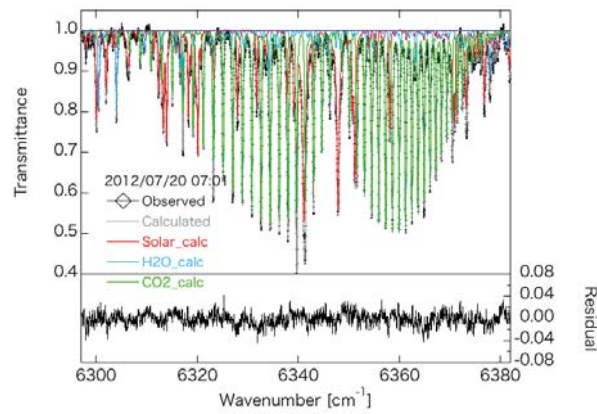Figure 2. 1.6 μm CO_2 absorption spectrum measured with the OSA.

Figure 3. Spectral fit performed for the 6297–6382 cm^{-1} region using an OSA spectrum.

(4) Preliminary results

The observations were made from February 15 to March 22, 2014 continuously in daytime (Table 1 and Figure 2).

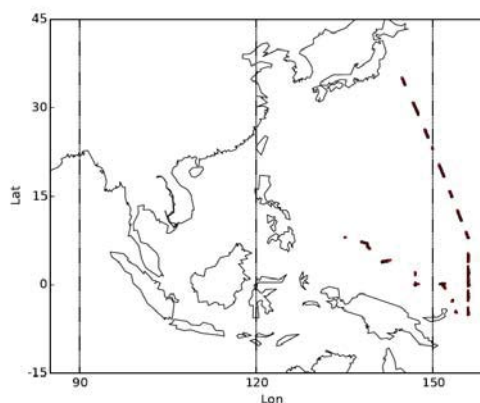| CO$_2$ observations		
Date	Start Time(JST)	End Time(JST)
2014/02/15	17:01	17:24
2014/02/16	7:01	16:40
2014/02/17	7:47	12:52
2014/02/18	6:33	15:37
2014/02/18	6:33	15:37
2014/02/20	9:17	11:36
2014/02/21	9:40	14:52
2014/02/22	12:39	15:16
2014/02/23	6:09	16:11
2014/02/24	6:34	16:27
2014/02/25	7:02	12:45
2014/02/26	12:39	14:05
2014/02/27	5:35	14:51
2014/02/28	5:33	14:44
2014/03/01	6:57	15:37
2014/03/02	5:45	16:09
2014/03/03	8:09	15:07
2014/03/04	7:08	13:30
2014/03/06	7:54	15:41
2014/03/07	5:28	16:05
2014/03/08	5:28	16:18
2014/03/09	5:28	16:09
2014/03/10	5:35	16:21
2014/03/11	5:28	16:05
2014/03/12	5:29	15:35
2014/03/13	5:34	16:10
2014/03/14	6:14	16:10
2014/03/15	5:59	16:34
2014/03/16	12:10	16:21
2014/03/17	7:07	16:27
2014/03/18	6:22	16:40
2014/03/19	8:22	16:10

Table 1. Period of CO$_2$ observations

Figure 2. Locations of CO$_2$ observations

(5) Data archive

The column-averaged dry-air mole fractions of CO$_2$ and CH$_4$ retrieved from the OSA spectra will be submitted to JAMSTEC Data Integration and Analyses Group (DIAG).

7.12 Underway pCO₂ observation

Personal:
Kei SHIOMI (JAXA)
Yoshiyuki NAKANO (JAMSTEC): Principal Investigator
Yoshiko ISHIKAWA(MWJ): Operation Leader

(1) Objectives

Concentrations of CO_2 in the atmosphere are increasing at a rate of 1.5 ppmv yr^{-1} owing to human activities such as burning of fossil fuels, deforestation, and cement production. Oceanic CO_2 concentration is also considered to be increased with the atmospheric CO_2 increase, however, its variation is widely different by time and locations. Underway pCO_2 observation is indispensable to know the pCO_2 distribution, and it leads to elucidate the mechanism of oceanic pCO_2 variation. We here report the underway pCO_2 measurements performed during MR14-02 cruise.

(2) Paramaeter

Atmospheric and oceanic CO_2 partial pressure (pCO_2)

(3) Instruments and Methods

Oceanic and atmospheric CO_2 concentrations were measured during the cruise using an automated system equipped with a non-dispersive infrared gas analyzer (NDIR; LI-7000, Li-Cor). Measurements were done every about one and a half hour, and 4 standard gases, atmospheric air, and the CO_2 equilibrated air with sea surface water were analyzed subsequently in this hour. The concentrations of the CO_2 standard gases were 249.25, 330.29, 360.28 and 420.25 ppmv. Atmospheric air taken from the bow of the ship (approx.30 m above the sea level) was introduced into the NDIR by passing through a electrical cooling unit, a mass flow controller which controls the air flow rate of 0.5 L min^{-1}, a membrane dryer (MD-110-72P, perma pure llc.) and chemical desiccant ($Mg(ClO_4)_2$). The CO_2 equilibrated air was the air with its CO_2 concentration was equivalent to the sea surface water. Seawater was taken from an intake placed at the approximately 4.5 m below the sea surface and introduced into the equilibrator at the flow rate of 4 - 5 L min^{-1} by a pump. The equilibrated air was circulated in a closed loop by a pump at flow rate of 0.6 - 0.8 L min^{-1} through two cooling units, a membrane dryer, the chemical desiccant, and the NDIR.

(4) Observation log

Cruise track during pCO_2 observation is shown in Figure 7.12-1.

(5) Preliminary results

Temporal variations of both oceanic and atmospheric CO_2 concentration (xCO_2) are shown in Fig. 7.12-2.

(6) Data Archive

Data obtained in this cruise will be submitted to the Data Management Group (DMG) of JAMSTEC, and will be opened to the public via "Data Research for Whole Cruise Information in JAMSTEC" in JAMSTEC home page.

(7) Reference

Dickson, A. G., Sabine, C. L. & Christian, J. R. (2007), Guide to best practices for ocean CO_2 measurements; PICES Special Publication 3, 199pp.
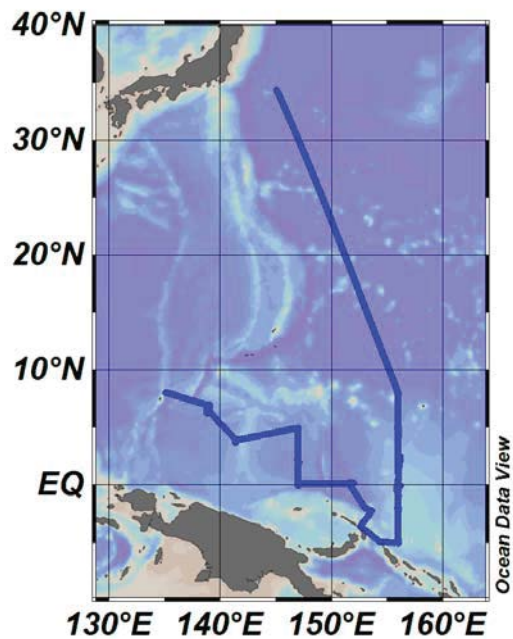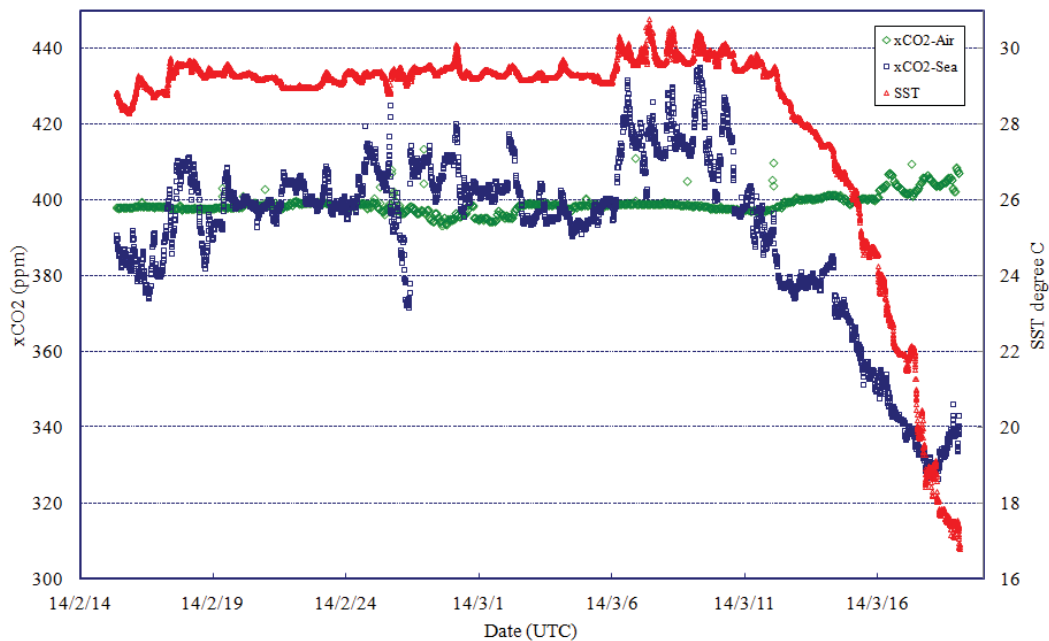

Figure 7.12-1 Observation map

Figure 7.12-2 Time series of atmospheric and oceanic CO_2 concentration (xCO_2). Green dots represent atmospheric xCO_2 variation and blue oceanic xCO2. SST variation (red) is also shown.

7.13. Doppler Radar

(1) Personnel

Masaki KATSUMATA   (JAMSTEC)   - Principal Investigator (Not on board)
Kazuho YOSHIDA   (GODI)   - Operation Leader

(2) Objective

The objective of the Doppler radar observation in this cruise is to investigate three dimensional rainfall and kinematic structures of precipitation systems and their temporal and special variations. The observation in this cruise is to compare the data to that from satellite-borne precipitation radar such as TRMM/PR and GPM/DPR to evaluate the accuracy of the radars.

(3) Method

The Doppler radar on board of Mirai is used. The specification of the radar is:

Frequency:	5290 MHz
Beam Width:	less than 1.5 degrees
Output Power:	250 kW (Peak Power)
Signal Processor:	RVP-7 (Vaisala Inc. Sigmet Product Line, U.S.A.)
Inertial Navigation Unit:	PHINS (Ixsea S.A.S., France)
Application Software:	IRIS/Open (Vaisala Inc. Sigmet Product Line, U.S.A.)

Parameters of the radar are checked and calibrated at the beginning and the end of the intensive observation. Meanwhile, daily checking is performed for (1) frequency, (2) mean output power, (3) pulse width, and (4) PRF (pulse repetition frequency).

During the cruise, the volume scan consisting of 21 PPIs (Plan Position Indicator) is conducted every 10 minutes. A dual PRF mode with the maximum range of 160 km is used for the volume scan. Meanwhile, a surveillance PPI scan is performed every 30 minutes in a single PRF mode with the maximum range of 300 km. At the same time, RHI (Range Height Indicator) scans of the dual PRF mode are also operated whenever detailed vertical structures are necessary in certain azimuth directions. Detailed information for each observational mode is listed in Table 7.13-1. The Doppler radar observation is from Mar.13 to 19 (during MR14-02) over the high sea and Japanese EEZ.

(4) Preliminary results

The data are successfully obtained continuously for the observation period described above. The data will be analyzed further after the cruise.

(5) Data archive

All data of the Doppler radar observation during this cruise will be submitted to the JAMSTEC Data Integration and Analysis Group (DIAG).

Table 5.2-1 Parameters for each observational mode

	Surveillance PPI	Volume Scan	RHI
Pulse Width	2 (microsec)	0.5 (microsec)	0.5 (microsec)
Scan Speed	18 (deg/sec)	18 (deg/sec)	Automatically determined
PRF	260 (Hz)	900/720 (Hz)	900 (Hz)
Sweep Integration	32 samples	50 samples	32 samples
Ray Spacing	1.0 (deg)	1.0 (deg)	0.2 (deg)
Bin Spacing	250 (m)	250 (m)	250 (m)
Elevation Angle	0.5	0.5, 1.0, 1.8, 2.6, 3.4, 4.2, 5.0, 5.8, 6.7, 7.7, 8.9, 10.3, 12.3, 14.5, 17.1, 20.0, 23.3, 27.0, 31.0, 35.4, 40.0	0.0 to 60.0
Azimuth	Full Circle	Full Circle	Optional
Range	300 (km)	160 (km)	160 (km)

Appendix

A list for all of the public application (project name and representative proposer) projects is shown below.

(1) The reconstruction of the ocean environmental change in the Quaternary period and geomagnetism strength change over the western equatorial Pacific
   Proposed by: Junichiro Kuroda (JAMSTEC)

(2) Estimation of the primary productivity by the dissolved O_2 isotope of the intermediate-to-deep water
   Proposed by: Osamu Abe (Nagoya University)

(3) Study on oceanic circulation, heat and fresh water transports, and their changes over the Pacific Ocean, and comprehensive study for physics, chemical and biology process over north-western Pacific, using Argo floats
   Proposed by: Toshio Suga (JAMSTEC)

(4) Lidar observations of clouds and aerosols
   Proposed by: Nobuo Sugimoto (NIES)

(5) Atmospheric aerosol and gas observations
   Proposed by: Yugo Kanaya (JAMSTEC)

(6) Study on formation process of the Lyra Basin
   Proposed by: Masao Nakanishi (Chiba University)

(7) Validation of GOSAT products over sea using a ship-borne compact system for measuring atmospheric trace gas column densities
   Proposed by: Kei Shiomi (JAXA)

(8) Aerosol optical characteristics measured by ship-borne sky radiometer
   Proposed by: Kazuma Aoki (University of Toyama)

(9) Study on standardization of ocean geophysics observation data and application to ocean bottom dynamics
   Proposed by Takeshi Matsumoto (University of the Ryukyus)